Ollscoil na hÉireann, Corcaigh

THE NATIONAL UNIVERSITY OF IRELAND, CORK

Coláiste na hOllscoile,

Corcaigh

UNIVERSITY COLLEGE CORK

CancerResearch@UCC

The characterization of macrophages in melanoma and the effect of electroporation on melanoma conditioned macrophages

Thesis presented by

Liam Friel Tremble, MSc.

Under the supervision of

Dr. Patrick Forde

Dr. Cynthia Heffron

For the degree of

Doctor of Philosophy

December 2019

Table of Contents

Abstract

Approximately 11,000 people are diagnosed with skin cancer in Ireland every year and approximately 1,000 of these present with malignant melanoma. Due to lifestyle changes and an increase in UV exposure, incidences are expected to continue to rise despite the presence of health campaigns.

Immune cells, called macrophages, have been documented to represent up to 50% of the tumour mass in some melanomas. However, we have only a nascent understanding of the role of these cells in tumour biology and treatment responses. One treatment offered to advanced melanoma patients is electrochemotherapy, which has exceptionally high complete local response rates of up to 80%, and is under investigation with the replacement of chemotherapy with non-cytotoxic drugs such as calcium. Calcium electroporation has shown the ability to induce comparable response rates and is under increased scrutiny due to the presence of a case report in which a systemic anti-melanoma response was seen following treatment.

While the effect of electroporation, and increasingly, calcium electroporation on tumour cells has been well documented. The effect of these treatments on bystander cells in the treatment area, such as tumour-associated macrophages, has not been investigated.

Here we present clinical findings of the presence of distinct macrophage populations recruited to melanoma tissue. Using their inflammatory phenotype, effect on gene expression within the tumour, and correlation with survival outcomes we give compelling evidence that melanomas contain distinct populations of both active, and relatively inactive macrophages, which can vary depending on the pathological features of the tumour, such as Breslow depth and BRAF mutational status.

Given the presence of an inflammatory population of macrophages in the tumour, we sought to develop an *in vitro* model in which we could examine the effect of electroporation on melanoma conditioned macrophages. Using an adapted model of bone marrow-derived monocyte development followed by melanoma conditioning, we were able to generate an immunologically active model of melanoma conditioned monocytes, which upregulated M2-associated surface receptors, similar to the predominant population of intratumoural macrophages. These conditioned cells showed no major increase in inducible nitric oxide synthase or arginase expression, as

was seen clinically, but were able to affect T cell proliferation and polarization, indicating an influential immunological phenotype.

In chapter 5, we investigate the effect of electroporation on these cells, and show that, similarly to tumour cells, their membranes do become reversibly electroporated. Using the parameters investigated in chapter 4 we show that calcium electroporation does impact their phenotype and functionality, and critically, influences their ability to subsequently activate and polarize T cells. Our data indicate that electroporation does not deplete intratumoural macrophages or inhibit their ability to drive cytotoxic T cell responses, suggesting that, from a macrophage perspective, calcium electroporation may be complementary to other immunogenic treatments.

Declaration

I hereby declare that I am the sole author of this thesis. This work has not been submitted for another degree, either at University College Cork or elsewhere.

I authorise University College Cork to lend and photocopy this thesis to other institutions or individuals for the purpose of scholarly research.

_____

Liam Friel Tremble

Acknowledgements

First and foremost I would like to thank my supervisor Dr Patrick Forde and co-supervisor Dr Cynthia Heffron for their endless support, availability and patience over the course of the last 3 years. It is without question that this thesis would not be near completion without their assistance at every step of the way. I cannot express my gratitude enough for their open doors and positive attitude from start to finish.

To all the staff and students at CancerResearch@UCC, thank you! Having at least some of my mental wellbeing intact at the end of this progress is thanks to you all. For the good times, and being there during the not so good times. For both the social outings and the invigorating scientific discussions (not that they were at all mutually exclusive). In particular to the soon to be doctors, Venkata Vamsi Bharadwaj Yallapragada, Joe Murphy and Glenn Hogan for our impromptu support sessions after tough days in the lab.

For scientific and practical support I am grateful to the army of people to which I am indebted to for their support. The list of people I wish to thank would require a few trees worth of paper, but I would like to especially thank Dr Derek Power, Dr James Clover and Juliet Barry for all of the time, support and enthusiasm they selflessly shared with me. A special thanks goes out to Dr Declan Soden for the opportunities afforded to me from the outset of this PhD, and to Dr Garrett Casey for what felt like endless lists of issues and requests that I would leave at his desk.

Finally, I would like to thank my parents and wonderful girlfriend for their eternal patience over the last few years, for making the hard choices that bit easier and supporting me throughout. After 3 years of describing my progress as “getting there” it is a privilege and some relief to finally be able to tell them “we got there.”

Abbreviations

5-FU	5-Fluorouracil
5YS	5-Year survival
Ab	Antibody
ADCC	Antibody-dependent cellular cytotoxicity
AE	Adverse event
AEEC	Animal Experimentation Ethics Committee
APC	Allophycocyanin
Arg	Arginase
ATP	Adenosine triphosphate
B16CM	B16F10 conditioned medium
BCG	Bacillus Calmette–Guérin
BMDM	Bone marrow-derived monocytes
BRAF	Serine/threonine-protein kinase B-Raf
BRIP1	BRCA1 interacting protein C-terminal helicase 1
BSA	Bovine serum albumin
BV605	Brilliant violet 605
CCL2	Chemokine (C-C motif) ligand 2
CCL3	Chemokine (C-C motif) ligand 3
CCR2	C-C chemokine receptor type 2
CCR5	C-C chemokine receptor type 5
CD	Cluster of differentiation
CDKN3	Cyclin-dependent kinase inhibitor 3
cDNA	Complementary DNA
CFSE	Carboxyfluorescein succinimidyl ester
CPI	T cell checkpoint inhibitor
CREC	Central Research Ethics Committee
CRISPR	Clustered regularly interspaced short palindromic repeats
cRPMI	Complete RPMI
CSF1	Colony-stimulating factor 1
CSF1R	Colony stimulating factor 1 receptor
CX3CL1	chemokine (C-X3-C motif) ligand 1
CX3CR1	CX3C chemokine receptor 1

CXCR3	C-X-C chemokine receptor type 3
CTLA-4	Cytotoxic T-lymphocyte-associated protein 4
Cy5.5	Cyanine5.5
Cy7	Cyanine7
DAMP	Damage associated molecular pattern
DC	Dendritic cell
ddH_2O	Double distilled water
DEPDC1	DEP domain containing 1
DFS	Disease-free survival
DNA	Deoxyribonucleic acid
ECT	Electrochemotherapy
EDTA	Ethylenediaminetetraacetic acid
Egr2	Early growth response protein 2
ELISA	Enzyme-linked immunosorbent assay
EP	Electroporation
FACS	Fluorescence-activated cell sorting
Fc	Fragment crystallisable region
FcγRIIIA	Fc γ receptor 3A
FcR	Fc receptor
FCS	Foetal calf serum
FFPE	Formalin-fixed paraffin embedded
FITC	Fluorescein isothiocyanate
FOLFIRINOX	Folinic acid, fluorouracil, irinotecan and oxaliplatin
FSC	Forward scatter
GAPDH	Glyceraldehyde 3-phosphate dehydrogenase
G-CSF	Granulocyte-colony stimulating factor
gDNA	Genomic DNA
GM-CSF	Granulocyte-macrophage colony-stimulating factor
GPCR	G-protein-coupled receptor
H&E	Haematoxylin and eosin stain
H&L	Heavy and light chain (antibody)
HEPES	4-(2-hydroxyethyl)-1-piperazineethanesulfonic acid
HLA-DR	Human Leukocyte Antigen – DR isotype

HMGB1	High mobility group box 1 protein
HRP	Horseradish peroxidase
ICOS	Inducible T-cell costimulator
IDO	Indolamine 2,3-dioxygenase
IDT	Integrated DNA Technologies, Inc
IFNγ	Interferon γ
IgG1	Immunoglobulin type G subclass 1
IgG4	Immunoglobulin type G subclass 4
IHC	Immunohistochemistry
IL-1	Interleukin 1
IL-1β	Interleukin 1β
IL-2	Interleukin 2
IL-4	Interleukin 4
IL-6	Interleukin 6
IL-8	Interleukin 8
IL-10	Interleukin 10
IL-12	Interleukin 12
IL-12b	Interleukin 12b
IL-13	Interleukin 13
iNOS	Inducible nitric oxide synthase
irAE	Immune related adverse event
LP	Long pass
LPS	Lipopolysaccharide
MAPK	Mitogen-activated protein kinase
M-CSF	Macrophage colony-stimulating factor
MDSC	Myeloid derived suppressor cell
MEF2C	Myocyte-specific enhancer factor 2C
MEK	Mitogen-activated protein kinase kinase
MEM	Eagle's modified essential medium
MFI	Mean fluorescent intensity
MHC II	Major histocompatibility complex class II
MMP-9	Matrix metallopeptidase 9
MO	Monocyte

mRPMI	RPMI supplemented for macrophages
mTOR	Mammalian target of rapamycin
MWCO	Molecular weight cut off
NED	N-1-napthylethylenediamine dihydrochloride
NGS	Next generation sequencing
NK	Natural killer
NO	Nitric oxide
NSCLC	Non-small cell lung cancer
NT	No treatment
NTCM	No treatment concentrated medium
OS	Overall survival
P/S	Penicillin and Streptomycin
PAMP	Pathogen associated molecular pattern
PAP-GM-CSF	Prostatic acid phosphatase- GM-CSF
PBMC	Peripheral blood mononuclear cell
PBS	Phosphate buffered saline
PCR	Polymerase chain reaction
PD-1	Programmed cell death protein 1
PDAC	Pancreatic ductal adenocarcinoma
PD-L1	Programmed death-ligand 1
PI	Propidium iodide
PIGF	Phosphatidylinositol-glycan biosynthesis class F protein
PT	Precise temperature control
qPCR	Quantitative polymerase chain reaction
RBC	Red blood cell
RFC4	Replication factor C subunit 4
RNA	Ribonucleic acid
RPMI 1640	Roswell Park Memorial Institute medium 1640
RT	Room temperature
SALL1	Sal-like protein 1
SSC	Side scatter
STAT3	Signal transducer and activator of transcription 3
Th1	T helper 1

THP-1	Human acute monocytic leukemia cell line
TLR	Toll-like receptor
TMB	3,3′,5,5′-Tetramethylbenzidine
TME	Tumour microenvironment
TNFα	Tumour necrosis factor α
TP53	Tumour protein 53
Treg	Regulatory T cell
uNTX	Urinary N-telopeptide
USA	United States of America
VCAM-1	Vascular cell adhesion protein 1
VEGF	Vascular endothelial growth factor
Ym1	chitinase-like 3
YUMM	Yale University Mouse Melanoma

Publications included as part of this thesis:

1. Tremble LF, Forde PF (2017) Clinical evaluation of macrophages in cancer: role in treatment, modulation and challenges. Cancer Immunology, Immunotherapy 66 (12):1509-1527. doi:10.1007/s00262-017-2065-0

2. Tremble LF, Moore AC, Forde PF (2019) Melanoma conditioned medium promotes cytotoxic immune responses by murine bone marrow derived monocytes despite their expression of 'M2' markers. Cancer Immunology, Immunotherapy. 2019 Sep;68(9):1455-1465. doi: 10.1007/s00262-019-02381-1

Oral Presentations

Young Cancer Researchers Network, 21-22 June 2018, Cork, Ireland. "Preclinical development of macrophage targeted therapies".

Poster Presentations

Young Cancer Researchers Network, 21-22 June 2018, Cork, Ireland. "Phenotypic evaluation of macrophages in murine and human melanoma"

20th International AEK Cancer Congress, Feb 27-Mar 1st, Heidelberg, Germany. "Melanoma conditioned bone marrow derived monocytes promote cytotoxic immune responses despite expression of 'M2' markers."

Phagocyte Functions Through Life: Development, Defence and Disease, Gordon Research Conference, 2-7 June 2019, New Hampshire, USA. "Clinical evaluation of the presence of macrophages in melanoma and their effect on intratumoural gene expression"

Publications obtained but not included within this thesis:

Tremble LF, O'Brien MA, Soden DM, Forde PF. Electrochemotherapy with cisplatin increases survival and induces immunogenic responses in murine models of lung cancer and colorectal cancer. Cancer Letters. 2019 Feb 1;442:475-482. doi: 10.1016/j.canlet.2018.11.015.

Tremble LF, O'Brien MA, Forde PF, Soden DM. ICOS activation in combination with electrochemotherapy generates effective anti-cancer immunological responses in murine models of primary, secondary and metastatic disease. Cancer Letters. 2018 Apr 28;420:109-115. doi: 10.1016/j.canlet.2018.01.081.

Chapter 1

Literature Review and introduction

Sections from this chapter have been published as;

Tremble LF, Forde PF (2017) Clinical evaluation of macrophages in cancer: role in treatment, modulation and challenges. Cancer Immunology, Immunotherapy 66 (12):1509-1527. doi:10.1007/s00262-017-2065-0

1.1 Abstract

The focus of immunotherapeutics has been placed firmly on anti-tumour T cell responses. Significant progress has been made in the treatment of both local and systemic malignancies, but low response rates and rising toxicities are limiting this approach. Advancements in the understanding of tumour immunology are opening up a new range of therapeutic targets, including immunosuppressive factors in the tumour microenvironment. Macrophages are a heterogeneous group of cells that have roles in innate and adaptive immunity and tissue repair, but become co-opted by tumours to support tumour growth, survival, metastasis and immunosuppression. Macrophages also support tumour resistance to conventional therapy. In preclinical models, interference with macrophage migration, macrophage depletion and macrophage re-education have all been shown to reduce tumour growth and support anti-tumour immune responses. Here we discuss the role of macrophages in prognosis and sensitivity to therapy, while examining the significant progress which has been made in modulating the behaviour of these cells in cancer patients.

-

1.2 Introduction

1.2.1 Historical context

The potential of utilizing the host immune system to eradicate cancers has been hotly debated over the course of the last century. Many doubted the ability to prime the host immune system to a tumour which has already successfully evaded detection and generated a profoundly immunosuppressive tumour microenvironment (TME). Over the last two decades a range of immunotherapies have made it to the clinic, clearly proving the point of principle, but the ability of immunotherapy to target more aggressive and less immunogenic tumours is still in doubt [1].

In order to comprehend the limitations of current T cell immunotherapeutics, namely T cell checkpoint inhibitors (CPIs), which skew the balance of stimulatory and inhibitory signals, it can be useful to imagine the tumours as exerting an immunosuppressive force, and the immune system as having a finite immune potential (**Figure 1.1**). Immunosuppression will rise with cancer progression and possibly plateau, but at a level both beyond the limit of the normal immune potential and even further from the immune potential of an immunocompromised cancer patient, thus even with a plentiful supply of neoantigens the immune system is rendered ineffective [2,3]. CPIs function to boost the immune potential of the host to a point at which it can feasibly compete and overcome the immunosuppression generated by the tumour [4,5]. While this is desirable in an anti-cancer context, the effect of such an untethered immune response in the host can have serious deleterious effects beyond the tumour [6,7].

The major successes in immunotherapies for cancer patients have relied upon the direct modulation of T cell activation, either by targeting T cell costimulatory proteins such as cytotoxic T-lymphocyte-associated protein 4 (CTLA-4) and Programmed cell death protein 1 (PD-1), or by adoptive T cell transfer using *ex-vivo* T cell activation [8-10]. However, the side effects associated with these drugs appear to be dose dependant, cumulative with previous cycles of therapy and additive with other similar regimes [11-13]. This apparent limit has led to a shift in research to identify suitable complimentary therapies that kill tumour cells in a way which primes the TME for T cell activation by inducing immunogenic forms of cell death [14,15].

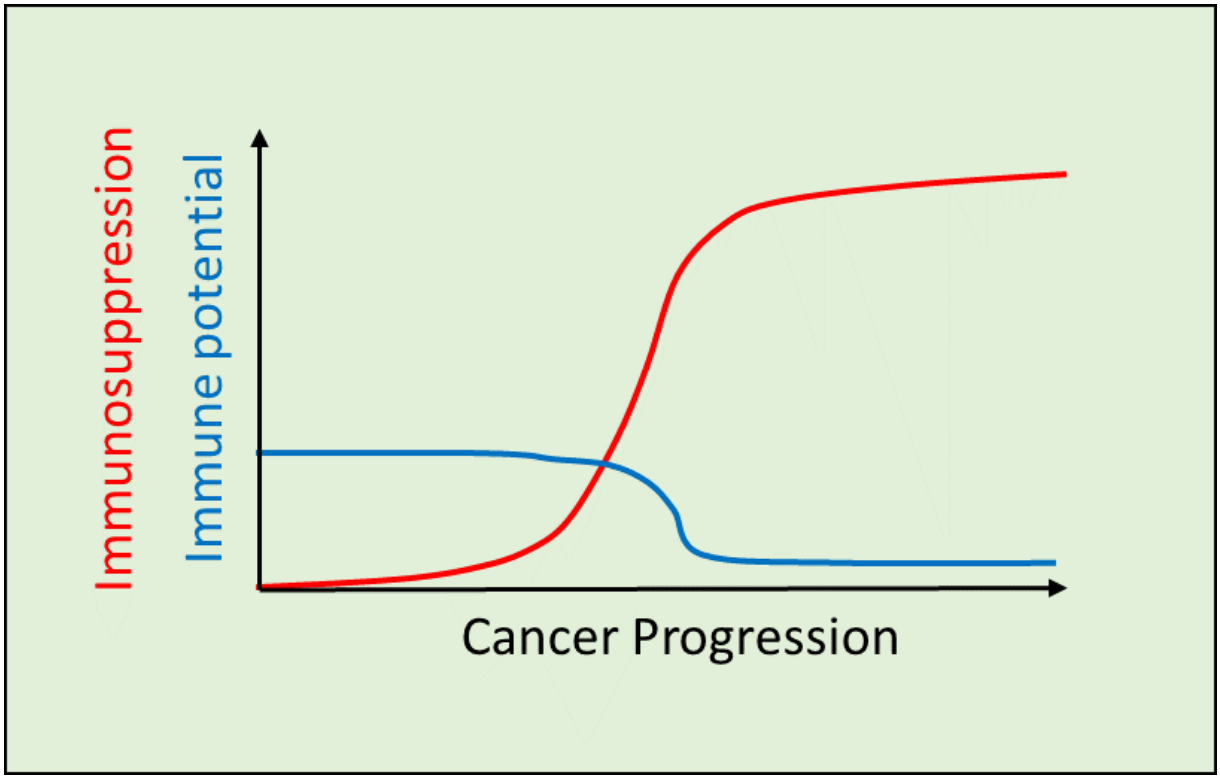

Figure 1.1 Magnitude of immune potential versus tumour generated immunosuppression
Diagrammatic hypothesis representing immunosuppression over time during cancer progression graphed with immune potential. Immune potential is the ability of the immune system to mount an effective adaptive immune response.

Developments in the field of immunology, and the elucidation of the myriad of components interacting in the TME, are leading to the development of a new range of immunotherapeutics that focus on an expanding set of targets with therapeutic and diagnostic potential [16,17].

In contrast to many approved immunotherapeutics that boost the immune potential, one interest has been in trying to actively reverse the immunosuppression generated by the tumour by disrupting immunosuppressive factors in the TME or by disrupting cells normally co-opted by tumours [18].

One specific vein of research has focused on a subset of the myeloid cell compartment comprising the monocyte-macrophage lineage which can be subverted and recruited to the tumour as tumour associated macrophages (TAMs). While TAMs can comprise up to 50% of the tumour mass, they have been less intensively studied than other immune subsets [19]. There is a growing body of literature showing their prognostic value, and they are emerging as promising therapeutic targets in oncology [20].

1.2.2 Synopsis of macrophage origin and classification

TAMs are predominantly derived from circulating populations of monocytes [21]. As a simplified paradigm, macrophages have been categorized as classically activated M1 (inflammatory) which are anti-tumour, or alternatively activated M2 (wound repair) which are pro-tumour [22]. The M1 M2 dichotomy was developed by *in vitro* observations but recent advances have led to a more complex spectrum of activation states. Both monocyte and macrophage populations frequently display hybrid M1/M2 phenotypes, or phenotypes that cannot be adequately defined using the M1:M2 system [23]. It has been identified that the M1/M2 system is leading to confusion and inconsistency between researchers and ultimately impeding progress [24].

Others advocate the use of *in vivo* function to classify M1 M2 macrophages, focusing on the inducible nitric oxide synthase (iNOS) (M1): arginase (M2) ratio. With cells being defined as inhibitors of cell growth and killers or as promoters of cell proliferation and wound repair (**Figure 1.2**) [25]. Flow cytometry has however led to the distinction of a range of macrophage and monocyte types based on their relative expression of various cell surface markers [26].

From a clinical perspective, the study of macrophages faces a unique challenge, in that we find it more amenable to study discretely defined subsets of cells, but it is becoming increasingly evident that this is not possible with such a heterogeneous set of cells. While many continue to report based on two distinct subtypes, it is important to remember that the activation states of macrophages incorporate discrete populations and spectrums or continuums where cells can adopt hybrid states [27].

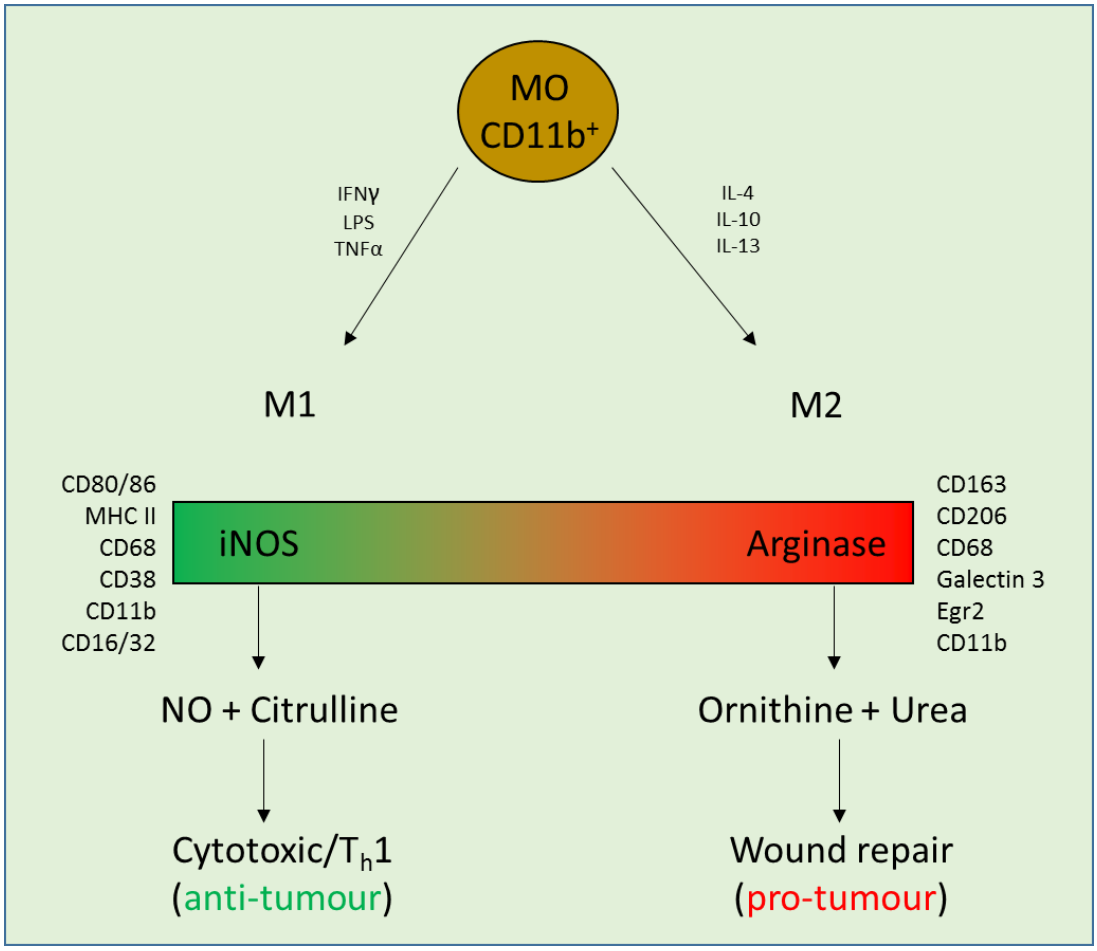

Figure 1.2 Synopsis of M1:M2 macrophage dichotomy

Cluster of differentiation (CD) 11b monocytes (MO) can mature with a heterogeneity of phenotypes which together represent a spectrum with M1 and M2 macrophages representing the two extremes of that spectrum. *In vitro*, Interferon γ (IFNγ), Lipopolysaccharide (LPS) and Tumour necrosis factor α (TNFα) drive M1 polarization whereas Interleukin 4 (IL-4), Interleukin 10 (IL-10) and interleukin 13 (IL-13) drive M2 polarization. M1 macrophages express CD68, CD11b, CD38, CD16/32, major histocompatibility complex class II (MHC II) and CD80/86, their primary function is dependent on the expression and function of inducible nitric oxide synthase (iNOS) which results in the extracellular accumulation of nitric oxide (NO) and citrulline which, along with other cytokines, can drive cytotoxic anti-tumour T helper 1 (T_h1) responses. M2 macrophages express CD68, CD11b, CD163, CD206, Galectin 3 and Early Growth Response Protein 2 (Egr2), their primary function is dependent on the expression and function of arginase which results in the extracellular depletion of arginine and the accumulation of ornithine and urea which are key to wound repair mechanisms but can also promote immune suppression and tumour progression. Legend: Monocyte (MO).

1.2.3 Contribution to tumourigenicity

Macrophages have been implicated in all aspects of tumour growth and spread, but they are also known to be critical mobilizers of the adaptive immune system (**Figure 1.3**) [28]. As such they play an enigmatic role in tumour development and the generation of anti-tumour responses.

In line with their roles in immune stimulation and antigen presentation, there is evidence high macrophage infiltration in the early stages of tumour growth can result in tumour destruction while low levels of infiltration support tumour growth [29,30]. Macrophages can promote anti-tumour responses but advanced tumours have been shown to polarize TAMs into an M2-like phenotype [31].

Tumours can secrete a range of chemoattractants that promote recruitment of monocyte and macrophage populations [32]. TAMs become co-opted to promote tumour cell proliferation and survival, tumour vascularization and immunosuppression along with supporting extravasation and growth of tumour cells at distal sites [33].

The importance of TAMs is evident across the literature, they can affect patient prognosis and determine sensitivity to a range of therapies. Preclinical studies and early stage clinical trials have implicated them as prime therapeutic targets [34,21].

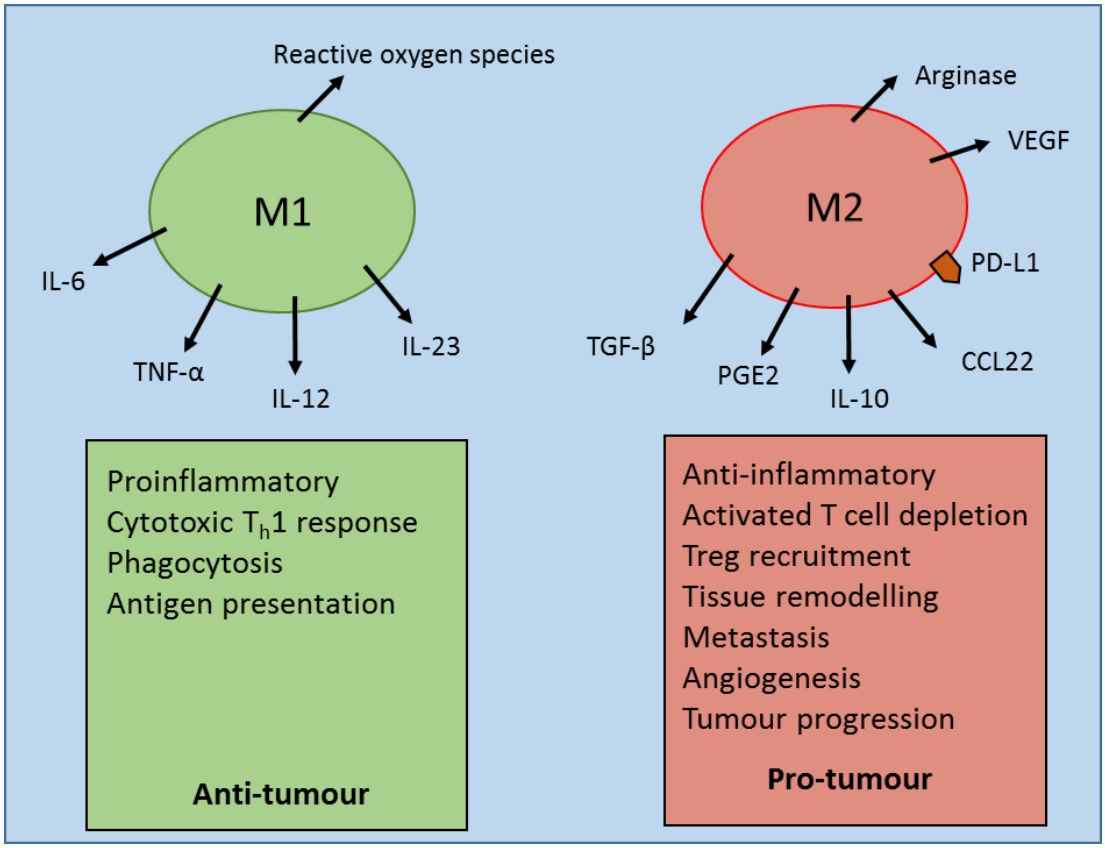

Figure 1.3 Synopsis of pro- and anti-tumoural effects exerted by macrophages

Key enzymes and cytokines produced by M1 and M2 macrophages that have the effect of driving or inhibiting cancer progression. M1 cells can drive inflammation and cytotoxic T_h1 responses while M2 cells can produce factors such as vascular endothelial growth factor (VEGF) and Prostaglandin E2 (PGE2), and are involved in the depletion of activated T cells, recruitment of regulatory T cells, tissue remodelling, angiogenesis and tumour progression.

1.3 Prognostic relevance of macrophages

1.3.1 Circulating and infiltrating macrophages

A high density of macrophage infiltration into the tumour has been cited as a negative prognostic indicator in a range of solid and haematological malignancies (**Tables 1.1-1.2**). Colorectal cancer displays a contrasting trend whereby high macrophage infiltration can result in increased patient survival [35-37].

Arguably the most robust prognostic evidence is available for breast cancer and Hodgkin's lymphoma. A distinct gene signature in breast cancer has shown high macrophage density is prognostic if combined with a high $CD4^+$ helper T cells to cytotoxic T cell ratio. The signature closely correlated to the development of secondary tumours that could accurately predict survival in women after complete resection [38]. A macrophage gene signature has been developed for Hodgkin's lymphoma that can accurately predict survival and response to therapy, indicating that the pro-tumour effect of macrophages is not restricted to solid tumours [39].

Table 1.1 The effect of macrophage infiltration and macrophage related biomarkers on prognosis in solid tumours

Tumour	Indicator	Prognostic Significance	Reference
Breast	High CSF1 gene expression	High grade, low estrogen receptor and progesterone receptor expression and high TP53 mutations	[40]
	High TAM infiltration	Shorter DFS	[41,42]
	High TAM density	Late clinical staging	[43] (M)
	High $CD68^+$ TAM density	Shorter DFS	[41]
	High $CD204^+$ TAM infiltration	Shorter relapse-free survival	[44]
Myxoid liposarcoma	High $CD68^+$ TAM infiltration	Shorter OS	[45]
Cervical	High $CD68^+$ TAM infiltration	Disease progression and high grade lesions	[46]
	High CCL2 expression and $CD68^+$ TAM infiltration	Lower relapse-free survival, lower OS, increased local and distant recurrence, vascular invasion, and larger tumour size.	[47]
Uveal Melanoma	Both High $CD68^+$ and $CD68^+CD163^+$ TAM infiltration	Shorter OS	[48]
Bladder	High $CD68^+$ TAM infiltration	Late clinical staging	[43] (M)
Oral	High $CD68^+$ TAM infiltration	Shorter OS	[43] (M)
Thyroid	High $CD68^+$ TAM infiltration	Shorter OS	[43] (M)
Ovarian	High $CD68^+$ infiltration	Shorter 5YS	[49]
	High $CD68^+$ density	Early clinical staging	[43] (M)
	High $CD68^+CD163^+$ TAM infiltration	Shorter PFS and OS	[50]
	High M1:M2 ratio in TME	Increased OS	[51]

	Serum soluble CD163	*Shorter DFS and OS	[52]
Gastric	High $CD68^+$ TAM infiltration	Shorter OS	[43] (M)
	High nest $CD68^+$ TAM	Higher 5YS	[53]
Prostate	High $CD68^+$ TAM density	Shorter median OS and poor clinical outcome	[54]
Glioma	High $CD163^+$ $CD204^+$ TAM infiltration	Correlates to histologic grade	[55]
Lung	M1:M2 gene signature	Increased OS	[56]
NSCLC	High $CD68^+$ HLA-DR^+ (M1) TAM infiltration to stroma and islets	Increased OS	[57]
	High $CD68^+$ TAM infiltration	Increased OS	[58]
Colorectal	High $CD68^+$ TAM infiltration	Increased OS	[43] (M)
	High $CD16^+$ TAM infiltration	Increased OS	[35]
	High $CD68^+$ TAM density at the tumour front	Increased OS and reduced liver metastasis	[36,37]

Clinical data linking macrophage infiltration and prevalence, via macrophage markers, with prognostic outcomes in patients with solid tumours. CD68, Colony-stimulating factor 1 (CSF1) and CD16 are markers used to identify macrophages, Human leukocyte antigen – DR isotype (HLA-DR) is used to identify M1-like macrophages. CD163 is a strong M2 marker while, CD204 and CD206 are markers also preferentially expressed by M2-like macrophages. Shaded in gray are indications where high M2-like macrophage numbers correspond to a positive prognosis. M denotes meta-study. Overall survival (OS), 5-year survival (5YS), Disease-free survival (DFS) non-small cell lung cancer (NSCLC), Tumour protein 53 (TP53).

Table 1.2 The effect of macrophage infiltration and macrophage related biomarkers on prognosis in haematological malignancies

Cancer	Indicator	Prognostic Significance	Reference
Angioimmunoblastic T-cell lymphoma	High CD163: CD68 ratio in the TME	Shorter OS	[59]
Hodgkin's lymphoma	TAM gene signature, High $CD68^+$ cells in lymph nodes	Shorter PFS, increased risk of relapse after haematopoietic stem cell transplant	[60]
	High $CD68^+$ $CD163^+$ infiltration	Shorter OS and reduced event-free survival	[61]
Follicular lymphoma	High $CD68^+$ infiltration	Shorter OS	[62]

Clinical data linking macrophage infiltration and prevalence, via macrophage markers, with prognostic outcomes in patients with haematological malignancies. CD68 is a marker used to identify all macrophages, CD163 is used to identify M2-like macrophages. Overall survival (OS), progression free survival (PFS), Tumour-associated macrophage (TAM), Tumour microenvironment (TME).

1.3.2 Histologic localization of macrophages

Histological examination of colorectal cancer, for which TAM infiltration is a positive prognostic indicator, revealed infiltration at the tumour front in colon cancer leads to enhanced survival and reduced liver metastasis, irrespective of cluster of differentiation (CD) 8^+ T cell infiltration [49,63,36,37]. The proximity of the TME to the intestinal microbiome has been hypothesized as a potential explanation for the differential behaviour of macrophages in colorectal cancer [64]. It is possible that the continuous supply of pathogen-associated molecular patterns (PAMPs) available to macrophages may outweigh the ability of the tumour to polarize the cells to an M2-like phenotype. This hypothesis may also explain why similar results have been seen in gastric cancer, in which tumours may have varying access to the intestinal microbiome depending on the localization of the tumour. Thus, high infiltration of macrophages in the tumour nests in gastric cancer is associated with enhanced antigen presentation and T cell activation, and a positive prognosis [53].

The histological localization of macrophages in breast cancer has shown no correlation with prognosis, while in endometrial cancer high TAM infiltration into the tumour hotspot (tumour core of necrotic cells) is associated with advanced clinical staging, myometrial invasion and histological differentiation [65,66,41]. Characterization in other tumour types is warranted.

1.3.3 Macrophage polarization

It is possible the results of many studies were adversely affected by failure to distinguish pro- and anti-tumour populations. When differentiated in non-small cell lung cancer (NSCLC), it was found that high M1-like macrophage infiltration was associated with prolonged survival, while the level of M2-like infiltration had no impact on survival [56,57]. This is in contrast to an earlier meta study examining the prognostic relevance of overall $CD68^+$ infiltration in NSCLC that found no link with overall survival (OS) [67].

Similarly, in patients with hepatocellular carcinoma after curative resection, high numbers of $CD11c^+$ dendritic cells and low numbers of $CD206^+$ macrophages correlated with extended OS, whereas $CD68^+$ TAM infiltration displayed no prognostic significance [68]. In ovarian cancer there is inconsistent evidence on the prognostic effect of $CD68^+$ cell infiltration, however differentiation of the populations revealed that a high M1-like:M2-like ratio is prognostically favorable [51,50,69,70]. Together these data indicate whole macrophage counts used to explore the prognostic effects in other cancers may not accurately reflect the true trend or scale of the effect imposed by pro-tumourigenic macrophage populations. The ability to draw robust prognostic indications from TAM frequency emphasizes their central role in disease progression.

1.4 Role of macrophages in therapeutic response

1.4.1 Chemotherapy

1.4.1.1 Effect of chemotherapy on macrophages

Conventional chemotherapies are considered immunosuppressive due to toxic systemic effects on rapidly proliferating leukocytes and bone marrow progenitors resulting in leukocyte depletion [71]. Chemotherapy has also been shown to stimulate the secretion of colony stimulating factor 1 (CSF1) by tumour cells, which is a potent chemoattractant for macrophages, and results in an accumulation of TAMs in the TME which contribute to chemoresistance [72].

1.4.1.2 Prognostic significance of macrophages in response to chemotherapy

High levels of infiltrating $CD68^+$ and $CD163^+$ cells are a negative prognostic marker for patients with oesophageal cancer undergoing preoperative neoadjuvant chemotherapy and indicates patients are less likely to respond to chemotherapy [73]. The CD8: CD68 cell ratio is a predictive biomarker for response to neoadjuvant chemotherapy in breast cancer patients [74,38]. These effects were found to be at least in part due to the upregulation of CSF1 by tumour cells in response to chemotherapy. A high density of $CD163^+$ cells at the invasive front in oral squamous cell carcinoma was found to correlate to a poorer outcome after surgery following 5- Fluorouracil (5-FU) based chemoradiotherapy [75].

On examination of the histologic localization of macrophages, $CD68^+$ in the parenchyma negatively correlated to lymphatic metastasis after neoadjuvant chemotherapy, in contrast to the number in the dense fibrous stroma which directly correlated to the number of positive lymph nodes, indicating the role of macrophages depends on intratumoural localization in breast cancer [74].

1.4.1.3 The role of macrophages in chemoresistance

Macrophages are central coordinators of immune responses during chemotherapy [76]. Blockade of macrophage recruitment increased the efficacy of paclitaxel in breast cancer, resulting in diminished growth of both primary and metastatic tumours [38]. Suppression of $CD8^+$ effector T cells by the production of Interleukin 10 (IL-10) has been shown to reduce anti-cancer cytotoxicity [77]. IL-10 production by macrophages also limits the efficacy of chemotherapy in breast cancer and was

subsequently shown to indirectly enhance tumour growth by down regulating Interleukin 12 (IL-12) production by dendritic cells (DCs) which is required for cytotoxic $CD8^+$ T cell responses [76].

Macrophages are critical mediators of wound and tissue repair and it is possible that these functions can be naturally adapted by the tumour to generate chemotherapeutic resistance [78]. M2-like macrophages derived from human acute monocytic leukemia (THP-1) cells, were shown to reduce apoptosis in addition to enhancing tissue repair and angiogenesis in response to etoposide, a topoisomerase inhibitor [79,80].

Both macrophage depletion and re-education to an M1 state have been shown to increase the efficacy of chemotherapy [81-83]. The induction of M1 polarization using host-produced histidine-rich glycoprotein to reduce signaling by the M2 driver Phosphatidylinositol-glycan biosynthesis class F protein (PIGF) has been shown to restore sensitivity to chemotherapy, reduce tumour growth and reduce metastasis, indicating that M1 polarization can combat all major aspects of disease [81].

Macrophage modulating therapies have an advantage over many other immunotherapeutics because they can be used to synergistically improve outcome with chemotherapy, whereas the results of combining CPIs with chemotherapy have shown very little or no effect on OS or quality of life [38].

1.4.2 Radiotherapy

1.4.2.1 Effect of radiotherapy on macrophages

Conventional fractionated radiotherapy is considered immunosuppressive, as radiation primarily leads to apoptotic cell death, but it can also lead to necrotic cell death and mitotic catastrophe [84,85].

The accumulation of macrophages in the TME after radiotherapy is due to the ability of macrophages to survive clinically relevant doses of radiotherapy coupled with an influx of monocytes after radiotherapy [86,87]. While this may seem attractive in the generation of an abscopal effect, there is much research showing that the influx of monocytes and macrophages is responsible for therapy failure due to their role in vasculogenesis and angiogenesis [88,89].

1.4.2.2 Role of macrophages in radioresistance

Murine models of oral and brain cancer have shown macrophages infiltrating the tumour after radiotherapy were primarily M2-like and supported vasculogenesis and tumour growth [90,91,89,92].

Curiously, ionizing radiation skews macrophages from an M2-like to an M1-like phenotype, suggesting an enigmatic role of macrophages in radiotherapy [93]. Characterization of the TME post irradiation reveals decreased levels of the anti-inflammatory markers CD163, IL-10, Vascular cell adhesion protein 1 (VCAM-1) and CD206 while significantly increasing the inflammatory markers iNOS, CD80, CD86 and Human Leukocyte Antigen-DR isotype (HLA-DR) [94]. However, irradiated macrophages were still able to enhance tumour cell invasion and supported the angiogenic process of tumour cells indicating the retention of M2-like traits. Blocking macrophage migration into the TME after radiotherapy has been shown to enhance responses in murine models [86].

1.4.2.3 Prognostic significance of macrophages in response to radiotherapy

Prognostically, there is limited evidence on the effect of macrophages in patients undergoing radiotherapy. Macrophages have been shown to predict response to short course pre-operative radiotherapy for colon cancer, with data suggesting a high infiltration of M1-like macrophages is likely to result in a reduced response, no effect was seen by M2-like macrophages [95].

1.4.3 T cell checkpoint inhibitors

CPIs have been the most notable achievement in the development of immunotherapy for cancer patients, but there has been limited interest in the role of myeloid cells in their clinical application to date.

Macrophages are key coordinators of adaptive immune responses, and express a range of T cell costimulatory and co-inhibitory molecules, known as the B7 family [96]. Crosstalk between tumour cells and macrophages can regulate the expression of B7 family molecules on both tumour cells and macrophages [97]. The TME is abundant in IL-10 and tumour necrosis factor α (TNF-α), which can both upregulate Programmed death-ligand 1 (PD-L1) expression on macrophages, via signal transducer and activator of transcription 3 (STAT3) signalling, which is responsible

for the inactivation and depletion of activated T cells [98-100]. PD-L1 has been implicated as a major signalling molecule associated with immune escape by tumours [101].

In addition to their role in facilitating T cell responses, macrophages are critical mediators of many therapeutics that employ antibodies with fully humanized fragment crystallisable region (Fc) domains [102]. While the primary function of antibodies is the activation or neutralization of their targets, the choice of antibody (Ab) Fc domains are known to influence their efficacy [103]. CD16, the receptor for Immunoglobulin type G subclass 1 (IgG1) is expressed primarily by macrophages and Natural killer (NK) cells and is responsible for the neutralization of antibody targets via antibody-dependent cellular cytotoxicity (ADCC) or phagocytosis [104,105]. The capacity to generate ADCC responses is dependent on two variables. Firstly, the ability of the antibody used to bind Fc receptors, and secondly on the activation state of the Fc receptor (FcR) expressing cell [106,107].

1.4.3.1 Anti-CTLA4

Ipilimumab is a fully human IgG1 monoclonal antibody (mAb) that interacts with Fc γ receptor 3A (FcγRIIIA) (CD16) expressing cells [108,109]. Ipilimumab efficacy relies on two mechanisms. Firstly, interference with CTLA4 binding on effector T cells, and secondly, FcγRIIIA mediated depletion of regulatory T cells (Tregs) by ADCC [110,111].

In a small study of 29 patients receiving Ipilimumab for the treatment of melanoma, responders had a higher number of $CD68^{+}CD163^{+}$ macrophages in the TME before treatment and decreased Treg infiltration after therapy. Responders had the highest level of circulating non-classical $CD16^{+}CD14^{low}$ macrophages at baseline [108]. In a study of 209 melanoma patients receiving Ipilimumab, low absolute monocyte counts and low levels of circulating $CD14^{+}HLA\text{-}DR^{-/low}$ Myeloid-derived suppressor cells (MDSCs) were significantly associated with improved survival [112]. These studies indicate macrophages play an active role in response.

1.4.3.2 Anti-PD-1/PD-L1

Both PD-1 and PD-L1 are expressed by macrophages, and as such the effect of these neutralizing antibodies may have a depletory effect on macrophage numbers

[113,114]. PD-1 is expressed on infiltrating macrophages and lymphocytes of melanoma patients responding to anti-PD-1 therapy [115]. Response was primarily correlated to the proliferation of intratumoural $CD8^+$ T cells and the role of $PD\text{-}1^+$ macrophages was not examined. A reduction of the proinflammatory Chemokine (C-C motif) ligand 3 (CCL3) is associated with prolonged survival in metastatic renal cell carcinoma patients receiving Atezolizumab [115,116].

Evaluation of immunologic correlates during CPI administration is required to improve our understanding of the biology of response and development of resistance. Due to the very limited number of patients receiving CPIs, our understanding of the global effect of CPIs on non-T cell immune subsets is still in its infancy.

1.5 Macrophage modulation in cancer

A wide range of efforts have been made to enhance anti-tumour responses by modulating the behaviour of macrophages. These can be distinguished into 3 groups:

1) Skewing of monocyte/macrophage ***polarization***

2) Inhibition of macrophage ***migration*** to the TME

3) ***Depletion*** of monocyte/macrophage populations

Interest has been shown in a wide range of modulatory mechanisms with varying degrees of success. The most promising include granulocyte-macrophage colony-stimulating factor (GM-CSF), the chemokine (C-C motif) ligand 2 (CCL2)/ C-C chemokine receptor type 2 (CCR2) axis and the CSF1/CSF1 receptor (CSF1R) axis.

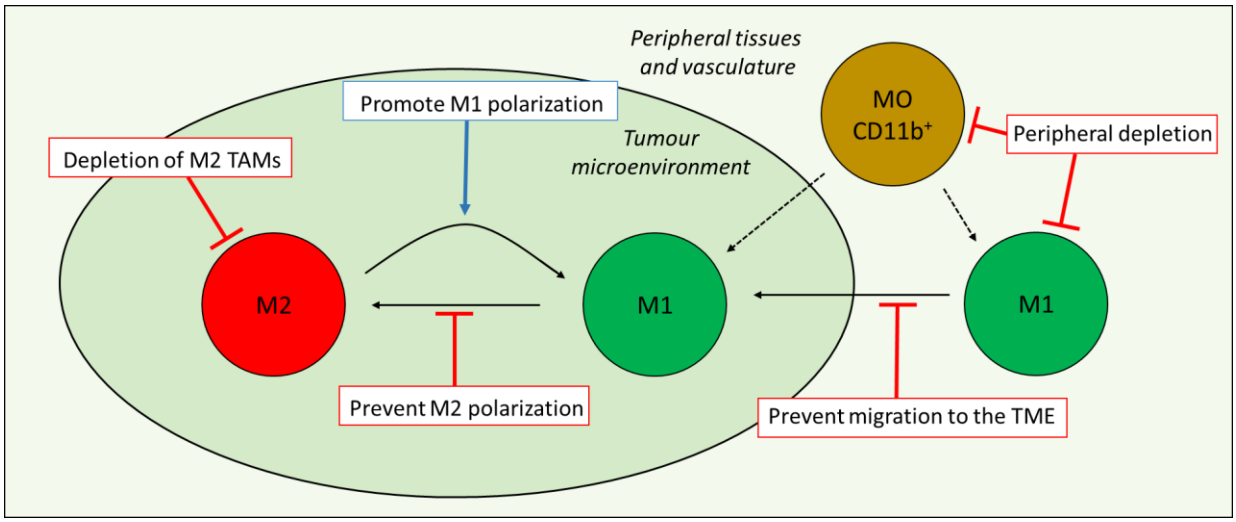

Figure 1.4 Mechanisms of macrophage targeting in cancer

Tumour associated macrophages are a negative prognostic marker in a range of cancer types and many attempts have been made to interfere with macrophage behaviour in the tumour microenvironment. Tumour-associated macrophages are readily trafficked to the tumour microenvironment, and are thought to have an unactivated or M1-like phenotype. Following recruitment to the tumour macrophages are polarized to an M2-like phenotype. Main mechanisms of treatment have focused at depleting intratumoural or peripheral macrophages, inhibiting the migration of macrophages to the TME, preventing M2 polarization or promoting M1 polarization.

1.5.1 Treatment with GM-CSF

GM-CSF promotes the expansion of granulocytes and monocytes, polarizes macrophages to an M1-like anti-tumour phenotype and can skew cells towards a type one phenotype capable of driving anti-tumour Th1 responses [117-121]. GM-CSF has been approved for the second line treatment of paediatric high-risk neuroblastoma in combination with Interleukin 2 (IL-2) and 13-cis-retinoic acid, and has been recommended for the amelioration of febrile neutropenia in solid and haematological malignancies by The American Society of Clinical Oncology [122].

There is currently a phase 2/3 trial in the recruitment phase examining the administration of recombinant GM-CSF, Bacillus Calmette–Guérin (BCG) and 4 lethally irradiated melanoma cell lines for the treatment of pre-malignant melanoma (NCT01729663).

Sipeleucel-T is a therapeutic vaccine approved for castration-resistant prostate cancer, composed of autologous peripheral blood mononuclear cells (PBMCs) cultured *ex vivo* with prostatic acid phosphatase-GM-CSF (PAP-GM-CSF) [123]. Despite gaining approval, it only modestly enhanced OS (25.8 vs 21.7 months) with no improvement in time to progression [124]. GVAX is a vaccine comprised of a patient's own cancer cells stimulated to secrete GM-CSF and then irradiated to prevent further proliferation [125]. GVAX has recently been given breakthrough designation for pancreatic cancer in combination with CRS-207, a listeria-based therapeutic vaccine, after positive phase 2 results [126]. Interestingly, GVAX has been shown to induce PD-L1 positive 'post-immunotherapy lymphoid aggregates' in murine models of pancreatic adenocarcinoma that may prime the tumour into an immunogenic state [127,128]. Building on that work the authors performed an early stage clinical trial with GVAX and Ipilimumab which showed clinical benefit [129]. These studies were performed before the approval of anti-PD-1 antibodies, and it is likely this combination will offer enhanced outcomes. A clinical trial is now recruiting (NCT02648282).

There have been fears surrounding the administration of GM-CSF due to observations of constitutive GM-CSF expression by advanced cancers [130]. GM-CSF can induce pleiotropic effects depending on its concentration and receptor, including differing effects on survival and proliferation [131]. Tumour cells can utilize GM-CSF in an autocrine or paracrine mechanism to stimulate growth and proliferation [132,133].

1.5.2 Interference with the CCL2/CCR2 axis

1.5.2.1 Rationale for the modulation of the CCL2/CCR2 axis

CCR2 is a chemokine receptor present on inflammatory monocytes that it is required for mobilization from the bone marrow and recruitment to the TME [134]. Tumours can upregulate CCL2 expression, its cognate ligand, from both tumour cells and stromal cells resulting in an upregulation of $CCR2^{+}$ inflammatory monocytes and matrix metallopeptidase 9^{+} (MMP-9) neutrophil infiltration [135-142].

CCL2 has been shown to increase the survival of PBMCs and clearance of apoptotic cells which may be beneficial in an anti-tumour context, however CCL2 also drives M2 polarization suggesting it is more likely to play a negative role in cancer patients [143,144]. Inhibition of the CCL2/CCR2 pathway has been shown to potently inhibit the development of metastasis in murine models of hepatocellular carcinoma, breast and prostate cancer [145-148]. Murine models of pancreatic ductal adenocarcinoma (PDAC) have shown that CCR2 inhibitors can induce a 3-fold reduction in tumour burden [149].

Both chemotherapies and radiotherapy have been shown to upregulate CCL2 production by tumour cells and stromal cells [150,151]. Addition of anti-CCL2 antibodies is additive with chemotherapy in models of ovarian and prostate cancer, and with radiotherapy in models of PDAC [152,153,147,154].

1.5.2.2 Prognostic significance of CCL2 and CCR2

CCL2 expression has been linked to cancer progression in hepatocellular carcinoma, prostate cancer, colorectal cancer, breast cancer and gastric cancer and has been shown to promote the induction of tumour growth, tumour cell migration, neovascularization and metastasis [155-159,137,160-166,146,141]. Prognostically, high CCL2 in combination with (Vascular endothelial growth factor) VEGF in tumour conditioned media has been shown to increase the chance of early relapse in breast cancer [167]. High intratumoural CCL2 expression is related to a lower 5-year survival (5YS) in gastric cancer [168]. Intratumoural expression of both CCL2 and CCR2 are associated with a lower OS and increased risk of recurrence in non-metastatic clear-cell renal cell carcinoma [169].

1.5.2.3 Clinical modulation of the CCL2/CCR2 axis

Clinical inhibition of CCL2 initially failed to generate significant effects. Carlumab, a monoclonal antibody against CCL2, was found to be safe and tolerable in patients but reduction in free CCL2 was short lived and failed to achieve an objective response in solid tumours (NCT01204996) [170,171]. MLN1202, a similar antibody, was trialled in patients with bone metastasis from solid tumours, and resulted in reduced urinary N-telopeptide (uNTX) levels but with minimal therapeutic success [172]. Further to the poor therapeutic responses, in murine models a bounce back effect in CCL2 levels was observed in which levels quickly returned to baseline or higher than pre-treatment levels resulting in accelerated death [173].

An orally active CCR2 antagonist PF-04136309, has been shown to reduce growth of PDAC and enhance survival. Phase 1b trials with the chemotherapy regime FOLFIRINOX (folinic acid, fluorouracil, irinotecan and oxaliplatin) have shown that it is safe, tolerable, and enhances survival [174]. Levels of peripheral circulating monocytes are inversely related to survival in pancreatic cancer [149]. Systemic CCR2 inhibition inhibits the mobilization of inflammatory monocytes from the bone marrow, consequently lowering monocyte infiltration to the TME. Preclinical models suggest the results in PDAC may translate into other tumour types, however the unique TME of PDAC, with high innate immune cell infiltration and T cell immune privilege, must be considered unique so recapitulation of the results in other tumour types is uncertain [175,176].

$CCR2^{+}$ macrophages suppress the infiltration of matrix $MMP\text{-}9^{+}$ neutrophils to the TME [177]. In murine models of cervical cancer, when macrophages are depleted in the TME, protumourigenic neutrophils are recruited. Consequently, no major difference in tumour incidence or tumour burden is seen between CCR2 null and wild type mice, with only a small delay from dysplasia to carcinoma being noted [178]. It is possible that this compensatory influx of neutrophils may be inhibited by the dense desmoplastic in pancreatic cancer, indicating the therapeutic benefit of PF-04136309 may be restricted to pancreatic cancer.

1.5.3 Interference with the CSF1/CSF1R axis

1.5.3.1 Rationale for modulation of the CSF1/CSF1R axis

CSF1 is a secreted cytokine that binds CSF1R on cells and which can control the production, migration, function and differentiation of macrophages [179]. CSF1R is predominantly expressed on myeloid cells of the monocyte-macrophage lineage and its inhibition has been used in various preclinical models for local macrophage/monocyte depletion [180-182]. CSF1R mediated depletion has been shown to increase the efficacy of chemotherapy, radiotherapy, angiogenic inhibitors, and CPIs [72,183,92,184,185]. In addition to enhancing monocyte migration, CSF1 binding has been shown to promote the development of M2-like macrophages [186,187].

Targeting CSF1R has the added advantage of being highly expressed on potently immunosuppressive MDSCs and can inhibit the migration of both macrophages and monocytic MDSCs to the TME [119, 120]. Along with M2-like macrophages, MDSCs secrete high levels of indolamine 2,3-dioxygenase (IDO) and have been implicated in resistance to CPIs and rapid outgrowth of B16 cell line tumours [119].

Unlike GM-CSF which results in upregulation of PD-L1 expression on immune infiltrates, inhibition of CSF1 signalling appears to upregulate CTLA-4 on tumour infiltrating $CD8^+$ T cells in addition to enhancing PD-L1 expression on macrophages and tumour cells, but with a concomitant decrease in PD-1 expression by monocytes and macrophages [185]. Inhibition of signalling by CSF1R on macrophages has been shown to enhance antigen presentation and T cell effector functions. Combination with CPIs was shown to induce tumour regression in murine models of PDAC [185].

While CCL2:CCR2 inhibitors can inhibit the mobilization of monocytes from the bone marrow and may result in a build-up of potentially pro-tumour cells elsewhere, anti-CSF1R antibodies deplete macrophages. There has been evidence that CSF1/CSF1R inhibition can increase metastasis in breast cancer via a compensatory increase in expression of granulocyte-colony stimulating factor (G-CSF), however this has not been seen in other tumour models [188].

1.5.3.2 Prognostic significance of CSF1 and CSF1R

CSF1R overexpression is associated with a negative prognosis in breast cancer patients [189]. In murine models, CSF1R overexpression is associated with reduced survival in endometrial, hepatocellular and colorectal cancer and targeting of both CSF1 and CSF1R have been shown to increase survival [190].

1.5.3.3 Clinical modulation of the CSF1/CSF1R axis

There are a range of anti-CSF1R antibodies currently in clinical trials designed to generate ADCC of tumour cells over expressing CSF1R and TAM depletion (**Table 1.3**).

CSF1R is a member of the KIT family of tyrosine kinases. Imatinib Mesylate can act as a tyrosine kinase inhibitor to these kinases. A trial using Imatinib in KIT^{+} patients showed clear clinical efficacy with 20/27 achieving stable disease, 1 complete response and 4 partial responses. Because of the promiscuity of Imatinib, toxicities due to off target effects were significant with 1 in 4 discontinuing treatment due to intolerable adverse events (AEs). [191-194].

There have been efforts to design tyrosine kinase inhibitors that target CSF1R, but they have lacked specificity to CSF1R and induced intolerable side effects unrelated to macrophage behavior [195]. A novel compound, DCC-3014, displays remarkable specificity and was due to be used in a First-In-Human trial by the end of 2016 but is yet to commence [196].

While the efficacy of CSF1R inhibitors has not yet led to their clinical approval, effective depletion of TAM numbers has been a positive development which may effectively compliment other therapies.

Table 1.3 Clinical trials involving CSF1R inhibitors

Name	Type	Cancer	Combination	Result	Reference
IMC-CS4 (Eli Lilly)	Fully human IgG1 mAb CSF1R	Breast	Monotherapy	Phase 1 ongoing	NCT02265536
		Prostate	Monotherapy	Phase 1 ongoing	NCT01346358
		Advanced solid tumours	Anti-PD-L1 or Anti-CTLA-4 Ab	Phase 1 ongoing	NCT02718911
AMG 820 (Amgen)	Fully human IgG1 mAb CSF1R	Advanced solid tumours	Monotherapy	Phase 1 completed (tolerable, 38% stable disease	NCT01444404
		Pancreatic, Colorectal, NSCLC	Anti-PD-1 Ab	Phase 1b/2 recruiting	NCT02713529
RG7155 (Roche)	humanized IgG1 mAb CSF1R	Advanced Solid Tumours	Monotherapy	Phase 1 ongoing	NCT01494688
			Anti-CD40 Ab	Phase 1 ongoing	NCT02760797
			Anti-PD-L1 Ab	Phase 1 ongoing	NCT02323191
		Diffuse-type Giant Cell	Monotherapy	Phase 1 (74% objective response)	[197]
PLX3397 (Plexxikon)	Oral small molecule inhibitor of CSF1R and other KIT kinases	Glioblastoma	Monotherapy	No efficacy	[198]
		Breast	Monotherapy	No efficacy	I-SPY-2 trial NCT01042379
		Advanced solid tumours	Monotherapy	Phase 1/2 ongoing	NCT02584647 NCT02071940 NCT02975700 NCT01499043 NCT01004861
		Advanced haematological malignancies	Monotherapy	Phase 1/2 ongoing	NCT01349049 NCT02390752
		Tenosynovial Giant Cell Tumours	Monotherapy	Phase 3 ongoing	NCT02371369

		Hodgkin Lymphoma	Monotherapy	Tolerable, limited efficacy	[199]
		Advanced Solid Tumours	Anti-PD-1 Ab	Phase1/2a ongoing	NCT02452424
		Pancreatic or Colorectal Cancers	Anti-PD-L1 Ab	Phase 1 ongoing	NCT02777710
		GIST	c-Kit inhibitor	Phase 1b ongoing	NCT02401815
		Malignant Peripheral Nerve Sheath Tumours	mTOR inhibitor	Phase 1 ongoing	NCT02584647
		V600E mutated melanoma	BRAF inhibitor	Phase 1b ongoing	NCT01826448
		Glioblastoma and prostate cancer	Radiotherapy	Phase 1b/2 ongoing	NCT01790503 NCT02472275
		Breast cancer and advanced solid tumours	Chemotherapy	Phase 1b ongoing	NCT01596751 NCT01525602
PLX7486 (Plexxikon)	Tyrosine kinase inhibitor of CSF1R and TrkA/B/C,	Advanced solid tumours	Monotherapy	Phase 1 ongoing	NCT01804530
FPA008 (FivePrime)	Humanized mAb CSF1R	Tenosynovial Giant Cell Tumours	Monotherapy	Phase 1/2 Ongoing	NCT02471716
		Selected advanced solid tumours	Nivolumab	Phase 1a/b	NCT02526017

A full list of clinical candidates targeting CSF1R for the prevention of malignancies in registered clinical trials. The company, drug format, treatment regimen, stage of clinical trial and clinical trial identifier codes are shown. Mammalian target of rapamycin (mTOR)

1.5.4 Combinations with T cell checkpoint inhibitors

Progress has not been aided by a relative under characterization of macrophage behaviour during the administration of current immunotherapeutics and analysis of how they may impact response. This is more striking when considering the central role monocytes and macrophages play in shaping the immune response [200]. There has been limited publication of the relationship between response to CPIs and myeloid cells, but the level of immunological interrogation of patients focusing on myeloid subsets is not clear.

Ipilimumab (10mg/kg) has been successfully trialed with subcutaneous recombinant GM-SCF in metastatic melanoma with an enhanced OS of 17.5 vs 12.7 months, and was better tolerated than Ipilimumab alone [201]. The mechanism resulting in reduced toxicities is not known, however there was no difference in the objective response rate and no significant change in PFS. There is currently a phase 2/3 clinical trial examining the combination of Nivolumab and Ipilimumab with or without GM-CSF in unresectable melanoma (NCT02339571).

Positive results of clinical trials examining macrophage modulation will intuitively result in future trials combining them with CPIs. Some of these combinational approaches are entering early stage clinical trials, but there have also been a number of trials which have indirectly combined CPIs with macrophage modulation and seen positive results.

Trabectedin is a drug approved for soft tissue sarcoma that binds the minor groove on deoxyribonucleic acid (DNA) resulting in a poorly characterized DNA damage in all cells, but critical to its anti-tumour efficacy is its ability to selectively induce apoptosis in monocytes and macrophages, reduce recruitment of $CD68^{+}$ monocytes to the TME and reduce CCL2 and Interleukin 8 (IL-8) levels [202-204]. Trabectedin has been shown to be synergistic with anti-PD-1 antibodies in murine models of ovarian cancer with the generation of systemic anti-tumour immunity [205]. It has been approved for the treatment of soft tissue sarcoma under the trade name Yondelis, and is currently in clinical trials for use in breast, prostate and paediatric sarcomas. The prolonged period of treatment required to see an effect on macrophage populations makes it unlikely to exert an observable effect in fast growing or late stage tumours.

MGN1703, a DNA-based toll-like receptor (TLR) agonist is being trialled in advanced solid malignancies with Ipilimumab (NCT02668770). Similarly, IMO-2125, a synthetic TLR-9 agonist which is expressed by plasmacytoid DCs but also to a lesser extent by monocytes and macrophages, is being trialled in combination with Ipilimumab in patients with metastatic melanoma (NCT02644967). If successful data emerges from these trials it will increasingly turn focus towards the role of innate immune system in response to CPIs [206].

Data emerging from the phase 3 clinical trial KEYNOTE-252/ECHO-301 suggests that Epacadostat, an IDO inhibitor, in combination with Pembrolizumab can improve outcome for stage III/IV unresectable or metastatic melanoma patients. IDO is primarily secreted by M2 macrophages but can also be produced directly by tumour cells in cancer patients. A phase 3 trial is currently recruiting 600 patients to further test this combination (NCT02752074).

1.6 Challenges of macrophage modulation

Side effects associated with CPIs are dose dependant (**Table 1.4**), it appears they are also cumulative to the cycles received and additive with other CPIs [207,11,12,14]. The most recent evidence to emerge from CheckMate 067 examining Ipilimumab and Nivolumab in advanced melanoma, has suggested the side effects are not cumulative but remain high with 58% of patients experiencing grade 3 or 4 AEs. Intuitively this has led to a shift in therapeutic design, which has been predominantly focused on engineering or stimulating T cells *ex vivo*. However, it is uncertain if these cells will be able to overcome the immunosuppressive environment that acts to 'turn off' these cells after readministration.

Table 1.4 Incidence of immune related AEs (irAE) seen in patients receiving Ipilimumab

	0.3 mg/kg	**3 mg/kg**	**10 mg/kg**
Incidence irAEs	26%	56%	70%
Incidence grade ¾ irAEs	0%	7%	25%
Incidence of drug discontinuation due AEs	13%	10%	27%

Numbers taken from [148].

The most notable and promising examples of successful macrophage modulation have been found in murine models on PDAC and these are now beginning to show efficacy in the clinical setting, but the unique composition of the pancreatic cancer TME may not accurately reflect the potential of macrophage modulation in other tumour types. It is hypothesized that the success seen may be due to the restricted flow of cells into and out of the microenvironment resulting in a reduced ability to compensate for a loss of macrophage function and consequent tumour inhibition [208]. It however appears likely that macrophage modulating therapies will compliment CPIs, and it will be of keen interest to see if the reduced AEs seen with GM-CSF and Ipilimumab will be seen with other therapies designed to reduce immunosuppressive factors in the TME.

While some have been quick to suggest that the ability to understand and direct macrophage behaviour represents an immunotherapy breakthrough it is clear from recent clinical evaluation that manipulation of macrophages as a stand-alone therapy in its current state is insufficient for therapeutic success [209]. However, it appears macrophage depletion may be a more effective strategy than macrophage re-education due to the profound immunosuppressive force exerted by advanced tumours [210].

In addition to the combination of macrophage modulation and immunotherapies, there is significant scope and promise for their combination with other therapies. For example, the anti-tumour effect of serine/threonine-protein kinase B-Raf (BRAF) inhibitors was noted to be reliant on host tumour-directed immune responses [211]. 50% of advanced melanomas are BRAF positive and initially respond to therapy, but tumours develop mechanisms of acquired resistance and become refractory [212]. In preliminary studies, inhibiting monocyte and MDSC influx to the TME synergistically enhanced the effect of BRAF inhibition [213,214]. There is mounting preclinical evidence to justify the use of macrophage modulating therapies with BRAF inhibitors in advanced melanoma.

Preclinical data in murine models has shown that the effect of immunotherapy in mouse models is more effective in the early stages of disease progression, which is generally defined by a low concentration of immunosuppressive elements in the TME [215-217]. While the reversal of this immunosuppression may restore sensitivity, delineation of the primary immunosuppressive factors responsible for the reduction in efficacy is difficult due to the plethora of interacting factors and systems in the TME. Significant literature is available on many factors, but their relative importance in determining sensitivity to therapy has not been fully elucidated. The clinical prognostic evidence on immunosuppressive factors in patients undergoing treatment is limited, but do suggest that they are key to the development of systemic and durable anti-cancer responses [3,218-220].

The form of cell death induced by existing anti-cancer treatments has been of intense interest [221]. Evidence of immunogenic cell death may not only reveal underlying mechanisms of response but may leave patients more responsive to combination or subsequent treatments which also induce immunostimulatory mechanisms [222]. Therapies such as electrochemotherapy (ECT), which involve the local delivery of

electrical pulses to tumour tissue, termed electroporation (EP), which are optimised to reversibly induce pores in the cell membrane, have been shown to induce an immunogenic form of cell death [223]. Using ECT the cells display enhanced uptake of chemotherapeutic which can allow a reduced dose of chemotherapy to be administered while retaining efficacy [224]. This may give treatment dual roles in increasing the immunogenicity of treatment, by supplying an ablative and immunogenic form of cell death with the reduction of immunosuppressive chemotherapeutics. Furthermore, recent clinical trials have substituted chemotherapy for calcium, which can retain the efficacy of treatment and may improve the immunogenic capacity of treatment. In line with this hypothesis, a case report has shown that an advanced melanoma patient given both calcium EP and ECT underwent a systemic and durable anti-cancer response [225]. As these effects have not been seen with ECT alone, it is hypothesized that the increased immunogenicity of calcium EP is responsible for the response seen. These effects have not been recapitulated in other patients treated, but may indicate that treatment is lowering the level of immunosuppression within the TME. Understanding the mechanisms involved will allow us to understand if macrophages play a role in this response or if macrophage targeting therapies can complement these effects.

Targeting of macrophages has been shown to profoundly shape the immune response and we now have a range of sophisticated therapeutics that are beginning to make impacts in the clinic. Rational design of immunotherapeutics that will increase their efficacy, response rates and generate systemic and durable response rates will require a holistic mind-set towards understanding the immune system. Given the central role that macrophages play in shaping the immune response they will play an integral role in immunotherapeutic design.

1.7 Current outlooks in melanoma

Cutaneous malignant melanoma is a form of skin cancer which affects approximately 20 people in every 100,000 per annum in caucasian populations, with a lifetime risk of 1 in 70 [226]. While incidence rates are rising globally due increased diagnosis rates as a result of screening and awareness, it is believed true incidence rates are also rising due to changing lifestyle habits resulting in increased exposure to the sun [227]. Incidence rates are higher in men and typically highest in countries in which ultraviolet light is highest, such as New Zealand and Australia [226]. Melanoma arises from the malignant transformation of pigment-containing cells known as melanocytes, which can penetrate into the subcutaneous fat and spread throughout the body. Melanomas commonly harbour mutations such as BRAF and Ras mutations but over 200 somatic driver mutations have been identified [228]. Many melanomas are frequently reported to arise from suspicious nevi, which have recently grown or changed phenotypically [229]. These pre-malignant nevi commonly harbour NRAS mutations [230].

Localized disease can be effectively treated with a wide local excision. 5-year survival for localized disease is over 95%, however for advanced disease survival rates can drop as low as 20% [231]. Survival rates for advanced melanoma are currently difficult estimate due to a spate of revolutionary drugs which have been approved in the last 8 years, but 5-year survival rates approaching 40% have been reported in some trials [232].

New treatments have relied on the discovery of specific BRAF mutations that are present in approximately 50% of advanced melanoma and can be effectively targeted along with the development of a range of immunotherapies [233]. There remains a high number of melanoma patients who fail to respond to therapy and prediction of responders from non-responders is currently poorly distinguishable [234]. Recent efforts are focused around the identification of novel targets and understanding the biology of response, of which require a holistic and comprehensive understanding of clinical disease [235,236].

1.8 Role of macrophages in melanoma

Melanoma has been characterized as an immunologically "hot" tumour to reflect the relatively high level of intratumoural immune cells and ability of tumour antigens to drive specific T cell responses [237,238]. The first T cell check point inhibitor to be approved, Ipilimumab, was first approved for use in metastatic melanoma, and since then other immunotherapies have been licenced for use in melanoma [8,9,239]. These therapies rely on the activation of T cell responses, however an oncolytic virus encoding GM-CSF was also approved for melanoma, which relies on myeloid cell activation to drive T cell responses [240,241]. While there has been much success, the factors determining response to these therapies are still poorly understood.

In patients receiving Ipilimumab, low circulating absolute monocyte counts and MDSCs but high levels of circulating non-classical monocytes and high intratumoural $CD163^+$ macrophage counts were associated with improved outcome [108,112]. Pre-treatment intratumoural $PD\text{-}1^+$ and $PD\text{-}L1^+$ along with $CD8^+$ T cells are all independent indicators of response to PD-1 inhibitors but cannot fully predict responders [115]. PD-1 and PD-L1 are expressed on tumour cells but also on tumour infiltrating macrophages [114]. In comparison to Ipilimumab which has an IgG1 subtype, the two anti-PD-1s approved for use in melanoma have Immunoglobulin type G subclass 4 (IgG4) design [242]. IgG4 is a poor inducer of effector immune responses by Fc binding, thus its main mechanism of action is thought to be the inhibition of signalling through the inhibitory receptor PD-1 [107]. $PD\text{-}1^+$ macrophages may act as a competitive inhibitor of anti-PD-1 inhibitors, but direct ADCC or effector functions are less likely to contribute to therapeutic response.

Melanomas are known to secrete immunosuppressive chemoattractants for macrophages such as transforming growth factor β (TGF- β), IL10, VEGFA, and VEGFC [243]. Macrophages are absent from some melanomas but have also been documented to represent up to 13% of total immune cell infiltrate, or up to 30% of the tumour mass in melanoma [244,245]. While much is understood of the role of macrophages in tumours, the specific understanding of their role in melanoma is poorly understood [246]. There is conflicting evidence on the prognostic significance of macrophage infiltration in melanoma [247,42,248-251]. Macrophages and DCs are critical linkers of innate and adaptive immunity in melanoma [252]. Macrophages

have been implicated in the development of acquired resistance to BRAF inhibitors, and other clinical indications have also suggested a physiological role, such as the increased response rate following addition of GM-CSF to an autologous melanoma vaccine [213,214,253]. In comparison to tumour infiltrating lymphocytes, which have been successfully targeted and are independent predictors of survival, the role of macrophages in melanoma appears to be more complex [254-256]. Clinical research on melanoma is impeded in comparison to other tumour types by low levels of fresh tissue availability. Many studies are restricted to metastatic tumour tissue or tissue from mucosal, acral cutaneous or uveal melanomas which are larger in size [257]. As a result, research on melanoma is predominantly derived from murine or *in vitro* studies.

Previous studies have shown that lymphocytic distribution and melanoma subtype can impact intratumoural macrophage polarization [258].

1.9 Challenges in the study of macrophages

1.9.1 Discrepancy between murine and human macrophages

Unlike T cells which display remarkable similarities between murine and human subsets, the interspecies variations between myeloid cells are more pronounced [259-262]. Differences between human monocytes and macrophages and their murine counterparts is particularly striking, with differences in cell surface markers, gene expression and functional activity [263]. Macrophage polarization of inflammation-like and wound repair-like phenotypes are conserved among evolutionarily diverse species, with relatively modest differences between human and murine cells, however these differences are significant when considered in the translation of treatment efficacy and must be taken into special account when considering the translation of research from murine to human models [264-266].

1.9.2 Factors influencing macrophage behaviour

Macrophage function is determined by a complex network of epigenetic and transcriptional regulation. As described in a seminal review by De Nardo and Ruffell (2019), 3 distinct factors determine macrophage phenotype and function, including the cells developmental origin, its tissue of residence, and the specific environmental stimuli [267]. These factors can affect the epigenetic state of an individual macrophage and act to determine the nature of response to a specific stimuli [268,269,262,270]. Thus two macrophages may respond differently to the same stimuli based on these criteria, and populations of macrophages are a heterogeneous group of discrete and individual cells. The phenotype of macrophages appear to be highly plastic, even among tissue resident macrophages. Macrophages have been shown to rapidly lose their specific phenotype following removal from their microenvironment, while both monocyte-derived macrophages, and tissue resident macrophages have been shown to change their transcriptional profile to match the new tissue specific macrophage prolife when transplanted into a distant tissue [271,272]. Specific transcription factors have been identified in the differentiation of specific macrophage subsets, such as Sal-like protein 1 (SALL1) and myocyte-specific enhancer factor 2C (MEF2C) for microglia[273]. While these transcription factors contribute to phenotype they are additive with other factors such as underlying epigenetics and environmental stimuli [271].

In addition to the ontology of macrophages, many stimuli which macrophages are exposed to leave a form of immunological memory. The term trained immunity has been used to describe the apparent non-specific immunological memory of the innate immune system [274]. Specific epigenetic markers have been documented in macrophages in response to specific stimuli that prime the cell for future responses [275,276]. The concept of trained immunity aligns with our current understanding of epigenetics to highlight the importance of cell ontogeny and the sum of previous and current stimuli in understanding macrophage behaviour. Studies have indicated that trained immunity can be detected in monocytes a year following vaccination with BCG [277]. It is currently unclear how the effects can last beyond the lifespan of individually affected monocytes and macrophages but is likely to be a reflection of the system wide effect of trained immunity on multiple branches of the immune system, including the adaptive immune response [278].

1.9.3 *In vitro* models of macrophage study

There are many models available for *in vitro* investigation of murine monocytes. Numerous cell lines exist, such as RAW 264.7 cells, however while these cells are a stable model of macrophage-like cells, they offer limited translational scope [279]. More physiologically representative models include the isolation of peritoneal macrophages from sacrificed animals or the development of bone marrow-derived macrophages from murine bone marrow [280,281]. Peritoneal macrophages are preferred for the study of tissue-resident macrophages, while bone-marrow derived monocytes (BMDMs) are used to study monocyte derived macrophages [282]. Within these systems there is significant heterogeneity in preparation methods and protocols which can ultimately affect their responsiveness [283-285]. Additionally *in vitro* cell culture of microglia, a specialized form of macrophage, has been shown to induce rapid and extensive down-regulation of microglia-specific genes following resection of brain tissue, indicating that all forms of cell culture may inhibit the recapitulation of true physiological behaviour [272].

1.9.4 The murine melanoma cell line, B16-F10

There are a limited number of highly cited cell lines representative of melanoma. A375 and SK-MEL derivatives are there most common human cell lines each with over 1000 separate Pubmed citations [286,287]. Murine cell lines are represented by the highly cited B16 derived cell lines, and the recently developed Yale University Mouse Melanoma (YUMM) cell lines, both of which are syngeneic with C57BL6 mice [288,289]. The B16 cell lines were initially differentiated into B16F1 to B16F10 derivatives which varied on their *in vivo* aggressiveness, with B16F10 the most aggressive. The B16F10 cell line was selected based on its ability to colonize the lung and it predominantly and quickly colonizes the liver and lung [290,291]. The B16F10 cell line has a number of potential immunogenic antigens but is poorly immunogenic *in vivo* [292,293]. The cell line is commonly transfected with ovalbumin to encourage antigen specific CD8+ T cell responses [294]. *In vitro* the cells have a doubling time of approximately 17hrs and readily secrete cytokines, including TNF-α, IL-1β, IL-6, and TGF-β, and exosomes which have discrete immunological profiles from the parenteral cells [295,296]. The B16F10 cell line does not contain any activating BRAF mutations, however some groups have modified the cell line to express the V600E mutation found in many human cancers [297].

1.9.5 Translation of research

Much of the available literature on macrophages has been developed on the inference that *in vitro* studies can be used to approximate true physiological behaviour. While significant progress has been made in the study of immunology based on *in vitro* observations, it is becoming increasingly accepted that such a format has limited applicability in the study of macrophages, which is ultimately reflected by the failure of all therapeutic interventions targeting macrophages in cancer discussed here [24,267]. In order to improve the translational value of macrophage research it is necessary to consider the specific research question, and perform research on macrophage populations which adequately reflect *in vivo* subsets, with the aim of minimizing potential epigenetic and functional differences between cell populations [298]. In this thesis, we present a step wise process for the optimal study of macrophages. It is currently unclear if macrophages exert a physiological role in

clinical disease and but we hypothesize that macrophages may be play a role in promoting T cell responses in melanoma. In chapter 3, we identify the presence and physiological activity of TAMs in human disease. In chapter 4, we present a concept to bench approach for the rational development of appropriate BMDMs. And in chapter 5, we build on this to utilize the *in vitro* model to study the potential effect of calcium electroporation on intratumoural macrophages during the treatment of melanoma.

1.10 Aims of thesis

This thesis had three specific aims;

1. To evaluate the presence and phenotype of macrophages in human melanoma.
2. To determine the effect of tumour conditioning on circulating monocytes
3. To determine the effect of calcium electroporation on the immunogenic capacity of TAMs.

Chapter 2

Materials and Methods

In this chapter we present an elongated form of the traditional materials and methods designed to provide complete description and clarity of all protocols and reagents used.

To ensure replicability of the presented methods and results, where multiple products of a given name are available from a specific supplier, and the specific reagent formulation, purity grade, or clone used, had a material impact on the results presented, such as in the case of antibodies, we have endeavoured to supply the name, supplier and where applicable, the clone of reagents used.

If following these definitions, there are multiple products which match the given criteria, we have supplied catalogue codes to the specific products used.

2.1 Ethical approval and ethical standards

Human studies were performed under ethical licencing from the Central Research Ethics Committee (CREC) of the Cork Research Hospital, with approvals ECM 4 (n) 17/10/17 and ECM 4 (m) 17/10/17. All patient information was anonymized and stored securely on encrypted hard drives.

Animal procedures were approved and licensed by the Animal Experimentation Ethics Committee (AEEC) in University College Cork under licence 2012-047 and performed according to the Irish Cruelty to Animals Act, 1876.

Animal husbandry and handling was performed according to the Directive 2010/63/EU. 61 mice were culled under a euthanasia-only licence, granted by the Animal Welfare Board of University College Cork, and was performed according to the Directive 2010/63/EU. Immediately following euthanasia, death was confirmed by observation of complete cervical dislocation.

2.2 Patient Cohort

Primary melanoma tumour blocks were randomly selected from BRAF tested tumours, for each tumour, a single block with a large area of both tumour and peritumoural tissue was selected. Patients were untreated prior to tumour excision. Pathological data and follow up data was obtained from patient charts. Tumour and cohort descriptions are provided (**Table 2.1**).

2.3 Immunohistochemistry

Primary melanoma tumours were formalin fixed and paraffin embedded by the Department of Pathology, Cork University Hospital. 3-5μm tissue sections were cut and mounted on Superfrost Plus™ slides (ThermoScientific). Slides were then dried at 37°C overnight. Slides were then kept at 4°C and stained within 1 month. Slides were incubated at 37°C overnight or at 60°C for 1hr to dry the slides and to enhance epitope retrieval.

Table 2.1 Pathological features of the tumours stained by immunohistochemistry

Patient Characteristics			
Characteristic		**No.**	**%**
Sex	Male	35	(61)
	Female	22	(39)
Age	Median	64 years	
	Range	18-85 years	
Subtype	Superficial spreading	20	(34)
	Nodular	19	(32)
	Acral lentiginous	7	(12)
	Lentigo maligna	6	(10)
	Desmoplastic	1	(2)
	Unknown	5	(8)
Primary location	Acral	11	(19)
	Head and neck	10	(18)
	Lower limb	15	(26)
	Upper limb	12	(21)
	Trunk	9	(26)
Breslow depth	<1mm	5	(8)
	1.01-2mm	7	(12)
	2.01-4mm	13	(22)
	>4.01mm	32	(54)
Stage	pT1a	2	(4)
	pT1b	3	(5)
	pT2a	7	(12)
	pT3a	8	(14)
	pT3b	4	(7)
	pT4a	5	(9)
	pT4b	28	(49)
Mitotic count	Median	6.5mm	
	Average	10.17mm	
	Range	0-51mm	
BRAF status	Positive	24	(42)
	Negative	33	(58)
Ulceration	Yes	33	(49)
	No	34	(51)
Tumour infiltrating lymphocytes	Absent	14	(24)
	Non-brisk	36	(63)
	Brisk	3	(5)
	Variable	2	(4)
	Unknown	2	(4)

Random primary melanoma tumours, screened for BRAF mutational status, were selected for analysis by immunohistochemistry. Patient and tumour descriptions are shown.

2.3.1 Manual IHC staining

Slides were washed in xylene (Ocon Chemicals) 3 times to remove wax and then placed in a decreasing alcohol (2-proponol, Merck) gradient of 90%, 90% and 70% in double distilled water (ddH_20) to rehydrate tissue sections. Slides were left in each solution for 2-3 minutes. Slides were then immersed in ddH_20 for at least 5min. For epitope retrieval, slides were placed in citrate buffer pH6 (1.92g/L anhydrous citric acid (Merck) in ddH_2O, adjusted to pH6 with HCl (Scharlau)) in a precise temperature control (PT) module for 20min at 95°C which was preheated to 65°C. Following epitope retrieval the slides were washed in ddH_20. Slides were placed in 3% H_2O_2 (Merck) in ddH_20 for 10min to quench endogenous peroxidase activity. A margin was drawn around the tissue with a 5mm hydrophobic pen (Merck). Slides were incubated in blocking solution (5% bovine serum albumin (BSA) (Merck) in phosphate buffered saline (PBS) (Merck)) for 1hr at room temperature (RT) in a humidified chamber. Blocking solution was washed from the slide with PBS and the slides were incubated in a 1 in 100 dilution of iNOS monoclonal antibody (**Table 2.2**) in blocking buffer for 60min at RT in a humidified chamber. The primary antibody was then washed from the slide with PBS and placed in 3 serial PBS washes for 5min each. Slides were then incubated at RT in a 1 in 1000 dilution of goat anti-rabbit alkaline phosphatase IgG heavy and light chain (H&L) secondary antibody (Abcam, ab97048) in blocking buffer for 30min. The secondary antibody was washed from the slide with PBS and then placed in 3 serial PBS washes for 5min each. Slides were covered in Liquid Fast-Red Substrate Kit (Abcam), briefly 1 drop of 75x Fast Red Chromogen was added to 3ml Liquid Fast Red Substrate (both supplied in Liquid Fast-Red Substrate Kit) within 15min of use and mixed well, this solution was then liberally added to cover the slide. Slides were incubated for 20-25min at RT in a humidified chamber. Fast red was washed from the slide with ddH_20 and the slides were left in ddH_20 for 5min. Slides were covered in Mayer's Haematoxylin (Merck) for 20-40sec. The slides were washed with ddH_20. Slides were dipped rapidly in Scott's Tap Water (Leica Biosystems) 6-10 times to blue the Mayer's Haematoxylin. Slides were coverslipped using aqueous mounting media (Vectamount).

2.3.2 Automated immunohistochemical staining

CD68, CD163 and arginase (Arg) staining (**Table 2.2**) was performed on an automated Benchmark Ultra system (Roche) using the UltraView Universal Alkaline Phosphatase Red Detection Kit (Roche) with the standard Ultraview protocol. Deparaffinization was performed with xylene, rehydration of tissue was performed with a decreasing concentration of alcohol. Antigen retrieval was performed in Cell Conditioning 1 solution (Ventana Medical Systems, Inc.) for 20min (Arg), 64min (CD163) or 20min (CD68), before addition of 1 drop of primary antibody for 60min (Arg) or 32min (CD163 and CD68). Slides were treated with the UltraView Universal Alkaline Phosphatase Red Detection Kit (Roche), counterstained in Haematoxylin II (Roche) for 4min, blued in Bluing Reagent (Roche) for 4min and cover slips were manually mounted in aqueous mounting medium (Vectamount).

All immunohistochemistry (IHC) slides were examined independently by two trained pathologists. The areas of highest staining were identified in peritumoural and intratumoural regions. Starting from this site, the number of positively stained cells were counted in 4 adjacent high powered fields, under a 40x magnification, which was equivalent to a total area of $1mm^2$. The number of positive cells between both pathologists was averaged to give a final value.

Due to a high number of specimens which were negative for $CD68^+$ and $iNOS^+$ cells in the tumoural and peritumoural tissue, CD68 and iNOS staining was stratified semi-quantitatively as positive (containing 1 or more positive cells) or negatively stained (no positive cells).

Table 2.2 Antibodies used for IHC analysis

Target	Clone	Supplier	Catalogue #
CD68	Kp-1	Cell Marque	168M
CD163	MRQ-26	Cell Marque	163M-18
Arginase	N/A	Atlas Antibodies	HPA003595
iNOS	SP126	Invitrogen	MA5-16422

Primary antibodies were used to stain specific targets in human FFPE primary melanoma tissues. Listed are the human specific antibodies used to identify macrophages and macrophage related enzymes, their clone, supplier and catalogue code required to source the antibodies used.

2.4 Gene expression analysis of human tissues

5μm serial sections were cut from primary melanoma formalin-fixed paraffin embedded (FFPE) blocks, which were previously selected for staining by IHC, and mounted on Superfrost Plus™ slides. The tumour margins were marked on a matched haematoxylin and eosin stain (H&E) by trained pathologists. HTG EdgeSeq technology was used with the oncology biomarker panel to perform gene expression. Cell lysis was performed on tumour tissue, as determined by the marked H&E, according to the manufacturer's instructions. All lysis and ribonucleic acid (RNA) sequencing was performed by Elda Biotech LTD under licence of HTG Molecular Diagnostics, Inc using proprietary protocols. In brief, nuclease protection probes and gene specific barcoded probes were added and complexed to lysed tissue by polymerase chain reaction (PCR). Individual probes were purified and the subsequent pooled library was run on Lumina next generation sequencing (NGS) technology [299].

24 samples were analysed along with 3 internal controls. 4 samples failed internal quality control analysis, as determined by comparison to internal controls and were omitted from all analyses. Pearson correlation values between internal controls were used to determine the acceptable variance within samples. Tumour and cohort descriptions are provided (**Table 2.3**) Normalized data on 2,550 oncology biomarker related genes was obtained from HTG EdgeSeq software and used for subsequent analyses.

Differentially expressed genes between groups were detected using the DESeq2 algorithm with adjusted *p* values. Heat maps were clustered using the Ward-Linkage method and generated using the Made4 package v.1.58 within the R environment. The full list of affected genes can be seen in **appendices 1-3**.

Table 2.3 Pathological features of the tumours selected for gene expression

Patient Characteristics			
Characteristic		**No.**	**%**
Sex	Male	13	(65)
	Female	7	(35)
Age	Median	70.5 years	
	Range	26-85 years	
Subtype	Superficial spreading	5	(25)
	Nodular	11	(55)
	Acral lentiginous	2	(10)
	Unknown	2	(10)
Primary location	Acral	4	(20)
	Head and neck	3	(15)
	Lower limb	5	(25)
	Upper limb	5	(25)
	Trunk	3	(15)
Breslow depth	<1mm	0	(0)
	1.01-2mm	1	(5)
	2.01-4mm	2	(10)
	>4.01mm	17	(85)
Stage	pT2a	1	(5)
	pT3a	3	(15)
	pT4b	16	(80)
Mitotic count	Median	12mm	
	Average	11.89mm	
	Range	0-30mm	
BRAF status	Positive	6	(30)
	Negative	14	(70)
Ulceration	Yes	15	(75)
	No	5	(25)
Tumour infiltrating lymphocytes	Absent	3	(15)
	Non-brisk	13	(65)
	Brisk	3	(15)
	Unknown	1	(5)

Random primary melanoma tumours, screened for BRAF mutational status, were selected for analysis by immunohistochemistry. 24 of these tumours were selected for gene expression analysis based on tumour tissue availability within the FFPE block. 4 failed internal quality control and were omitted from analysis. Above cohort descriptives characterizing both the patient and the melanoma of tumours which were successfully analysed for gene expression and presented in chapter 3.

2.5 B16F10 cell line maintenance

The B16F10 cell line is a highly aggressive murine melanoma cell line which readily metastasizes to the lung and liver when grown *in vivo*. The cell line was purchased from and authenticated by the Developmental Therapeutics Program, Division of Cancer Treatment and Diagnosis Tumor Repository (United States of America, USA) and maintained in Roswell Park Memorial Institute medium 1640 (RPMI-1640) (Merck; R8758) supplemented with 10% foetal calf serum (FCS) (Merck) and 50units/ml penicillin and 50µg/ml streptomycin (P/S) (Merck) [289]. Cell lines were

regularly tested for the presence of mycoplasma infection. This solution is referred to as complete RPMI (cRPMI). Cells were cultured at 37°C in a humidified chamber with 5% CO_2. To wash or pellet the cells, the cells were centrifuged at 200g. Cells were grown in tissue culture treated tissue culture flasks (Sarstedt) or tissue culture treated 6/12/24 or 96 well plates (Sarstedt).

To isolate cells the medium was decanted, the flasks/plates were rinsed in PBS and 1 volume of trypsin-ethylenediaminetetraacetic acid (EDTA) solution (Merck) was added to the cells. The cells were incubated at 37°C until the cells had detached (5-10min). The trypsin-EDTA solution was then quenched with 2 volumes of cRPMI.

2.6 Cell counting

A 200µL aliquot of cells were taken and added to 200µl solution A100 (Chemometec) and 200µl solution B (Chemometec). The solution was mixed well for 30sec to allow complete cell lysis and then added to a NucleoCassette™ (Chemometec). The cells were counted using a Mammalian Cell Counter NucleoCounter® NC-100™ (Chemometec).

2.7 *In vivo* B16F10 subcutaneous tumour model

The cells were counted and resuspended at $5x10^6$ cells/ml in serum and antibiotic free RPMI (Merck). Cells were kept at 37°C. 4-8 week old female C57BL6J mice (Envigo, UK) had their left flank shaved. 200µl of cell solution ($1x10^6$ cells) was injected into the left flank using a 26 gauge syringe [300]. Subcutaneous tumour volumes were monitored daily and measured using a Vernier callipers. Tumour volume measurements were calculated using the equation: volume= $ab^2\pi/6$. Where *a* is the largest diameter of the tumour and *b* is the greatest diameter of the tumour perpendicular to a.

2.8 Isolation of murine blood for flow cytometry

Blood samples were taken at different times during tumour growth, using volume as a measure of tumour development. Mice were anaesthetized with intraperitoneal delivery of ketamine (75mg/kg, Chanelle) and Medetomidine (1mg/kg, Chanelle) in PBS. 200µl 0.5M EDTA taken up by a 27 gauge syringe to prevent clotting. Blood was isolated by cardiac puncture. The blood was kept at room temperature and red blood cell (RBC) lysis was performed within 90min. The volume of RBC lysis buffer

added (155mM NH_4Cl (Merck), 12mM $NaHCO_3$ (Merck), 0.1mM EDTA) was greater than 10x the volume of blood obtained. RBC lysis buffer was left to incubate for 7min at RT with continuous agitation. The cells were then washed in fluorescence-activated cell sorting (FACS) buffer (2% FCS, 0.1% sodium azide (Merck) and 1mM EDTA in PBS). RBC lysis was repeated if RBC contamination was visible.

2.9 Development of BMDMs

Healthy 4-8 week old female C57BL6J were euthanized humanely by cervical dislocation. Tibia and femur bones were isolated. Muscle, cartilage and other material was removed from the bone. Bones were transferred to a laminar flow hood to maintain sterility and placed in 100% ethanol (Brenntag) for 90 seconds to sterilize the surface of the bones. The bones were then transferred to PBS. Both ends of the bone were removed using sterile scissors. The bone marrow was then flushed from the bone with RPMI supplemented for macrophages (mRPMI) (RPMI supplemented with 10% FCS, 1% P/S, 0.01mM β-mercaptoethanol (Merck), 1mM sodium pyruvate (Merck) and 1x Eagle's modified essential medium (MEM) non-essential amino acids (Merck)) using a 26 gauge syringe (Braun) and passed through a 70μm filter (BD Falcon) to obtain a single cell suspension. Cells were washed in mRPMI. All centrifugation of BMDM populations was performed at 270g for 7min. The cells were resuspended in 50ml RBC lysis buffer (155mM NH_4Cl, 12mM $NaHCO_3$, 0.1mM EDTA) at RT for 8min with continuous agitation. Cells were washed and resuspended in 10ml mRPMI. Cells were counted and resuspended at a concentration of $5x10^5$ cells/ml in mRPMI supplemented with 50ng/ml recombinant carrier free mouse Macrophage colony-stimulating factor (M-CSF, Biolegend) [301,285]. Cells were seeded in either 10cm bacteriological petri dishes (Sarstedt) with 10ml of cell solution added or in 35mm suspension dishes (Sarstedt) with 1.81ml of cell solution added. Cells were left undisturbed at 37°C in a humidified chamber with 5% CO_2 for 5 days unless otherwise specified.

2.10 Development of B16F10 conditioned media

To generate B16F10 conditioned medium (B16CM) $2x10^6$ B16F10 cells were seeded in 20ml RPMI supplemented with 2% FCS and 1% P/S. For no treatment controls (NTCM) 20ml of RPMI was supplemented with 2% FCS and 1% P/S with no cells added. Flasks were incubated for 48hrs at 37°C. Supernatants were isolated and

centrifuged to remove any cells or cellular debris. Supernatants were stored at 4-8°C for a maximum of 48hrs. Either B16F10 conditioned medium (B16CM) or No treatment concentrated medium (NTCM) was added to Vivaspin 20 ultracentrifugation tubes (GE Healthcare) with a molecular weight cut-off (MWCO) of 3,000Da and centrifuged at 8000g for 1-3hrs until was reduced to 0.5-0.8ml [302,303]. Ultracentrifugation with a MWCO filter of 3,000Da allowed the retention of all proteins greater than 6,000Da in size. Medium, including salts and other components under 6000Da in size can pass through the MWCO filter and into the lower chamber, while the remaining fluid containing components of 6000Da or larger was retained and concentrated in the upper chamber. B16CM and NTCM were used to treat BMDMs at a final concentration of 1x, as shown in **figure 2.1**.

2.11 Harvesting of BMDMs

Different methods were used to isolate cells and samples depending on the assays which were to be performed.

When cell viability was required, such as for reseeding cells or flow cytometry, the supernatant was isolated, and the dish was rinsed once in PBS, the PBS was retained along with the supernatant.

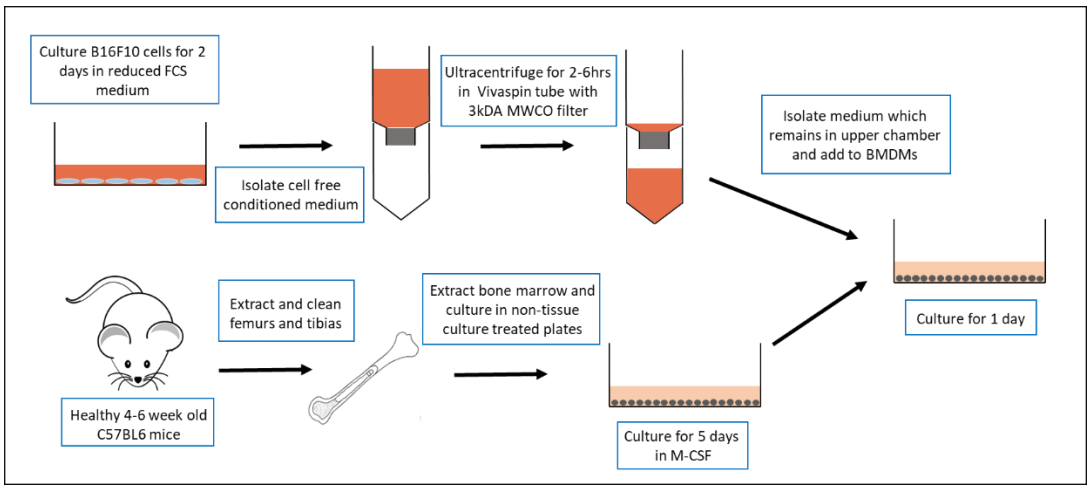

Figure 2.1 Protocol for the development of melanoma conditioned macrophages.
B16F10 cells were grown in RPMI with 2% FCS and 1% P/S for 48hrs. The supernatant was isolated and ultracentrifuged with a MWCO filter for 3kDa. Separately BMDMs were generated from the bone marrow of healthy 4-6 week old C57BL6J mice by culturing the cells in M-CSF. Following 5 days of culture melanoma conditioned media was added to the BMDMs for 24hrs.

Adherent cells were isolated by adding 5mM EDTA in PBS and incubating on ice for 5min. These cells were added to the suspension cells. Isolation of all cells from each dish was confirmed by light microscopy, and if necessary a further incubation in EDTA on ice was performed.

Where only supernatant was required, such as for Enzyme-linked immunosorbent assays (ELISA) or Griess assays, the supernatant was gently lifted from the dish minimizing agitation of cells. The supernatant was then washed at 500g for 5min to remove cells and cellular debris from the supernatant. Assays were performed immediately where possible or supernatant was stored at 4°C for up to 24hrs or at -20°C for up to 7 days.

When cell viability was not required, such as prior to analysis by quantitative polymerase chain reactions (qPCRs) or arginase assays, cells were isolated with a cell scraper to detach adherent cells. Cells were then washed twice in PBS before cell lysis in an assay dependent lysis buffer (specified in relevant protocols). Following cell lysis, a Bradford Assay (see below) was performed to normalize the protein concentration of cell lysates.

2.12 Flow cytometry

Cells were washed in FACS buffer and $1x10^6$ cells were transferred to FACS tubes (BD Biosciences). Cells were resuspended in 500µl blocking buffer (1 part FACS buffer to 1 part FCS) and incubated for 10min at RT. The cells were washed twice in FACS buffer. All flow cytometry wash steps are defined as the addition of 2ml of FACS buffer to each tube and centrifuging at cell type specific speed for 5min, after decanting the supernatant, the cells were vortexed to resuspend. Fluorescently conjugated antibodies (**Table 2.4**) were added to the cells (suspended in 100µl of FACS buffer remaining after discarding the rest of the FACS buffer). Where possible master mixes of antibodies were prepared in advance of use. Once antibodies were added, FACS tubes were kept in the dark. Cells were incubated at RT for 20-30min and washed twice.

Where granzyme B staining was required, surface markers were stained first. Cells were fixed in 2% paraformaldehyde for 20min. Cells were washed 3 times in

Intracellular staining permeabilisation wash buffer (Biolegend) and granzyme B-PE-Cy7 antibody was then added for 30min. Cells were washed twice in FACS buffer. Cells were resuspended in 200-500µl FACS buffer and read on a custom BD flow cytometer (**Table 2.5**).

Table 2.4 List of all antibodies used for flow cytometry experiments

Target (clone)	Conjugate	Isotype	Volume per $1x10^6$ cells (µl)	Supplier
CD11b (M1/70)	BV 605	Rat IgG2b,κ	0.75	BD Biosciences
Ly6C (HK1.4)	Pacific Blue	Rat IgG2c,κ	1	Biolegend
Ly6G (1A8)	FITC	Rat IgG2a,κ	1.5	BD Biosciences
CCR2 (475301)	APC	Rat IgG2b	2	R&D Biosystems
CD115 (AFS98)	PE-Cy7	Rat IgG2b,κ	1	Invitrogen
F4/80 (BM8)	PE	Rat IgG2a,κ	1	Biolegend
CD206 (C068C2)	PerCP/Cy5.5	Rat IgG2a, κ	1	Biolegend
Granzyme B (QA16A02)	PE-Cy7	Rat IgG1, κ	3	Biolegend
CD3 (C363.29B)	PE	Rat IgG2b, κ	1	Novusbio
CD4 (RM 4-5)	FITC	Rat IgG2a, κ	1	eBioscience
CD8 (53-6.7)	FITC	Rat IgG2a, κ	1	Biolegend
CXCR3 (CXCR3-173)	PE-Cy7	Armenian hamster IgG	1	eBioscience
CD25 (PC61.5)	APC	Rat IgG1, λ		eBioscience

Primary antibodies were used to identify specific protein targets in murine immune cells and murine bone marrow-derived cells by flow cytometry. Listed above are the targets of each antibody, the clone of the antibody, the fluorochrome to which the antibody was bound, the isotype of the antibody constant domain, the volume which was added to stain cells, and the suppliers of each antibody. C-X-C chemokine receptor type 3 (CXCR3), brilliant violet 605 (BV605), Fluorescein isothiocyanate (FITC), propidium iodide (PI), phycoerythrin (PE), phycoerythrin- cyanine7 (PE-Cy7), Peridinin-chlorophyll-protein complex (PerCP), Allophycocyanin (APC).

Compensation controls were performed on anti-rat anti-hamster Ig κ negative and positive CompBeads (BD biosciences). 1 drop of positive and negative beads were mixed and 1μl of each antibody was added to the relevant single stain control tube. Single stain controls were run for each new experiment and used to set up the compensation controls. Each single stain control was used to gate a true positive and negative signal for each fluorochrome. Successful compensation was confirmed with the use of fluorescence minus one control tubes, performed on cells. Isotype controls and unstained controls were run for every experiment. The same volume of isotype control antibody was added as of the corresponding antibody and the cells were incubated for the same length of time as the experimental tubes.

Results were analysed on FlowJo® software (version 10.5.0). Positive staining was determined by comparison to both unstained and isotype control antibodies. All experiments included an initial gate which excluded doublets by comparison of height and width of forward scatter (FSC) readings. Subsequently FSC and side scatter (SSC) low events were excluded from analysis to gate out non-cellular debris (**Figure 2.2**). Isotype controls and gating strategies for all flow cytometry graphs are shown (**Figures 2.3-2.9)**. Axes in flow cytometric graphs are 'logicle' scaled and not logarithmically scaled, except for forward and side scatter (FSC and SSC) which are linearly scaled.

Table 2.5 Lasers, filters, channels and fluorophores detected on a custom BD LSR flow cytometer used for all experiments.

Laser	Dichroic filter (nm)	Filter (nm)	Fluorophores detected
UV 355nm	505LP	525/50	
		450/50	
Violet 405nm	595LP	610/20	BV605
	505LP	525/50	
		450/50	Pacific Blue
Blue 488nm	505LP	525/50	FITC
	675LP	685/35	PI, PerCP/Cy5.5
Yellow/Green 561nm	755LP	780/60	PE-Cy7
	685LP	710/50	
	635LP	660/20	
	600LP	610/20	
		582/15	PE
Red 640nm	735LP	780/60	
	685LP	710/50	
		670/14	APC

A flow cytometer was used to identify specific populations of immune cells. The flow cytometer was a custom BD LSR flow cytometer in which the filters and channels were specifically chosen. Above is a list of the lasers, filters and channels used to identify the presence and level of antibody staining. *Long pass (LP), Brilliant violet 605 (BV605), Fluorescein isothiocyanate (FITC), propidium iodide (PI), phycoerythrin- (PE), phycoerythrin- cyanine7 (PE-Cy7), Peridinin-chlorophyll-protein complex (PerCP), Allophycocyanin (APC).

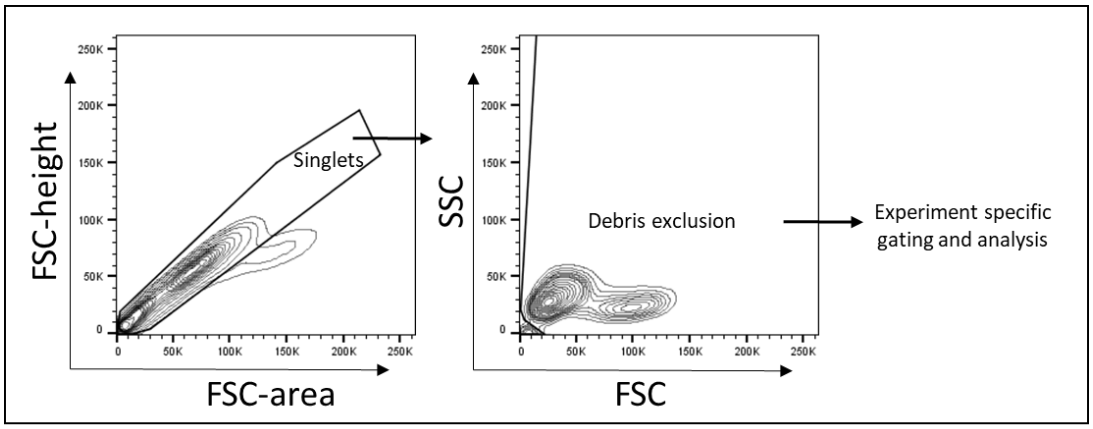

Figure 2.2 Exclusion of doublets and debris from flow cytometric data

Prior to flow cytometry analysis, singlets were gated by comparison of FSC-area and FSC-height as shown (left). Subsequently debris was excluded by gating all events except those with a near zero size and granularity (right).

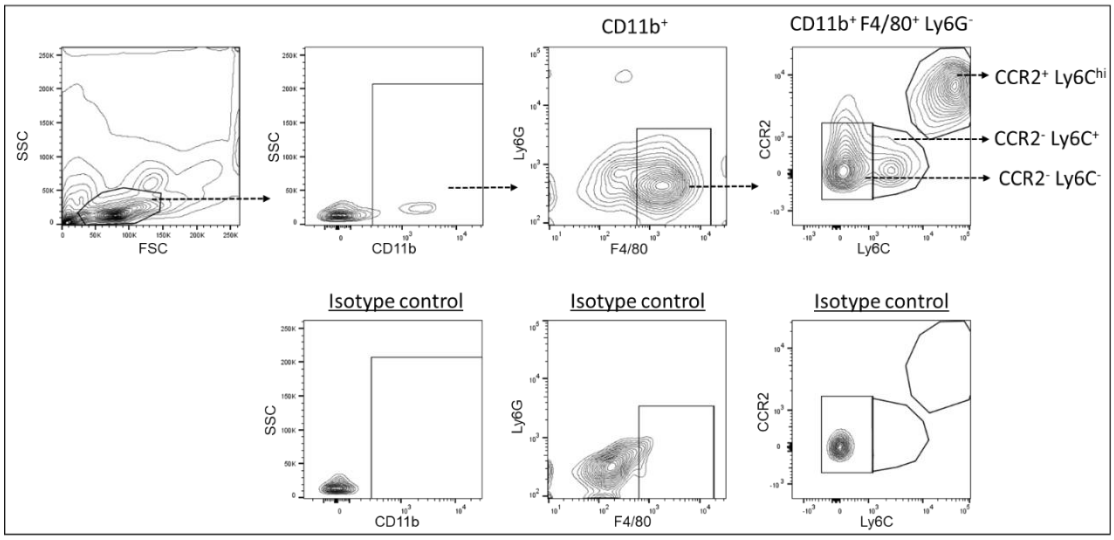

Figure 2.3 Gating of circulating monocyte populations

Flow cytometry graphs showing the gating strategy used to identify $CD11b^+$ $F4/80^+$ $Ly6G^-$ cells in peripheral murine blood and the subsequent stratification of these cells into $CCR2^+$ $Ly6C^{hi}$, $CCR2^-$ $Ly6C^+$ and $CCR2^-$ $Ly6C^-$ populations (top) as seen in **figure 4.1**. Also shown are the isotype controls used to determine positive staining (bottom).

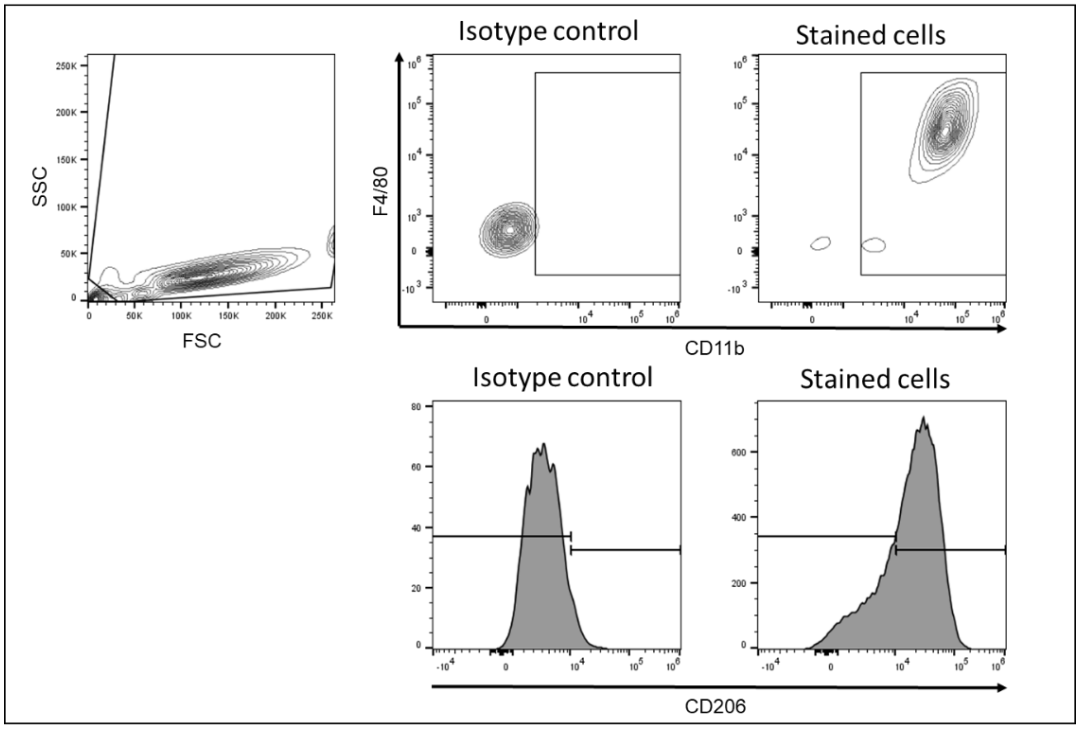

Figure 2.4 Gating of monocytic cells from BMDMs for CD206 analysis

Flow cytometry graphs showing the gating strategy used to identify $CD11b^+$ cells from treated BMDMs (top) and the gating strategy to identify $CD206^+$ cells (bottom) used in **figure 4.6**.

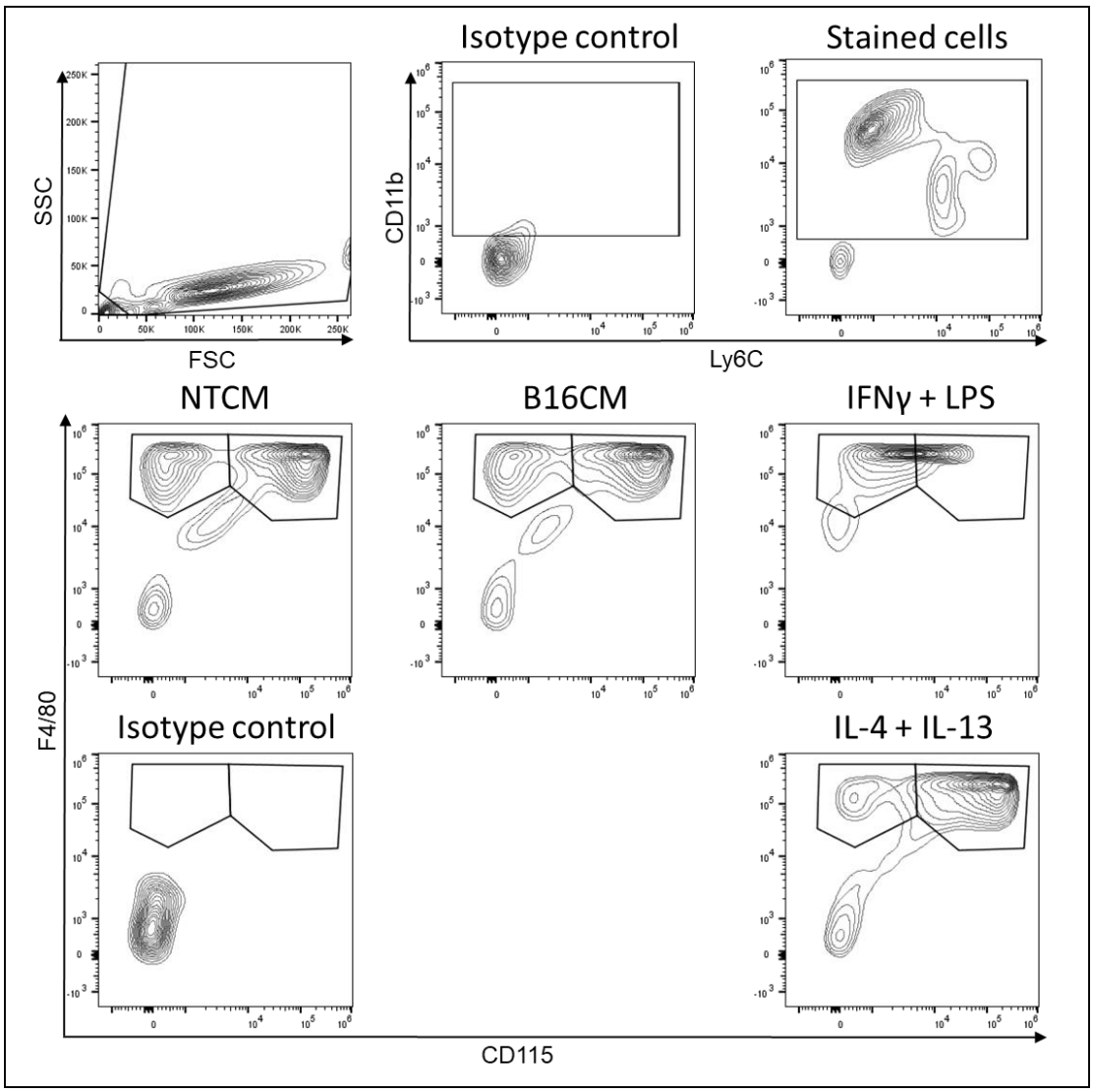

Figure 2.5 Gating of monocytic cells from BMDMs for CD115 analysis

Flow cytometry graphs showing the gating strategy used to identify $CD11b^+$ cells from treated BMDMs (top), along with representative graphs of treatment groups showing the gating strategy to identify $F4/80^+$ $CD115^-$ and $F4/80^+$ $CD115^+$ populations across treatment conditions (middle and bottom), which were used in **figure 4.6.**

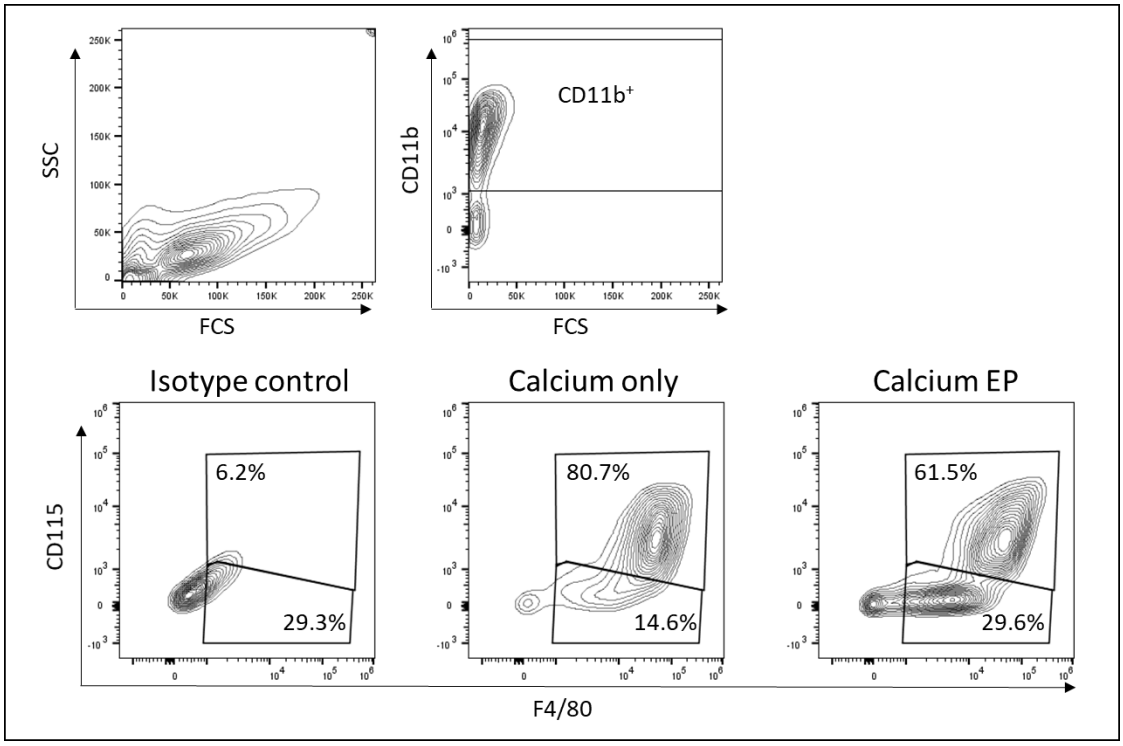

Figure 2.6 Gating used to identify CD115^{+} F4/80^{hi} BMDMs following electroporation

BMDMs were isolated 72hrs after treatment. Cells were gated as CD11b^{+} (top). Cells were then identified as CD115^{-} F4/80^{+} or CD115^{+} F4/80^{hi}. Shown are isotype control staining and representative images of BMDMs treated passively or with EP which were used to determine gating of distinct populations used in **figure 5.5a**.

2.13 Bradford Assay

Bradford assays were performed to normalise cell lysates by protein content [304]. Protein standards, 0-55µg/ml in 5µg/ml increments, were made using a 1mg/ml BSA in ddH_20 solution. 800µl of samples and standards were added to 1.5ml Eppendorfs. 200µl Protein Assay Dye Reagent Concentrate (Bio-Rad) was then added to each Eppendorf. Eppendorfs were vortexed vigorously and 200µl of each sample was added in triplicate to a flat bottom, optically clear 96 well plate. The absorbance of the wells was measured at 595nm using a SpectraMax M2 (Molecular Devices).

2.14 Arginase assay

Cells were washed twice in PBS and lysed by the addition of 10mM Tris-HCl pH7.4, 1x cOmplete™ EDTA-free protease inhibitor cocktail (Roche) and 1% Triton X-100 (Merck) for 30min on ice with vigorous vortexing every 10min. To make 1M Tris-HCl, 12.1g Trizma® base (Merck) was added 80ml ddH_2O. The solution was brought to pH7.4 with HCl and the volume was made up to 100ml with ddH_20. This was diluted 1 in 100 in ddH_20 on the day of use to make a 10mM solution.

The samples were centrifuged at 13,000g for 20min to remove any cellular debris from the solution. A Bradford assay was performed to normalize the protein concentration of cell lysates. Each sample was seeded in sextuplicate. 40µL of cell lysate was added to each well.

An arginase assay kit was used to assay arginase activity of cell lysates (Merck-MAK112). For each sample 3 wells were run as samples, and 3 samples were run as sample blank wells. Sample blank wells were incubated in the absence of substrate buffer (supplied in kit) and acted as negative controls in which there is no arginase activity [305].

As positive and negative controls, 3 wells were seeded with 50µl 1mM urea standard (supplied in kit) and 3 wells were seeded with 50µl ddH_20.

10µl of substrate buffer (supplied in kit) was added to each sample well and each sample well blank received no addition. The plates were mixed well and sealed to stop evaporation. Plates were incubated at 37°C for 2hrs. 200µl of urea reagent (supplied in kit) was added to all wells and 10µl of substrate buffer was added to the sample blank wells. The plates were incubated at RT for 60min. If turbidity appeared in the

wells, the plate was centrifuged at 200g for 5min and the supernatants were transferred to a new plate without agitation of precipitate at the bottom of the wells. The absorbance was read at 430nm using a SpectraMax M2 (Molecular Devices). In this assay, arginase catalyses the conversion of arginine to urea and ornithine. The urea produced reacts with the colour development reagent to generate a coloured product proportional to the arginase activity present, the comparison of sample wells which received substrate buffer before incubation at 37°C and sample blank wells which only received substrate buffer following incubation at 37°C permits a calculation of the level of arginase activity from each sample.

2.15 Griess assay

Supernatants of BMDM treatment cultures were isolated. Supernatants were centrifuged at 500g for 5min to remove any cells or cellular debris from the solution. A 100µM nitrite standard was prepared using a 1 in 1000 dilution of a 0.1M sodium nitrate (Merck) in ddH_2O. 100, 50, 25, 12.5, 6.25, 3.125 and 1.5625µM standards were prepared using a serial dilution in ddH_2O. 50µl of supernatant and standards were added in triplicate to flat bottomed optically transparent 96 well plates (Sarstedt). 50µl of control media was plated in triplicate. 1% sulphanilamide was made by dissolving 1g sulphanilamide (Merck) in a solution of 1 part 85% phosphoric acid (Merck) to 16 parts ddH_20. 50µl 1% sulphanilamide solution was added to each well, plates were mixed well and stored in the dark at RT for 10min. 50µl 0.1% (w/v) N-1-napthylethylenediamine dihydrochloride (NED, Merck) in ddH_20 solution was added to each well, the plate was mixed well and stored in the dark at RT for a further 10min. The absorbance of each well was read at 535nm on a SpectraMax M2 (Molecular Devices) plate reader within 30min [306].

2.16 RNA extraction

RNA extraction was performed using RNeasy plus minikit (Qiagen). All reagents used were contained in this kit unless specified. Following trypsinisation, cells were washed 3 times in PBS. To lyse the cells 350µl RLT buffer was added to the cell pellet and vortexed for 1min. To eliminate the presence of genomic DNA in the product, the cell lysate was transferred to a genomic DNA (gDNA) eliminator column and centrifuged at 8,000g for 30sec. The flow through was collected and added to an equal volume of 70% ethanol to provide appropriate conditions for the binding of RNA to the RNeasy

spin column. The samples were mixed well and transferred to an RNeasy spin column. The column was placed in a 2ml collection tube and centrifuged at 8,000g for 15sec. The flow through was discarded and a series of solutions are sequentially added to wash the spin column. 700µl of buffer RW1 was added to the spin column. The column was centrifuged at 8,000g for 15sec and the flow through discarded. 500µl of buffer RPE was added to the spin column. The column was centrifuged at 8,000g for 15sec and the flow through discarded. Another 500µl of buffer RPE was added to the spin column. The column was centrifuged at 8,000g for 2min and the flow through discarded. The spin tube was removed and placed in a new collection tube and centrifuged for a further 1min at 8,000g to completely dry the tube and prevent contamination of the RNA product with RPE buffer. RNA was then eluted from the spin column by adding 30-50µl RNase free water and centrifuging for 1min at 8,000g.

2.17 DNA and RNA quantification

Both RNA and DNA content were measured using a NanoDrop spectrophotometer. 1µl of RNA or DNA solution was placed on the stage of the spectrophotometer for measurement. The stage was washed with RNase/DNase free ddH_2O before use and between samples. The spectrophotometer was zeroed with the same stock of RNase/DNase free ddH_2O in which the samples were prepared. Both RNA and DNA absorb at 260nm. The A260/280 was confirmed to be within 0.1 of 1.8 (for DNA) or 2 (for RNA) in all samples, as many protein, phenol and other common contaminants absorb strongly at or near 280nm, and thus this is a measurement of DNA or RNA purity. The A260/230 values were also confirmed to be within the range of 2.0-2.2. Common contaminants from DNA and RNA extraction kits can absorb at 230nm and these contaminants can impair the efficacy of downstream applications. Following RNA/DNA concentration measurements, the samples were normalized to a maximum concentration of 60ng/ml for RNA or 100ng/µl for DNA.

2.18 Reverse Transcription

RNA samples were normalized with RNase free water following the determination of RNA content by NanoDrop analysis (section 2.16). Reverse transcription was performed in 20µl reaction volumes using an Omniscript Reverse Transcriptase kit (Qiagen) with 1µM oligo(dt)15 (Promega) and 1µM random hexamers (Qiagen) for 60min at 37°C. A mixture of oligo nucleotides and random hexamers were used as

primers to ensure reverse transcription of transcripts with a diversity of lengths and from diverse start points in an effort to ensure samples were not enriched for any genes.

2.19 Quantitative PCR (qPCR)

Complementary DNA (cDNA) samples were normalized with DNase free water following the determination of DNA content by NanoDrop analysis. Primers were designed based on publically available genetic sequences and by using the IDT primer design tool (Integrated DNA Technologies, Inc). Two sets of primers were synthesized by IDT for each gene of interest, one with a short amplicon and one with a long amplicon. Primers were validated by visualization of a DNA bands on a 2% agarose gel following PCR amplification of BMDM samples and electrophoresis. qPCR was performed using Luna® Universal qPCR Master Mix (New England Biolabs) with 500nM of forward and reverse primers (**Table 2.6**) and 100ng cDNA. Reactions were analysed on an AriaMx Real-time PCR System (Agilent). The thermal profile used included a hot start of 3min at 95°C followed by 40 amplification cycles. Each amplification cycle consisted of denaturation for 15sec at 95°C, followed by annealing for 15sec at 52.5°C and elongation for 30sec at 60°C. A melting curve was performed (30sec at 95°C, 30sec at 65°C and 30sec at 95°C) at the end of each analysis to confirm efficiency of the primers.

Data presented was normalized using the 2^ΔΔCT method with normalization to the housekeeping gene β-actin. Data was also analysed using glyceraldehyde 3-phosphate dehydrogenase (GAPDH) to ensure validity of results, no changes in trends or significance were seen using GAPDH or β-actin analysis.

Table 2.6 Primers used for qPCR experiments

Protein	Gene	Direction	Sequence (5'-3')
B-actin	*ACTB*	Fwd	GAG GTA TCC TGA CCC TGA AGT A
		Rev	GCT CGA AGT CTA GAG CAA CAT AG
GAPDH	*GAPDH*	Fwd	CGA GAA ACC TGC CAA GTA TGA
		Rev	CCT GTT GCT GTA GCC GTA TT
IL-6	*IL6*	Fwd	CTT CCA TCC AGT TGC CTT CT
		Rev	CCT TCT GTG ACT CCA GCT TAT C
Arginase 1	*ARG1*	Fwd	GAA CTG GCT GAA GTG GTT AGT
		Rev	TAG GAG TAG GAA GGT GGT CAT AG
CD206	*MRC1*	Fwd	GTG GTC CTC CTG ATT GTG ATA G
		Rev	AGT GGC TTA CGT GGT TGT T
Ym1	*CHIL3*	Fwd	CAG GCC AAT AGA AGG GAG TTT
		Rev	GAG TAG CAG CCT TGG AAT GT
IL-10	*IL10*	Fwd	GGA GCA GGT GAA GAG TGA TTT
		Rev	TCC AAG GAG TTG TTT CCG TTA G
TGF-β	TGFB	Fwd	CTG AAC CAA GGA GAC GGA ATA C
		Rev	CTC TGT GGA GCT GAA GCA ATA G
IL-12b	*IL12B*	Fwd	GCA AGC TCA GGA TCG CTA TTA
		Rev	AGA AGG CCC TGG TTT CTT ATC
CD68	*CD68*	Fwd	GAT TGA GGA AGG AAC TGG TGT AG
		Rev	CTT CCA CCC TGA ATT GGG TAT AG

Above are complementary DNA sequences used to identify specific murine mRNA sequences. mRNA was isolated, reverse transcribed, amplified and measured to determine relative gene expression in bone marrow-derived macrophages. Interleukin 12b (IL-12b), chitinase-like 3 (Ym1).

2.20 BMDM and $CD4^+$/$CD8^+$ T cell cocultures

Spleens were isolated from healthy 4-8 week old female C57BL6J mice and passed through a 70μm filter. RBCs were lysed in RBC lysis buffer (**see section 2.8**) and $CD4^+$ or $CD8^+$ T cells were isolated using negative selection magnetic bead labelling kits (Miltenyi Biotec) according to the manufacturer's instructions. Splenic cells were washed once in separation buffer (PBS with 0.5% BSA). All solutions, including separation buffer, separation kit reagents, and splenic cells, were kept on ice during separation. The following volumes are per $1x10^7$ cells, where more starting cells were used for isolation the volumes added were scaled appropriately. Cells were resuspended in 40μl separation buffer and 10μl of Biotin-Antibody Cocktails (supplied in kit) were added. Cells were vortexed and incubated on ice for 5min. A further 30μl of separation buffer and 20μl of Anti-Biotin MicroBeads (supplied in kit) were added. Cells were vortexed and incubated on ice for 10min. During incubation, an LS column (Miltenyi Biotec) containing magnetic beads was placed in a QuadroMACS™ Separator magnet (Miltenyi Biotec) and was washed by adding 3ml of separation buffer. The run through was discarded. The column was kept wet at all times, adding additional separation buffer when required to prevent the column running dry. Following 10min incubation with Anti-Biotin MicroBeads, the cell solution was added to the LS column. The flow through containing unlabelled cells was collected. The column was rinsed with a further 3ml separation buffer and the run through was added to the negatively selected faction representing enriched $CD4^+$ or $CD8^+$ T cells.

In each kit all other cells are selected for by the cocktail of antibodies provided in the Biotin-Antibody Cocktail solution, these cells are bound by biotin-avidin reactions to magnetic microbeads and retained in the LS column while the $CD4^+$ or $CD8^+$ T cells are free to pass through. Once the LS column is removed from the magnetic field, these positively selected cells can be eluted from the LS column. These cells were not required for further use in the experiments performed in this thesis.

Following separation, the negatively selected T cells were washed once in PBS. Cells were then resuspended in 2ml 5μM carboxyfluorescein succinimidyl ester (CFSE) in warm PBS for precisely 8min. Cells were then washed in cRPMI 3 times.

Confirmation of separation and CFSE analysis was performed by flow cytometry. An aliquot of cells was taken pre-separation and an aliquot of the negatively selected faction were taken both before and after CFSE staining. The cells were stained with PE conjugated CD4 or CD8. The concentration of $CD4^+$ or $CD8^+$ T cells was confirmed to be above 85% in all negatively selected T cell enriched samples before further use, and CFSE staining was confirmed. An example of the gating used is shown (**Figure 2.7**).

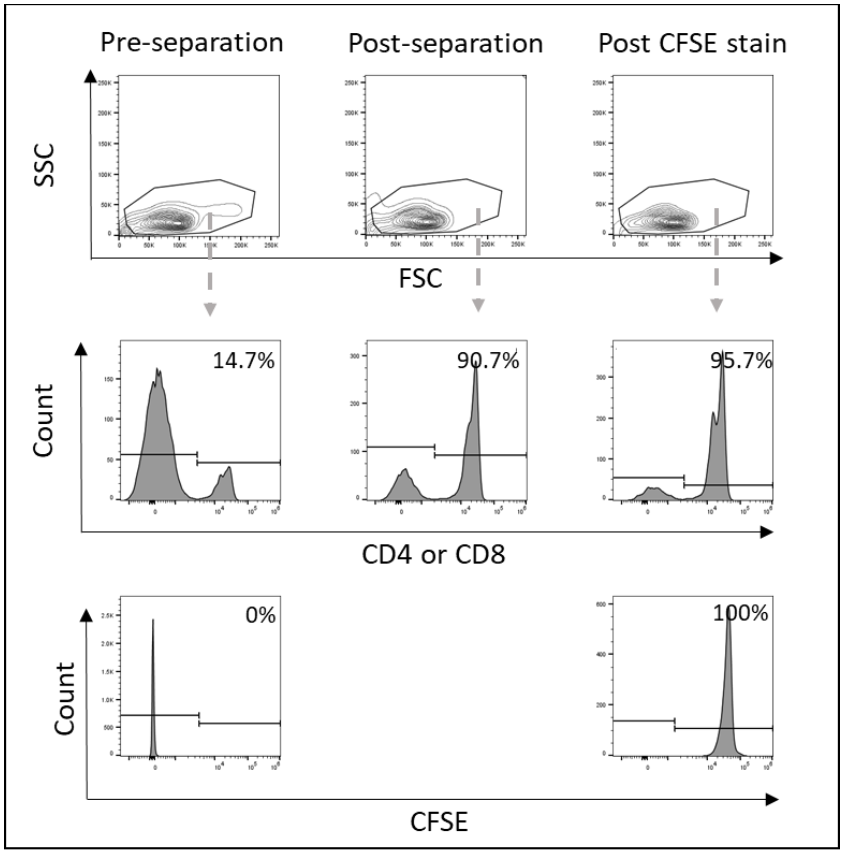

Figure 2.7 Concentration and CFSE staining of $CD4^+$ or $CD8^+$ T cells following magnetic bead separation and CFSE labelling

Aliquots of T cells were taken before magnetic bead separation, post magnetic bead separation and post CFSE staining. All aliquots were stained for FACS analysis with either CD4-PE or CD8-PE. Cells were gated by FSC and SSC to remove debris from analysis (top). Cells were then gated based on CD8 expression (middle row). All samples were confirmed to be >85% purity prior to further use. CFSE was confirmed to have stained 100% of cells by gating relative to aliquots taken before CFSE staining (bottom).

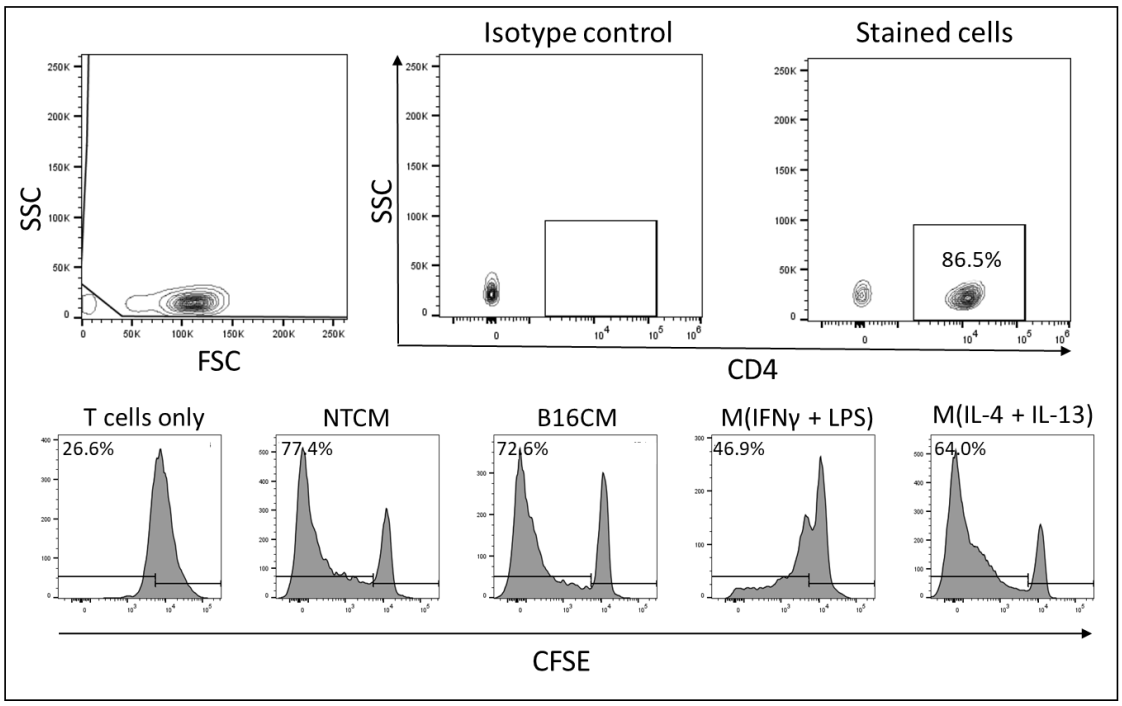

Figure 2.8 Identification of CD4$^+$ T cell purity and gating of CFSE^{lo} cells following coculture

Flow cytometry graphs showing gating strategy used to identify CD4$^+$ T cells following coculture (top) and to differentiate proliferating T cells (bottom) seen in **figures 4.8 and 5.6.**

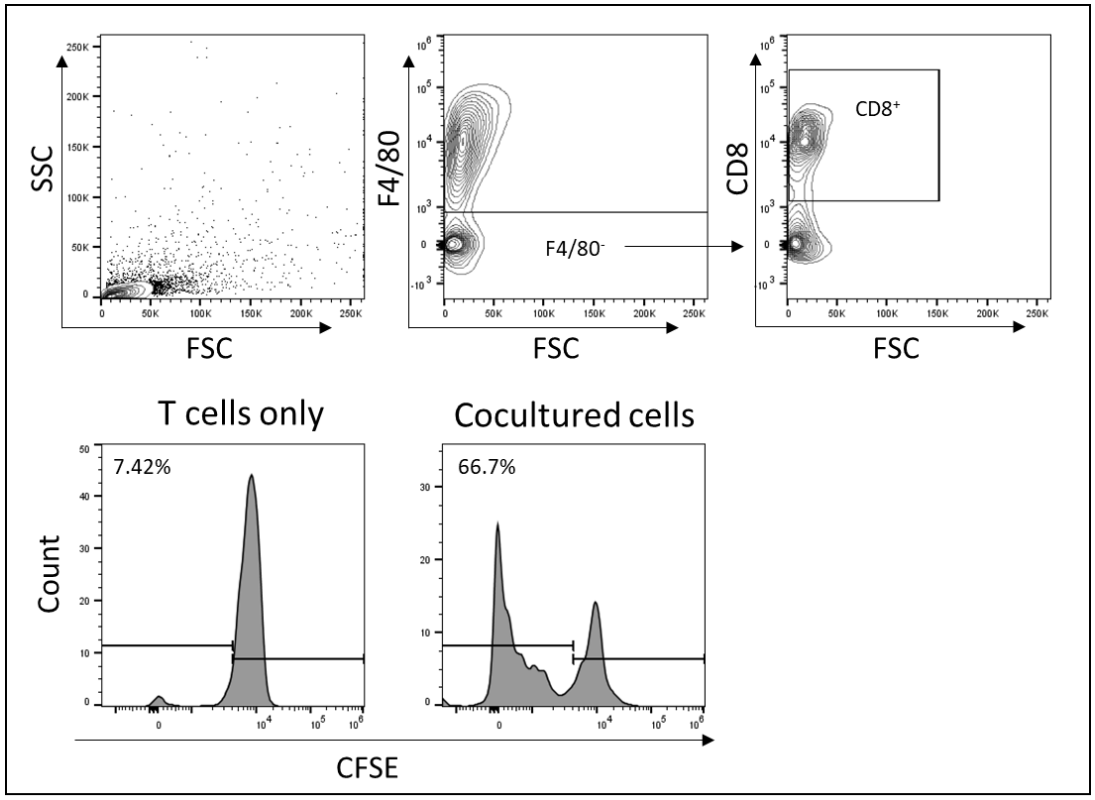

Figure 2.9 Gating used to identify CD8$^+$ T cell proliferation

Flow cytometry graphs showing representative graphs of the gating strategy used to gate for CD8$^+$ T cells (top) seen in **figures 4.9 and 5.7**. Also shown is the CFSE staining of a T cell only aliquot and a sample coculture reaction, showing gating of cells which have proliferated (bottom).

Before the coculture experiments BMDMs were treated for 24hrs and washed 3 times to prevent contamination of coculture reactions with treatment conditions. CFSE stained T cells were cocultured with pre-treated and washed BMDMs at a concentration of $5x10^5$/ml T cells and $5x10^5$/ml BMDMs in 200µl reactions in round bottom suspension 96 well plates (Sarstedt) to ensure the aggregation of T cells and BMDMs [307]. The cocultures were incubated at 37°C for 5-7 days. Harvesting of experiments was timed by checking for the presence of significant T cell proliferation as determined by a decrease in CFSE staining in positive control sample wells (**Figure 2.8-2.9**).

2.21 Reversible Electroporation

Cells were trypsinised, counted and aliquoted into polystyrene FACS tubes (BD biosciences) with $2x10^6$ cells added to each tube. The cells were washed once in 4-(2-hydroxyethyl)-1-piperazineethanesulfonic acid (HEPES) EP buffer (10mM HEPES (Merck), 250mM Sucrose (Merck), 1mM $MgCl_2$ (Merck) in ddH_20) and resuspended in a final volume of 1.6ml of EP buffer with or without calcium (Merck) or bleomycin (Mylan). 800µl of the 1.6ml was added to an electroporation cuvette (VWR).

For all experiments involving calcium, Milli-Q® ultrapure water from a Milli-Q® Integral Water Purification System for Ultrapure Water (Merck) was used instead of ddH_2O, to ensure buffers had no calcium contamination.

Cells were electroporated at room temperature in 0.4cm cuvettes (Fisherbrand) at 700V/cm (280V across 0.4cm), unless specified, using 8 square wave pulses of 99µsec at 1Hz using a BTX ECM 2001 square wave electroporator (BTX, San Diego, USA) [308]. For no electroporation controls, cells were left in FACS tubes at RT while other cells were subjected to electroporation. Following electroporation all cells were placed at 37°C for 20-40min to allow electroporated cells to recover their cell membrane integrity following electroporation. Following incubation, the inner surfaces of the electrodes were vigorously washed and the cells were transferred to a new FACS tube. Cells were washed in cRPMI and resuspended in 1ml of cRPMI. Cells were then seeded in 6 well plates with 2ml media and incubated at 37°C in a humidified chamber with 5% CO_2 for 24hrs.

2.22 Colony forming assay

Following electroporation the cells were seeded for 24hrs to allow cells to recover. The cell concentration was determined empirically for each treatment to ensure 60-90% confluency of cells after 24hrs. Supernatants and non-adhered cells were discarded to select for adherent (viable) cells. Cells were counted and resuspended at a standardized concentration of 400 cells/well in cRPMI. 4ml of cell solution was added to each well of a 6 well plate. All samples were run in triplicate. The plates were incubated at 37°C in a humidified chamber with 5% CO_2 for 10-14 days until visible colonies were established in the no treatment control well [309]. The supernatant was removed from the wells and 3-4ml of methanol (Honeywell) was added to each well for 5-10min. Methanol was removed and Prodiff stain 2 (Acquascience), composed of buffered methyl thionins, was added to the wells so that the entire surface of the well was covered for 5-10min. Prodiff solution was removed and the plates were washed under running ddH_20. Plates were allowed to dry for 1-2 days. Once fully dry the underside of the plates was cleaned with 70% ethanol spray (Brenntag) to remove any marks from the underside of the plate. The fluorescence of the plate was then read using a Li-Cor plate reader (Odyssey) at 800nm.

2.23 Enzyme-linked immunosorbent assay (ELISA)

Mouse Interferon γ (IFNγ), IL-4 and IL-10 ELISA Max™ Deluxe Sets (Biolegend) were used for ELISAs according to the manufacturer's instructions. Coating buffer A was made by mixing 4 parts ddH_20 with 1 part 5x Coating buffer (supplied in kit). Capture antibody (supplied in kit) was diluted 1 in 200 in 1x coating buffer. Nunc™ MaxiSorp™ ELISA plates (supplied in kit) were coated with 100µl per well of diluted capture antibody, sealed with cling film and stored overnight at 4°C. The capture antibody was emptied from the plate and the plate was washed. For each wash step the plate was washed 4 times in wash buffer (PBS + 0.05% Tween (Merck)). Assay diluent was made by diluting 1 part 5x assay diluent (supplied) with 4 parts PBS. The plate was blocked by adding 200µl assay diluent to each well. The plate was sealed and placed on a plate shaker at 500rpm with a 0.3cm orbit for 1hr at RT, all subsequent incubation steps were performed with the plate sealed and on a shaking incubator at RT. The antibody diluent was eluted and the plate was washed.

Standards were made by reconstituting 1 vial of standard (supplied in kit) in 200µl assay diluent. These solutions were diluted in assay diluent to generate serial dilutions to be used as standards. IFNγ standards were made at 2000, 1000, 500, 250, 125, 62.5 and 31.25pg/ml. IL-4 standards were made 125, 62.5, 31.25, 15.63, 7.8, 3.9 and 2.0. IL-10 standards were made at 1000, 500, 250, 125, 62.5, 31.25 and 15.63pg/ml. Assay diluent alone was used as a negative control.

100µl of supernatants and standards were added to the appropriate wells in triplicate and the plate was incubated for a further 2hrs. The samples were eluted and the plate was washed. Detection antibody was made by diluting the 200x detection antibody (supplied) in assay diluent. 100µl diluted detection antibody was added to each well and the plates were incubated for 1hr. Detection antibody was eluted from the plate and the plate was washed. Avidin- Horseradish peroxidase (HRP) solution was made by diluting the 1000x Avidin-HRP (supplied in kit) in assay diluent. 100µl diluted Avidin-HRP solution was added to each well and the plate was incubated for 30min. Avidin-HRP was eluted from the plate and the plate was washed. Equal volumes of substrate solution A (supplied in kit) and substrate solution B (supplied in kit) were mixed to make 3,3′,5,5′-Tetramethylbenzidine (TMB) substrate. 100µl of TMB substrate was added to each well, the plate was tapped to mix well and stored in the dark for 15-30min until a strong colour change developed. 100µl 1M HCl stop solution was added to each well and the plate was read on a SpectraMax M2 (Molecular Devices) plate reader at 570nm and 450nm. The 570nm reading provided a measure of non-specific values which were subtracted from the 450nm values before analysis.

2.24 Statistical analysis

2.24.1 Chapter 3

All statistical analyses was carries out in the R environment, v.3.4.4. Boxplots shown represent the mean, with interquartile ranges (boxes) and 95% confidence interval (whiskers), with outliers shown.

Spearman's correlations were used to determine significance, correlation coefficients between continuous variables. The Wilcoxon rank sum test was used to determine significance between continuous and discrete variables.

Where a large number of zero values were obtained in immunohistochemical measurements (CD68 staining), semi-quantitative measurements were used for data analysis. A Spearman correlation was used in **figure 3.2d** to show the association of intratumoural $CD68^+$ cells with Breslow depth, however the Wilcoxon rank sum test value of this association is also presented in **table 3.1**, both were non-significant.

Gene expression data was analysed using normalized gene values as presented by HTG EdgeSeq technology. Differentially expressed genes between groups were detected using the DESeq2 algorithm with adjusted *p* values. Heat maps were clustered using the Ward-Linkage method and generated using the Made4 package v.1.58 within the R environment. Kaplan-Meier plots and associated statistical testing was performed using the survminer package in R, v.0.4.4. Survival probabilities were calculated using the Cox proportional hazards model and differences between groups were analysed using the log-rank test.

2.24.2 Chapter 4 and 5

Statistical analysis for data present in chapter 4 and 5 was performed using GraphPad Prism version 5.03. Flow cytometry data was analysed using FlowJo version 10.5.3. Differences between groups were determined by paired and un-paired student's t-tests as appropriate.

Chapter 3

Immunohistochemical evaluation of the presence and phenotype of $CD68^+$ and $CD163^+$ macrophages in human melanoma

3.1 Abstract

The density and phenotype of tumour-associated macrophages have been linked with prognosis in a range of solid tumours. While there is strong preclinical evidence that tumour-associated macrophages promote aspects of tumour progression, it can be difficult to infer clinical activity from surface markers and ex vivo behaviour. Here, we investigated the association of macrophage infiltration with prognosis and functional changes in the tumour microenvironment in primary human melanoma. 57 formalin-fixed paraffin embedded primary melanomas were analysed by immunohistochemical analysis of CD68, CD163, iNOS and arginase expression. RNA sequencing was performed on serial sections of 20 of the stained tumours to determine the influence of macrophage infiltration on gene expression. $CD68^+$ cells were found to be a functionally active subset of macrophages that are associated with increased iNOS and arginase staining and altered gene expression within the tumour. In comparison, while there is a greater accumulation of $CD163^+$ macrophages in larger tumours, these cells are comparatively inactive, with no association with the level of iNOS or arginase staining, and no effect on gene expression within the tumour. Infiltration of either subset of macrophages did not correlate to overall survival. Thus, melanomas contain distinct macrophage populations with diverse phenotypes, but with no observable prognostic role.

3.2 Introduction

Macrophage infiltration as determined by evaluation of FFPE has been shown to be a prognostic indicator in a range of solid malignancies [310]. The markers used to identify macrophages vary, and there is no consensus on markers which reflect true physiological subsets [311].

In the majority of cancers the macrophage marker CD163 correlates with more advanced tumours and to a worse prognostic outcome, except in the cases of gastric cancer and colorectal cancers [36,37,53,310]. Other markers, such as CD68, have been used to stain macrophages, but have been linked to both favourable and unfavourable outcomes [53,43].

Previous studies have attempted to delineate the prognostic influence of macrophage infiltration in melanoma. Both the number of $CD68^{+}$ cells and soluble CD163 have correlated to poor OS, however only CD68 counts at the invasive front of the tumour were independent predictors of reduced survival [248].

Macrophages have been implicated in all aspects of tumour progression including proliferation, survival, immunosuppression, angiogenesis and metastasis [312]. Furthermore macrophages have been implicated in resistance to various therapies such as chemotherapy and radiotherapy [76,79,81,89].

However, much evidence of the effect of intratumoural infiltration has been inferred from *in vitro* analysis which is based on the hypothesis that the expression of surface markers is reflective of functional phenotype, however it is known the diversity of functional phenotypes and macrophage plasticity are controlled by a much more intricate underlying system of epigenetics that cannot be represented by the known subset of surface markers [268,313]. The precise nature of macrophages continues to be unravelled, and during the process of unravelling, further findings continue to add additional layers of complexity to an already poorly understood science [200]. Recently horizontal transformation from macrophage-like cells to fibroblast-like cells has been observed, and the source or stability of discrete populations are still not known [60]. As such, macrophage markers may not be considered stable markers of distinct cells. However, whether they represent stable populations or a continuous flow of cells through a transition state, we can use these markers to identify distinct subsets of macrophage-like cells at any point in time.

Another source of concern is the discrepancy of results in murine and human intervention studies [20]. It is known that monocyte and macrophage markers vary between mice and humans, such as F4/80, which is a monocyte and macrophage marker in mice, but its homolog, EMR1, is an eosinophil-specific receptor in humans [314]. But cross-species differences have also been seen in the outcomes of interventions targeting conserved targets. Anti-CSF1R antibodies which inhibit macrophage migration to the tumour have been effective in the treatment of murine malignancies, however clinical trials have observed no therapeutic benefit in humans, indicating a differential physiological role or reliance on macrophage behaviour between mice and human disease [310,180,213]. The influence of macrophages on tumour biology in human malignancies is not fully known as macrophages are also known to adopt unreactive senescent and quiescent states [315].

Another central concern is the sensitivity of macrophages to environmental stimuli, which adds question to the compatibility of *ex vivo* studies [316]. Macrophages are known to be activated by environmental stimuli including adherence to the extracellular matrix and a wide range of innocuous stimuli such as adherence to plastic, thus *ex vivo* studies contain inherent limitations [317,318,316]. An alternative approach is to investigate the presence and associations of macrophages in FFPE tissues. While this approach reduces the level of artificially introduced environmental impacts, it comes with its own experimental limitations. From a clinical standpoint, this approach has significant advantages in being able to draw on the existing biobanks with associated patient data [319].

Here we evaluate the presence of $CD68^+$ and $CD163^+$ macrophages in human primary melanoma lesions, and determine their correlation with the canonical M1:M2 enzymes iNOS and arginase [320]. To further investigate if these cells have a biological role, we investigate their link with OS and determine if they correlate to differential gene expression within the tumour.

3.3 Results

3.3.1 Correlation of $CD68^+$ and $CD163^+$ macrophage infiltration with pathological features of melanoma

Primary untreated melanoma lesions were stained with CD68 and CD163 antibodies to identify macrophages, and with iNOS and arginase to identify enzymatic activity. CD68, iNOS and arginase specifically stained cytoplasmic compartments (**Figure 3.1**). CD163 stained both the cytoplasm and plasma membrane of target cells, with increased staining intensity seen at the plasma membrane. CD68 and iNOS staining was specific to cells with a distinct macrophage morphology. CD163 stained a much larger number of cells, but was not restricted to cells of a distinct macrophage-like morphology. Arginase staining was less frequent and was completely negative in almost half of stained sections. In positive sections, stained cells showed a distinct macrophage (**Figure 3.1e**) or neutrophil (**Figure 3.1f**) morphology, thus arginase staining as presented in this study is a reflection of a subset of both neutrophils and macrophages. Many ulcerated tumours showed a distinct influx of a high number of $arginase^+$ neutrophils to the peritumoural ulcerated tissue. There was a statistically significant positive correlation between peritumoural $arginase^+$ cells and ulceration, accompanied by a significant decrease in peritumoural $CD68^+$ cell infiltration.

The number of positive cells per mm^2 were measured in both intratumoural tissue and peritumoural tissue. 21 specimens were negative for intratumoural $CD68^+$ cells and 30 were negative for peritumoural $CD68^+$ cells, as such CD68 data was stratified into those with and without the presence of stained cells. Previous reports have similarly found that tumours of the same subtype may be negative or positive for the presence of $CD68^+$ cells [321].

There was no significant correlation between the infiltration of $CD163^+$ and $CD68^+$ cells, indicating that these cells represent distinct, but potentially non-mutually exclusive, macrophage subsets (**Figure 3.2a-b**). The correlation of CD68 and CD163 macrophage infiltration with pathological features of the tumour were determined using Spearman correlations and Wilcoxon Rank sum tests (**Table 3.1**). No differences in cell density were seen between baseline characteristics such as age, gender, tumour stage, or tumour infiltrating lymphocytes. Intratumoural $CD163^+$ macrophages were found to increase with Breslow depth (**Figure 3.2c**). There was a

decrease in the number of peritumoural $CD68^+$ macrophages in tumours with a thicker Breslow depth (**Figure 3.3a**), however there was no significant correlation with intratumoural $CD68^+$ macrophages and tumour size. The nature of this non-significant trend was in contrast to intratumoural $CD163^+$ cells, with the trend suggesting potentially decreased numbers of $CD68^+$ cells in tumours with a thicker Breslow depth (**Figure 3.2d**). A reduced number of peritumoural $CD68^+$ cells were also seen in ulcerated tumours (**Figure 3.3b**).

Table 3.1 Association of pathological tumour features with $CD68^+$ and $CD163^+$ macrophage infiltration

	CD68		**CD163**	
	Peritumoural	**Intratumoural**	**Peritumoural**	**Intratumoural**
Age (years)	0.4	0.19	0.233 (0.162)	0.502 (0.092)
Gender	0.425	0.834	0.498	0.78
Breslow depth (mm)	**0.004**	0.5	0.937 (0.011)	**0.0191 (0.315)**
Stage	0.28	0.72	0.62	0.213
BRAF status	**0.027**	**0.001**	0.443	0.726
Mitotic count (mm)	**0.01**	0.13	0.908 (-0.017)	0.501 (-0.017)
Ulceration (mm)	0.12	0.36	0.074 (0.356)	0.208 (0.255)
Ulceration (Yes/No)	**0.01**	0.224	0.549	0.683
TIL distribution	0.683	0.455	0.166	0.353

The association of the number of $CD68^+$ and $CD163^+$ cells with patient and tumour characteristics was determined using Wilcoxon Rank Sum test and Spearman Correlations. The significance value for each relationship is shown above, and where relevant the correlation coefficient between two continuous variables is also shown. Data is presented as significance values (correlation coefficients), n=57. With significant correlations in bold text.

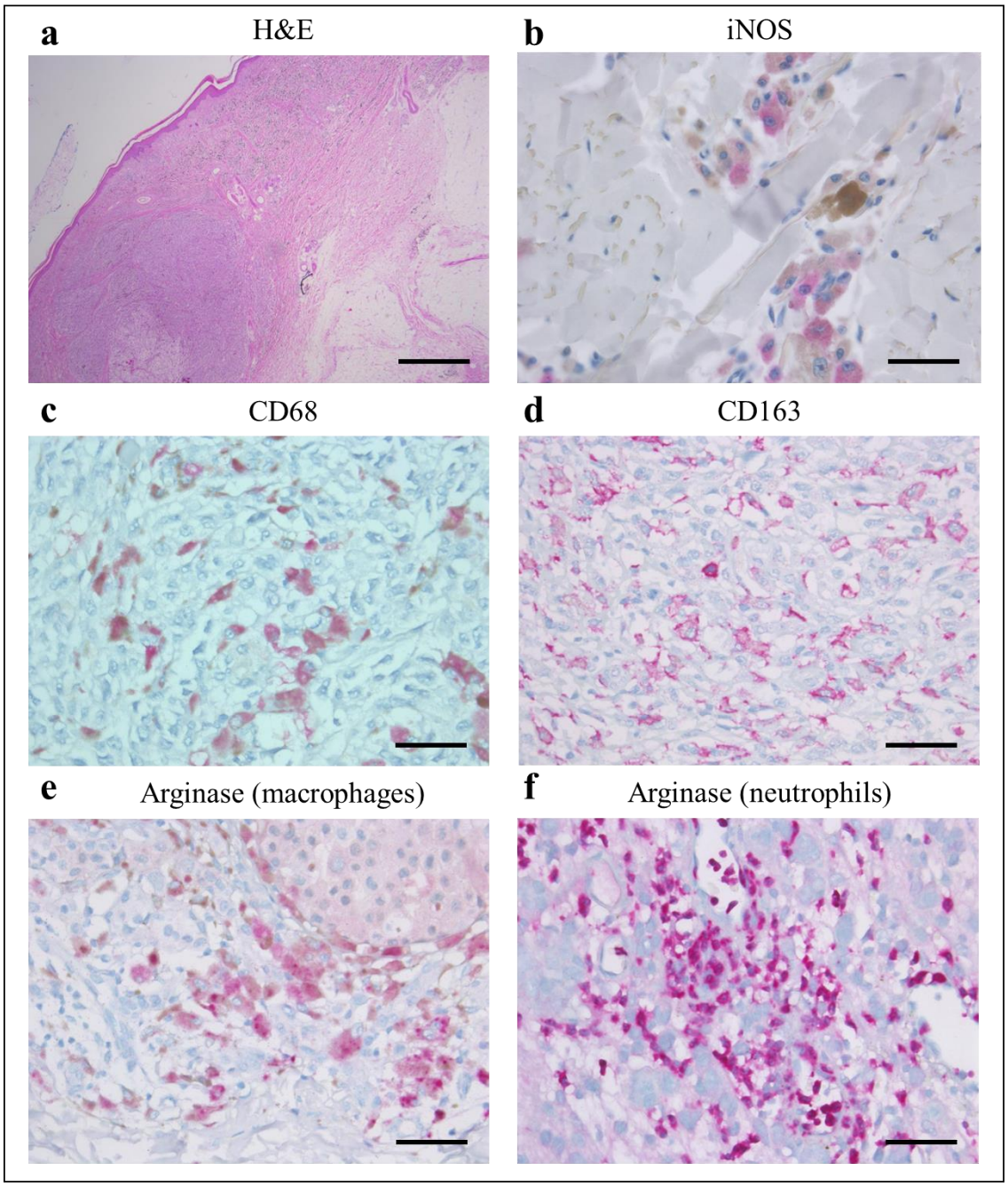

Figure 3.1 Staining of primary melanoma tumours

FFPE tumours were cut and stained by H&E (a), along with immunohistochemical staining of iNOS (b), CD68 (c), CD163 (d) and arginase (e-f). Immunohistochemical staining was performed using an alkaline phosphatase coupled to Fast-Red to produce a red/pink reaction. Images are shown at 40x (a), 400x (b) or 100x (c-f) magnification. Scale bars 1mm (4x), 400μm (10x), and 100μm (40x).

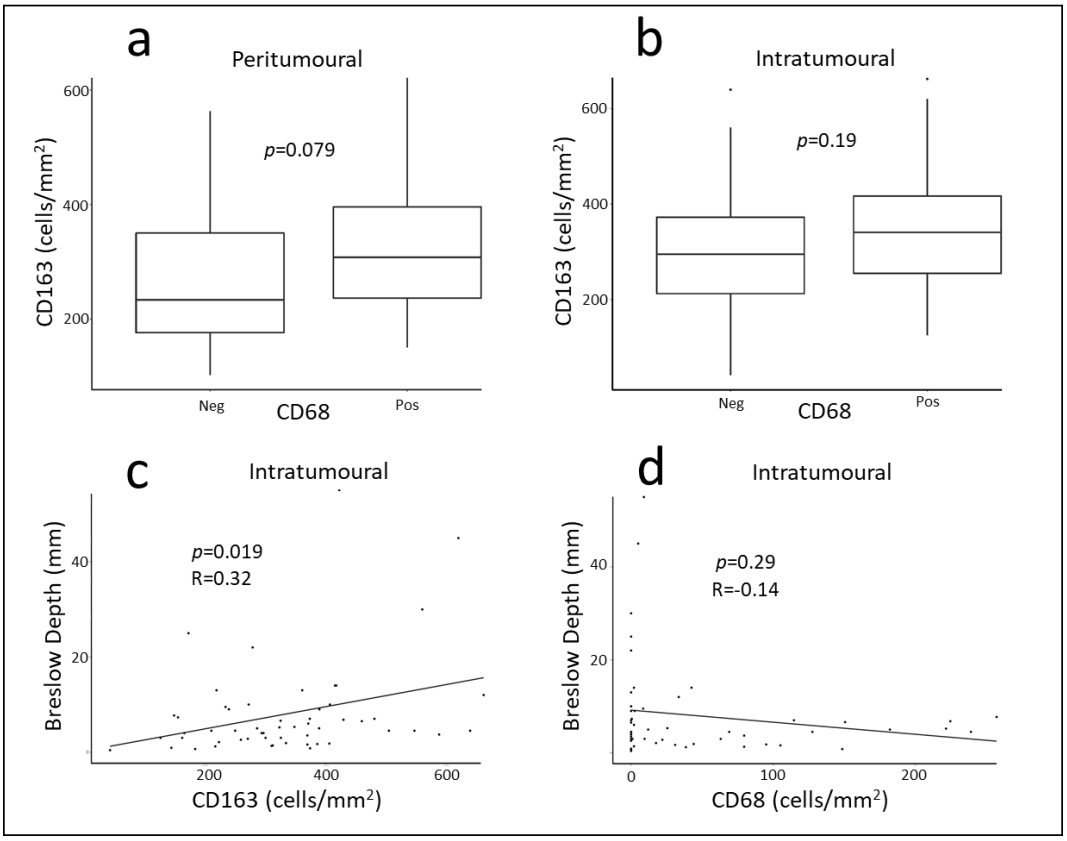

Figure 3.2 Differential CD68$^+$ and CD163$^+$ macrophage recruitment to primary melanoma lesions
The number of CD68$^+$ and CD163$^+$ cells were determined by immunohistochemistry in primary melanoma tumours. The number of positive cells were counted in the peritumoural and intratumoural regions. CD68$^+$ and CD163$^+$ cells were shown to be differentially recruited (a-b). Intratumoural CD163$^+$ macrophage infiltration was positively correlated to Breslow depth, while intratumoural CD68$^+$ macrophage infiltration showed no significant correlation. Boxplots shown represent the mean, with interquartile ranges (boxes) and 95% confidence interval (whiskers), with outliers shown. Correlations with discrete variables were analysed using Wilcoxon Rank Sum tests, and between continuous variables with Spearman correlations. n=57.

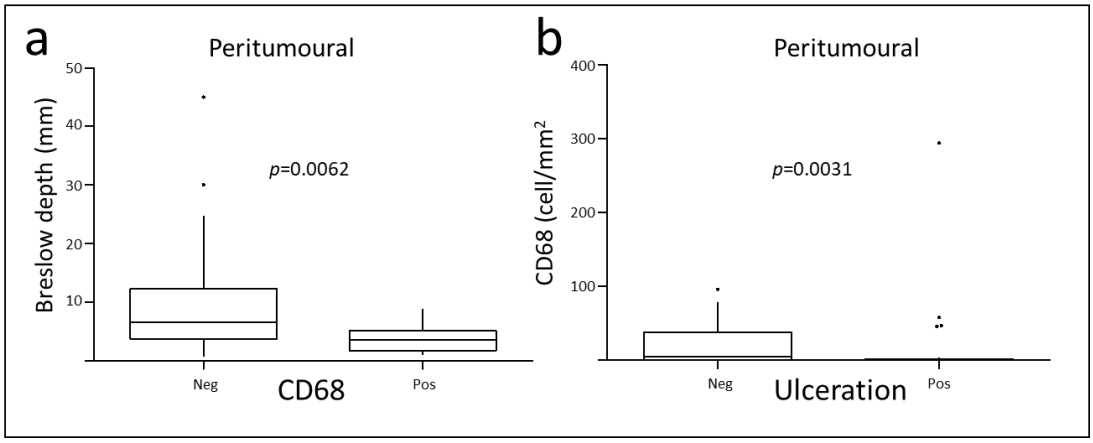

Figure 3.3 Reduced peritumoural CD68$^+$ macrophage infiltration in thick and ulcerated tumours

The number of CD68$^+$ macrophages were determined by immunohistochemistry in primary melanoma tumours. The number of positive cells were counted in the peritumoural region. a) Tumours with no peritumoural CD68$^+$ macrophages had a greater Breslow depth. b) Decreased numbers of peritumoural CD68$^+$ macrophages were seen in ulcerated tumours. Boxplots shown represent the mean, with interquartile ranges (boxes) and 95% confidence interval (whiskers), with outliers shown. Correlations with discrete variables were analysed using Wilcoxon Rank Sum tests, n=57.

3.3.2 Correlation of CD68$^+$ and CD163$^+$ macrophage infiltration with the number of iNOS$^+$ and arginase$^+$ cells

Given that CD68$^+$ and CD163$^+$ macrophages represent distinct subsets with distinct staining profiles based on a number of pathological features, we next set out to determine if these differences reflected different immunological profiles within the tumour by measuring the expression of the macrophage enzymes iNOS and arginase. These enzymes were selected as they are constitutively active when expressed, thus they are likely to have a meaningful impact on tumour biology, and they are highly cited in the literature, however it must be stated that while these enzymes are associated with inflammatory or tissue repair phenotypes respectively, it is important not to infer a distinct M1 or M2 phenotype in these cells. Strong positive correlations were seen between intratumoural CD68$^+$ macrophages and the number of both iNOS$^+$ and arginase+ cells. Specimens with intratumoural CD68$^+$ macrophages had a higher level of both arginase$^+$ and iNOS$^+$ cells (**Figure 4a-b**), while specimens with peritumoural CD68$^+$ macrophages also showed a strong increase in peritumoural arginase levels (**Figure 4c**). In contrast, there were no strong positive or negative correlations between CD163$^+$ macrophage density and the number of either iNOS$^+$ or

arginase+ cells. Intratumoural CD163$^+$ macrophage density was significantly correlated to the number of iNOS$^+$ cells showing no meaningful change in the number of iNOS$^+$ cells regardless of CD163$^+$ macrophage density (**Figure 4d**). Thus strong differences exist between the correlations of CD68$^+$ and CD163$^+$ macrophage populations and iNOS or arginase activity.

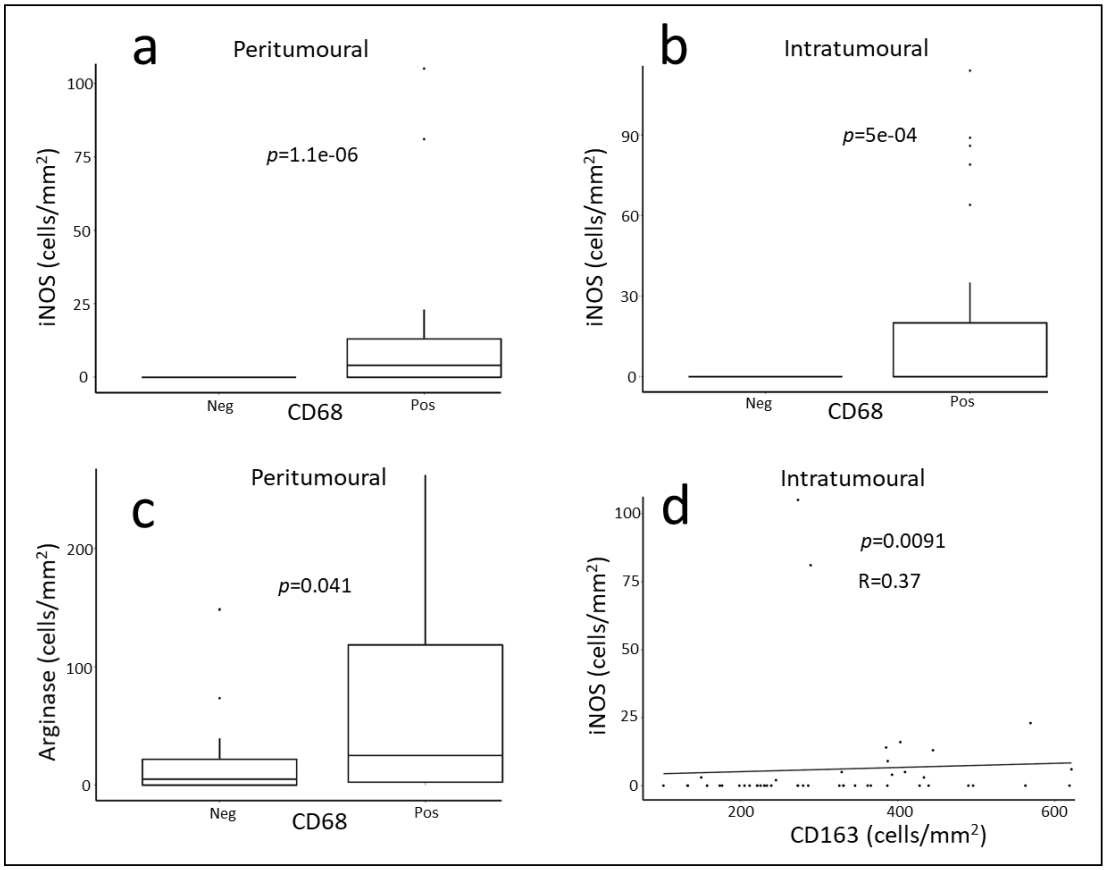

Figure 3.4 Association of CD68$^+$ and CD163$^+$ macrophage infiltration with iNOS$^+$ and arginase$^+$ cells

The number of CD68$^+$, CD163$^+$, iNOS$^+$ and arginase$^+$ cells were determined by immunohistochemistry in primary melanoma tumours. The number of positive cells were counted in the peritumoural and intratumoural regions. a-b) Peritumoural and intratumoural CD68$^+$ macrophages were positively correlated to the number of iNOS$^+$ cells. c) Peritumoural CD68$^+$ macrophages were found to positively correlate to arginase$^+$ cells. d) Intratumoural CD163$^+$ macrophages were found to correlate to the number of iNOS$^+$ cells, however the trend line shows that this is a near zero trend. Boxplots shown represent the mean, with interquartile ranges (boxes) and 95% confidence interval (whiskers), with outliers shown. Correlations with discrete variables were analysed using Wilcoxon Rank Sum tests, and between continuous variables with Spearman correlations. n=57.

3.3.3 Effect of $CD68^+$ and $CD163^+$ macrophage infiltration on total intratumoural gene expression

While an increase in the number of $iNOS^+$ and $arginase^+$ cells in tumours with $CD68^+$ macrophages is indicative an active $CD68^+$ macrophage phenotype, both iNOS and Arginase activity reflect a very small component of macrophage behaviour which is unlikely to independently determine the influence of macrophages on tumour biology. To determine if the macrophage infiltration could have an effect on global gene expression within the tumour tissue we performed RNA sequencing on serial sections of the same FFPE tissue. In addition to seeing no effect of $CD163^+$ macrophage infiltration on iNOS or arginase staining, no effect was seen on gene expression within the tumour tissue. Analysis of both peritumoural and intratumoural $CD68^+$ macrophage infiltration correlated to differential expression of a number of genes within the tumour tissue (**Figure 3.5**). This effect was all the more notable given an average of 7-15 fold more $CD163^+$ macrophages in the tumour in comparison to $CD68^+$ macrophages. The genes affected were not specific to monocytic cells and were reflective of a broad range of processes within the tumour such cell proliferation, cell death and differentiation.

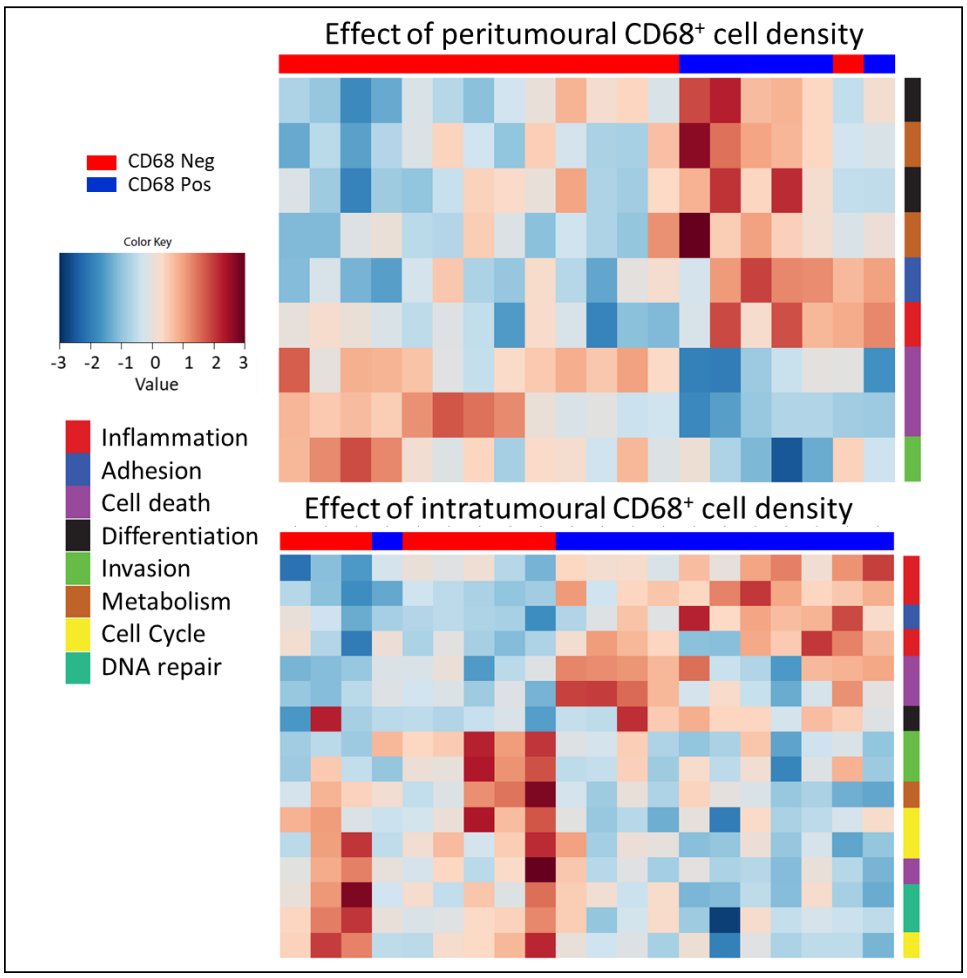

Figure 3.5 The correlation of CD68$^+$ macrophage recruitment with differential gene expression

The number of CD68$^+$ and CD163$^+$ macrophages were determined by immunohistochemistry in primary melanoma tumours. Intratumoural gene expression of the same FFPE blocks was measured using next-generation sequencing technology. Using Deseq2 algorithms both peritumoural and intratumoural CD68$^+$ macrophages were shown to correlate to differential regulation of a number of genes within the tumour. CD68 positive samples are marked as blue along the upper margin, while CD68 negative samples are marked as red. Gene associated signalling pathways are colour coded on the right hand margin. No effect was observed by the level of CD163$^+$ macrophage infiltration. Data was displayed using the Ward-Linkage method for significant genes from a database of 2550 oncology biomarker genes, n=20.

3.3.4 Effect of CD68$^+$ and CD163$^+$ macrophage infiltration on OS

To determine if the markedly different functional phenotypes of CD68$^+$ and CD163$^+$ could impact patient outcome we analysed the effect of macrophage density on OS (**Figure 3.6**). No significant correlations were seen in survival probability between tumours with or without CD68$^+$ macrophage infiltration or high or low CD163$^+$ macrophage infiltration (**Figure 3.6a-d**).

Previous studies have showed contrasting prognostic trends of CD68 M1-like and CD163 M2-like macrophages in other tumour types such as lung cancer and ovarian cancer [51,56]. Non-significant trends of increased intratumoural CD68$^+$ (p=0.2) and CD163$^+$ (p=0.052) macrophage density were associated with improved and worse survival respectively. These results are in line with previous literature which have failed to show a prognostic significance of TAM density in melanoma.

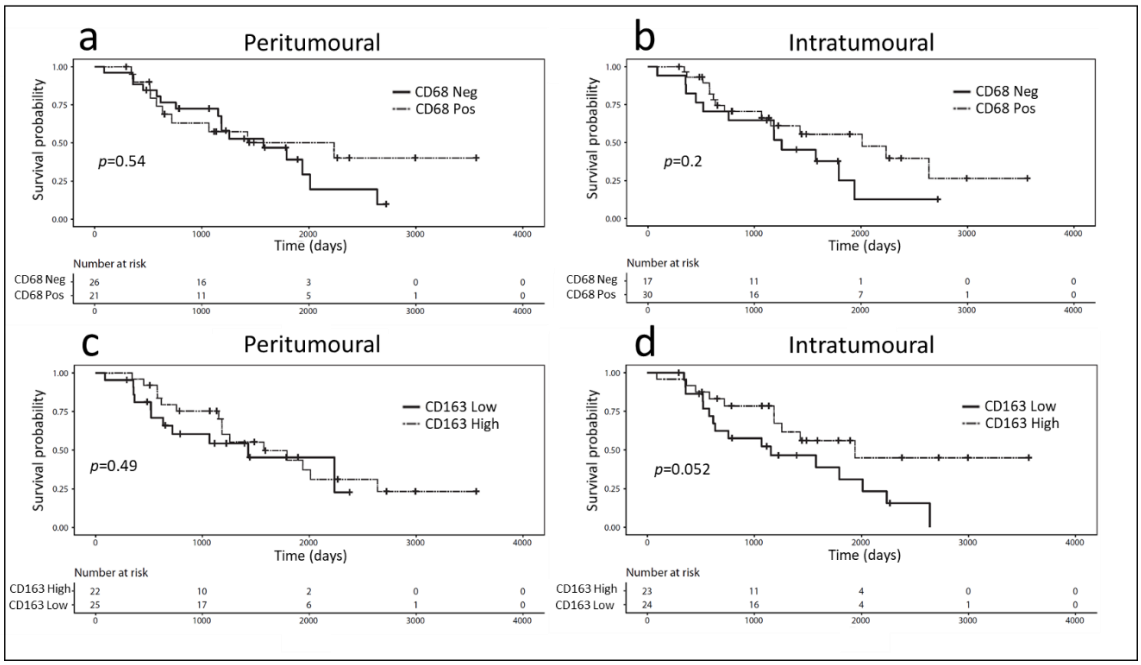

Figure 3.6 Correlation of CD68$^+$ and CD163$^+$ macrophage infiltration with OS

The number of peritumoural and intratumoural CD68$^+$ and CD163$^+$ macrophages were determined by immunohistochemistry in primary melanoma tumours. Patients were stratified based on the density of infiltrating macrophages and survival probabilities were predicted using Cox proportional hazards model, and visualised with a Kaplan-Meyer curve. Tumours were stratified as having CD68$^+$ macrophages (positive) or having no CD68$^+$ cells present (negative) (a-b). The level of CD163$^+$ infiltration was stratified as high or low (c-d). Survival probabilities were calculated using the Cox proportional hazards model and differences between groups were analysed using the log-rank test, n=57.

3.3.5 Correlation of iNOS$^+$ and arginase$^+$ cell infiltration with pathological features of melanoma

Having shown the effect of CD68$^+$ and CD163$^+$ macrophage infiltration, we next observed if the number of iNOS$^+$ or arginase$^+$ cells independently correlated to pathological features of the tumour (**Table 3.2).** There were no correlations with age, gender, Breslow depth, tumour stage, mitotic count or tumour infiltrating lymphocytes. BRAF positive tumours were found to have significantly increased levels of peritumoural and intratumoural iNOS$^+$ cells (**Figure 3.7a-b**). Ulceration and BRAF status correlated to the number of iNOS$^+$ and arginase$^+$ cells. Notably the presence of ulceration resulted in significantly reduced peritumoural and intratumoural iNOS$^+$ cells (**Figure 3.7c-d**) and the presence and size of ulceration was positively correlated to the number of arginase$^+$ cells (not shown).

Table 3.2 Association of pathological tumour features with iNOS$^+$ and Arginase$^+$ cell density, presented as significance values

	Arginase		**iNOS**	
	Peritumoural	**Intratumoural**	**Peritumoural**	**Intratumoural**
Age (years)	0.242	0.861	0.28	0.17
Gender	0.921	0.721	0.62	0.69
Breslow depth (mm)	0.947	0.671	0.4	0.2
Stage	0.894	0.482	0.09	0.16
BRAF status	0.416	0.693	**0.0002**	**0.0002**
Mitotic count (mm)	0.492	0.084	0.28	0.35
Ulceration (mm)	**0.00015**	0.416	0.15	0.67
Ulceration (Yes/No)	0.795	0.33	**0.008**	**0.005**
TIL distribution	0.278	0.582	0.96	0.77

The association of the number of arginase$^+$ and iNOS$^+$ cells with patient and tumour characteristics was determined using Wilcoxon Rank Sum test and Spearman Correlations. Data is presented as significance values, n=57. With significant correlations in bold text.

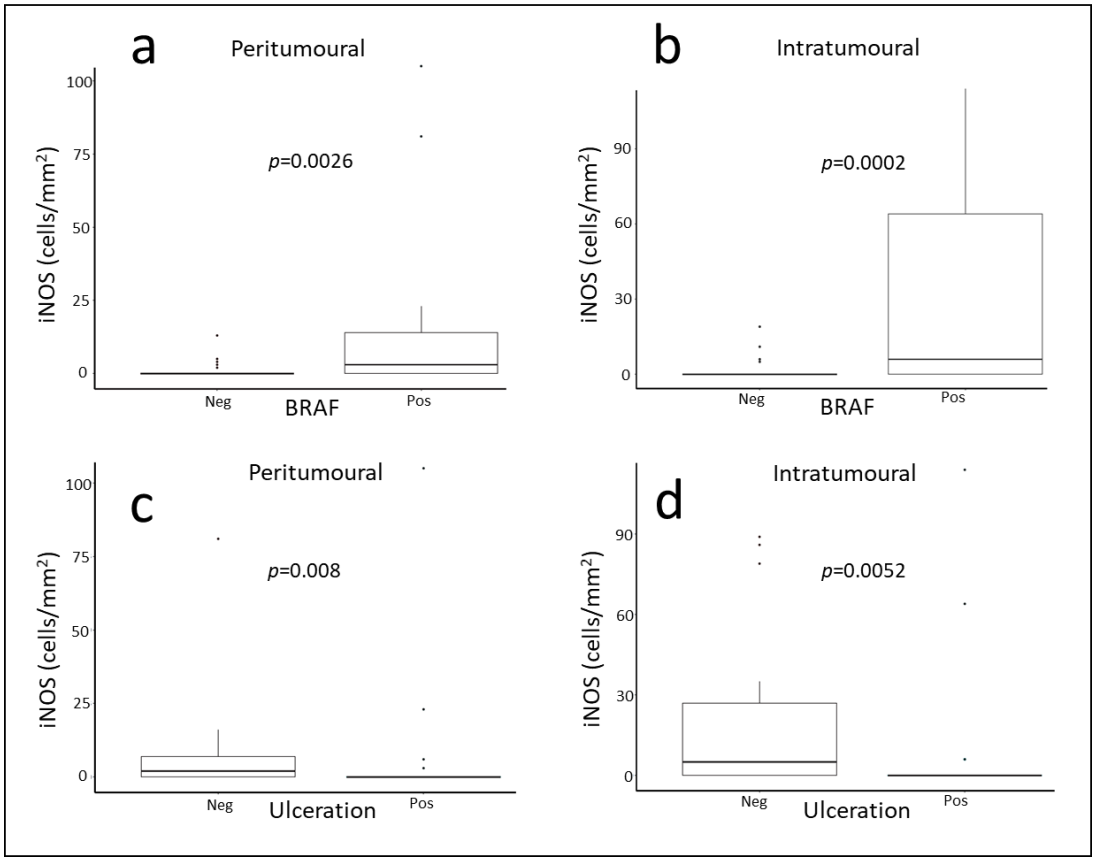

Figure 3.7 Correlation of iNOS$^+$ cell density with ulceration and BRAF status

The number of peritumoural and intratumoural iNOS$^+$ cells were determined by immunohistochemistry in primary melanoma tumours. Shown are significant correlations of iNOS$^+$ cell density with the pathological features BRAF status (a-b) and ulceration (c-d). Boxplots shown represent the mean, with interquartile ranges (boxes) and 95% confidence interval (whiskers), with outliers shown. Correlations with discrete variables were analysed using Wilcoxon Rank Sum tests. n=57.

3.3.6 Correlation of BRAF mutational status with CD68$^+$ macrophage recruitment and total intratumoural gene expression.

In addition to the positive correlations of CD68$^+$ macrophages with iNOS$^+$ cells and iNOS$^+$ cells with BRAF status, we found that there were a significantly higher number of CD68$^+$ macrophages in BRAF positive melanomas (**Figure 3.8b-c**). BRAF status had significant effects on gene expression within the tumour (**Figure 3.8a**). The genes affected by BRAF were independent from the subset affected by CD68$^+$ macrophage infiltration, with the exception of VCAM1 and Cyclin-dependent kinase inhibitor 3 (CDKN3), indicating distinct physiological regulation by CD68$^+$ infiltration and BRAF positivity. BRAF positive tumours had upregulated genes involved in angiogenesis, cell death and metabolism but down regulated genes associated with proliferation, cell cycle and inflammation.

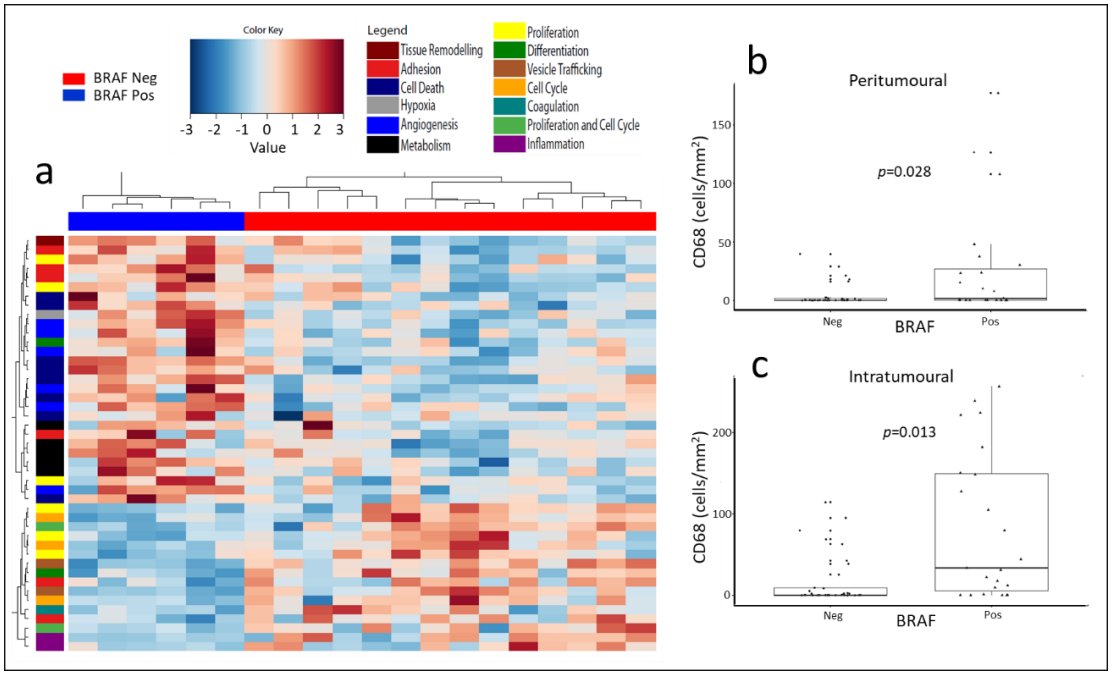

Figure 3.8 The effect of BRAF status on CD68$^+$ macrophage density and gene expression

The number of CD68$^+$ macrophages were determined by immunohistochemistry in primary melanoma tumours. a) Intratumoural gene expression of the same FFPE blocks was measured using next-generation sequencing technology. The BRAF status of samples is shown along the upper margin with BRAF mutation positive samples marked blue and BRAF negative samples marked red. Using Deseq2, genes differentially expressed based on BRAF status were identified. Gene associated signalling pathways are colour coded on the left hand margin. Using Wilcoxon rank sum tests it was shown there was a higher number of peritumoural and intratumoural CD68$^+$ macrophages in BRAF$^+$ tumours (b-c). Data was displayed using the Ward-Linkage method for significant genes from a database of 2550 oncology biomarker genes, n=20.

3.4 Discussion

Previous reports have cited CD68 as a pan-macrophage marker and CD163 as an M2-like macrophage marker [322]. Staining of primary melanoma specimens has shown that $CD68^+$ cells are significantly less prevalent than $CD163^+$ cells. In many melanomas there were no $CD68^+$ macrophages within tumours or peritumoural tissue, but there were high levels of $CD163^+$ macrophages across almost all cases. Thus, from our study, it is clear that CD68 is not a pan-macrophage marker in melanoma.

$CD68^+$ and $CD163^+$ macrophages represent distinct physiological subsets [323]. While M2 macrophages are commonly regarded as promoting disease progression we saw no evidence of a biological role of these cells except an accumulation of cells during disease progression, as seen by the positive correlation between intratumoural $CD163^+$ macrophages and Breslow depth. Despite the high numbers of $CD163^+$ cells (up to 1161 positive cells per mm^2), there was no correlation with an increase in $iNOS^+$ or $arginase^+$ cells, implying they do not align with traditional M1:M2 phenotyping. Furthermore they had no significant effect on gene expression within the tumour, indicating that a high number of these cells may not physiologically impact tumour biology. While there was a non-significant trend with reduced OS, it is possible that this trend is reflective of the increased Breslow depth of tumours with a high number of $CD163^+$ cells, and not an independent negative prognostic effect of the cells themselves [324].

Our study cohort was selected from patients who underwent routine BRAF status testing and was thus skewed towards advanced melanoma patients. Therefore the lack of observed correlations of macrophage markers with tumour stage cannot be meaningfully interpreted and will require analysis in an appropriately powered cohort. Previous investigations have suggested there is an increase in the density of $CD68^+$ macrophages in advanced tumour stages [325].

The contrasting trends of $CD68^+$ macrophages and $CD163^+$ macrophages against Breslow depth is striking in suggesting a differential expression pattern, albeit with the former being non-significantly correlated. There is much evidence that tumours exert a strong polarizing effect on recruited cells, and it remains to be determined whether the $CD68^+$ and $CD163^+$ infiltration is reflective of differential recruitment, or a system in which $CD68^+$ cells are recruited and polarized to a $CD163^+$ phenotype

which is less functionally active in the parameters we observed, such as arginase and iNOS activity and influencing gene expression within the tumour [326-328]. This system would explain both the increased prevalence of $CD68^+$ macrophages in less progressed tumours and increased accumulation of $CD163^+$ macrophages in more advanced tumours. Previous reports have shown that there is a continuous supply of monocytes to diverse tumour types, even tumours such as pancreatic ductal adenocarcinoma which has a dense desmoplastic barrier surrounding the tumour tissue that can impair cell infiltration, and that tumours exert a strong polarizing effect on TAMs to a more M2-like phenotype [174,149,329,330].

A high density of intratumoural and peritumoural $CD163^+$ macrophages were detected in many tumours however this failed to translate into a difference in global gene expression within the tumour tissue. Previous reports have shown an association between $CD163^+$ macrophage infiltration and angiogenesis and cyclooxygenase-2 expression [331]. Specific analysis of these genes with unadjusted *p* values, which may not have been detected by DESeq2 analysis of total gene expression datasets, showed no correlation of $CD163^+$ macrophage density with the expression of the genes VEGFA/B/C, ANGPT1/2 or PTGS1/2.

The strong positive correlations between $CD68^+$ macrophage infiltration and the number of $iNOS^+$ cells gives strong reason to suggest that these cells are more M1-like cells [332]. However the positive correlation with $arginase^+$ cells is more surprising but possibly representative of a more immunologically active subset capable of a range of responses [333].

This argument is upheld by the effect of $CD68^+$ macrophage infiltration on gene expression within the tumour, in which increased infiltration can impact genes involved in a range of processes such as cell death and cell cycle in addition to the role of regulation of inflammation.

While no correlation of $CD68^+$ or $CD163^+$ cell density was found on overall survival, non-significant trends were seen which align with previous observations in other tumour types in which $CD68^+$ cells can be associated with improved prognosis and $CD163^+$ cells can be associated with worse prognosis in a range of solid malignancies [310].

The increased presence of $CD68^+$ cells and inflammatory markers in $BRAF^+$ tumours, could indicate that BRAF status may play a role in determining the response of patients to immunotherapies or immunogenic treatments. Recently $CD68^+$ macrophages have been found to promote tumour hypoxia and drive resistance to anti-PD-1 antibodies in murine models [334]. Conversely, M1-like $CD68^+$ macrophages were also found to potentiate the synergistic effects of VEGF inhibitors with BRAF inhibitors in murine melanoma [335]. However, clinically CD68 has been found to be a biomarker of response to Ipilimumab [108]. Melanoma patients with BRAF mutations were found to have a longer progression free survival and higher overall survival in response to Nivolumab, with or without Ipilimumab, thus $CD68^+$ macrophages may potentiate the favourable effect of BRAF status during treatment with immunotherapies [336].

While the two were positively associated, the different genes affected by BRAF status and the presence $CD68^+$ macrophages indicate non-redundant roles of BRAF status and $CD68^+$ cell infiltration. The p53-DREAM pathway genes CDKN3, DEP domain containing 1 (DEPDC1), Survivin, BRCA1 interacting protein C-terminal helicase 1 (BRIP1), Replication factor C subunit 4 (RFC4) were all strongly associated and down regulated in tumours with intratumoural $CD68^+$ macrophage infiltration [337]. None of these genes were affected by BRAF status, indicating that this pathway is regulated by macrophages.

The highly active functional phenotype of $CD68^+$ macrophages may indicate $CD68^+$ macrophages may be a more viable therapeutic target for therapies looking to boost or interfere with TAM behaviour. Previous clinical interventions have targeted CSF1R due to the increased prevalence of this receptor and the quality of antibodies which can be raised against this target [310]. As CSF1R is a G-protein-coupled receptor (GPCR) the opsonisation and depletory effects of targeting are augmented by the inhibition of survival signalling in targeted cells [338-340]. Therapeutic targeting of CD68 cells has been impeded by the discrepancies between human CD68 and its murine homolog, macrosialin, which is not restricted to monocytic cells in mice [341]. However, CD68 has been shown to represent differential macrophage subsets to both CSF1R and CD163 and thus depletion of $CD68^+$ macrophages, if cell specific targeting could be achieved, could improve therapeutic outcomes [342-344].

While CD68 has commonly been recognised as a specific monocyte and macrophage marker, a major issue with targeting of CD68 is its wide expression in a number of cell types [341]. Immunohistochemical analysis and RNA sequencing have shown that CD68 levels on fibroblasts and endothelial cells can match levels shown on macrophages, and lower levels can be also be detected on tumour cell lines and lymphoid cells [342]. This presents major challenges for the effective specific targeting of $CD68^+$ macrophages therapeutically. There is merit in investigating if other interventions can be developed which can boost the activity or number of $CD68^+$ macrophages in the TME. However these results do suggest a hypothesis for the clinical failure of anti-CSF1R antibodies, which do not distinguish between $CD68^+$ and $CD163^+$ macrophages, and in which the majority of targeted cells are likely to be less functionally active.

Chapter 4

The development of a preclinical model for the study of melanoma conditioned macrophages

Results from this chapter have been published as;

Tremble LF, Moore AC, Forde PF (2019) Melanoma conditioned medium promotes cytotoxic immune responses by murine bone marrow derived monocytes despite their expression of 'M2' markers. Cancer Immunology, Immunotherapy. 2019 Sep;68(9):1455-1465.

4.1 Abstract

Macrophages have been shown to infiltrate a wide range of malignancies and are often considered to promote tumour survival, growth and spread. However, the source and behaviour of discrete tumour associated macrophage populations are still poorly understood. Here we show a novel method for the rational development of bone marrow derived monocytes appropriate for the study of processes which involve the contribution of circulating inflammatory monocytes. We have shown that in response to tumour conditioned medium these cells upregulate CD206 and CD115, markers traditionally associated with M2-type macrophages. Treated cells show reduced capacity for cytokine secretion but significantly impact $CD4^+$ and $CD8^+$ T cell proliferation and polarization. Coculture with conditioned bone marrow derived monocytes significantly reduced $CD4^+$ T cell proliferation but increased $CD8^+$ T cell proliferation and granzyme B expression with significant induction of IFNγ secretion by both $CD4^+$ and $CD8^+$ T cells, indicating that these cells may have a role in promoting anti-cancer immunity.

4.2 Introduction

The difficulties of *in vitro* macrophage research have been documented at length [24]. At its heart are the inadequacies of current models and uncertainty over whether they translate to *in vivo* physiological behaviour [345].

In vivo research of macrophages continues to question basic physiological questions such as the native activation state of macrophage populations, the source of distinct macrophage populations and the epigenetic or other differences between macrophage populations that may influence their behaviour in response to specific environmental stimuli, all of which may affect the relevancy of previously published literature.

The M1 M2 dichotomy of macrophage polarization has been widely used in cancer research, with M1 macrophages considered to promote anti-cancer immune responses and M2 macrophages supporting tumour survival, growth and spread. TAMs are generally considered to be M2-like in nature and thus a negative presence in tumour biology. This has been supported by a wide range of studies evaluating the presence and phenotypes of macrophages in human cancers, whereby TAMs express M2 markers and have been associated with poorer prognostic outcomes, with the exception of colorectal and gastric cancers [310].

The protocols used for the generation of bone marrow derived monocytes and macrophages differ widely across the literature. Limited guidelines are available for the development of BMDMs, including the growth factors to be used and the source of cells [24]. It has been suggested these guidelines in combination with comprehensive reporting standards will aid the process of unifying experimental protocols and increase the comparability and reproducibility of published research. However, there are still a wide range of protocol aspects which vary and which have significant impacts on the resultant populations [303,316,346].

Monocytes develop into macrophages, however the distinction between monocyte and macrophage populations is unclear. Current theories suggest that monocytes migrate from the bone marrow to the circulation and exist as two distinct populations. One population are primed for inflammatory responses, these cells have been referred to as inflammatory monocytes and are defined as $CD11b^{+}$ $Ly6G^{-}$ $Ly6C^{hi}$ and $CCR2^{+}$. A second population defined as $CD11b^{+}$ $Ly6C^{+}$ and $CCR2^{-}$ are commonly referred to as non-classical monocytes and are primed for M2 responses [347]. It has been suggested

that inflammatory monocytes over time or in the absence of inflammatory stimuli evolve into non-classical monocytes [348].

In addition to functional differences, these cells also differ in migration potential. Inflammatory monocytes rely on CCR2 to home towards the sites of inflammation whereas non-classical monocytes rely predominantly on CX3C chemokine receptor 1 (CX3CR1) and C-C chemokine receptor type 5 (CCR5) expression to direct their homing capacity [349]. Both populations are likely to accumulate at tumour sites due to leaky vasculature and tumour expression of CCL2, chemokine CX3C motif ligand 1 (CX3CL1) and Regulated on activation, normal T cell expressed and secreted (RANTES, also known as CCL5), the reciprocal ligands for CCR2, CX3CR1 and CCR5 respectively. However, it is intuitive that variations will exist between tumour types and tumour models, depending on ligand expression and tumour accessibility and penetrability. Studies examining the presence of monocytes and macrophages in tumour lesions have frequently reported the presence of TAMs which have an M2-like phenotype, as was observed in chapter 3. This may in part be due to the shorter half-life of inflammatory monocytes, recruitment of TAMs from tissue resident subsets rather than circulating monocytes, selective proliferation of M2-like TAMs in the tumour microenvironment or conditioning by the tumour of monocytes to an M2-like phenotype.

From a tumour immunology point of view the relative contribution of these factors is poorly defined and may vary significantly between tumour types, but circulating monocytes have been shown to infiltrate murine tumours [350].

The type of model in use must also be taken into consideration. Differences exist between murine and human cell types, including macrophages, in which cell markers can vary significantly [343,351]. The translation of murine models to human disease contains inherent limitations. Efforts to decrease these limitations include the use of orthotopic tumour models and the use of human cell lines in immunocompromised mice, however differences in murine anatomy and the absence of a competent immune system still limit the relevance of these models [352-355]. It is still common to use subcutaneous tumour models in mice [356,357].

There are a limited number of cell lines available for the study of murine melanoma. Many commonly cited cell lines derivate from a common B16 progenitor, and do not

contain BRAF mutations as is commonly reported in human disease [289]. Other cell lines have more recently been developed, such as the YUMM lines, which offer a selection of transgenic variants for targeted research [288]. The B16F10 cell line is one of the most cited murine melanoma cell line due to its aggressive nature in which it easily and quickly metastasizes *in vivo* [289,291]. However, the cell line is poorly immunogenic and is commonly transfected with ovalbumin in order to facilitate antigen specific cytotoxic $CD8^+$ T cell responses [358]. Subcutaneous B16F10 tumours have previously been shown by histologic examination to be infiltrated by a wide range of immune cells including $CD68^+$ and $CD206^+$ macrophages [359,360].

The nature of monocytes and macrophages infiltrating a tumour are likely to impact their functional contribution to tumour biology, thus for each tumour type and tumour model this must be individually assessed.

Here we present a concept to bench process for the rational development of an *in vitro* model for the study of monocytes and macrophages in a murine model of melanoma. We show the effect of tumour conditioning on these cells and their role in anti-cancer immunity.

4.3 Results

4.3.1 Prevalence of inflammatory monocytes during murine disease

Melanomas are one of the most immunogenic cancer types characterized by a high volume of tumour infiltrating leukocytes, and are consequently considered one of the tumours most likely to benefit from immunotherapy [361]. B16F10 cells are a highly aggressive cell line which can be used for the study of murine melanoma. Injected subcutaneously they readily form primary tumours which metastasise. We used this model of tumour growth to examine the role of TAMs in murine melanoma. Circulating monocytes were analysed during tumour growth (**Figure 4.1**). Monocytes were gated as $CD11b^{+}$ $F4/80^{+}$ $Ly6G^{-}$ and distinguished as $Ly6C^{+}$ $CCR2^{-}$ or $Ly6C^{-}$ $CCR2^{-}$ non-inflammatory monocytes or as $Ly6C^{hi}$ $CCR2^{+}$ inflammatory monocytes (**Figure 4.1**).

Inflammatory monocytes were found to be present in circulation and increased as a proportion of total $CD11b^{+}$ $F4/80^{+}$ $Ly6G^{-}$ monocytes during disease progression ($p<0.01$)(**Figure 4.1**). The proportion of other $CD11b^{+}$ $Ly6G^{-}$ monocytes decreased during tumour progression ($p<0.01$). B16F10 tumours were excised, washed and plated for 24hrs, tumours were confirmed to secrete CCL2 (>1000pg/ml/10^{6} cells, data not shown), the primary chemoattractant for CCR2.

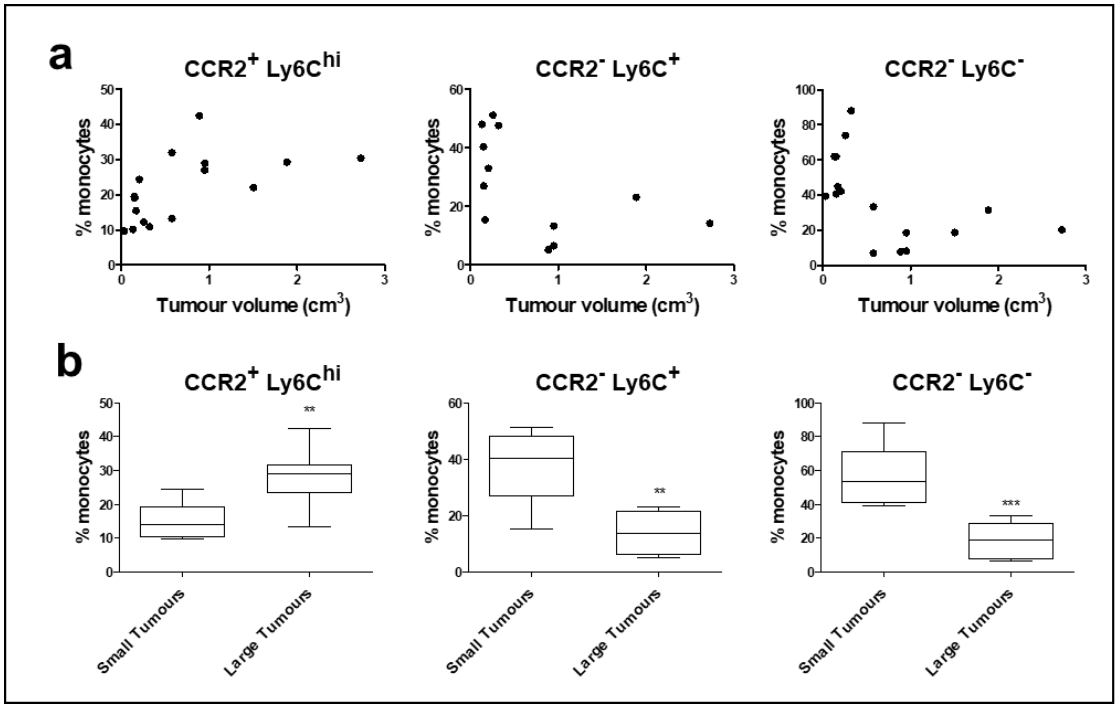

Figure 4.1 Circulating monocyte populations in subcutaneous B16F10 tumour bearing mice

Mice were subcutaneously inoculated with B16F10 cells. At various points of tumour development blood was isolated and analysed by flow cytometry. Monocytes were gated according to forward scatter, side scatter and as $CD11b^+$, $F4/80^+$ and $Ly6G^-$. a) Scatter plots of tumour size against the relative proportion of $CCR2^-$ $Ly6C^{hi}$ (left) $CCR2^-$ $Ly6C^+$ (middle), and $CCR2^-$ $Ly6C^-$ (right) in the blood. b) Box plots of the data shown in (a) showing the proportion of cells when stratified between small ($<0.5cm^3$) and large ($>0.5cm^3$) tumours. Data shown is representative of n=6 per group. ** $p<0.01$ ***$p<0.001$ compared to small tumours.

4.3.2 Development of BMDMs enriched for inflammatory monocyte-like cells

In line with the three R's of animal research, replacement, reduction and refinement, we next sought to develop monocytes *in vitro* from murine bone marrow which reflect the cells previously seen *in vivo* (**Figure 4.1**) [362]. Bone marrow was cultured in the presence of 50ng/ml M-CSF and analysed by flow cytometry daily to track their development (**Figure 4.2**). Monocytic cells were defined as $CD11b^+$ $CD115^+$ $F4/80^+$ and with varying CCR2 and Ly6C expression [348]. Analysis of CD11b versus Ly6C allowed the identification of distinct monocyte subsets.

The proportion of monocyte subsets varied between suspension and adherent populations, however once grouped on Ly6C and CD11b expression, other cell markers remained consistent indicating homogeneity of adherent and suspension populations, as such all cells were harvested for further use.

By day 5 non-monocytic $CD11b^{-}$ $Ly6C^{-}$ cells composed just 3 ± 1% of total cells. $CD11b^{+}$ $Ly6C^{+}$ cells were negative for CD115 and F4/80 (**Figure 4.3**) and are likely to represent an immature population of monocytic cells at a midway point to development, by day 5 however they represented a minimal proportion of the population at 10 ± 3%.

$CD11b^{hi}$ $Ly6C^{-}$, $CD11b^{hi}$ $Ly6C^{+}$ and $CD11b^{+}$ $Ly6C^{hi}$ populations were all positive for CD115 and F4/80 (**Figure 4.3**). F4/80 is a murine marker of monocytes which is present on monocytes and highly expressed on macrophages. $CD11b^{+}$ $Ly6C^{hi}$ cells most accurately reflected inflammatory monocyte populations with CCR2 positivity and were $Ly6G^{-}$ (**Figures 4.4-4.5**). These cells peaked in frequency at day 4, after which a gradual decline was seen from day 5 to day 7.

In order to study the effect of tumour conditioning on peripheral monocytes infiltrating into the tumour, day 5 BMDMs were used which were comprised of 78 ± 3% $CD11b^{hi}$ $Ly6C^{-}$cells, 3 ± 1% $CD11b^{hi}$ $Ly6C^{-}$cells and 8 ± 0.07% inflammatory monocyte-like $CD11b^{+}$ $Ly6C^{hi}$ cells. Thus monocytic subsets represented 89 ± 4% of cell populations used for subsequent experiments.

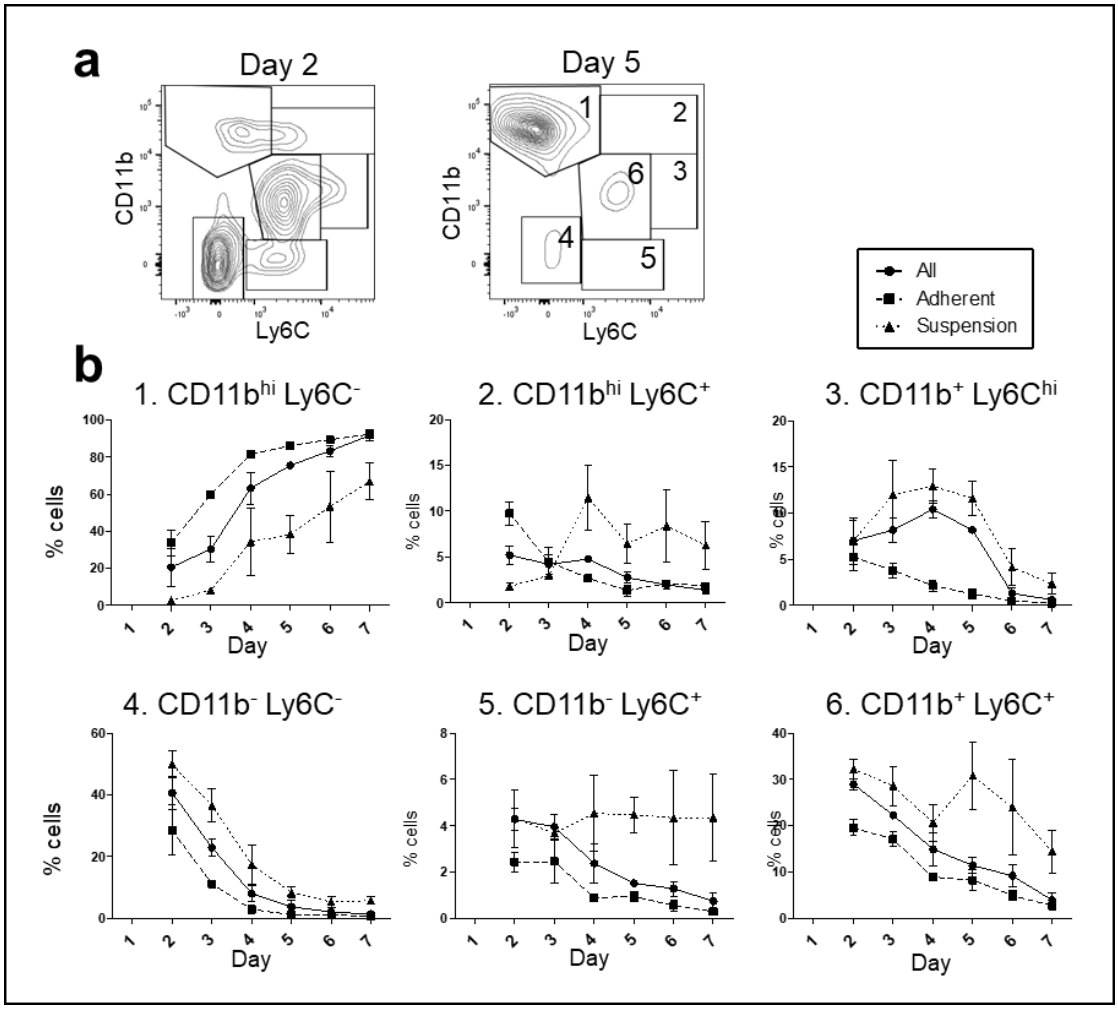

Figure 4.2 The development of bone marrow derived monocytes

Bone marrow was isolated and following RBC lysis was cultured in the presence of 50ng/ml M-CSF for between 2 and 7 days. a) Representative graphs showing CD11b and Ly6C expression of whole BMDM populations on day 2 (left) and day 5 (middle). b) Adherent only, suspension only and mixed populations were each analysed by flow cytometry from day 2 to day 7 to track the development of BMDMS. Populations shown correspond to the gating shown in (a). Data shown is representative of an n=3 per group.

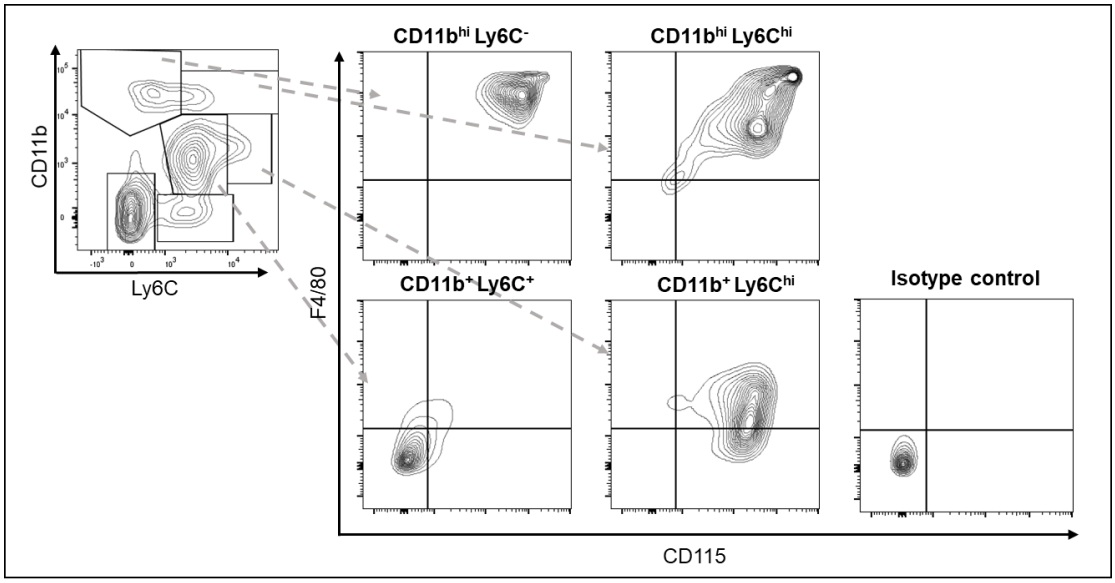

Figure 4.3 CD115 and F4/80 expression of BMDM subpopulations

Bone marrow was isolated and following RBC lysis was cultured in the presence of 50ng/ml M-CSF for 5 days. Shown are representative flow cytometry graphs showing the F4/80 and CD115 expression of the four monocytic populations identified in **figure 4.2a**, along with isotype control staining.

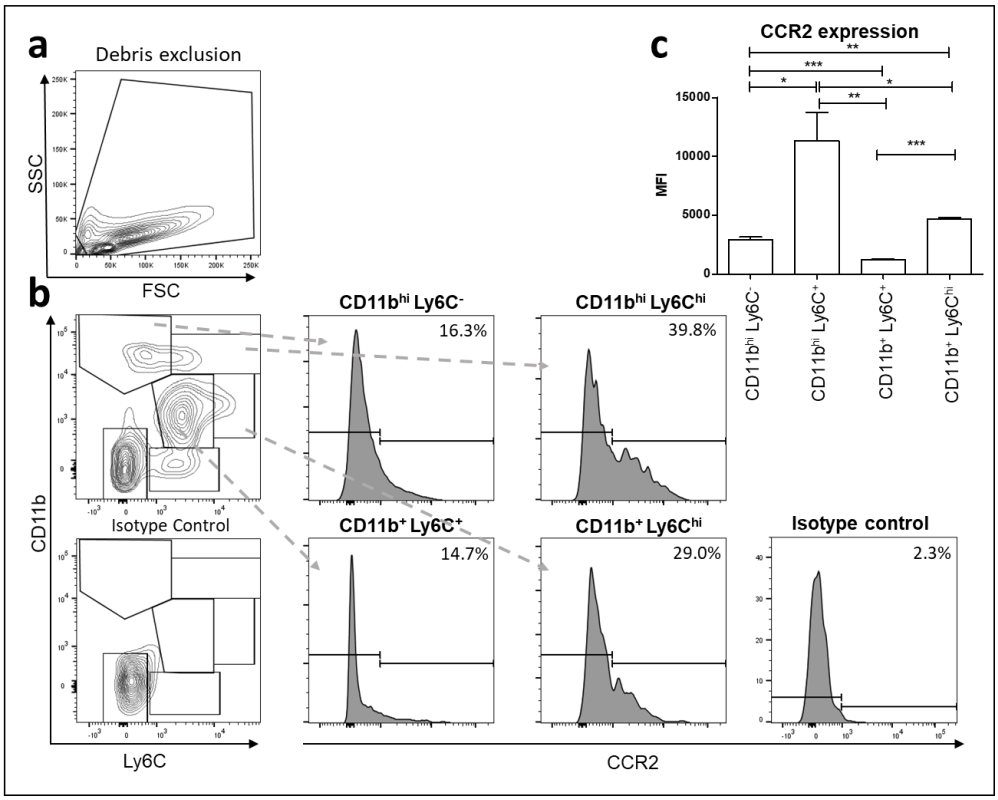

Figure 4.4 CCR2 expression of BMDM subpopulations

Bone marrow was isolated and following RBC lysis was cultured in the presence of 50ng/ml M-CSF for 5 days. a) Flow cytometry graphs showing the forward scatter and side scatter gating strategy used to gate BMDMs in **figure 4.2**. b) CCR2 expression of the four monocytic populations identified in **figure 4.2a**. c) Bar chart showing the mean CCR2 fluorescent intensity of the monocytic populations shown in (b).

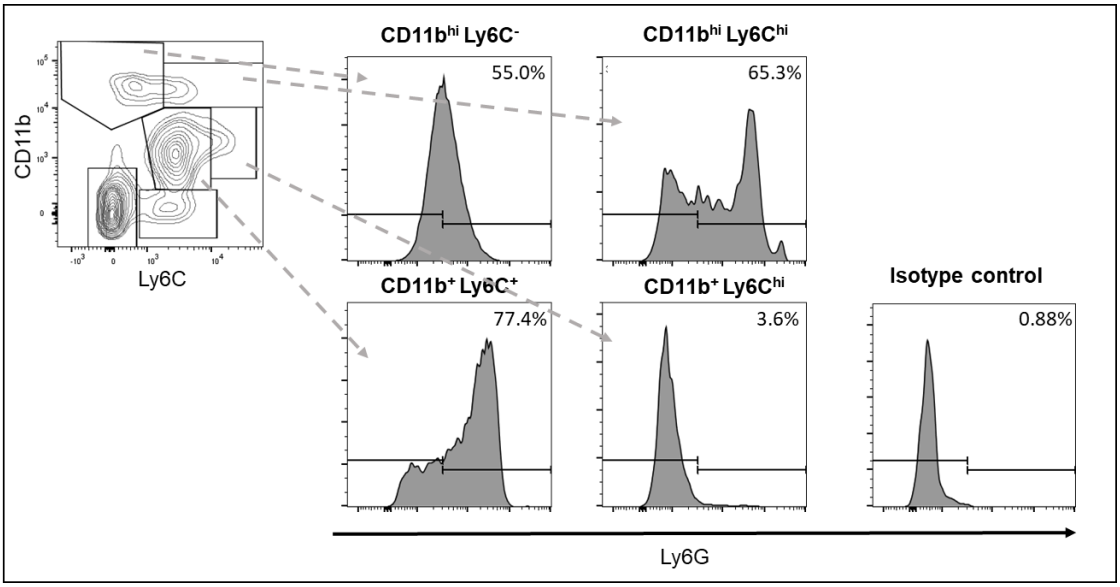

Figure 4.5 Ly6G expression of BMDM subpopulations

Bone marrow was isolated and following RBC lysis was cultured in the presence of 50ng/ml M-CSF for 5 days. Shown are representative flow cytometry graphs showing the Ly6G expression of the four monocytic populations identified in **figure 4.2a**, along with isotype control staining.

4.3.3 The effect of melanoma conditioning on BMDM surface markers

To study the effect of tumour conditioning on monocytes we treated BMDMs with concentrated melanoma conditioned medium derived from B16F10 cells, termed B16 conditioned medium (B16CM). As this contained a low level of serum, which has been shown to influence macrophage polarization, our no treatment negative controls were treated with an equivalent amount of ultracentrifuged medium with serum which was not exposed to B16F10 cells. To clarify this distinction we have labelled our no treatments as 'no treatment concentrated medium' (NTCM) [363]. Of note, FCS has been documented to contain varying cytokines, chemokines, growth factors and extracellular vesicles, all of which can influence macrophage polarization. To control for this the FCS for each experiment was derived from the same batch and the same stock solution.

Treatments with either IFNγ and Lipopolysaccharide (LPS) or interleukin 4 (IL-4) and interleukin 13 (IL-13) were included as M1 and M2 controls, while their biological relevance is questionable, they have been included as assay positive controls and to give the results presented here context in comparison to other similar literature.

B16CM increased the expression of the 'M2' marker CD206 on $CD11b^+$ cells, although not to the extent of IL-4 and IL-13 conditioned BMDMs (**Figure 4.6a**) [364]. B16CM was also shown to increase CD115 expression on $CD11b^+$ cells to a similar extent as treatment with IL-4 and IL-13.

To determine if this apparent 'M2'-like shift was reflected in arginine metabolism which has been proposed as a central feature of the M1 M2 dichotomy, we determined the arginase activity of cell lysates and the secretion of nitrate species (**Figure 4.6b-c**). B16CM increased arginase activity but was significantly lower than IL-4/IL-13 treated BMDMs and comparable to IFNγ/LPS treated BMDMs. All populations fell below the detectable limit of nitrate detection indicating little or no iNOS activity in these cells, except for IFNγ/LPS treated BMDMs.

Thus while B16CM treated BMDMs showed indication of an M2-like phenotype by CD206 and CD115 expression, supported by the absence of nitric oxide species secretion, the arginase activity was comparable to IFNγ/LPS treated M1-like BMDMs and not IL-4/IL-13 treated M2-like BMDMs.

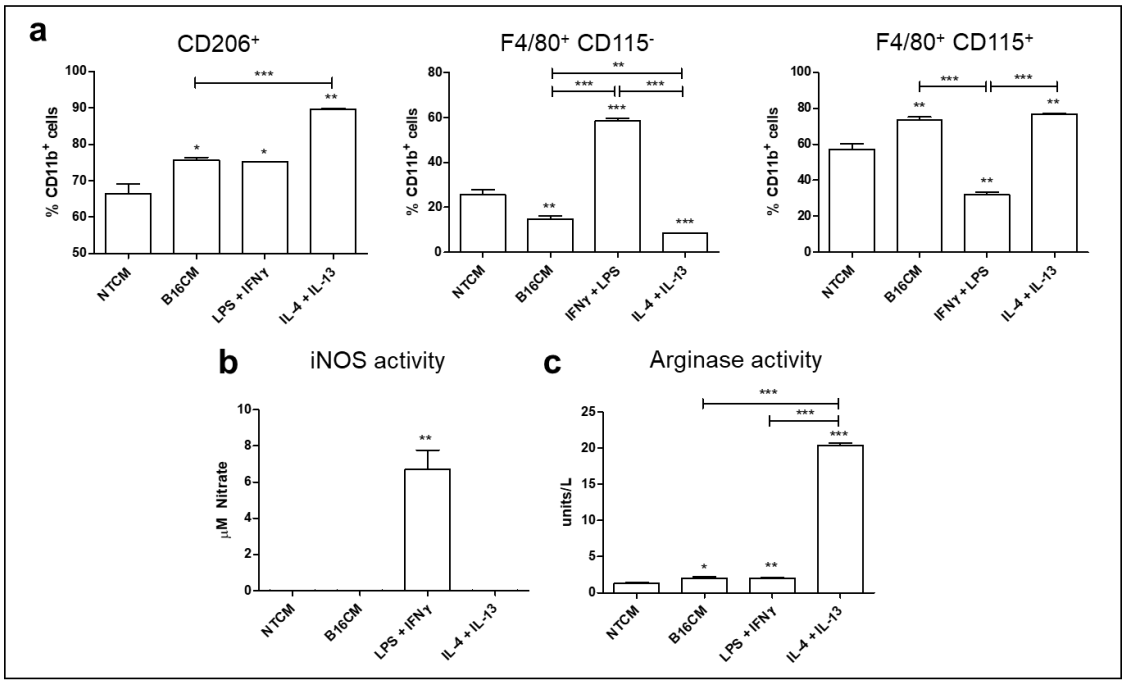

Figure 4.6 The effect of B16CM on the expression of CD206 and CD115 and activity of iNOS and Arginase by BMDMs

BMDMs were treated on day 5 with NTCM, B16CM, IFNγ/LPS or IL-4/13 for 24hrs. a) Cells were analysed by flow cytometry to determine the level of CD206 expression or CD115 expression on $CD11b^+$ BMDMs. b) Culture supernatants were analysed by Griess assay to determine the levels of iNOS activity c) Arginase activity was measured in cell lysates following treatment. Data was analysed using paired student's t-tests. Data shown is representative of an n=3 per group. * $p<0.05$, ** $p<0.01$, *** $p<0.001$ compared to NTCM unless specified.

4.3.4 The effect of melanoma conditioning on BMDM gene expression

In order to determine the functional phenotype of these BMDMs we next evaluated the gene expression of BMDMs 4hrs and 24hrs following treatment.

CD68 is a scavenger receptor expressed by monocytes and macrophages, which can be upregulated during activation [365]. In addition to the increase in surface markers CD206 and CD115 previously shown (**Figure 4.6**), gene expression of the surface markers, CD206 and CD68, were both shown to be increased by B16CM treatment after 4hrs and an increase in CD68 expression was still visible at 24hrs (**Figure 4.7a**).

Analysis of *ARG1* gene expression, the inducible form of arginase commonly seen in 'M2' macrophages, and stained for in chapter 3, revealed no observable increase in expression and at 24hrs a significant decrease was observed (**Figure 4.7b**).

No change in IL-10, IL-12 or IL-6 expression was found after B16CM treatment. IL-4/IL-13 treatment was shown to induce expression of TGFβ at 4hrs after treatment and IL-6 24hrs after treatment. IFNγ/LPS treatment showed no effect on TGFβ expression but increased IL-10, IL-12 and IL-6 expression 4hrs after treatment. The inflammatory genes IL-6 and IL-12 were still significantly increased 24hrs following treatment.

Ym1 is a protein which has been linked to invasion. B16CM treatment was shown to reduce Ym1 expression after 24hrs and was significantly lower than IL-4 and IL-13 treated BMDMs and IFNγ/LPS treated BMDMs after 4hrs.

Thus, while B16CM was shown to impact surface marker expression by flow cytometry and qPCR, there was very little change in the expression of functional cytokines and enzymes.

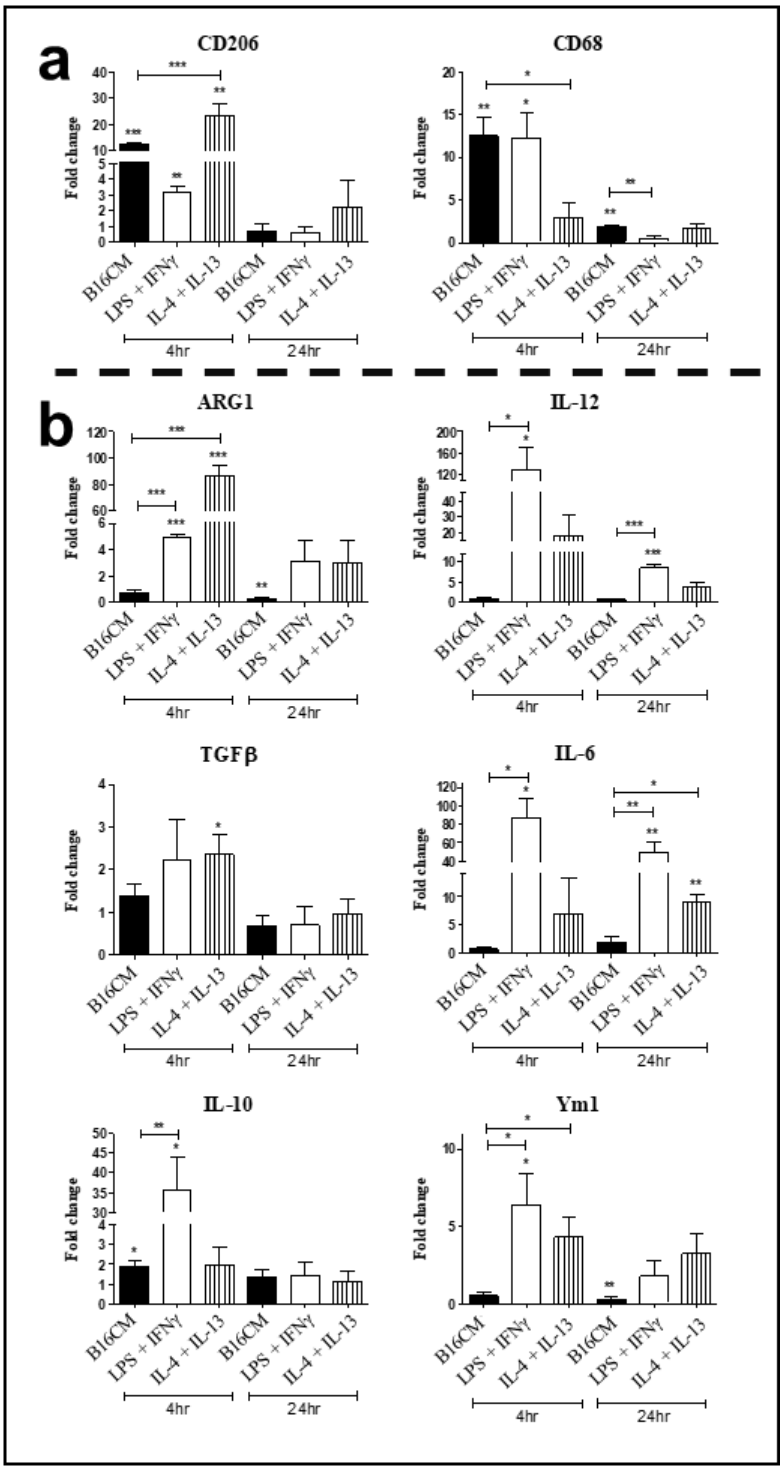

Figure 4.7 The effect of B16CM on gene expression of BMDMs

BMDMs were treated on day 5 with NTCM, B16CM, IFNγ/LPS or IL-4/13 for 4 or 24hrs. Total RNA was isolated and analysed for relative gene expression by qPCR. Results were normalized to NTCM only. a) Gene expression for the surface receptors CD206 and CD68 was measured following treatment. b) Gene expression of the functional proteins ARG1, TGFβ, IL-10, IL-12, IL-6 and Ym1 was measured following treatment. Data shown is representative of an n=3 per group. Data was analysed using paired student's t-tests. * $p<0.05$, ** $p<0.01$, *** $p<0.001$ compared to NTCM (a mean value of 1 in all graphs due to normalization of data) unless specified.

4.3.5 The effect of melanoma conditioned BMDMs on $CD4^+$ T cell responses

To determine if the limited functional capacity seen in gene expression would translate to a reduced influence in determining tumour immunology we next sought to identify the effect of B16CM treated BMDMs on $CD4^+$ T cell activity (**Figure 4.8**).

NTCM treated BMDMs were able to induce the proliferation of $CD4^+$ T cells, to a similar level as IL-4/IL-13 treated BMDMs, however B16CM treated BMDMs significantly decreased the proportion of activated T cells.

Analysis of culture supernatants showed NTCM, B16CM and IFNγ/LPS treated BMDMs failed to generate IL-4 secretion by $CD4^+$ T cells, however IL-4/IL-13 treated BMDMs resulted in a significant increase in IL-4 secretion.

While macrophages were able to directly secrete IFNγ (shown in grey, **Figure 4.8d**, $p<0.05$), coculture revealed significant additional IFNγ secretion from $CD4^+$ T cells across all conditions. B16CM treated BMDMs significantly increased secretion of IFNγ compared to NTCM and IL-4/13 treated BMDMs but not to the extent of IFNγ/LPS treated cells.

Flow cytometric analysis of activated $CD4^+$ T cells showed the induction of CXCR3 and CD25 on $CD4^+$ T cells by NTCM treated BMDMs. B16CM treated cells resulted in a decrease of $CXCR3^+$ T cells but had no effect on the number of $CD25^+$ T cells. Both IFNγ/LPS and IL-4/IL-13 treated BMDM cocultures resulted in significantly lower numbers of $CD25^+$ and $CXCR3^+$ T cells compared to NTCM treated cells. The trend indicated they were also lower than T cells cocultured with B16CM treated cells, however this trend was only significant for the expression of CXCR3 T cells cocultured with IFNγ/LPS treated BMDMs.

While B16CM treated BMDMs reduced $CD4^+$ T cell proliferation and the level of activated T cells positive for the Th1 marker CXCR3, they also increased IFNγ secretion which is central to driving Th1 type anti-cancer immune responses. To further investigate the effect on the anti-tumour immune response we investigated the effect of treated BMDMs directly on $CD8^+$ T cells.

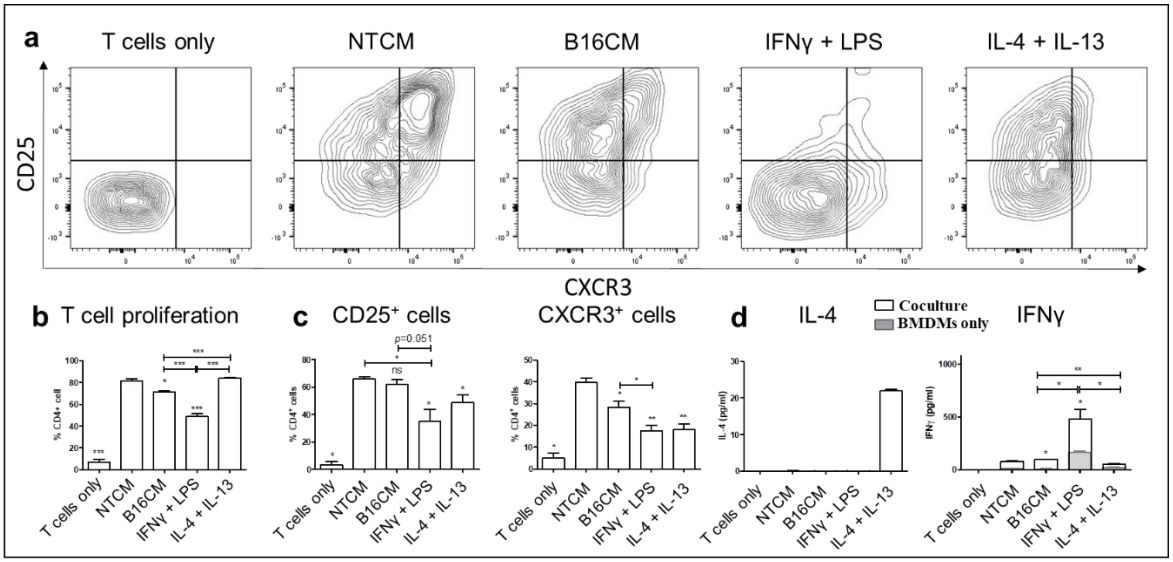

Figure 4.8 The effect of treated BMDMs on CD4$^+$ T cell expansion and polarization

Day 5 BMDMs were treated for 24hrs. Following treatment the cells were washed twice and cocultured with freshly isolated CFSE labelled splenic CD4$^+$ T cells from syngeneic mice for 7 days. Cells were analysed by flow cytometry and supernatants were analysed by ELISA. a) T cells were gated for by CD4 expression. Shown are representative graphs of CXCR3 against CD25 for each of the treatment groups. b). CD4$^+$ T cell proliferation was determined by reduced CFSE staining. c) Bar charts showing the number of CD25$^+$ and CXCR3$^+$ CD4$^+$ T cells determined using the gating shown in (a). d) Shown in white bar charts are the IL-4 and IFNγ levels in supernatants following coculture, overlaid in grey are the level of the same cytokines following culture of treated BMDMs alone. Data shown is representative of an n=3 per group. Data was analysed using paired student's t-tests * p<0.05, ** p<0.01, *** p<0.001 compared to NTCM unless specified.

4.3.6 The effect of melanoma conditioned BMDMs on $CD8^+$ T cell responses

To determine if B16CM treated BMDMs could have an effect on cytotoxic $CD8^+$ T cell behaviour we examined the proliferation of $CD8^+$ T cells cocultured with treated BMDMs.

B16CM treated BMDMs were shown to significantly increase the proliferation of $CD8^+$ T cells in comparison to NTCM, IFNγ/LPS and IL-4/13 treated cells. IFNγ/LPS and IL-4/13 treated cells had no significant impact on $CD8^+$ T cell expansion (**Figure 4.9**).

Along with increased $CD8^+$ T cell proliferation, B16CM treated BMDMs were found to increase the granzyme B levels of $CD8^+$ T cells. This increase was above the level seen following coculture with either IFNγ/LPS or IL-4/13 treated BMDMs indicating that B16CM treated BMDMs may prime $CD8^+$ T cells for cytotoxic responses.

All BMDMs were found to stimulate secretion of IFNγ by $CD8^+$ T cells. B16CM significantly increased IFNγ secretion, and this was also significantly higher than that induced by IL-4/IL-13 treated BMDMs, but was over 10 fold less than IFNγ secreted by cells cocultured with IFNγ/LPS treated BMDMs.

Although B16CM treated BMDMs in coculture significantly increased IL-10 levels compared to T cells alone this was lower than the levels seen by B16CM treated BMDMs alone in culture. This trend was seen in cocultures with all BMDM treatments except for cocultures with IFNγ/LPS treated BMDMs which were significantly higher following inclusion of T cells ($p<0.01$) indicating $CD8^+$ T cell secretion of IL-10 is absent except when cocultured IFNγ/LPS treated BMDMs.

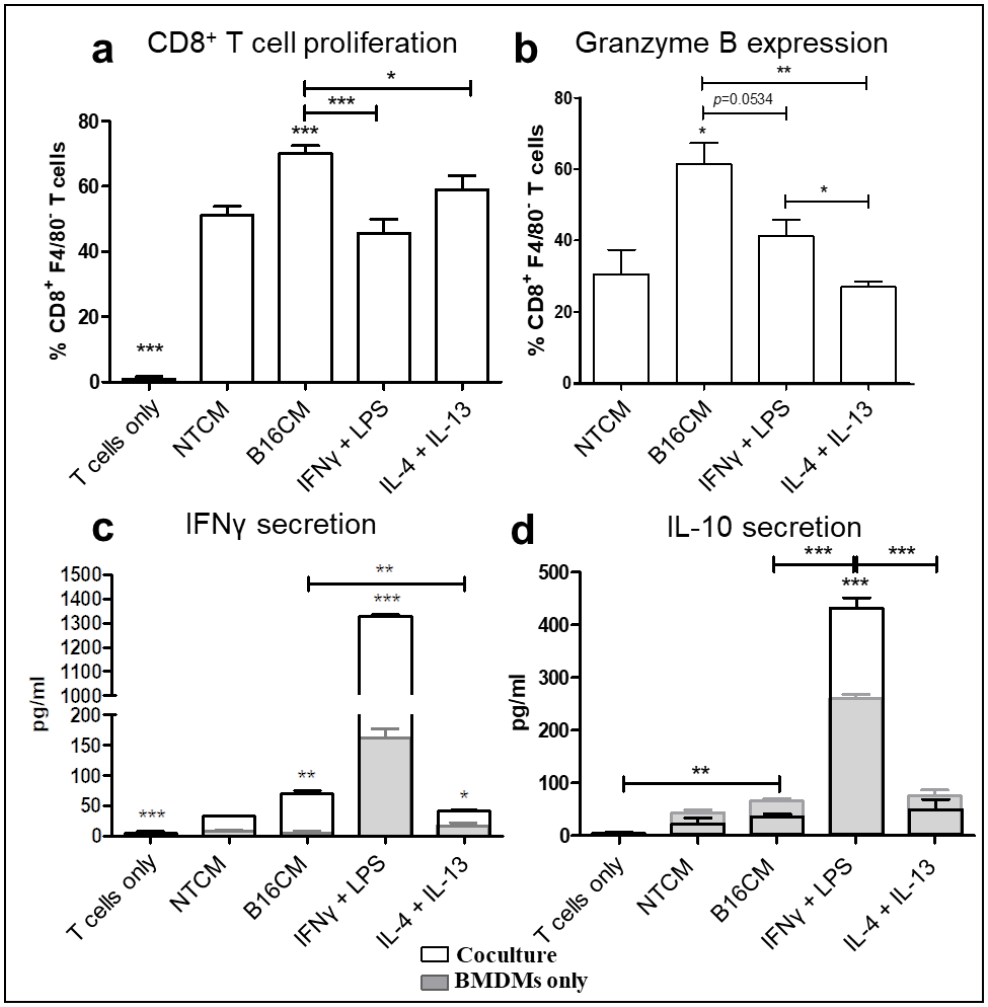

Figure 4.9 The effect of treated BMDMs on CD8$^+$ T cell expansion and polarization

Day 5 BMDMs were treated for 24hrs. Following treatment, BMDMs were washed twice and cocultured with freshly isolated CFSE labelled splenic CD8$^+$ T cells from syngeneic mice. Cells were incubated for 5 days. a) CD8$^+$ T cell proliferation was determined by reduced CFSE staining. b) Granzyme B levels were determined by flow cytometry. c-d) Shown in white bar charts are the IFNγ and IL-10 levels in supernatants following coculture, overlaid in grey are the level of the same cytokines following culture of treated macrophages alone. Data shown is representative of an n=3 per group. Data was analysed using paired student's t-tests. * p<0.05, ** p<0.01, *** p<0.001 compared to NTCM unless specified.

4.4 Discussion

It has been noted that M-CSF derived BMDMs adopt an M2-like phenotype. This polarization phenomenon cannot be avoided with the use of BMDMs derived from M-CSF of GM-CSF (GM-CSF derived cells conversely adopt a relative M1-like phenotype and the inclusion of a dendritic cell population). Many protocols involve the culturing of cells for 7-14 days, however it is likely that this may be subversive in dissecting the minutiae of monocyte/macrophage function, as it often requires powerful signalling to see any shift away from an M-CSF induced M2-like phenotype. Other studies have used M-CSF withdrawal or GM-CSF pulsing prior to stimulation to induce a 'M0' phenotype prior to activation, however all starting states are subjective to the protocol used and the results presented should be noted in that context. To aid reproducibility we have retained a simplified protocol but future work is required to determine if the results presented can be recapitulated under different BMDM culturing conditions [24].

Due to the leaky vasculature of tumour tissue it was traditionally presumed that peripheral circulating monocytes were readily trafficked the tumour microenvironment. However, it has been shown in a murine model of colon adenoma that the tumour may contain a dominant population of self-maintaining macrophages distinct from circulating populations [366]. However, using a subcutaneous B16F10 model of murine melanoma which secretes CCL2 we have shown that the levels of circulating $CCR2^{+}$ inflammatory monocytes increases during tumour progression. Using the B16 cell line variant B16BL6 tumour model, it has been shown that the level of monocytic proliferation in the tumour is low and that bone marrow is likely to provide a continuous flow of poorly proliferating monocytes to the tumour [367]. A recent paper has also shown that circulating inflammatory monocyte levels correlate to both intratumoural macrophage infiltration and patient survival in colorectal cancer [329].

In order to form an *in vitro* model to study the effect of B16F10 tumours on these cells we opted to treat M-CSF derived BMDMs on day 5 with conditioned medium. This population, which is 89 ± 4% mature monocytic cells, is enriched for inflammatory monocyte-like cells and limits the M2 polarizing effect of M-CSF itself.

The model contains inherent limitations including the purity of the cell population and also the effect of tumour conditioning is effected by B16F10 secreted factors only and does not account for any cell-cell interactions or biochemical effects such as hypoxia or low pH commonly exerted in the TME.

Due to limited availability of clinical tissue, the function of TAMs is often inferred from surface markers commonly expressed by M2-like cells seen during examination of formalin fixed paraffin embedded tissue [310].

Here we have shown that expression of cell surface markers traditionally associated with 'M2' macrophages, may not reflect functional activity and these cells expressing 'M2' markers may instead promote anti-cancer immune responses via $CD8^+$ T cell expansion, IFNγ expression and increased cytotoxicity. B16CM increased the expression of cell surface markers CD206, CD115 and CD68 but this did not translate into a change in IL-10 or IFNγ production as determined by ELISA or IL-6, IL-10, IL-12 or TGFβ expression as determine by qPCR. These results reflect previous studies showing that B16F10 conditioned medium can inhibit cytokine production by murine lymphocytic preparations and that melanoma derived exosomes can promote mixed M1 M2 polarization in macrophages, although melanoma derived exosomes were able to augment the production of cytokines such as TNFα, IL-1β and IL-10 [368,327].

TGF-β can be secreted by M2-like macrophages and can promote tumour cell stemness and migration while both TGF-β and IL-10 are potent inhibitors of effective T cell responses [369,370]. A reduction in these immunosuppressive mediators is positive in an anti-cancer context but the inability of B16CM treated BMDMs to produce IL-6 or IL-12 which are both potent inflammatory mediators required for the induction of IFNγ secreting T cells indicates a more ambiguous role in disease [371].

Coculture with T cells showed a marginal decrease in $CD4^+$ T cell expansion by B16CM treated BMDMs but an increase in $CD8^+$ T cell expansion. Coculture of B16CM treated BMDMs with either $CD4^+$ or $CD8^+$ coculture also increased IFNγ secretion by T cells, which has been identified as a central cytokine in driving anti-cancer Th1 immune responses.

These results are in contrast to other studies which have shown that direct treatment of T cells with cell line conditioned medium or fractionated exosomes from

conditioned medium reduces T cell proliferation and induces a suppressive $CD8^+$ T cell phenotype [372].

Intratumoural depletion of Tregs has been shown to control the growth of murine models of melanoma as these cells can inhibit the cytotoxic anti-tumour effect of $CD8^+$ T cells [373,374]. Tregs have also been shown to correlate to prognosis in human melanoma indicating that they play an influential role in disease [375-377]. There is intimate cross talk between melanoma derived factors, including melanoma derived exosomes and cytokines, and T cells that can affect their function [378,295,373,296,379]. The ability of B16CM treated BMDMs to induce $CD8^+$ T cell proliferation and cytotoxicity without increasing the frequency of $CD25^+$ T cells may indicate that these cells could counteract the direct inhibitory effect of conditioned medium on T cells.

Similar factors such as cytokines and exosomes are present in FCS, and while controlled for in this study, serum free growth media are becoming increasingly available and may permit more sensitive studies to be performed on the effect of cell line conditioned media or their constituents.

Due to their role in a wide range of tumour promoting activities, macrophages have been viewed as actionable targets in the development of novel anti-cancer therapeutics, however these efforts have been largely unsuccessful. Understanding the role of TAMs is essential for the development of effective therapeutics, these results suggest that the presence of M2 markers on macrophages, as are commonly reported on TAMs, does not prohibit them from promoting T cell responses.

Chapter 5

The effect of electroporation on melanoma conditioned macrophages

5.1 Abstract

Electroporation in combination with chemotherapy is an established treatment used on solid malignancies that results in enhanced chemotherapeutic uptake. Recent advances have begun to transition to the use of non-toxic compounds in lieu of chemotherapy, death, such as calcium which can also induce tumour cell death. While the effect of treatment on tumour cell death has been well characterized and has been shown to induce an immunogenic form of cell death, the effect of treatment on intratumoural immune cells has not been investigated. Here we present the first study showing the effect of tumour electroporation on immune cells, using melanoma-conditioned BMDMs. Similar to tumour cells, macrophage cell membranes are susceptible to poration following pulsing and subsequently reseal. Melanoma conditioned BMDMs are resistant to calcium electroporation induced cell death in comparison to B16F10 melanoma cells. However treatment with electroporation with or without bleomycin or calcium was shown to affect macrophage phenotype and function. Coculture of calcium electroporated macrophages revealed that both the capacity of macrophages to stimulate and to direct T cell responses are affected following exposure to treatment.

5.2 Introduction

EP is a local treatment application which can be used to form transient pores in the cell membrane. Electrodes are placed in direct proximity to the tissue of interest and a series of pulses are delivered which exceed the dielectric potential of the cell membrane resulting in the formation of pores which can persist for several seconds to several minutes before resealing and leaving cells intact and viable.

EP has been used in a cancer context to increase the uptake of chemotherapeutics, especially hydrophobic drugs, such as bleomycin, which can have poor rates of passive cell penetration. However, EP has also been used in combination with non-toxic drugs such as calcium, which when delivered in sufficient concentrations can induce rapid cell death [225]. Due to variations in tissue resistance and conductivity, EP can be safely used in proximity to healthy tissue and vasculature, making it an attractive alternative in a range of tumour types.

EP with chemotherapy, termed ECT, is routinely used for the treatment of dermal lesions but endoscopic devices have been designed for the treatment of oesophageal and colorectal cancers. Other devices are currently in development to facilitate EP of other organ sites. Complete response rates in excess of 80% have regularly been reported for treatment of dermal lesions with ECT.

ECT with bleomycin has been shown to induce an immunogenic form of cell death characterized by enhanced ecto-calreticulin and adenosine triphosphate (ATP) and high-mobility group protein 1 (HMGB1) release by treated cells. An influx of immune cells is also seen following treatment, including macrophages, indicating that ECT may be utilized to induce an anti-cancer immune response [380]. However, while ECT has been shown to repress distal tumour growth in murine models, this is not seen in clinically advanced cancer patients [380].

The substitution of chemotherapy with calcium was rationally designed in part due to the hypothesized immunogenic effects of calcium uptake, and to abrogate the immunosuppressive effects of chemotherapy. Promisingly, a case study in malignant melanoma treated with calcium EP in combination with ECT has reported remission of both local treated and distal untreated tumours, indicating a systemic anti-cancer immune response or other abscopal effect [225].

Due to the immunogenic potential of EP treatments, the effect of treatment in combination with other immunogenic modalities, including T cell check point inhibitors, is under investigation [381,382]. However the direct effect of EP on intratumoural immune cells is not known. Here, using a BMDM model of melanoma TAMs, we show for the first time that EP can induce reversible pore formation on macrophages that can impact their size, viability, phenotype, function and role in T cell activation.

5.3 Results

5.3.1 Optimization of B16F10 electroporation parameters

As electrical parameters of tumour EP are optimized to induce tumour cell death, we first optimized the *in vitro* delivery of EP on B16F10 tumour cells. Cell poration was measured in parallel with the subsequent viability of cells 30min following EP (**Figure 5.1a**). At 800V/cm the sum of non-viable cells and porated cells surpassed 100%, indicating that a proportion of electroporated cells did not regain membrane integrity. As such 700V/cm was selected as an appropriate voltage to induce reversible EP in B16F10 cells.

Using this voltage preliminary data was generated to ensure cell viability at 24, 48, and 72hrs post treatment (**Figure 5.1b**). Using previously optimised concentrations of bleomycin (10nM) and calcium (0.5-5mM) we examined the nature of cell death following treatment. No loss in viability was observed following EP. A daily increase in viability was observed however this was considered likely to be an artefact of experimental technique, in which B16F10 cells do not respond optimally to repeated trypsinisations within short periods and the nature of the EP buffer used.

Significantly decreased viability was seen in cells treated with bleomycin ECT 3 days post treatment compared to EP only ($p<0.01$) and in contrast a significant decrease was seen in 24hrs post treatment in cells treated with calcium EP ($p<0.001$). This reduction in viability which was no longer apparent at 48 or 72hrs indicates that cells not killed by treatment are able to recover following treatment. As expected these results indicated a differential timing of cell death following EP with calcium and bleomycin.

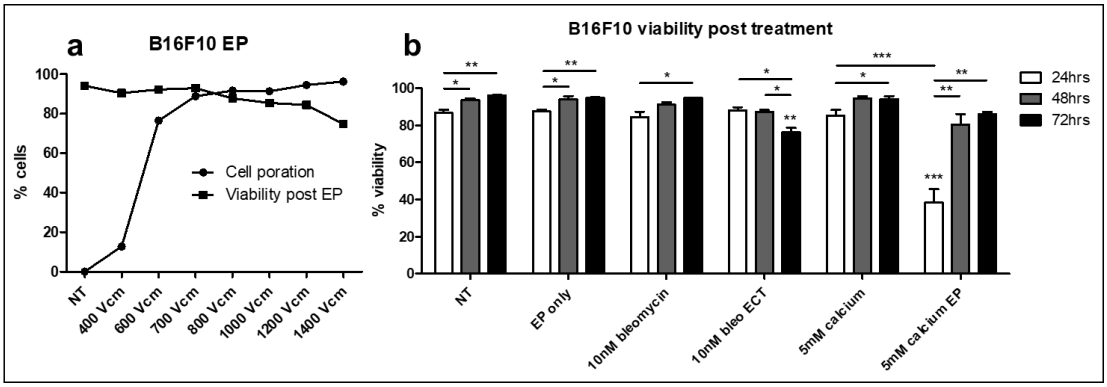

Figure 5.1 Optimisation of electroporation parameters in B16F10 cells

a) B16F10 cells were electroporated at a range of voltages, cell poration was measured by PI uptake during EP and cell viability was determined by PI uptake 30min following electroporation. b) Cells were electroporated at 700V/cm with or without drug and were analysed for viability 24, 48 and 72hrs post treatment. Data was analysed using paired student's t-tests. Data shown is representative of an n=3 per group. * $p<0.05$, ** $p<0.01$, *** $p<0.001$ compared to NT at the same time point unless specified. No Treatment (NT)

5.3.2 Loss of B16F10 cell viability following Ep with calcium or bleomycin

To further determine the nature of cell death following treatment, we performed serial matched viability analysis on B16F10 cells following calcium EP at a range of calcium concentrations (**Figure 5.2a-d**). No cell death was observed in cells treated with 500μM calcium, indicating doses of 2.5mM or greater are required to generate therapeutic cell death in a B16F10 model of melanoma. A significant drop in viability was seen in cells treated with 2.5mM calcium or higher in combination with EP, which had occurred by 30min post treatment. The level of cell death continued to increase for 6hrs, but an increase in viability was seen in all conditions by 8hrs after treatment. The doubling time of B16F10 cells is approximately 15hrs, so improved viability is likely a result of replication by intact cells rather than the recovery of cells which had lost membrane integrity for up to 6hrs. For further studies we chose to use 500μM as a low ineffective dose and 5mM as the upper dose as rates of cell death between 5 and 10mM were non-significant.

To determine if cells not acutely killed following calcium EP had any loss in malignant potential, we performed clonogenic assays on cells which were viable 24hrs following treatment (**Figure 5.2e**). No change was seen in clonogenic ability, indicating that cells not killed acutely have normal replicative potential.

Conversely, we performed clonogenics with viable cells selected 24hrs following EP with bleomycin (**Figure 5.2f**). No colonies were established in comparison to all controls (p<0.001), indicating all cells were killed by treatment. These results are in agreement with previous literature indicating that electrochemotherapy results in cell death by loss of replicative potential.

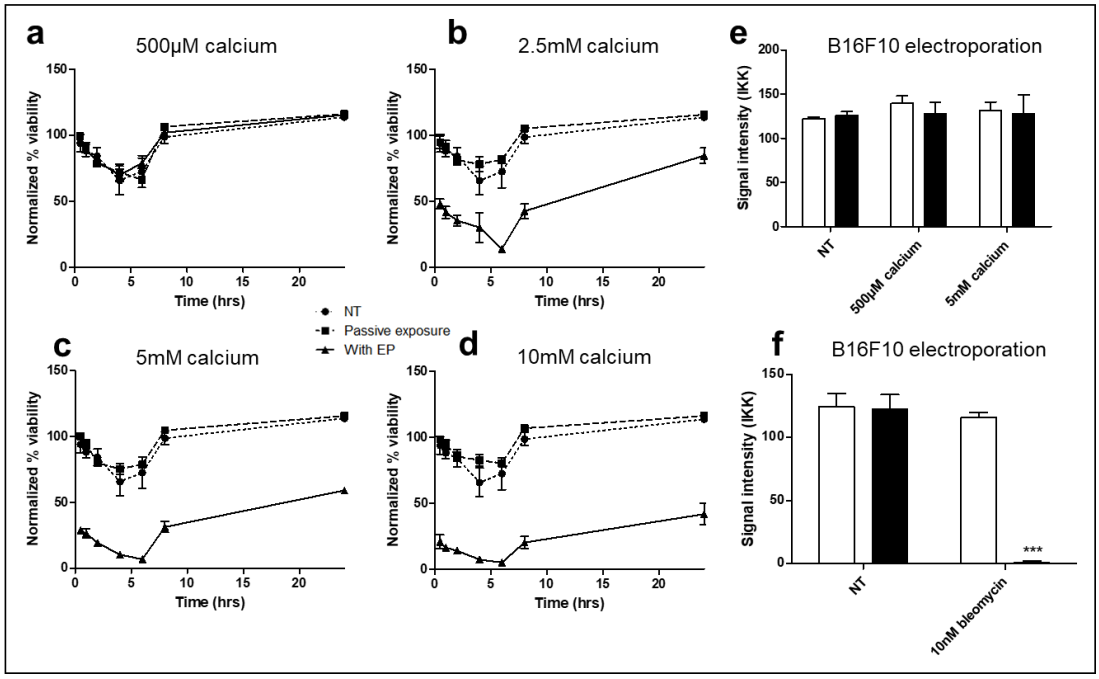

Figure 5.2 Cell death following electroporation with bleomycin or calcium

B16F10 cells were electroporated at 700V/cm with or without drug. a-d) Serial matched measurements of cell viability were taken following calcium EP. e-f) Viable cells were isolated 24hrs post treatment by selection of adherent cells and seeded at a low concentration for clonogenic analysis. Data was analysed using paired student's t-tests. Data shown is representative of an n=3 per group (a-d and f) and an n=9 per group (e). *** p<0.001 compared to all other conditions. No treatment (NT)

5.3.3 Poration of BMDMs following EP with or without calcium

Using the above optimised parameters melanoma conditioned BMDMs were electroporated. The efficiency of EP in the presence of calcium was also investigated as extracellular calcium is known to affect membrane resealing and other membrane dynamics through its role in voltage generation (**Figure 5.3a**) [383]. EP induced cell poration in 64.26% ±4.64% of BMDMs, which was unchanged by the addition of calcium (**Figure 5.3b**).

Although calcium did not affect the level of porated cells, there was a shift in cell size following EP with calcium, with calcium EP resulting in phenotypically smaller cells as determined by forward scatter (p<0.001) (**Figure 5.3a and 5.3c**). This effect was induced by both 5mM calcium and the lower dose 500µM which was non-lethal in B16F10 cells.

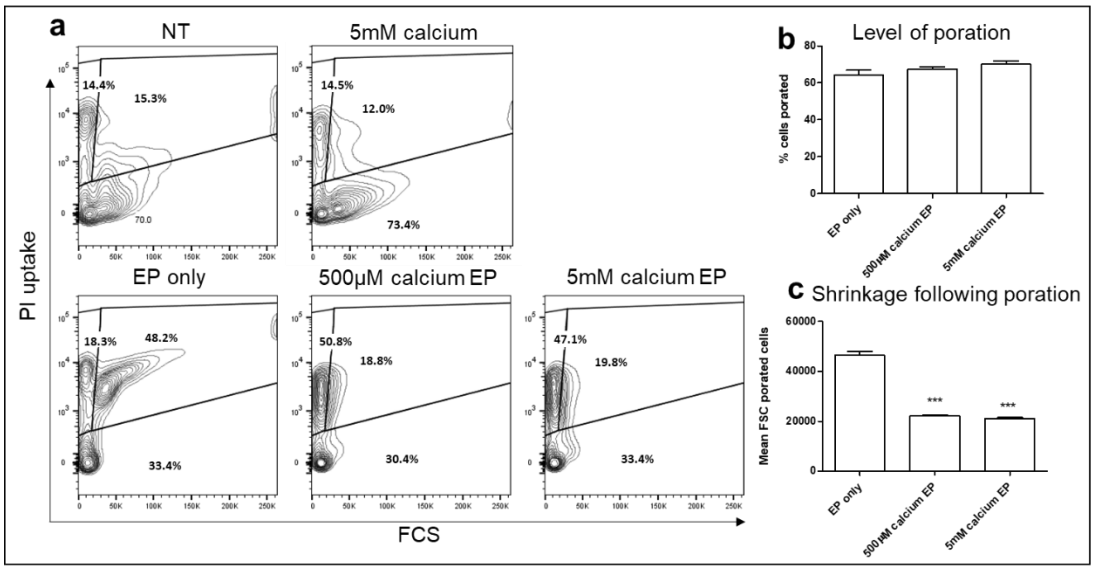

Figure 5.3 Electroporation of melanoma conditioned BMDMs

Melanoma conditioned BMDMs were electroporated at the same parameters as were used for B16F10 cells. a-b) Poration was measured by PI uptake during EP. Total number of porated cells were calculated by addition of the PI^+ FCS^{lo} and PI^+ FCS^{hi} gates from (a). c) Cell size was determine by flow cytometric forward scatter readings, graphed is the MFI of PI^+ FCS^{lo} and PI^+ FCS^{hi} events from (a). Data was analysed using paired student's t-tests. Data shown is representative of an n=3 per group. *** p<0.001 compared to EP only. No Treatment (NT)

5.3.4 Effect of EP with calcium or bleomycin on BMDM viability

Following determination that BMDMs are porated we next analysed the viability of cells following treatment with EP with or without calcium or bleomycin (**Figure 5.4**). As BMDMs have limited replicative potential the effect of therapy was followed for up to 5 days. At 1hr post treatment, all cells except those treated with EP with 5mM calcium ($p<0.05$) were as viable as untreated cells (**Figure 5.4a**). These results indicate that following poration, in which over 60% of cells are porated, cells regain membrane integrity.

At 24hrs post treatment, cells treated with EP with or without bleomycin displayed a marked reduction in viability, indicating an EP related toxicity in BMDMs (**Figure 5.4b**). This is likely due to sensitivity to the composition of their cytoplasmic contents which can be distorted by loss of cytoplasm and gain of extracellular medium during treatment. 500μM calcium was protective to electroporated cells, resulting in significantly reduced death compared to EP alone ($p<0.05$). There was no significant difference between 500μM calcium EP and non-treated cells although there was a slight trend of decreased viability. This protective role of calcium was lost in the presence of 5mM calcium ($p=0.0678$). Thus low levels of calcium are most protective for conditioned BMDMs following treatment.

At 5 days post treatment the decrease in viability of electroporated cells was less pronounced but still present ($p<0.01$) (**Figure 5.4c**). The addition of bleomycin decreased the viability of non-treated and electroporated cells, however bleomycin induced a larger level of cell death in combination with EP compared to passive exposure (29.95±13.45% vs 45.89±16.12%, $p=0.0642$). Both doses of calcium proved protective at 5 days post treatment, with no significant change from non-treated or passive calcium exposure and increased viability compared to EP alone ($p<0.05$).

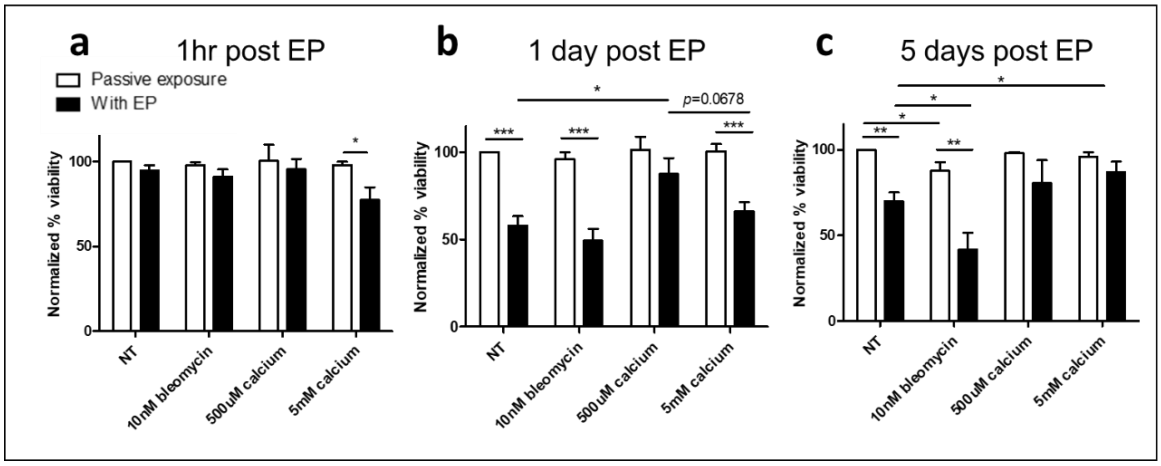

Figure 5.4 Viability of melanoma conditioned BMDMs following electroporation with bleomycin or calcium

Melanoma conditioned BMDMs were electroporated in the presence of bleomycin or calcium. Viability was determined by PI uptake at 1hr (a), 1 day (b) and 5 days (c) post treatment. Data was analysed using paired student's t-tests. Data shown is representative of an n=7 per group. * $p<0.05$, ** $p<0.01$, *** $p<0.001$ compared to NT or EP only as appropriate unless specified. No treatment (NT)

5.3.5 Effect of EP with calcium or bleomycin on BMDM surface markers and arginase activity

Following confirmation that some BMDMs can survive EP, we next sough to phenotype cells to determine any shifts in behaviour. Cells were isolated 72hrs post treatment and the canonical M1:M2 enzymes, iNOS and arginase, were assayed in combination with cell surface markers. Viable $CD11b^{+}$ BMDMs can be separated in a binary fashion into $F4/80^{+}$ $CD115^{-}$ or $F4/80^{hi}$ $CD115^{+}$ cells. An upregulation of F4/80 accompanied with CD115 induction is indicative in murine myeloid cells of a transition from monocyte to macrophage [285]. The linear evolution of these cells is poorly understood, however this shift is commonly associated with an upregulation of M2-like behaviour [348]. EP resulted in a significant decrease in this maturation process (**Figure 5.5a),** which was maintained in cells treated with bleomycin EP. However the addition of calcium, in a dose dependent manner, reduced this decrease ($p<0.001$). The M2-like phenotype of these matured cells was reflected by the CD206 expression of $CD11b^{+}$ cells (**Figure 5.5b**).

All cells assayed were negative for detectable nitrates in supernatant using Griess assay (data not shown). While EP induced a decrease in $F4/80^{hi}$ $CD115^{+}$ cells, there was no change in arginase activity in these cells (**Figure 5.5c**). And despite a relative increase in $F4/80^{hi}$ $CD115^{+}$ in cells treated with calcium EP, these cells displayed marked reduction in arginase activity, that was independent of EP, indicating that passive exposure to calcium can induce metabolic effects in BMDMs.

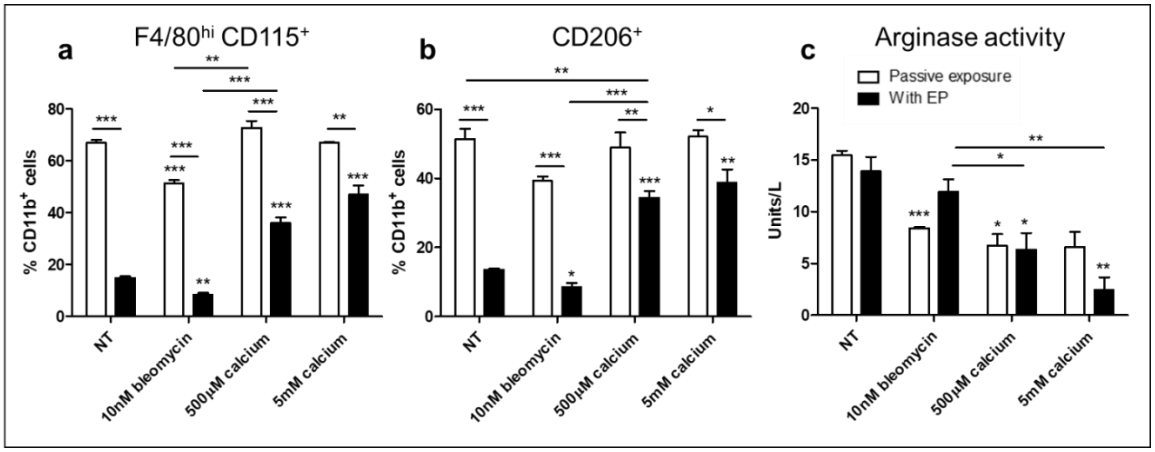

Figure 5.5 Phenotypic evaluation of melanoma conditioned BMDMs following electroporation with bleomycin or calcium

Melanoma conditioned BMDMs were electroporated in the presence of bleomycin or calcium and cultured for 72hrs. a-b) Cells were analysed by flow cytometry for macrophage activation markers. BMDMs were identified as $CD11b^+$ (**Figure 2.5**) and gated according to F4/80, CD115 and CD206 expression. c) Intracellular arginase activity was assayed following cell lysis. Data was analysed using paired student's t-tests. Data shown is representative of an n=3 per group. * $p<0.05$, ** $p<0.01$, *** $p<0.001$ compared to NT or EP only as appropriate unless specified. No Treatment (NT)

5.3.6 Effect of calcium electroporation of BMDMs on subsequent $CD4^+$ T cell activation

Due to enhanced survival of cells treated with calcium EP, and increased maturation coupled with decreased arginase activity this treatment was selected as the most promising for further immunological studies. The effect of treated BMDMs on $CD4^+$ T cells was determined by coculture experiments using BMDMs isolated 24hrs after treatment in combination with freshly isolated splenic $CD4^+$ T cells.

Calcium EP of BMDMs was found to decrease their ability to stimulate $CD4^+$ T cell proliferation compared to BMDMs treated with EP only (**Figure 5.6a**). Cells treated with or without EP resulted in no detectable IL-10 in supernatant (**Figure 5.6c**), however calcium treatment induced IL-10 secretion. This effect was further increased by 5mM calcium in combination with EP ($p<0.05$). IFNγ secretion patterns inversely reflected IL-10 expression (**Figure 5.6d**). EP alone induced high levels, and the addition of calcium reduced IFNγ secretion. These results suggest that while EP alone may promote relative Th1 responses, calcium EP shifts this towards a Treg response. This is also reflected by the Th2 cytokine IL-4, which often accompanies Treg responses, and which was detectable in trace amounts following treatment with calcium EP (**Figure 5.6b**).

A decrease in IFNγ was reflected by decreased CXCR3 expression on activated T cells (**Figure 5.6f)** following calcium EP. There was a decrease also in the Treg marker, CD25, following calcium EP ($p<0.01$), however CD25 expression is also coupled to T cell activation and could reflect decreased activation as is mirrored in the reduced T cell proliferation (**Figure 5.6a**).

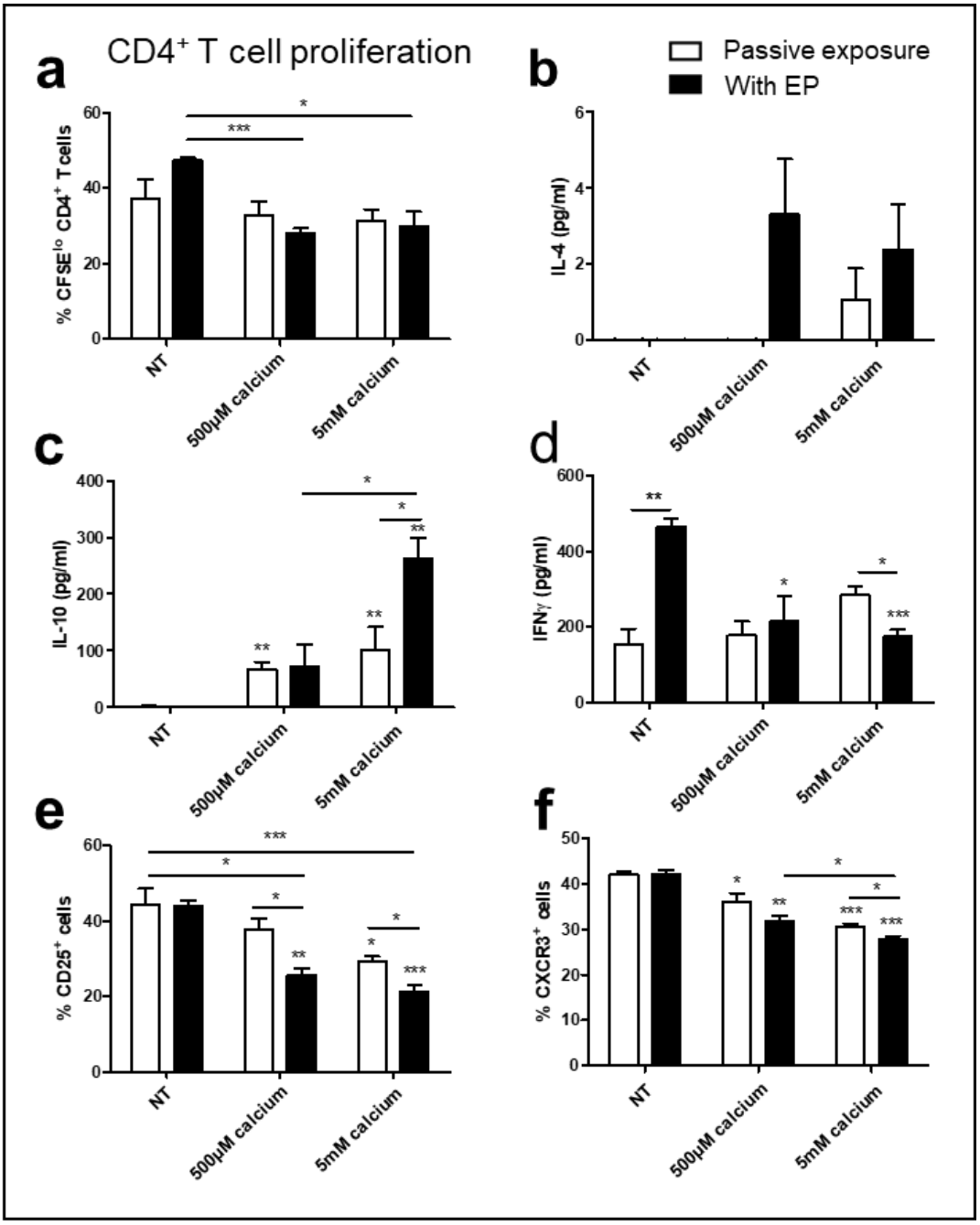

Figure 5.6 Effect of melanoma conditioned BMDMs following electroporation on CD4$^+$ T cells

Melanoma conditioned BMDMs were electroporated in the presence of bleomycin or calcium and cultured for 24hrs. Cells were then cocultured with freshly isolated CFSE labelled CD4$^+$ T cells. T cell proliferation was measured by reduced CFSE expression (a). Levels of IL-4 (b), IL-10 (c) and IFNγ (d) in the supernatant were measured by ELISA. Activated T cells were gated by low CFSE expression and CD25 (e) and CXCR3 (f) expression was determined by flow cytometry. Data was analysed using paired student's t-tests. Data shown is representative of an n=3 per group. * p<0.05, ** p<0.01, *** p<0.001 compared to NT or EP only as appropriate unless specified. No treatment (NT)

5.3.7 Effect of calcium electroporation of BMDMs on subsequent $CD8^+$ T cell activation

To fully elucidate the role of electroporated macrophages in anti-cancer immunity we subsequently examined the effect of treated BMDMs on cytotoxic $CD8^+$ T cell responses. In contrast to $CD4^+$ T cell activation, calcium EP was shown to increase the $CD8^+$ T cell activation potential of melanoma conditioned BMDMs, as seen by a reduction in CFSE mean fluorescent intensity (MFI) (**Figure 5.7a**). EP of BMDMs had no effect on subsequent $CD8^+$ T cell proliferation, however calcium treatment increased activation in an apparently dose dependent manner (p=0.0892). Intracellular granzyme B was detectable in both BMDMs and $CD8^+$ T cells (**Figure 5.7b-c**). BMDM calcium treatment resulted in an increase in granzyme B in both BMDMs and cocultured $CD8^+$ T cells. EP decreased BMDM granzyme B levels (p<0.05), which was also evident in decreased BMDM granzyme B levels in 500μM calcium EP (non-significant) and 5mM calcium EP (p=0.05) compared to respective passive treatments. BMDM EP had no effect on $CD8^+$ T cell granzyme B levels across any of the tested conditions compared to respective passive treatments. Passive exposure of BMDMs to calcium increased the granzyme B levels of cocultured $CD8^+$ T cells.

Secretion of IL-10 and IFNγ were also measured as $CD8^+$ T cells are significant sources of both IL-10 and IFNγ *in vivo* (**Figure 5.7d-e**). Similarly to $CD4^+$ T cell coculture, passive calcium treatment induced a dose dependent increase in IL-10 levels, which was independently of EP, however calcium levels were of a 4 to 6 fold lower concentration than from $CD4^+$ T cell cocultures. No changes were observed in IFNγ secretion levels except by cocultures with BMDMs treated with 5mM EP in which increased secretion was observed (p<0.05).

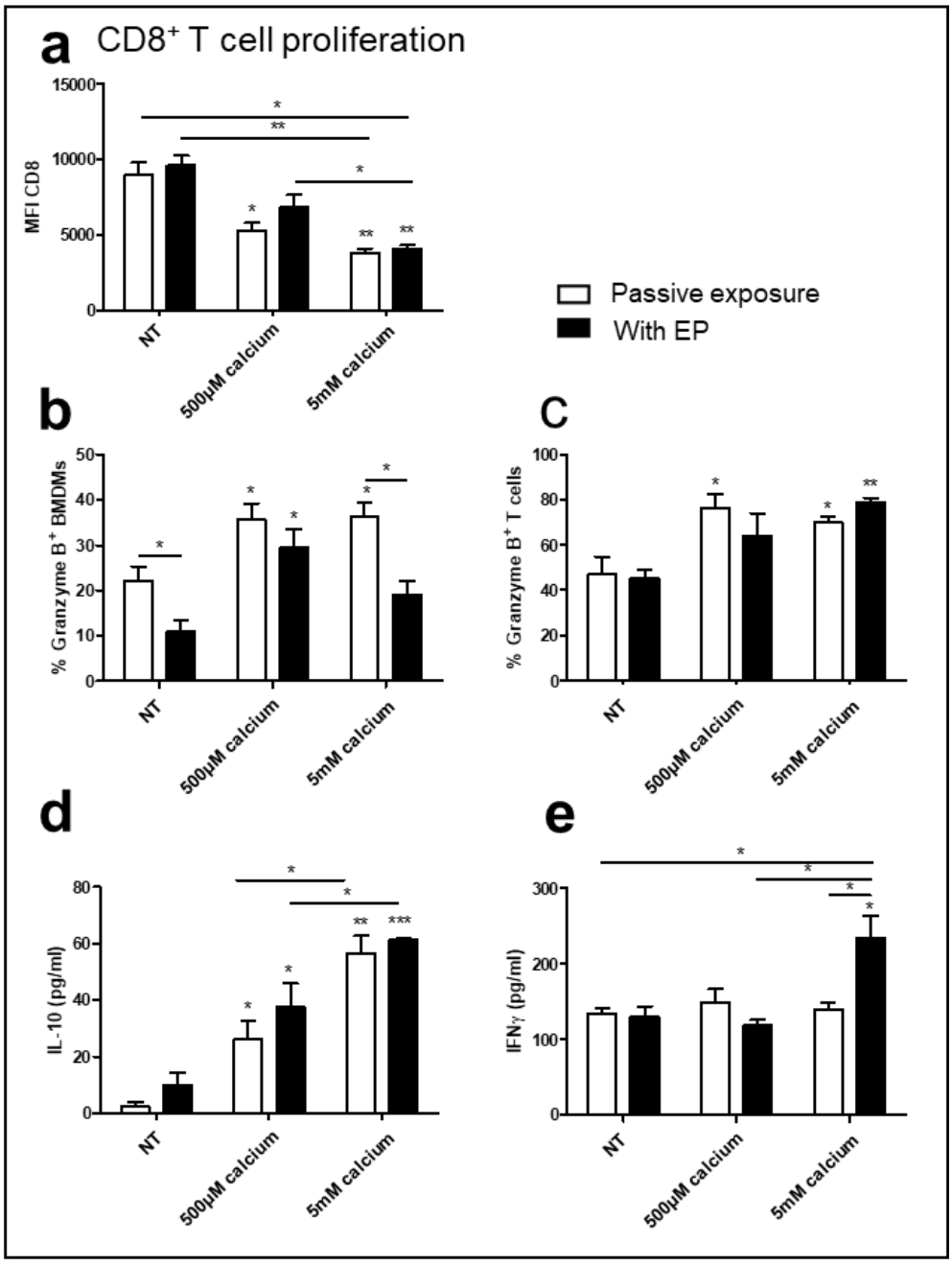

Figure 5.7 Effect of melanoma conditioned BMDMs following electroporation on CD8$^+$ T cells

Melanoma conditioned BMDMs were electroporated in the presence of bleomycin or calcium and cultured for 24hrs. Cells were then cocultured with freshly isolated CFSE labelled CD8$^+$ T cells. T cell proliferation was measured by reduced CFSE expression (a). Intracellular levels of granzyme B were determined by flow cytometry in treated BMDMs (b) and cocultured activated CD8$^+$ T cells. Levels of IL-10 (d) and IFNγ (e) in the supernatant were measured by ELISA. Data was analysed using paired student's t-tests. Data shown is representative of an n=3 per group. * p<0.05, ** p<0.01, *** p<0.001 compared to NT or EP only as appropriate unless specified. Mean fluorescent intensity (MFI). No treatment (NT)

5.4 Discussion

ECT is a well-established treatment modality with high complete response rates. The EP pulses are optimized to result in reversible cell poration with minimal ablative effects [384,385]. The cytotoxic effects of ECT are manifested by intracellular bleomycin during cell proliferation following treatment, as supported by the cell death shown (**Figure 5.5**) [385]. Despite promising indications, calcium EP is not yet well established and is currently restricted to use on an investigative basis.

The fundamental mechanism of cell death following calcium EP is different to ECT as no chemotherapeutic is present. It has previously been suggested that calcium EP results in necrotic cell death as a result of severe ATP depletion [386]. In agreement with this, here we have shown that the cell death following treatment is acute, in which cells do not regain membrane integrity or lose viability within 6hrs of treatment (**Figure 5.5**). Cells which survive this initial insult show no loss of proliferative potential.

Having successfully generated these treatment models in a melanoma cell line, we subsequently examined the effect of these electroporation parameters on syngenic BMDMs treated with B16F10 conditioned medium to mimic melanoma conditioning. These cells were shown to be susceptible to EP and regained membrane integrity following treatment. However, EP resulted in a subsequent reduction in viability at 24hrs which was still evident 5 days following treatment. In tandem with this effect was a selective depletion of $CD115^{+}$ $F4/80^{hi}$ and $CD206^{+}$ cells. $CD115^{+}$ $F4/80^{hi}$ and $CD206^{+}$ are macrophage-like cells and also M2-like, in contrast to $CD115^{-}$ $F4/80^{mid}$ cells which are monocyte-like and M1-like. It is commonly considered that M2-like cells can support tumour growth and inhibit anti-cancer T cell responses while M1-like cells can exert inflammatory responses that can support anti-cancer immune responses [387-389]. While $CD115^{+}$ $F4/80^{hi}$ cells were depleted by EP, cell populations retained their arginase activity, indicating the retention an M2-like phenotype. EP alone of BMDMs showed no subsequent effect on T cell proliferation or polarization as determined by surface markers but did result in increased IFNγ secretion in $CD4^{+}$ T cell cocultures.

ECT did not induce any further cell death in comparison to EP alone in the first 24hrs (**Figure 5.7**). By day 5 there is a further reduction in viability caused by ECT beyond

the loss of viability seen with EP alone ($p<0.01$). In a tumour context, there is a continual supply of TAMs from circulating monocytes and while it has been shown that some murine models contain populations of self-maintaining macrophage populations, it is likely that a continuous supply from the circulation is the predominant source of TAMs [185,390,366,391]. Therefore, while it is likely to effect coculture behaviour, it cannot be speculated whether viability declines seen after the first 24hrs will have a meaningful effect on *in vivo* macrophage tumour biology. ECT followed the same trend of $CD115^+$ $F4/80^{hi}$ and $CD206^+$ depletion as EP but did non-significantly decrease arginase activity indicating that ECT may impair M2-like responses.

Calcium EP of melanoma conditioned BMDMs displayed a remarkably different response profile compared to EP alone. Immediately following treatment cell size was significantly reduced. Following treatment an initial loss in viability was seen in cells treated with 5mM calcium EP, however the scale of cell death in comparison to B16F10 cells was markedly reduced. At 1hr following treatment with 5mM calcium there was a reduction of viability of 73.26±3.28% of cells in B16F10 cells compared to only 22.62±7.42% in melanoma conditioned BMDMs ($p<0.01$ difference in means).

By 24hrs calcium had played a protective role in improving viability following EP, and by day 5 no significant difference was observable between untreated cells and cells treated with calcium EP.

Calcium is known to influence a variety of signalling pathways, and among other pathways is coupled to purinergic receptor signalling in macrophages, which are known to regulate migration and activation [392]. Thus it is intuitive that calcium treatment will induce phenotypic and functional changes in treated macrophages.

Calcium EP diminishes the reduction of $F4/80^{hi}$ $CD115^+$ cells seen following EP despite the initial phenotypic shift towards cell shrinking, but instead of increasing arginase expression associated with these cells, there is a down regulation of arginase activity. This effect, with lower (500μM) doses is independent of EP, indicating that passive calcium treatment can impart lasting effects on BMDMs. Mirroring this effect, calcium treatment of BMDMs in the absence of EP affected subsequent $CD8^+$ T cell proliferation and both $CD4^+$ and $CD8^+$ T polarization and activation.

Cells were washed following treatment 3 times, negating the possibility of prolonged exposure to EP buffer or calcium treatments. However calcium is known to interact with and affect the plasma membrane. Providing a hypothesis for the effects of calcium seen in the absence of EP, such as decrease arginase activity.

The interaction of calcium with the plasma membrane is poorly understood but has been shown to be both complex and specific [393]. Calcium can interact with the phosphate groups of phosphatidylcholine which can constitute 40-80% of the plasma membrane and can affect lipid clustering which has been shown, among other process to control T cell activation, and is known to affect macrophage intracellular signalling [394-396]. Extracellular calcium depletion has also been shown to reduce macrophage phagocytosis and cytokine secretion, and the influx of calcium is coupled to signalling via TRPV2 [397-399]. Thus the effect of passive exposure to calcium resulting in functional differences is not anomalous with previous results, however physiological extracellular calcium concentrations are approximately 2mM while culture media range from 0.7-1.7mM, indicating that the effect observed may equally be due to the temporary removal of extracellular calcium in negative controls while in calcium free EP buffers during experiments [399].

Over active ATPase activity by cells attempting to regain homeostatic intracellular calcium concentrations has been hypothesized as a potential cause of severe ATP depletion following calcium EP [400,401]. However it is possible that calcium free buffers result in cytoplasmic calcium depletion which is also energetically taxing on cells. Further research is required to determine if low levels of calcium in EP buffers can reduce energetic stress on cells following treatment.

That calcium EP can upregulate IL-10 secretion from both $CD4^+$ and $CD8^+$ T cell cocultures in a dose dependent manner indicates that high dose calcium administration may inhibit anti-cancer immune responses as directed by exposed macrophages. However they exert complex effects, also increasing $CD8^+$ T cell proliferation and granzyme B levels in activated T cells indicating the expansion of cytotoxic immune responses in a dose dependent manner. Most strikingly, $CD8^+$ T cell cocultures with BMDMs treated with high dose (5mM) calcium electroporation were the only treatment which displayed an increase in IFNγ. IFNγ is a potent activator of Th1 anti-cancer immune responses.

When administered in combination with EP, calcium dosage can affect the level of tumour cell death [402,403]. From this data, it is clear melanoma conditioned BMDMs are susceptible to poration by EP but relatively resistant to calcium EP induced cell death. However exposed cells are phenotypically and functionally altered. To our knowledge, this is the first study examining the effect of EP, as designed for the treatment of solid tumours, on immune cells which are also exposed to treatment. *In vivo* investigation is required to see if the increase in cytotoxic $CD8^+$ T cell activity will be seen in a disease setting. Further investigation of other immune cell types, is required to determine if immune responses are compromised, and if therapeutic administration can be optimized to balance immunogenic tumour cell death with the retention and optimisation of the immune response by exposed immune cells.

Chapter 6

General Discussion

It is known that tumours can polarize macrophages to an M2-like phenotype through a variety of mechanisms, including hypoxia, lactate, and immunosuppressive cytokines [404-406,369]. We have shown that human melanoma tumours contain distinct macrophage populations with different biological activity and a predominance of $CD163^+$ M2-like TAMs in the TME and peritumoural tissue. Thus the high level of $CD163^+$ macrophages seen in the TME is in line with expected observations. Our results are also in alignment with the hypothesis that M2 macrophages accumulate during the course of disease, although we cannot offer a mechanism, others have speculated that this is reflective of an continual influx of monocyte-derived macrophages which are then polarized to an M2-like phenotype in the TME, and which is supported by numerous *in vitro* and preclinical studies [250,407-410].

In contrast, a much smaller population of $CD68^+$ macrophages exist in and around some human melanoma tumours, but not in all cases. These may reflect recently recruited monocytes. While previous studies have reported CD68 as a pan-macrophage marker, from our study and previous published literature it is clear CD68 is not a pan-macrophage marker [322,411]. The nature of these cells is unknown as *in vitro* CD68 is expressed on both M1-like and M2-like macrophages [412]. However there was a clear correlation of $CD68^+$ macrophages with increased $arginase^+$ and $iNOS^+$ cells in the tumour. While the expression of iNOS was restricted to cells with a macrophage morphology, arginase expression was present in both macrophages and neutrophils. $CD68^+$ recruitment is associated with an increased immunologically active microenvironment from an iNOS and arginase perspective. Thus it is hypothesized that $CD68^+$ macrophages have an active phenotype. The failure to draw consistent prognostic indications from macrophage infiltration in melanoma could be due to reduced macrophage activity, whereby the cells have no effect on tumour progression, or the prognostic effect is masked by opposing biological effects. Other studies have similarly indicated that $CD68^+$ macrophages can be absent in some melanomas [247].

$CD68^+$ infiltration was also positively associated with BRAF status. These findings are significant in the context of BRAF inhibition, in which macrophages have been implicated in therapeutic resistance [413]. Similarly, macrophage derived factors such as hepatocyte growth factor (HGF) and epidermal growth factor (EGF) have been implicated in the resistance to BRAF inhibitors [414,415]. BRAF activity is known to

increase glycolysis, and subsequent dependence on glycolysis is a major mechanism through which BRAF inhibitors can reduce tumour growth [416,417]. Increased lactate levels, which can be expected as a result of overactive glycolysis, can polarize macrophages to an M2-like phenotype [405]. M2 polarization of macrophages can reactive mitogen-activated protein kinase (MAPK) signalling in tumour cells via VEGF secretion [413,335]. While these studies focused on M2-like macrophages, M1-like macrophages were also shown to mediate resistance of melanoma cells to mitogen-activated protein kinase kinase (MEK) inhibition. These results serve as a valid hypothesis for macrophages contributing to developed resistance to BRAF inhibitors, whereby preventing M2 polarization of TAMs could prolong the duration of response to BRAF inhibitors.

The evaluation of $CD68^+$ macrophage phenotype may very between tumour and tissue type. Other studies have shown that $CD163^+$ cells can also express iNOS, indicating the existence of non-binary macrophage subsets [418]. Recent advances of RNA sequencing technology have been expanded to use on FFPE tissue [419]. Because of discrepancies between murine models and human disease and the difficulty of performing detailed examination of fresh human tissue it is hoped that single cell RNA sequencing which can give more complete phenotypic descriptions on a cellular level may reveal a more complete description. Current preclinical targeting of TAMs is largely based on presumptions of TAMs adopting an M2 phenotype and contributing to tumour progression, supported by prognostic links with intratumoural TAM accumulation, in many tumours types. Further interrogation of RNA sequencing data will provide a more detailed description of the many discrete physiological roles of TAMs.

It is largely believed that any effective immunotherapeutic, must effectively stimulate effective T cell responses or provide a source of effective T cells. As such the role of macrophages in immunotherapy has largely been in the context of their ability to promote or inhibit T cell responses [267]. Specifically, the current focus in the literature is on preventing M2 macrophage polarization of macrophages. Contrary to this, our study has shown that it is possible to have M2-like macrophages, which can promote T cell responses. Thus our results indicate that macrophage polarization can build upon an existing ability to promote T cell response and further enhance responses to immunotherapies.

In support of the hypothesis of $CD68^+$ macrophages having a meaningful role in tumour biology, the correlations of $CD68^+$ and $CD163^+$ macrophage infiltration in our study with total gene expression in the tumour were positive and negative respectively. While both peritumoural and intratumoural recruitment of $CD68^+$ cells correlated to the regulation of a number of genes, involved in cell death and inflammation, among other processes, there was no correlation between $CD163^+$ macrophage recruitment and gene expression. These results also undermine the rational of targeting TAM inhibition in the TME, as they indicate that TAMs may be functionally inert in the TME. Therapeutic strategies should instead focus on preserving or boosting the function of $CD68^+$ M1-like macrophages.

There has been intense interest in the contribution of circulating inflammatory monocytes to tumour growth in murine models. In PDAC inhibition of the mobilization of inflammatory monocytes from the bone marrow, and consequent the reduction of recruitment to the tumour has been associated with positive prognostic outcomes in both murine and human disease [149]. Central to this hypothesis is the effect of tumour conditioning on monocytes recruited to the TME, in which they initially contribute to destructive inflammation, and then become polarized by the tumour to support tumour progression [420]. It is currently unclear how the positive prognostic outcomes seen in lung cancer and ovarian cancer with increased M1-like macrophage density can be aligned with the negative prognostic role of inflammatory monocyte infiltration in PDAC [43,56].

The focus of research on PDAC has led to observations in other murine models, such as colorectal cancer, in which the frequency of circulating inflammatory monocytes can inversely correlate to survival [329].

While the nature of the effect of these cells in the TME is unclear and may vary depending on the tumour type, the identification of inflammatory monocytes as a prognostic influencer has identified an actionable therapeutic target for cancer treatment. It is likely that the role of recruited monocytes in tumour biology depends on the specific cancer type and anatomical site.

In agreement with other murine tumour models, in a murine model of melanoma, we observed increased levels of circulating inflammatory monocyte as disease progressed. To determine the role of these cells in the TME, we developed a novel

protocol of BMDM generation, optimised for the study of inflammatory monocytes, and determined the effect of tumour conditioning on these cells using melanoma, B16F10, cell line conditioned medium.

For *in vitro* research of monocytes and macrophages there are competing factors in determining the protocols used. From one perspective, we must standardize the protocols used to increase the repeatability and comparability of the literature [24]. However, given the known role of epigenetics in determining the behaviour of monocytes and macrophages, it is also essential that we rationally design protocols of BMDM generation to accurately reflect *in vivo* subsets we wish to study [268]. A reasonable outcome may be that there will be a central database of a limited number of protocols from which researchers select depending on the cell of interest. The protocol presented here is rationally robust and future studies comparing BMDM protocols to *in vivo* subsets will continue to question previous protocols.

Using our model, interestingly, as we had seen a predominant population of inactive $CD163^+$ macrophages in human melanoma, conditioned medium had the effect of increasing the murine M2-associated surface markers, CD115 and CD206. This increase in M2 markers was upregulated in the absence of any major impact on functional protein expression such as arginase, iNOS, IL-10 or IL-6. In effect these results mirror the clinical hypothesis shown in chapter 3, in which $CD68^+$ inflammatory monocytes are recruited to the TME and polarized to an M2 $CD163^+$ phenotype.

Furthermore, analysis of the effect of conditioned BMDMs revealed they retained the ability to promote cytotoxic T cell responses, indicating that neutralization of inflammatory monocyte recruitment will not induce favourable outcomes in murine melanoma. These results are in contrast to other tumour models in which TAMs have been shown to skew T cell polarization to a Treg phenotype [421,422,313]. However, many studies are based on the hypothesis that BMDMs cultured with M-CSF and IL-4 with or without IL-13 are representative of TAMs, in lieu of tumour conditioning or in combination with tumour conditioning [423]. Many studies exist such as a study using human breast cancer cell line conditioned medium on freshly isolated peripheral blood monocytes, co-treats with IL-4, IL-10 and M-CSF, in addition to cell line conditioned medium before showing conditioned medium can decrease T cell

proliferation [313,424,425]. Abbreviated culturing of BMDMs has been shown to be representative of inflammatory monocytes and limits the polarizing effect of M-CSF [285]. The use of these shortened culturing protocols on other tumour models has not yet been evaluated, however the number of studies using shortened protocols is increasing, probably reflecting a growing consensus of issues with other longer protocols [426-428]. Prolonged exposure to M-CSF may induce an artificial, non-physiological and irreversible M2 phenotype which masks the effect of tumour conditioning. Our results showing an increase of cytotoxic $CD8^+$ T cells and IFNγ offer a novel role for 'M2-like' TAMs in the TME which could be harnessed to increase the rates of tumour rejection.

Previous efforts to target macrophages in the TME have relied on CSF1R targeting or the use of trabectedin, which is a cytotoxic agent selective for macrophages [429]. However the range of delivery methods and treatments which can effective harness or manipulate macrophage behaviour have increased greatly in recent years. Nanoparticles such as liposomes can effectively deliver encapsulated drugs specifically to phagocytic macrophages [430]. There are a range of epigenetic regulators which can effectively control macrophage polarization [268]. Recent advances in clustered regularly interspaced short palindromic repeats (CRISPR) allow effective tissue targeting [431]. In this context, the ability of TAMs to promote cytotoxic T cell responses is significant, epigenetic regulators which can impair glycolysis and the citric acid cycle but maintain an M2 macrophage phenotype may offer superior alternatives in comparison to regulators which boost M1 polarization [432].

ECT is commonly administered clinically with high complete response rates. One advantage of treatment is the localized effect of treatment with adjacent exposed healthy tissue remaining apparently unaffected [433,434]. Facial nerves, parotid ducts, eyelids and tear apparatus have all been exposed to treatment with no observed damage and retention of normal function [433]. Treatment can also be performed in proximity to vasculature, at distances which may otherwise be considered too closely associated for surgical interventions. The safety of nearby tissues may be tissue specific, while no serious adverse events have been recorded for the treatment of routine dermal lesions, the combination of ECT with subsequent radiotherapy has suggested that ECT may be the cause of osteoradionecrosis following treatment of tumours on the floor of

the mouth, and reconstructive surgery is common following treatment of tumours located in the bucca, floor of mouth, or base of tongue [435].

While adjacent tissues are commonly unaffected, non-neoplastic cells within the TME are exposed to equivalent EP. The TME contains a wide diversity and high concentration of stromal cells and immune cells. Preliminary *in vitro* studies have been performed examining the effect of EP on fibroblast and vascular endothelial and non-vascular endothelial cell lines. Vascular endothelial cells have been shown to be highly sensitive to treatment with markedly reduced survival [436,437]. Fibroblast cell lines have been shown to be resistant to ECT induced cell death in comparison to tumour cells, indicating a cell type specific sensitivities [436,438]. *In vitro* results have been corroborated by *in vivo* studies which have observed restricted blood flow and irreversible damaged of intratumoural vasculature following ECT, a phenomenon which has been exploited for the palliative treatment of bleeding melanoma lesions [439,440].

Investigation of the effect of EP and ECT on intratumoural immune cells has not yet been investigated. It is known that ECT can induce an immunogenic form of cell death in cancer cells, however, immunogenic cell death is only relevant in the presence of a competent immune system [223]. Calcium electroporation results in a rapid form of cell death, indicating that it is likely to represent an immunogenic form of cell death [441,442]. However, due to the delayed versus acute death seen in ECT versus calcium electroporation, it is likely that the supply of PAMPs and damage associated molecular patterns (DAMPs) are supplied over different time courses following the respective treatments, which could affect the immunogenicity of treatments (**Figure 5.5**). The case report of a systemic anti-cancer response seen in an advanced melanoma patient following treatment with ECT and calcium EP, indicates that calcium EP may be superior in generating an immunogenic response [225].

Activating an immune response following treatment is critical to the development of effective, safe and durable cancer treatments. The potential of harnessing this response more reliably by optimising therapeutic regimens or by designing combination treatments is dependent on understanding the immune response following treatment. The focus of the study presented here is to evaluate the effect of treatment on macrophages present within the tumour at the time of treatment, as these cells are

likely to represent a significant proportion of the immune compartment following treatment in addition to the cells which may infiltrate the tumour following treatment [380]. Having shown that TAMs can boost cytotoxic $CD8^+$ T cell responses, we next examined if delivery of treatment could be optimized to enhance this effect.

Using a model of melanoma conditioned macrophages, we have shown that macrophages are less susceptible to membrane poration than tumour cells when given equivalent treatment. While macrophage membranes reseal, there is a significant loss of viability following treatment. Promisingly, the ability of surviving macrophages to stimulate T cell responses following treatment is not impaired. These results are significant in the context of immunogenic cell death shown following ECT [443,223]. The efficacy of Ipilimumab in melanoma patients has been shown to be almost doubled when combined with local ablative therapies, and there is significant interest in the combination of Ipilimumab with ECT, with further clinical evaluation ongoing (EU clinical trials number 2014-004420-22) [444,445]. As discussed in **section 1.7.8**, the improved tolerability of Ipilimumab when combined with GM-CSF may indicate that beneficial intratumoural macrophage behaviour can improve therapeutic delivery [201].

ECT is regularly given to advanced melanoma patients in Europe and the US where treatment with immunotherapies is offered to all suitable patients. There are no powered prospective studies showing a significant effect of ECT on response to immunotherapies [382,444]. However there are studies which provide sufficient evidence to justify a powered controlled trial [444]. Because of the affordability of ECT and absence of a patentable element of treatment, it is unclear who would fund such a trial, which would require highly costly immunotherapies.

Further to the promising clinical observations in response to ECT in combination with immunotherapy, there is significant progress being made in the field of electroporation to expand treatment opportunities to new organ types, to optimize therapy to enhance responses, and to optimise delivery to facilitate pain free delivery. Substitution of chemotherapy with calcium, without any loss of efficacy, has been a major breakthrough. The use of calcium with high frequency electrical parameters, which are also under development, could revolutionize the field of electroporation in which theatres and cytotoxic drugs are no longer required. Thus EP could offer an ideal

accompaniment to costly immunotherapeutics, which is tolerable, easily administered, economical, and can enhance response rates.

To position EP treatments as a potential co-treatment to immunotherapy, it is necessary to comprehensively understand treatment and optimise the immunogenicity of treatment. Understanding the effect of treatment on the immune compartment is critical to improving treatment. To fully understand the immune response it is necessary to establish the effect of treatment on exposed cells, the immune cell recruitment following treatment, and the *in vivo* immune responses following treatment. The data presented here is positive, in indicating the effect of calcium electroporation on intratumoural macrophages can be immunostimulatory at the correct calcium concentration.

Our understanding of the potential of tissue resident macrophages to self-maintain, independent of circulating monocytes has revolutionized our understanding of terminal macrophage differentiation [446]. It has recently been established that tissue resident macrophages can contribute to TAMs in a murine model of colorectal cancer and self-maintain [366]. It is difficult to perform lineage determination in clinical disease however circulating monocytes are still considered to be the predominant source of TAMs. Analysis of long term effects of bleomycin on BMDMs is not possible, as BMDMs have limited replicative potential when grown *in vitro* [447]. The reduction of viability following ECT is in line with the hypothesis that macrophages are susceptible to bleomycin induced cell death following treatment, as has been previously shown [448]. However the induction of immunological memory following ECT in combination with agonistic anti-inducible T-cell costimulatory (ICOS) antibodies has previously been shown in murine models, indicating that the immune response is intact [381].

The addition of calcium to EP treatment did not affect the level of membrane poration, however it played a protective role in increasing viability at 24hrs and 5 days following treatment. Calcium prevented the decrease of the activation markers F4/80 and CD206 following EP. F4/80 is an epidermal growth factor-transmembrane 7 family protein and a G-protein coupled receptor, which can promote the generation Tregs [449]. CD206 mediated engagement of tumoural mucins has also been shown to promote a suppressive phenotype [450]. However the addition of calcium had no effect on T cell

proliferation and did not increase Treg polarization. Furthermore a higher dose of calcium resulted in a marked increase if IFNγ levels following coculture indicating the promotion of a type 1 cytotoxic T cell response. These results indicate that using a dose in the region of 5mM calcium in combination with EP will induce favourable immunogenic responses following treatment.

The lowered arginase activity of treated cells and increased $CD8^+$ T cell proliferation, $CD8^+$ T cell cytotoxicity, and IFNγ secretion in response to calcium appears to be conducive to the generation of anti-cancer cytotoxic responses, which provides a hypothesis to explain the clinical case report of systemic anti-cancer response following calcium EP [225]. The beneficial effects of antitumour T cell mediated effects have been shown at length and are a positive indicator for the translation of the current treatment regimen to *in vivo* murine models [451]. Due to the local delivery of electroporation and tissue contact required, subcutaneous tumour models are frequently adopted, and while appropriate for the current study in melanoma there are indications this treatment could be effective in other orthotopic tumour models [452].

There are a range of local ablative and non-ablative treatments being investigated as appropriate combination treatments for immunotherapeutics, however we propose that given the results shown here, calcium EP may provide an effective and cost effective additional or sole therapy for patients and enhance the efficacy of costly systemic anti-cancer therapies.

References

1. Graciotti M, Berti C, Klok HA, Kandalaft L (2017) The era of bioengineering: how will this affect the next generation of cancer immunotherapy? J Transl Med 15 (1):142. doi:10.1186/s12967-017-1244-2

2. Kalathil SG, Thanavala Y (2016) High immunosuppressive burden in cancer patients: a major hurdle for cancer immunotherapy. Cancer immunology, immunotherapy : CII 65 (7):813-819. doi:10.1007/s00262-016-1810-0

3. Dennis KL, Blatner NR, Gounari F, Khazaie K (2013) Current status of interleukin-10 and regulatory T-cells in cancer. Curr Opin Oncol 25 (6):637-645. doi:10.1097/CCO.0000000000000006

4. Grywalska E, Pasiarski M, Góźdź S, Roliński J (2018) Immune-checkpoint inhibitors for combating T-cell dysfunction in cancer. Onco Targets Ther 11:6505-6524. doi:10.2147/OTT.S150817

5. Seidel JA, Otsuka A, Kabashima K (2018) Anti-PD-1 and Anti-CTLA-4 Therapies in Cancer: Mechanisms of Action, Efficacy, and Limitations. Frontiers in oncology 8:86-86. doi:10.3389/fonc.2018.00086

6. Farzaneh L, Kasahara N, Farzaneh F (2007) The strange case of TGN1412. Cancer Immunol Immunother 56 (2):129-134. doi:10.1007/s00262-006-0189-8

7. Hassel JC, Heinzerling L, Aberle J, Bahr O, Eigentler TK, Grimm MO, Grunwald V, Leipe J, Reinmuth N, Tietze JK, Trojan J, Zimmer L, Gutzmer R (2017) Combined immune checkpoint blockade (anti-PD-1/anti-CTLA-4): Evaluation and management of adverse drug reactions. Cancer Treat Rev 57:36-49. doi:10.1016/j.ctrv.2017.05.003

8. Hodi FS, O'Day SJ, McDermott DF, Weber RW, Sosman JA, Haanen JB, Gonzalez R, Robert C, Schadendorf D, Hassel JC, Akerley W, van den Eertwegh AJ, Lutzky J, Lorigan P, Vaubel JM, Linette GP, Hogg D, Ottensmeier CH, Lebbe C, Peschel C, Quirt I, Clark JI, Wolchok JD, Weber JS, Tian J, Yellin MJ, Nichol GM, Hoos A, Urba WJ (2010) Improved survival with ipilimumab in patients with metastatic melanoma. N Engl J Med 363 (8):711-723. doi:10.1056/NEJMoa1003466

9. Robert C, Schachter J, Long GV, Arance A, Grob JJ, Mortier L, Daud A, Carlino MS, McNeil C, Lotem M, Larkin J, Lorigan P, Neyns B, Blank CU, Hamid O, Mateus C, Shapira-Frommer R, Kosh M, Zhou H, Ibrahim N, Ebbinghaus S, Ribas A

(2015) Pembrolizumab versus Ipilimumab in Advanced Melanoma. N Engl J Med 372 (26):2521-2532. doi:10.1056/NEJMoa1503093
10. Prasad V (2018) Immunotherapy: Tisagenlecleucel - the first approved CAR-T-cell therapy: implications for payers and policy makers. Nature reviews Clinical oncology 15 (1):11-12. doi:10.1038/nrclinonc.2017.156
11. Larkin J, Chiarion-Sileni V, Gonzalez R, Grob JJ, Rutkowski P, Lao CD, Cowey CL, Schadendorf D, Wagstaff J, Dummer R, Ferrucci PF, Smylie M, Hogg D, Hill A, Marquez-Rodas I, Haanen J, Guidoboni M, Maio M, Schoffski P, Carlino MS, Lebbe C, McArthur G, Ascierto PA, Daniels GA, Long GV (2019) Five-Year Survival with Combined Nivolumab and Ipilimumab in Advanced Melanoma. 381 (16):1535-1546. doi:10.1056/NEJMoa1910836
12. Ascierto PA, Del Vecchio M, Robert C, Mackiewicz A, Chiarion-Sileni V, Arance A, Lebbe C, Bastholt L, Hamid O, Rutkowski P, McNeil C, Garbe C, Loquai C, Dreno B, Thomas L, Grob JJ, Liszkay G, Nyakas M, Gutzmer R, Pikiel J, Grange F, Hoeller C, Ferraresi V, Smylie M, Schadendorf D, Mortier L, Svane IM, Hennicken D, Qureshi A, Maio M (2017) Ipilimumab 10 mg/kg versus ipilimumab 3 mg/kg in patients with unresectable or metastatic melanoma: a randomised, double-blind, multicentre, phase 3 trial. Lancet Oncol 18 (5):611-622. doi:10.1016/s1470-2045(17)30231-0
13. Weber J (2007) Review: anti-CTLA-4 antibody ipilimumab: case studies of clinical response and immune-related adverse events. The oncologist 12 (7):864-872. doi:10.1634/theoncologist.12-7-864
14. Law AM, Lim E, Ormandy CJ, Gallego-Ortega D (2017) The innate and adaptive infiltrating immune systems as targets for breast cancer immunotherapy. Endocr Relat Cancer 24 (4):R123-r144. doi:10.1530/erc-16-0404
15. Liu Y, Zeng G (2012) Cancer and Innate Immune System Interactions: Translational Potentials for Cancer Immunotherapy. J Immunother 35 (4):299-308. doi:10.1097/CJI.0b013e3182518e83
16. Cassetta L, Fragkogianni S, Sims AH, Swierczak A, Forrester LM, Zhang H, Soong DYH, Cotechini T, Anur P, Lin EY, Fidanza A, Lopez-Yrigoyen M, Millar MR, Urman A, Ai Z, Spellman PT, Hwang ES, Dixon JM, Wiechmann L, Coussens LM, Smith HO, Pollard JW (2019) Human Tumor-Associated Macrophage and Monocyte Transcriptional Landscapes Reveal Cancer-Specific Reprogramming,

Biomarkers, and Therapeutic Targets. Cancer cell 35 (4):588-602.e510. doi:10.1016/j.ccell.2019.02.009
17. Sturey R, Patnaik A (2017) Neutrophils and anti-cancer immunity: a paradigm shift in cancer immunotherapy. Oncoscience 4 (11-12):164-165. doi:10.18632/oncoscience.378
18. Hanahan D, Weinberg RA (2011) Hallmarks of cancer: the next generation. Cell 144 (5):646-674. doi:10.1016/j.cell.2011.02.013
19. Solinas G, Germano G, Mantovani A, Allavena P (2009) Tumor-associated macrophages (TAM) as major players of the cancer-related inflammation. J Leukoc Biol 86 (5):1065-1073. doi:10.1189/jlb.0609385
20. Poh AR, Ernst M (2018) Targeting Macrophages in Cancer: From Bench to Bedside. Front Oncol 8 (49). doi:10.3389/fonc.2018.00049
21. Noy R, Pollard JW (2014) Tumor-associated macrophages: from mechanisms to therapy. Immunity 41 (1):49-61. doi:10.1016/j.immuni.2014.06.010
22. Shapouri-Moghaddam A, Mohammadian S, Vazini H, Taghadosi M, Esmaeili SA, Mardani F, Seifi B, Mohammadi A, Afshari JT, Sahebkar A (2018) Macrophage plasticity, polarization, and function in health and disease. 233 (9):6425-6440. doi:10.1002/jcp.26429
23. Mosser DM, Edwards JP (2008) Exploring the full spectrum of macrophage activation. Nat Rev Immunol 8 (12):958-969. doi:10.1038/nri2448
24. Murray PJ, Allen JE, Biswas SK, Fisher EA, Gilroy DW, Goerdt S, Gordon S, Hamilton JA, Ivashkiv LB, Lawrence T, Locati M, Mantovani A, Martinez FO, Mege JL, Mosser DM, Natoli G, Saeij JP, Schultze JL, Shirey KA, Sica A, Suttles J, Udalova I, van Ginderachter JA, Vogel SN, Wynn TA (2014) Macrophage activation and polarization: nomenclature and experimental guidelines. Immunity 41 (1):14-20. doi:10.1016/j.immuni.2014.06.008
25. Mills CD, Ley K (2014) M1 and M2 macrophages: the chicken and the egg of immunity. J Innate Immun 6 (6):716-726. doi:10.1159/000364945
26. Bronte V, Brandau S, Chen SH, Colombo MP, Frey AB, Greten TF, Mandruzzato S, Murray PJ, Ochoa A, Ostrand-Rosenberg S, Rodriguez PC, Sica A, Umansky V, Vonderheide RH, Gabrilovich DI (2016) Recommendations for myeloid-derived suppressor cell nomenclature and characterization standards. Nat Commun 7:12150. doi:10.1038/ncomms12150

27. Mills CD, Lenz LL, Ley K (2015) Macrophages at the fork in the road to health or disease. Front Immunol 6:59. doi:10.3389/fimmu.2015.00059
28. Oishi Y, Manabe I (2018) Macrophages in inflammation, repair and regeneration. International immunology 30 (11):511-528. doi:10.1093/intimm/dxy054
29. Konig S, Nitzki F, Uhmann A, Dittmann K, Theiss-Suennemann J, Herrmann M, Reichardt HM, Schwendener R, Pukrop T, Schulz-Schaeffer W, Hahn H (2014) Depletion of cutaneous macrophages and dendritic cells promotes growth of basal cell carcinoma in mice. PloS one 9 (4):e93555. doi:10.1371/journal.pone.0093555
30. Nesbit M, Schaider H, Miller TH, Herlyn M (2001) Low-level monocyte chemoattractant protein-1 stimulation of monocytes leads to tumor formation in nontumorigenic melanoma cells. J Immunol 166 (11):6483-6490
31. Sica A, Schioppa T, Mantovani A, Allavena P (2006) Tumour-associated macrophages are a distinct M2 polarised population promoting tumour progression: potential targets of anti-cancer therapy. Eur J Cancer 42 (6):717-727. doi:10.1016/j.ejca.2006.01.003
32. Dandekar RC, Kingaonkar AV, Dhabekar GS (2011) Role of macrophages in malignancy. Ann Maxillofac Surg 1 (2):150-154. doi:10.4103/2231-0746.92782
33. Qian B, Pollard JW (2010) Macrophage Diversity Enhances Tumor Progression and Metastasis. Cell 141 (1):39-51. doi:10.1016/j.cell.2010.03.014
34. Mantovani A, Allavena P (2015) The interaction of anticancer therapies with tumor-associated macrophages. J Exp Med 212 (4):435-445. doi:10.1084/jem.20150295
35. Sconocchia G, Zlobec I, Lugli A, Calabrese D, Iezzi G, Karamitopoulou E, Patsouris ES, Peros G, Horcic M, Tornillo L, Zuber M, Droeser R, Muraro MG, Mengus C, Oertli D, Ferrone S, Terracciano L, Spagnoli GC (2011) Tumor infiltration by FcγRIII (CD16)+ myeloid cells is associated with improved survival in patients with colorectal carcinoma. Int J Cancer 128 (11):2663-2672. doi:10.1002/ijc.25609
36. Forssell J, Oberg A, Henriksson ML, Stenling R, Jung A, Palmqvist R (2007) High macrophage infiltration along the tumor front correlates with improved survival in colon cancer. Clin Cancer Res 13 (5):1472-1479. doi:10.1158/1078-0432.ccr-06-2073

37. Zhou Q, Peng RQ, Wu XJ, Xia Q, Hou JH, Ding Y, Zhou QM, Zhang X, Pang ZZ, Wan DS, Zeng YX, Zhang XS (2010) The density of macrophages in the invasive front is inversely correlated to liver metastasis in colon cancer. J Transl Med 8:13. doi:10.1186/1479-5876-8-13
38. DeNardo DG, Brennan DJ, Rexhepaj E, Ruffell B, Shiao SL, Madden SF, Gallagher WM, Wadhwani N, Keil SD, Junaid SA, Rugo HS, Hwang ES, Jirstrom K, West BL, Coussens LM (2011) Leukocyte complexity predicts breast cancer survival and functionally regulates response to chemotherapy. Cancer Discov 1 (1):54-67. doi:10.1158/2159-8274.cd-10-0028
39. Steidl C, Farinha P, Gascoyne RD (2011) Macrophages predict treatment outcome in Hodgkin's lymphoma. Haematologica 96 (2):186-189. doi:10.3324/haematol.2010.033316
40. Beck AH, Espinosa I, Edris B, Li R, Montgomery K, Zhu S, Varma S, Marinelli RJ, van de Rijn M, West RB (2009) The macrophage colony-stimulating factor 1 response signature in breast carcinoma. Clin Cancer Res 15 (3):778-787. doi:10.1158/1078-0432.ccr-08-1283
41. Gwak JM, Jang MH, Kim DI, Seo AN, Park SY (2015) Prognostic value of tumor-associated macrophages according to histologic locations and hormone receptor status in breast cancer. PloS one 10 (4):e0125728. doi:10.1371/journal.pone.0125728
42. Tsutsui S, Yasuda K, Suzuki K, Tahara K, Higashi H, Era S (2005) Macrophage infiltration and its prognostic implications in breast cancer: the relationship with VEGF expression and microvessel density. Oncol Rep 14 (2):425-431
43. Zhang QW, Liu L, Gong CY, Shi HS, Zeng YH, Wang XZ, Zhao YW, Wei YQ (2012) Prognostic significance of tumor-associated macrophages in solid tumor: a meta-analysis of the literature. PloS one 7 (12):e50946. doi:10.1371/journal.pone.0050946
44. Miyasato Y, Shiota T, Ohnishi K, Pan C, Yano H, Horlad H, Yamamoto Y, Yamamoto-Ibusuki M, Iwase H, Takeya M, Komohara Y (2017) High density of CD204-positive macrophages predicts worse clinical prognosis in patients with breast cancer. Cancer Sci 108 (8):1693-1700. doi:10.1111/cas.13287
45. Nabeshima A, Matsumoto Y, Fukushi J, Iura K, Matsunobu T, Endo M, Fujiwara T, Iida K, Fujiwara Y, Hatano M, Yokoyama N, Fukushima S, Oda Y, Iwamoto Y (2015) Tumour-associated macrophages correlate with poor prognosis in myxoid

liposarcoma and promote cell motility and invasion via the HB-EGF-EGFR-PI3K/Akt pathways. Br J Cancer 112 (3):547-555. doi:10.1038/bjc.2014.637
46. Hammes LS, Tekmal RR, Naud P, Edelweiss MI, Kirma N, Valente PT, Syrjanen KJ, Cunha-Filho JS (2007) Macrophages, inflammation and risk of cervical intraepithelial neoplasia (CIN) progression--clinicopathological correlation. Gynecol Oncol 105 (1):157-165. doi:10.1016/j.ygyno.2006.11.023
47. Zijlmans HJ, Fleuren GJ, Baelde HJ, Eilers PH, Kenter GG, Gorter A (2006) The absence of CCL2 expression in cervical carcinoma is associated with increased survival and loss of heterozygosity at 17q11.2. J Pathol 208 (4):507-517. doi:10.1002/path.1918
48. Bronkhorst IH, Ly LV, Jordanova ES, Vrolijk J, Versluis M, Luyten GP, Jager MJ (2011) Detection of M2-macrophages in uveal melanoma and relation with survival. Invest Ophthalmol Vis Sci 52 (2):643-650. doi:10.1167/iovs.10-5979
49. Wan T, Liu JH, Zheng LM, Cai MY, Ding T (2009) [Prognostic significance of tumor-associated macrophage infiltration in advanced epithelial ovarian carcinoma]. Ai Zheng 28 (3):323-327
50. Lan C, Huang X, Lin S, Huang H, Cai Q, Wan T, Lu J, Liu J (2013) Expression of M2-polarized macrophages is associated with poor prognosis for advanced epithelial ovarian cancer. Technol Cancer Res Treat 12 (3):259-267. doi:10.7785/tcrt.2012.500312
51. Zhang M, He Y, Sun X, Li Q, Wang W, Zhao A, Di W (2014) A high M1/M2 ratio of tumor-associated macrophages is associated with extended survival in ovarian cancer patients. J Ovarian Res 7:19. doi:10.1186/1757-2215-7-19
52. No JH, Moon JM, Kim K, Kim YB (2013) Prognostic significance of serum soluble CD163 level in patients with epithelial ovarian cancer. Gynecol Obstet Invest 75 (4):263-267. doi:10.1159/000349892
53. Ohno S, Inagawa H, Dhar DK, Fujii T, Ueda S, Tachibana M, Suzuki N, Inoue M, Soma G, Nagasue N (2003) The degree of macrophage infiltration into the cancer cell nest is a significant predictor of survival in gastric cancer patients. Anticancer Res 23 (6d):5015-5022
54. Lissbrant IF, Stattin P, Wikstrom P, Damber JE, Egevad L, Bergh A (2000) Tumor associated macrophages in human prostate cancer: relation to clinicopathological variables and survival. Int J Oncol 17 (3):445-451

55. Komohara Y, Ohnishi K, Kuratsu J, Takeya M (2008) Possible involvement of the M2 anti-inflammatory macrophage phenotype in growth of human gliomas. J Pathol 216 (1):15-24. doi:10.1002/path.2370
56. Yuan A, Hsiao Y-J, Chen H-Y, Chen H-W, Ho C-C, Chen Y-Y, Liu Y-C, Hong T-H, Yu S-L, Chen JJW, Yang P-C (2015) Opposite Effects of M1 and M2 Macrophage Subtypes on Lung Cancer Progression. Sci Rep 5:14273
57. Ma J, Liu L, Che G, Yu N, Dai F, You Z (2010) The M1 form of tumor-associated macrophages in non-small cell lung cancer is positively associated with survival time. BMC Cancer 10 (1):112. doi:10.1186/1471-2407-10-112
58. Ohri CM, Shikotra A, Green RH, Waller DA, Bradding P (2009) Macrophages within NSCLC tumour islets are predominantly of a cytotoxic M1 phenotype associated with extended survival. Eur Respir J 33 (1):118-126. doi:10.1183/09031936.00065708
59. Niino D, Komohara Y, Murayama T, Aoki R, Kimura Y, Hashikawa K, Kiyasu J, Takeuchi M, Suefuji N, Sugita Y, Takeya M, Ohshima K (2010) Ratio of M2 macrophage expression is closely associated with poor prognosis for Angioimmunoblastic T-cell lymphoma (AITL). Pathol Int 60 (4):278-283. doi:10.1111/j.1440-1827.2010.02514.x
60. Steidl C, Lee T, Shah SP, Farinha P, Han G, Nayar T, Delaney A, Jones SJ, Iqbal J, Weisenburger DD, Bast MA, Rosenwald A, Muller-Hermelink HK, Rimsza LM, Campo E, Delabie J, Braziel RM, Cook JR, Tubbs RR, Jaffe ES, Lenz G, Connors JM, Staudt LM, Chan WC, Gascoyne RD (2010) Tumor-associated macrophages and survival in classic Hodgkin's lymphoma. N Engl J Med 362 (10):875-885. doi:10.1056/NEJMoa0905680
61. Kamper P, Bendix K, Hamilton-Dutoit S, Honoré B, Nyengaard JR, d'Amore F (2011) Tumor-infiltrating macrophages correlate with adverse prognosis and Epstein-Barr virus status in classical Hodgkin's lymphoma. Haematologica 96 (2):269-276. doi:10.3324/haematol.2010.031542
62. Farinha P, Masoudi H, Skinnider BF, Shumansky K, Spinelli JJ, Gill K, Klasa R, Voss N, Connors JM, Gascoyne RD (2005) Analysis of multiple biomarkers shows that lymphoma-associated macrophage (LAM) content is an independent predictor of survival in follicular lymphoma (FL). Blood 106 (6):2169-2174. doi:10.1182/blood-2005-04-1565

63. Sconocchia G, Zlobec I, Lugli A, Calabrese D, Iezzi G, Karamitopoulou E, Patsouris ES, Peros G, Horcic M, Tornillo L, Zuber M, Droeser R, Muraro MG, Mengus C, Oertli D, Ferrone S, Terracciano L, Spagnoli GC (2011) Tumor infiltration by FcgammaRIII (CD16)+ myeloid cells is associated with improved survival in patients with colorectal carcinoma. Int J Cancer 128 (11):2663-2672. doi:10.1002/ijc.25609
64. Pinto ML, Rios E, Duraes C, Ribeiro R, Machado JC, Mantovani A, Barbosa MA, Carneiro F, Oliveira MJ (2019) The Two Faces of Tumor-Associated Macrophages and Their Clinical Significance in Colorectal Cancer. Front Immunol 10:1875. doi:10.3389/fimmu.2019.01875
65. Medrek C, Ponten F, Jirstrom K, Leandersson K (2012) The presence of tumor associated macrophages in tumor stroma as a prognostic marker for breast cancer patients. BMC Cancer 12:306. doi:10.1186/1471-2407-12-306
66. Ohno S, Ohno Y, Suzuki N, Kamei T, Koike K, Inagawa H, Kohchi C, Soma G, Inoue M (2004) Correlation of histological localization of tumor-associated macrophages with clinicopathological features in endometrial cancer. Anticancer Res 24 (5c):3335-3342
67. Mei J, Xiao Z, Guo C, Pu Q, Ma L, Liu C, Lin F, Liao H, You Z, Liu L (2016) Prognostic impact of tumor-associated macrophage infiltration in non-small cell lung cancer: A systemic review and meta-analysis. Oncotarget 7 (23):34217-34228. doi:10.18632/oncotarget.9079
68. Shu QH, Ge YS, Ma HX, Gao XQ, Pan JJ, Liu D, Xu GL, Ma JL, Jia WD (2016) Prognostic value of polarized macrophages in patients with hepatocellular carcinoma after curative resection. J Cell Mol Med 20 (6):1024-1035. doi:10.1111/jcmm.12787
69. Klimp AH, Hollema H, Kempinga C, van der Zee AG, de Vries EG, Daemen T (2001) Expression of cyclooxygenase-2 and inducible nitric oxide synthase in human ovarian tumors and tumor-associated macrophages. Cancer Res 61 (19):7305-7309
70. Colvin EK (2014) Tumor-Associated Macrophages Contribute to Tumor Progression in Ovarian Cancer. Front Oncol 4:137. doi:10.3389/fonc.2014.00137
71. Lyman GH, Williams CC, Preston D (1980) The use of lithium carbonate to reduce infection and leukopenia during systemic chemotherapy. N Engl J Med 302 (5):257-260. doi:10.1056/nejm198001313020503
72. Paulus P, Stanley ER, Schafer R, Abraham D, Aharinejad S (2006) Colony-stimulating factor-1 antibody reverses chemoresistance in human MCF-7 breast

cancer xenografts. Cancer Res 66 (8):4349-4356. doi:10.1158/0008-5472.can-05-3523
73. Sugimura K, Miyata H, Tanaka K, Takahashi T, Kurokawa Y, Yamasaki M, Nakajima K, Takiguchi S, Mori M, Doki Y (2015) High infiltration of tumor-associated macrophages is associated with a poor response to chemotherapy and poor prognosis of patients undergoing neoadjuvant chemotherapy for esophageal cancer. J Surg Oncol 111 (6):752-759. doi:10.1002/jso.23881
74. Mitrofanova I, Zavyalova M, Telegina N, Buldakov M, Riabov V, Cherdyntseva N, Kzhyshkowska J (2017) Tumor-associated macrophages in human breast cancer parenchyma negatively correlate with lymphatic metastasis after neoadjuvant chemotherapy. Immunobiology 222 (1):101-109. doi:10.1016/j.imbio.2016.08.001
75. Matsuoka Y, Yoshida R, Nakayama H, Nagata M, Hirosue A, Tanaka T, Kawahara K, Nakagawa Y, Sakata J, Arita H, Hiraki A, Shinohara M (2015) The tumour stromal features are associated with resistance to 5-FU-based chemoradiotherapy and a poor prognosis in patients with oral squamous cell carcinoma. APMIS 123 (3):205-214. doi:10.1111/apm.12344
76. Ruffell B, Chang-Strachan D, Chan V, Rosenbusch A, Ho CM, Pryer N, Daniel D, Hwang ES, Rugo HS, Coussens LM (2014) Macrophage IL-10 blocks CD8+ T cell-dependent responses to chemotherapy by suppressing IL-12 expression in intratumoral dendritic cells. Cancer cell 26 (5):623-637. doi:10.1016/j.ccell.2014.09.006
77. De Palma M, Lewis CE (2011) Cancer: Macrophages limit chemotherapy. Nature 472 (7343):303-304. doi:10.1038/472303a
78. Krzyszczyk P, Schloss R, Palmer A, Berthiaume F (2018) The Role of Macrophages in Acute and Chronic Wound Healing and Interventions to Promote Pro-wound Healing Phenotypes. Frontiers in physiology 9:419-419. doi:10.3389/fphys.2018.00419
79. Genin M, Clement F, Fattaccioli A, Raes M, Michiels C (2015) M1 and M2 macrophages derived from THP-1 cells differentially modulate the response of cancer cells to etoposide. BMC Cancer 15:577. doi:10.1186/s12885-015-1546-9
80. Ruffell B, Coussens LM (2015) Macrophages and therapeutic resistance in cancer. Cancer cell 27 (4):462-472. doi:10.1016/j.ccell.2015.02.015
81. Rolny C, Mazzone M, Tugues S, Laoui D, Johansson I, Coulon C, Squadrito ML, Segura I, Li X, Knevels E, Costa S, Vinckier S, Dresselaer T, Akerud P, De

Mol M, Salomaki H, Phillipson M, Wyns S, Larsson E, Buysschaert I, Botling J, Himmelreich U, Van Ginderachter JA, De Palma M, Dewerchin M, Claesson-Welsh L, Carmeliet P (2011) HRG inhibits tumor growth and metastasis by inducing macrophage polarization and vessel normalization through downregulation of PlGF. Cancer cell 19 (1):31-44. doi:10.1016/j.ccr.2010.11.009
82. De Palma M, Lewis CE (2013) Macrophage regulation of tumor responses to anticancer therapies. Cancer cell 23 (3):277-286. doi:10.1016/j.ccr.2013.02.013
83. Germano G, Frapolli R, Belgiovine C, Anselmo A, Pesce S, Liguori M, Erba E, Uboldi S, Zucchetti M, Pasqualini F, Nebuloni M, van Rooijen N, Mortarini R, Beltrame L, Marchini S, Fuso Nerini I, Sanfilippo R, Casali PG, Pilotti S, Galmarini CM, Anichini A, Mantovani A, D'Incalci M, Allavena P (2013) Role of macrophage targeting in the antitumor activity of trabectedin. Cancer cell 23 (2):249-262. doi:10.1016/j.ccr.2013.01.008
84. Park B, Yee C, Lee K-M (2014) The Effect of Radiation on the Immune Response to Cancers. Int J Mol Sci 15 (1):927-943. doi:10.3390/ijms15010927
85. Obeid M, Panaretakis T, Joza N, Tufi R, Tesniere A, van Endert P, Zitvogel L, Kroemer G (2007) Calreticulin exposure is required for the immunogenicity of [gamma]-irradiation and UVC light-induced apoptosis. Cell Death Differ 14 (10):1848-1850
86. Ahn GO, Tseng D, Liao CH, Dorie MJ, Czechowicz A, Brown JM (2010) Inhibition of Mac-1 (CD11b/CD18) enhances tumor response to radiation by reducing myeloid cell recruitment. Proc Natl Acad Sci U S A 107 (18):8363-8368. doi:10.1073/pnas.0911378107
87. Crittenden MR, Cottam B, Savage T, Nguyen C, Newell P, Gough MJ (2012) Expression of NF-kappaB p50 in tumor stroma limits the control of tumors by radiation therapy. PloS one 7 (6):e39295. doi:10.1371/journal.pone.0039295
88. Martin BJ (2013) Inhibiting vasculogenesis after radiation: a new paradigm to improve local control by radiotherapy. Semin Radiat Oncol 23 (4):281-287. doi:10.1016/j.semradonc.2013.05.002
89. Wang SC, Yu CF, Hong JH, Tsai CS, Chiang CS (2013) Radiation therapy-induced tumor invasiveness is associated with SDF-1-regulated macrophage mobilization and vasculogenesis. PloS one 8 (8):e69182. doi:10.1371/journal.pone.0069182

90. Okubo M, Kioi M, Nakashima H, Sugiura K, Mitsudo K, Aoki I, Taniguchi H, Tohnai I (2016) M2-polarized macrophages contribute to neovasculogenesis, leading to relapse of oral cancer following radiation. Sci Rep 6:27548. doi:10.1038/srep27548
91. Crittenden MR, Cottam B, Savage T, Nguyen C, Newell P, Gough MJ (2012) Expression of NF-κB p50 in Tumor Stroma Limits the Control of Tumors by Radiation Therapy. PloS one 7 (6):e39295. doi:10.1371/journal.pone.0039295
92. Shiao SL, Ruffell B, DeNardo DG, Faddegon BA, Park CC, Coussens LM (2015) TH2-Polarized CD4(+) T Cells and Macrophages Limit Efficacy of Radiotherapy. Cancer Immunol Res 3 (5):518-525. doi:10.1158/2326-6066.cir-14-0232
93. Teresa Pinto A, Laranjeiro Pinto M, Patrícia Cardoso A, Monteiro C, Teixeira Pinto M, Filipe Maia A, Castro P, Figueira R, Monteiro A, Marques M, Mareel M, dos Santos SG, Seruca R, Adolfo Barbosa M, Rocha S, José Oliveira M (2016) Ionizing radiation modulates human macrophages towards a pro-inflammatory phenotype preserving their pro-invasive and pro-angiogenic capacities. Sci Rep 6:18765. doi:10.1038/srep18765
94. Klug F, Prakash H, Huber PE, Seibel T, Bender N, Halama N, Pfirschke C, Voss RH, Timke C, Umansky L, Klapproth K, Schakel K, Garbi N, Jager D, Weitz J, Schmitz-Winnenthal H, Hammerling GJ, Beckhove P (2013) Low-dose irradiation programs macrophage differentiation to an iNOS(+)/M1 phenotype that orchestrates effective T cell immunotherapy. Cancer cell 24 (5):589-602. doi:10.1016/j.ccr.2013.09.014
95. Shaikh S, Noshirwani A, West N, Perry S, Jayne D (2015) Can macrophages within the microenvironment of locally invasive rectal cancers predict response to radiotherapy? Lancet 385 Suppl 1:S87. doi:10.1016/s0140-6736(15)60402-0
96. Greenwald RJ, Freeman GJ, Sharpe AH (2005) The B7 family revisited. Annu Rev Immunol 23:515-548. doi:10.1146/annurev.immunol.23.021704.115611
97. Che F, Heng X, Zhang H, Su Q, Zhang B, Chen Y, Zhang Z, Du Y, Wang L (2017) Novel B7-H4-mediated crosstalk between human non-Hodgkin lymphoma cells and tumor-associated macrophages leads to immune evasion via secretion of IL-6 and IL-10. Cancer Immunol Immunother 66 (6):717-729. doi:10.1007/s00262-017-1961-7

98. Riley JL (2009) PD-1 signaling in primary T cells. Immunol Rev 229 (1):114-125. doi:10.1111/j.1600-065X.2009.00767.x
99. Hutchins AP, Diez D, Miranda-Saavedra D (2013) The IL-10/STAT3-mediated anti-inflammatory response: recent developments and future challenges. Brief Funct Genomics 12 (6):489-498. doi:10.1093/bfgp/elt028
100. Rodríguez-García M, Porichis F, de Jong OG, Levi K, Diefenbach TJ, Lifson JD, Freeman GJ, Walker BD, Kaufmann DE, Kavanagh DG (2011) Expression of PD-L1 and PD-L2 on human macrophages is up-regulated by HIV-1 and differentially modulated by IL-10. J Leukoc Biol 89 (4):507-515. doi:10.1189/jlb.0610327
101. Hartley G, Regan D, Guth A, Dow S (2017) Regulation of PD-L1 expression on murine tumor-associated monocytes and macrophages by locally produced TNF-alpha. Cancer Immunol Immunother 66 (4):523-535. doi:10.1007/s00262-017-1955-5
102. Bournazos S, Wang TT, Ravetch JV (2016) The Role and Function of Fcγ Receptors on Myeloid Cells. Microbiol Spectr 4 (6):10.1128/microbiolspec.MCHD-0045-2016. doi:10.1128/microbiolspec.MCHD-0045-2016
103. Tiller KE, Tessier PM (2015) Advances in Antibody Design. Annual review of biomedical engineering 17:191-216. doi:10.1146/annurev-bioeng-071114-040733
104. Kohrt HE, Houot R, Marabelle A, Cho HJ, Osman K, Goldstein M, Levy R, Brody J (2012) Combination strategies to enhance antitumor ADCC. Immunotherapy 4 (5):511-527. doi:10.2217/imt.12.38
105. Sliwkowski MX, Mellman I (2013) Antibody therapeutics in cancer. Science 341 (6151):1192-1198. doi:10.1126/science.1241145
106. Tse SM, Furuya W, Gold E, Schreiber AD, Sandvig K, Inman RD, Grinstein S (2003) Differential role of actin, clathrin, and dynamin in Fc gamma receptor-mediated endocytosis and phagocytosis. J Biol Chem 278 (5):3331-3338. doi:10.1074/jbc.M207966200
107. Vidarsson G, Dekkers G, Rispens T (2014) IgG subclasses and allotypes: from structure to effector functions. Frontiers in immunology 5:520-520. doi:10.3389/fimmu.2014.00520
108. Romano E, Kusio-Kobialka M, Foukas PG, Baumgaertner P, Meyer C, Ballabeni P, Michielin O, Weide B, Romero P, Speiser DE (2015) Ipilimumab-dependent cell-mediated cytotoxicity of regulatory T cells ex vivo by nonclassical

monocytes in melanoma patients. Proc Natl Acad Sci U S A 112 (19):6140-6145. doi:10.1073/pnas.1417320112
109. Sondermann P, Huber R, Oosthuizen V, Jacob U (2000) The 3.2-A crystal structure of the human IgG1 Fc fragment-Fc gammaRIII complex. Nature 406 (6793):267-273. doi:10.1038/35018508
110. Simpson TR, Li F, Montalvo-Ortiz W, Sepulveda MA, Bergerhoff K, Arce F, Roddie C, Henry JY, Yagita H, Wolchok JD, Peggs KS, Ravetch JV, Allison JP, Quezada SA (2013) Fc-dependent depletion of tumor-infiltrating regulatory T cells co-defines the efficacy of anti-CTLA-4 therapy against melanoma. J Exp Med 210 (9):1695-1710. doi:10.1084/jem.20130579
111. Bulliard Y, Jolicoeur R, Windman M, Rue SM, Ettenberg S, Knee DA, Wilson NS, Dranoff G, Brogdon JL (2013) Activating Fc gamma receptors contribute to the antitumor activities of immunoregulatory receptor-targeting antibodies. J Exp Med 210 (9):1685-1693. doi:10.1084/jem.20130573
112. Martens A, Wistuba-Hamprecht K, Geukes Foppen M, Yuan J, Postow MA, Wong P, Romano E, Khammari A, Dreno B, Capone M, Ascierto PA, Di Giacomo AM, Maio M, Schilling B, Sucker A, Schadendorf D, Hassel JC, Eigentler TK, Martus P, Wolchok JD, Blank C, Pawelec G, Garbe C, Weide B (2016) Baseline Peripheral Blood Biomarkers Associated with Clinical Outcome of Advanced Melanoma Patients Treated with Ipilimumab. Clin Cancer Res 22 (12):2908-2918. doi:10.1158/1078-0432.ccr-15-2412
113. Wang F, Li B, Wei Y, Zhao Y, Wang L, Zhang P, Yang J, He W, Chen H, Jiao Z, Li Y (2018) Tumor-derived exosomes induce PD1(+) macrophage population in human gastric cancer that promotes disease progression. Oncogenesis 7 (5):41. doi:10.1038/s41389-018-0049-3
114. Gordon SR, Maute RL, Dulken BW, Hutter G, George BM, McCracken MN, Gupta R, Tsai JM, Sinha R, Corey D, Ring AM, Connolly AJ, Weissman IL (2017) PD-1 expression by tumour-associated macrophages inhibits phagocytosis and tumour immunity. Nature 545 (7655):495-499. doi:10.1038/nature22396
115. Tumeh PC, Harview CL, Yearley JH, Shintaku IP, Taylor EJM, Robert L, Chmielowski B, Spasic M, Henry G, Ciobanu V, West AN, Carmona M, Kivork C, Seja E, Cherry G, Gutierrez AJ, Grogan TR, Mateus C, Tomasic G, Glaspy JA, Emerson RO, Robins H, Pierce RH, Elashoff DA, Robert C, Ribas A (2014) PD-1

blockade induces responses by inhibiting adaptive immune resistance. Nature 515 (7528):568-571. doi:10.1038/nature13954
116. McDermott DF, Sosman JA, Sznol M, Massard C, Gordon MS, Hamid O, Powderly JD, Infante JR, Fassò M, Wang YV, Zou W, Hegde PS, Fine GD, Powles T (2016) Atezolizumab, an Anti–Programmed Death-Ligand 1 Antibody, in Metastatic Renal Cell Carcinoma: Long-Term Safety, Clinical Activity, and Immune Correlates From a Phase Ia Study. J Clin Oncol 34 (8):833-842. doi:10.1200/JCO.2015.63.7421
117. Nicola NA (1987) Granulocyte colony-stimulating factor and differentiation-induction in myeloid leukemic cells. Int J Cell Cloning 5 (1):1-15. doi:10.1002/stem.5530050102
118. Helft J, Böttcher J, Chakravarty P, Zelenay S, Huotari J, Schraml Barbara U, Goubau D, Reis e Sousa C GM-CSF Mouse Bone Marrow Cultures Comprise a Heterogeneous Population of CD11c+ MHCII+ Macrophages and Dendritic Cells. Immunity 42 (6):1197-1211. doi:10.1016/j.immuni.2015.05.018
119. Verreck FAW, de Boer T, Langenberg DML, Hoeve MA, Kramer M, Vaisberg E, Kastelein R, Kolk A, de Waal-Malefyt R, Ottenhoff THM (2004) Human IL-23-producing type 1 macrophages promote but IL-10-producing type 2 macrophages subvert immunity to (myco)bacteria. Proc Natl Acad Sci U S A 101 (13):4560-4565. doi:10.1073/pnas.0400983101
120. Ferlazzo G, Klein J, Paliard X, Wei WZ, Galy A (2000) Dendritic cells generated from CD34+ progenitor cells with flt3 ligand, c-kit ligand, GM-CSF, IL-4, and TNF-alpha are functional antigen-presenting cells resembling mature monocyte-derived dendritic cells. J Immunother 23 (1):48-58
121. Eksioglu EA, Mahmood SS, Chang M, Reddy V (2007) GM-CSF promotes differentiation of human dendritic cells and T lymphocytes toward a predominantly type 1 proinflammatory response. Exp Hematol 35 (8):1163-1171. doi:10.1016/j.exphem.2007.05.001
122. Smith TJ, Khatcheressian J, Lyman GH, Ozer H, Armitage JO, Balducci L, Bennett CL, Cantor SB, Crawford J, Cross SJ, Demetri G, Desch CE, Pizzo PA, Schiffer CA, Schwartzberg L, Somerfield MR, Somlo G, Wade JC, Wade JL, Winn RJ, Wozniak AJ, Wolff AC (2006) 2006 update of recommendations for the use of white blood cell growth factors: an evidence-based clinical practice guideline. J Clin Oncol 24 (19):3187-3205. doi:10.1200/jco.2006.06.4451

123. Anassi E, Ndefo UA (2011) Sipuleucel-T (provenge) injection: the first immunotherapy agent (vaccine) for hormone-refractory prostate cancer. P T 36 (4):197-202
124. Kantoff PW, Higano CS, Shore ND, Berger ER, Small EJ, Penson DF, Redfern CH, Ferrari AC, Dreicer R, Sims RB, Xu Y, Frohlich MW, Schellhammer PF (2010) Sipuleucel-T Immunotherapy for Castration-Resistant Prostate Cancer. N Engl J Med 363 (5):411-422. doi:doi:10.1056/NEJMoa1001294
125. Simons JW, Sacks N (2006) Granulocyte-macrophage colony-stimulating factor-transduced allogeneic cancer cellular immunotherapy: the GVAX vaccine for prostate cancer. Urologic oncology 24 (5):419-424. doi:10.1016/j.urolonc.2005.08.021
126. Le DT, Wang-Gillam A, Picozzi V, Greten TF, Crocenzi T, Springett G, Morse M, Zeh H, Cohen D, Fine RL, Onners B, Uram JN, Laheru DA, Lutz ER, Solt S, Murphy AL, Skoble J, Lemmens E, Grous J, Dubensky T, Jr., Brockstedt DG, Jaffee EM (2015) Safety and survival with GVAX pancreas prime and Listeria Monocytogenes-expressing mesothelin (CRS-207) boost vaccines for metastatic pancreatic cancer. Journal of clinical oncology : official journal of the American Society of Clinical Oncology 33 (12):1325-1333. doi:10.1200/JCO.2014.57.4244
127. Lutz ER, Kinkead H, Jaffee EM, Zheng L (2014) Priming the pancreatic cancer tumor microenvironment for checkpoint-inhibitor immunotherapy. Oncoimmunology 3 (11):e962401. doi:10.4161/21624011.2014.962401
128. Zheng L (2014) Does vaccine-primed pancreatic cancer offer better candidates for immune-based therapies? Immunotherapy 6 (10):1017-1020. doi:10.2217/imt.14.87
129. Le DT, Lutz E, Uram JN, Sugar EA, Onners B, Solt S, Zheng L, Diaz LA, Jr., Donehower RC, Jaffee EM, Laheru DA (2013) Evaluation of ipilimumab in combination with allogeneic pancreatic tumor cells transfected with a GM-CSF gene in previously treated pancreatic cancer. J Immunother 36 (7):382-389. doi:10.1097/CJI.0b013e31829fb7a2
130. Adachi N, Yamaguchi K, Morikawa T, Suzuki M, Matsuda I, Abe MK (1994) Constitutive production of multiple colony-stimulating factors in patients with lung cancer associated with neutrophilia. Br J Cancer 69 (1):125-129

131. Ruef C, Coleman DL (1990) Granulocyte-macrophage colony-stimulating factor: pleiotropic cytokine with potential clinical usefulness. Reviews of infectious diseases 12 (1):41-62. doi:10.1093/clinids/12.1.41
132. Oshika Y, Nakamura M, Abe Y, Fukuchi Y, Yoshimura M, Itoh M, Ohnishi Y, Tokunaga T, Fukushima Y, Hatanaka H, Kijima H, Yamazaki H, Tamaoki N, Ueyama Y (1998) Growth stimulation of non-small cell lung cancer xenografts by granulocyte-macrophage colony-stimulating factor (GM-CSF). Eur J Cancer 34 (12):1958-1961
133. Hercus TR, Thomas D, Guthridge MA, Ekert PG, King-Scott J, Parker MW, Lopez AF (2009) The granulocyte-macrophage colony-stimulating factor receptor: linking its structure to cell signaling and its role in disease. Blood 114 (7):1289-1298. doi:10.1182/blood-2008-12-164004
134. Tsou C-L, Peters W, Si Y, Slaymaker S, Aslanian AM, Weisberg SP, Mack M, Charo IF (2007) Critical roles for CCR2 and MCP-3 in monocyte mobilization from bone marrow and recruitment to inflammatory sites. The Journal of clinical investigation 117 (4):902-909. doi:10.1172/JCI29919
135. Chiu HY, Sun KH, Chen SY, Wang HH, Lee MY, Tsou YC, Jwo SC, Sun GH, Tang SJ (2012) Autocrine CCL2 promotes cell migration and invasion via PKC activation and tyrosine phosphorylation of paxillin in bladder cancer cells. Cytokine 59 (2):423-432. doi:10.1016/j.cyto.2012.04.017
136. Craig MJ, Loberg RD (2006) CCL2 (Monocyte Chemoattractant Protein-1) in cancer bone metastases. Cancer Metastasis Rev 25 (4):611-619. doi:10.1007/s10555-006-9027-x
137. Saji H, Koike M, Yamori T, Saji S, Seiki M, Matsushima K, Toi M (2001) Significant correlation of monocyte chemoattractant protein-1 expression with neovascularization and progression of breast carcinoma. Cancer 92 (5):1085-1091
138. Kitamura T, Qian BZ, Soong D, Cassetta L, Noy R, Sugano G, Kato Y, Li J, Pollard JW (2015) CCL2-induced chemokine cascade promotes breast cancer metastasis by enhancing retention of metastasis-associated macrophages. J Exp Med 212 (7):1043-1059. doi:10.1084/jem.20141836
139. Silzle T, Kreutz M, Dobler MA, Brockhoff G, Knuechel R, Kunz-Schughart LA (2003) Tumor-associated fibroblasts recruit blood monocytes into tumor tissue. Eur J Immunol 33 (5):1311-1320. doi:10.1002/eji.200323057

140. Arendt LM, McCready J, Keller PJ, Baker DD, Naber SP, Seewaldt V, Kuperwasser C (2013) Obesity promotes breast cancer by CCL2-mediated macrophage recruitment and angiogenesis. Cancer Res 73 (19):6080-6093. doi:10.1158/0008-5472.can-13-0926
141. Zhao L, Lim SY, Gordon-Weeks AN, Tapmeier TT, Im JH, Cao Y, Beech J, Allen D, Smart S, Muschel RJ (2013) Recruitment of a myeloid cell subset (CD11b/Gr1 mid) via CCL2/CCR2 promotes the development of colorectal cancer liver metastasis. Hepatology 57 (2):829-839. doi:10.1002/hep.26094
142. Okuma T, Terasaki Y, Kaikita K, Kobayashi H, Kuziel WA, Kawasuji M, Takeya M (2004) C-C chemokine receptor 2 (CCR2) deficiency improves bleomycin-induced pulmonary fibrosis by attenuation of both macrophage infiltration and production of macrophage-derived matrix metalloproteinases. J Pathol 204 (5):594-604. doi:10.1002/path.1667
143. Roca H, Varsos ZS, Sud S, Craig MJ, Ying C, Pienta KJ (2009) CCL2 and interleukin-6 promote survival of human CD11b+ peripheral blood mononuclear cells and induce M2-type macrophage polarization. J Biol Chem 284 (49):34342-34354. doi:10.1074/jbc.M109.042671
144. Tanaka T, Terada M, Ariyoshi K, Morimoto K (2010) Monocyte chemoattractant protein-1/CC chemokine ligand 2 enhances apoptotic cell removal by macrophages through Rac1 activation. Biochem Biophys Res Commun 399 (4):677-682. doi:10.1016/j.bbrc.2010.07.141
145. Lu X, Kang Y (2009) Chemokine (C-C motif) ligand 2 engages CCR2+ stromal cells of monocytic origin to promote breast cancer metastasis to lung and bone. J Biol Chem 284 (42):29087-29096. doi:10.1074/jbc.M109.035899
146. Loberg RD, Ying C, Craig M, Yan L, Snyder LA, Pienta KJ (2007) CCL2 as an important mediator of prostate cancer growth in vivo through the regulation of macrophage infiltration. Neoplasia 9 (7):556-562
147. Loberg RD, Ying C, Craig M, Day LL, Sargent E, Neeley C, Wojno K, Snyder LA, Yan L, Pienta KJ (2007) Targeting CCL2 with systemic delivery of neutralizing antibodies induces prostate cancer tumor regression in vivo. Cancer Res 67 (19):9417-9424. doi:10.1158/0008-5472.can-07-1286
148. Li X, Yao W, Yuan Y, Chen P, Li B, Li J, Chu R, Song H, Xie D, Jiang X, Wang H (2015) Targeting of tumour-infiltrating macrophages via CCL2/CCR2

signalling as a therapeutic strategy against hepatocellular carcinoma. Gut 66 (1):157-167. doi:10.1136/gutjnl-2015-310514
149. Sanford DE, Belt BA, Panni RZ, Mayer A, Deshpande AD, Carpenter D, Mitchem JB, Plambeck-Suess SM, Worley LA, Goetz BD, Wang-Gillam A, Eberlein TJ, Denardo DG, Goedegebuure SP, Linehan DC (2013) Inflammatory monocyte mobilization decreases patient survival in pancreatic cancer: a role for targeting the CCL2/CCR2 axis. Clin Cancer Res 19 (13):3404-3415. doi:10.1158/1078-0432.ccr-13-0525
150. Qian DZ, Rademacher BLS, Pittsenbarger J, Huang C-Y, Myrthue A, Higano CS, Garzotto M, Nelson PS, Beer TM (2010) CCL2 is induced by chemotherapy and protects prostate cancer cells from docetaxel - induced cytotoxicity. The Prostate 70 (4):433-442. doi:10.1002/pros.21077
151. Nakasone ES, Askautrud HA, Kees T, Park J-H, Plaks V, Ewald AJ, Fein M, Rasch MG, Tan Y-X, Qiu J, Park J, Sinha P, Bissell MJ, Frengen E, Werb Z, Egeblad M (2012) Imaging tumor-stroma interactions during chemotherapy reveals contributions of the microenvironment to resistance. Cancer cell 21 (4):488-503. doi:10.1016/j.ccr.2012.02.017
152. Geller MA, Bui-Nguyen TM, Rogers LM, Ramakrishnan S (2010) Chemotherapy induces macrophage chemoattractant protein-1 production in ovarian cancer. Int J Gynecol Cancer 20 (6):918-925. doi:10.1111/IGC.0b013e3181e5c442
153. Moisan F, Francisco EB, Brozovic A, Duran GE, Wang YC, Chaturvedi S, Seetharam S, Snyder LA, Doshi P, Sikic BI (2014) Enhancement of paclitaxel and carboplatin therapies by CCL2 blockade in ovarian cancers. Mol Oncol 8 (7):1231-1239. doi:10.1016/j.molonc.2014.03.016
154. Kalbasi A, Komar C, Tooker GM, Liu M, Lee JW, Gladney WL, Ben-Josef E, Beatty GL (2017) Tumor-Derived CCL2 Mediates Resistance to Radiotherapy in Pancreatic Ductal Adenocarcinoma. Clin Cancer Res 23 (1):137-148. doi:10.1158/1078-0432.ccr-16-0870
155. Gorlov IP, Sircar K, Zhao H, Maity SN, Navone NM, Gorlova OY, Troncoso P, Pettaway CA, Byun JY, Logothetis CJ (2010) Prioritizing genes associated with prostate cancer development. BMC Cancer 10:599. doi:10.1186/1471-2407-10-599
156. Hu H, Sun L, Guo C, Liu Q, Zhou Z, Peng L, Pan J, Yu L, Lou J, Yang Z, Zhao P, Ran Y (2009) Tumor cell-microenvironment interaction models coupled with clinical validation reveal CCL2 and SNCG as two predictors of colorectal cancer

hepatic metastasis. Clin Cancer Res 15 (17):5485-5493. doi:10.1158/1078-0432.ccr-08-2491
157. Tonouchi H, Miki C, Tanaka K, Kusunoki M (2002) Profile of monocyte chemoattractant protein-1 circulating levels in gastric cancer patients. Scand J Gastroenterol 37 (7):830-833
158. Tao LL, Shi SJ, Chen LB, Huang GC (2014) Expression of monocyte chemotactic protein-1/CCL2 in gastric cancer and its relationship with tumor hypoxia. World J Gastroenterol 20 (15):4421-4427. doi:10.3748/wjg.v20.i15.4421
159. Li X, Yao W, Yuan Y, Chen P, Li B, Li J, Chu R, Song H, Xie D, Jiang X, Wang H (2017) Targeting of tumour-infiltrating macrophages via CCL2/CCR2 signalling as a therapeutic strategy against hepatocellular carcinoma. Gut 66 (1):157-167. doi:10.1136/gutjnl-2015-310514
160. Hembruff SL, Jokar I, Yang L, Cheng N (2010) Loss of transforming growth factor-beta signaling in mammary fibroblasts enhances CCL2 secretion to promote mammary tumor progression through macrophage-dependent and -independent mechanisms. Neoplasia 12 (5):425-433
161. Fujimoto H, Sangai T, Ishii G, Ikehara A, Nagashima T, Miyazaki M, Ochiai A (2009) Stromal MCP-1 in mammary tumors induces tumor-associated macrophage infiltration and contributes to tumor progression. Int J Cancer 125 (6):1276-1284. doi:10.1002/ijc.24378
162. Yoshimura T, Howard OM, Ito T, Kuwabara M, Matsukawa A, Chen K, Liu Y, Liu M, Oppenheim JJ, Wang JM (2013) Monocyte chemoattractant protein-1/CCL2 produced by stromal cells promotes lung metastasis of 4T1 murine breast cancer cells. PloS one 8 (3):e58791. doi:10.1371/journal.pone.0058791
163. Chun E, Lavoie S, Michaud M, Gallini CA, Kim J, Soucy G, Odze R, Glickman JN, Garrett WS (2015) CCL2 Promotes Colorectal Carcinogenesis by Enhancing Polymorphonuclear Myeloid-Derived Suppressor Cell Population and Function. Cell Rep 12 (2):244-257. doi:10.1016/j.celrep.2015.06.024
164. Snyder L, Kesavan P, Kaiser E, Rudnick K, McCabe F, Millar H, Nakada M, Yan L (2007) Neutralization of CCL2 inhibits tumor angiogenesis and pancreatic tumor growth. Mol Cancer Ther 6 (11 Supplement):A69 [Abstract]
165. Youngs SJ, Ali SA, Taub DD, Rees RC (1997) Chemokines induce migrational responses in human breast carcinoma cell lines. Int J Cancer 71 (2):257-266

166. Roca H, Varsos ZS, Pienta KJ (2009) CCL2 is a negative regulator of AMP-activated protein kinase to sustain mTOR complex-1 activation, survivin expression, and cell survival in human prostate cancer PC3 cells. Neoplasia 11 (12):1309-1317
167. Ueno T, Toi M, Saji H, Muta M, Bando H, Kuroi K, Koike M, Inadera H, Matsushima K (2000) Significance of macrophage chemoattractant protein-1 in macrophage recruitment, angiogenesis, and survival in human breast cancer. Clin Cancer Res 6 (8):3282-3289
168. Zhang J, Yan Y, Cui X, Zhang J, Yang Y, Li H, Wu H, Li J, Wang L, Li M, Liu X, Wang J, Duan X (2017) CCL2 expression correlates with Snail expression and affects the prognosis of patients with gastric cancer. Pathol Res Pract 213 (3):217-221
169. Wang Z, Xie H, Zhou L, Liu Z, Fu H, Zhu Y, Xu L, Xu J (2016) CCL2/CCR2 axis is associated with postoperative survival and recurrence of patients with non-metastatic clear-cell renal cell carcinoma. Oncotarget 7 (32):51525-51534. doi:10.18632/oncotarget.10492
170. Sandhu SK, Papadopoulos K, Fong PC, Patnaik A, Messiou C, Olmos D, Wang G, Tromp BJ, Puchalski TA, Balkwill F, Berns B, Seetharam S, de Bono JS, Tolcher AW (2013) A first-in-human, first-in-class, phase I study of carlumab (CNTO 888), a human monoclonal antibody against CC-chemokine ligand 2 in patients with solid tumors. Cancer Chemother Pharmacol 71 (4):1041-1050. doi:10.1007/s00280-013-2099-8
171. Pienta KJ, Machiels JP, Schrijvers D, Alekseev B, Shkolnik M, Crabb SJ, Li S, Seetharam S, Puchalski TA, Takimoto C, Elsayed Y, Dawkins F, de Bono JS (2013) Phase 2 study of carlumab (CNTO 888), a human monoclonal antibody against CC-chemokine ligand 2 (CCL2), in metastatic castration-resistant prostate cancer. Invest New Drugs 31 (3):760-768. doi:10.1007/s10637-012-9869-8
172. Lim SY, Yuzhalin AE, Gordon-Weeks AN, Muschel RJ (2016) Targeting the CCL2-CCR2 signaling axis in cancer metastasis. Oncotarget 7 (19):28697-28710. doi:10.18632/oncotarget.7376
173. Bonapace L, Coissieux M-M, Wyckoff J, Mertz KD, Varga Z, Junt T, Bentires-Alj M (2014) Cessation of CCL2 inhibition accelerates breast cancer metastasis by promoting angiogenesis. Nature 515 (7525):130-133
174. Nywening TM, Wang-Gillam A, Sanford DE, Belt BA, Panni RZ, Cusworth BM, Toriola AT, Nieman RK, Worley LA, Yano M, Fowler KJ, Lockhart AC,

Suresh R, Tan BR, Lim K-H, Fields RC, Strasberg SM, Hawkins WG, DeNardo DG, Goedegebuure SP, Linehan DC Targeting tumour-associated macrophages with CCR2 inhibition in combination with FOLFIRINOX in patients with borderline resectable and locally advanced pancreatic cancer: a single-centre, open-label, dose-finding, non-randomised, phase 1b trial. Lancet Oncol 17 (5):651-662. doi:10.1016/S1470-2045(16)00078-4

175. Beatty GL, Winograd R, Evans RA, Long KB, Luque SL, Lee JW, Clendenin C, Gladney WL, Knoblock DM, Guirnalda PD, Vonderheide RH (2015) Exclusion of T Cells From Pancreatic Carcinomas in Mice Is Regulated by Ly6C(low) F4/80(+) Extratumoral Macrophages. Gastroenterology 149 (1):201-210. doi:10.1053/j.gastro.2015.04.010

176. Beatty GL, Chiorean EG, Fishman MP, Saboury B, Teitelbaum UR, Sun W, Huhn RD, Song W, Li D, Sharp LL, Torigian DA, O'Dwyer PJ, Vonderheide RH (2011) CD40 agonists alter tumor stroma and show efficacy against pancreatic carcinoma in mice and humans. Science 331 (6024):1612-1616. doi:10.1126/science.1198443

177. Pahler JC, Tazzyman S, Erez N, Chen Y-Y, Murdoch C, Nozawa H, Lewis CE, Hanahan D (2008) Plasticity in Tumor-Promoting Inflammation: Impairment of Macrophage Recruitment Evokes a Compensatory Neutrophil Response. Neoplasia 10 (4):329-IN322

178. Pahler JC, Tazzyman S, Erez N, Chen YY, Murdoch C, Nozawa H, Lewis CE, Hanahan D (2008) Plasticity in tumor-promoting inflammation: impairment of macrophage recruitment evokes a compensatory neutrophil response. Neoplasia 10 (4):329-340

179. Jones CV, Ricardo SD (2013) Macrophages and CSF-1: implications for development and beyond. Organogenesis 9 (4):249-260. doi:10.4161/org.25676

180. Lyons YA, Pradeep S, Wu SY, Haemmerle M, Hansen JM, Wagner MJ, Villar-Prados A, Nagaraja AS, Dood RL, Previs RA, Hu W, Zhao Y, Mak DH, Xiao Z, Melendez BD, Lizee GA, Mercado-Uribe I, Baggerly KA, Hwu P, Liu J, Overwijk WW, Coleman RL, Sood AK (2017) Macrophage depletion through colony stimulating factor 1 receptor pathway blockade overcomes adaptive resistance to anti-VEGF therapy. Oncotarget 8 (57):96496-96505. doi:10.18632/oncotarget.20410

181. Strachan DC, Ruffell B, Oei Y, Bissell MJ, Coussens LM, Pryer N, Daniel D (2013) CSF1R inhibition delays cervical and mammary tumor growth in murine

models by attenuating the turnover of tumor-associated macrophages and enhancing infiltration by CD8(+) T cells. Oncoimmunology 2 (12):e26968. doi:10.4161/onci.26968
182. Meziani L, Mondini M, Petit B, Boissonnas A, Thomas de Montpreville V, Mercier O, Vozenin MC (2018) CSF1R inhibition prevents radiation pulmonary fibrosis by depletion of interstitial macrophages. 51 (3). doi:10.1183/13993003.02120-2017
183. Mitchem JB, Brennan DJ, Knolhoff BL, Belt BA, Zhu Y, Sanford DE, Belaygorod L, Carpenter D, Collins L, Piwnica-Worms D, Hewitt S, Udupi GM, Gallagher WM, Wegner C, West BL, Wang-Gillam A, Goedegebuure P, Linehan DC, DeNardo DG (2013) Targeting tumor-infiltrating macrophages decreases tumor-initiating cells, relieves immunosuppression, and improves chemotherapeutic responses. Cancer Res 73 (3):1128-1141. doi:10.1158/0008-5472.can-12-2731
184. Priceman SJ, Sung JL, Shaposhnik Z, Burton JB, Torres-Collado AX, Moughon DL, Johnson M, Lusis AJ, Cohen DA, Iruela-Arispe ML, Wu L (2010) Targeting distinct tumor-infiltrating myeloid cells by inhibiting CSF-1 receptor: combating tumor evasion of antiangiogenic therapy. Blood 115 (7):1461-1471. doi:10.1182/blood-2009-08-237412
185. Zhu Y, Knolhoff BL, Meyer MA, Nywening TM, West BL, Luo J, Wang-Gillam A, Goedegebuure SP, Linehan DC, DeNardo DG (2014) CSF1/CSF1R blockade reprograms tumor-infiltrating macrophages and improves response to T-cell checkpoint immunotherapy in pancreatic cancer models. Cancer Res 74 (18):5057-5069
186. Martinez FO, Gordon S, Locati M, Mantovani A (2006) Transcriptional profiling of the human monocyte-to-macrophage differentiation and polarization: new molecules and patterns of gene expression. J Immunol 177 (10):7303-7311
187. Pyonteck SM, Akkari L, Schuhmacher AJ, Bowman RL, Sevenich L, Quail DF, Olson OC, Quick ML, Huse JT, Teijeiro V, Setty M, Leslie CS, Oei Y, Pedraza A, Zhang J, Brennan CW, Sutton JC, Holland EC, Daniel D, Joyce JA (2013) CSF-1R inhibition alters macrophage polarization and blocks glioma progression. Nat Med 19 (10):1264-1272. doi:10.1038/nm.3337
188. Swierczak A, Cook AD, Lenzo JC, Restall CM, Doherty JP, Anderson RL, Hamilton JA (2014) The promotion of breast cancer metastasis caused by inhibition

of CSF-1R/CSF-1 signaling is blocked by targeting the G-CSF receptor. Cancer Immunol Res 2 (8):765-776. doi:10.1158/2326-6066.cir-13-0190
189. Richardsen E, Uglehus RD, Johnsen SH, Busund LT (2015) Macrophage-colony stimulating factor (CSF1) predicts breast cancer progression and mortality. Anticancer Res 35 (2):865-874
190. Aharinejad S, Paulus P, Sioud M, Hofmann M, Zins K, Schafer R, Stanley ER, Abraham D (2004) Colony-stimulating factor-1 blockade by antisense oligonucleotides and small interfering RNAs suppresses growth of human mammary tumor xenografts in mice. Cancer Res 64 (15):5378-5384. doi:10.1158/0008-5472.can-04-0961
191. Cassier PA, Gelderblom H, Stacchiotti S, Thomas D, Maki RG, Kroep JR, van der Graaf WT, Italiano A, Seddon B, Domont J, Bompas E, Wagner AJ, Blay JY (2012) Efficacy of imatinib mesylate for the treatment of locally advanced and/or metastatic tenosynovial giant cell tumor/pigmented villonodular synovitis. Cancer 118 (6):1649-1655. doi:10.1002/cncr.26409
192. Panagopoulos I, Brandal P, Gorunova L, Bjerkehagen B, Heim S (2014) Novel CSF1-S100A10 fusion gene and CSF1 transcript identified by RNA sequencing in tenosynovial giant cell tumors. Int J Oncol 44 (5):1425-1432. doi:10.3892/ijo.2014.2326
193. Dewar AL, Cambareri AC, Zannettino AC, Miller BL, Doherty KV, Hughes TP, Lyons AB (2005) Macrophage colony-stimulating factor receptor c-fms is a novel target of imatinib. Blood 105 (8):3127-3132. doi:10.1182/blood-2004-10-3967
194. Blay JY, El Sayadi H, Thiesse P, Garret J, Ray-Coquard I (2008) Complete response to imatinib in relapsing pigmented villonodular synovitis/tenosynovial giant cell tumor (PVNS/TGCT). Ann Oncol 19 (4):821-822. doi:10.1093/annonc/mdn033
195. Cannarile MA, Weisser M, Jacob W, Jegg AM, Ries CH, Ruttinger D (2017) Colony-stimulating factor 1 receptor (CSF1R) inhibitors in cancer therapy. J Immunother Cancer 5 (1):53. doi:10.1186/s40425-017-0257-y
196. Smith BD, Leary CB, Lu W-P, Kaufman MD, Flynn DL (2016) The highly specific CSF1R inhibitor DCC-3014 exhibits immunomodulatory and anti-invasive activities in cancer models. Cancer Res 76 (14 Supplement):4889 [Abstract]. doi:10.1158/1538-7445.am2016-4889

197. Ries CH, Cannarile MA, Hoves S, Benz J, Wartha K, Runza V, Rey-Giraud F, Pradel LP, Feuerhake F, Klaman I, Jones T, Jucknischke U, Scheiblich S, Kaluza K, Gorr IH, Walz A, Abiraj K, Cassier PA, Sica A, Gomez-Roca C, de Visser KE, Italiano A, Le Tourneau C, Delord JP, Levitsky H, Blay JY, Ruttinger D (2014) Targeting tumor-associated macrophages with anti-CSF-1R antibody reveals a strategy for cancer therapy. Cancer cell 25 (6):846-859. doi:10.1016/j.ccr.2014.05.016
198. Butowski N, Colman H, De Groot JF, Omuro AM, Nayak L, Wen PY, Cloughesy TF, Marimuthu A, Haidar S, Perry A, Huse J, Phillips J, West BL, Nolop KB, Hsu HH, Ligon KL, Molinaro AM, Prados M (2016) Orally administered colony stimulating factor 1 receptor inhibitor PLX3397 in recurrent glioblastoma: an Ivy Foundation Early Phase Clinical Trials Consortium phase II study. Neuro-oncology 18 (4):557-564. doi:10.1093/neuonc/nov245
199. Moskowitz CH, Younes A, de Vos S, Bociek RG, Gordon LI, Witzig TE, Gascoyne RD, West B, Nolop K, Steidl C (2012) CSF1R Inhibition by PLX3397 in Patients with Relapsed or Refractory Hodgkin Lymphoma: Results From a Phase 2 Single Agent Clinical Trial. Blood 120 (21):[Abstract 1638]
200. Reynolds G, Haniffa M (2015) Human and Mouse Mononuclear Phagocyte Networks: A Tale of Two Species? Front Immunol 6:330-330. doi:10.3389/fimmu.2015.00330
201. Hodi FS, Lee S, McDermott DF, Rao UN, Butterfield LH, Tarhini AA, Leming P, Puzanov I, Shin D, Kirkwood JM (2014) Ipilimumab plus sargramostim vs ipilimumab alone for treatment of metastatic melanoma: a randomized clinical trial. JAMA 312 (17):1744-1753. doi:10.1001/jama.2014.13943
202. Allavena P, Germano G, Belgiovine C, D'Incalci M, Mantovani A (2013) Trabectedin: A drug from the sea that strikes tumor-associated macrophages. Oncoimmunology 2 (6):e24614. doi:10.4161/onci.24614
203. López-Guerrero JA, Romero I, Poveda A (2015) Trabectedin therapy as an emerging treatment strategy for recurrent platinum-sensitive ovarian cancer. Chin J Cancer 34 (1):41-49. doi:10.5732/cjc.014.10278
204. Germano G, Frapolli R, Simone M, Tavecchio M, Erba E, Pesce S, Pasqualini F, Grosso F, Sanfilippo R, Casali PG, Gronchi A, Virdis E, Tarantino E, Pilotti S, Greco A, Nebuloni M, Galmarini CM, Tercero JC, Mantovani A, D'Incalci M, Allavena P (2010) Antitumor and Anti-inflammatory Effects of Trabectedin on

Human Myxoid Liposarcoma Cells. Cancer Res 70 (6):2235-2244. doi:10.1158/0008-5472.can-09-2335
205. Guo Z, Wang H, Meng F, Li J, Zhang S (2015) Combined Trabectedin and anti-PD1 antibody produces a synergistic antitumor effect in a murine model of ovarian cancer. J Transl Med 13:247. doi:10.1186/s12967-015-0613-y
206. Kanzler H, Barrat FJ, Hessel EM, Coffman RL (2007) Therapeutic targeting of innate immunity with Toll-like receptor agonists and antagonists. Nat Med 13 (5):552-559. doi:10.1038/nm1589
207. Tarhini A (2013) Immune-Mediated Adverse Events Associated with Ipilimumab CTLA-4 Blockade Therapy: The Underlying Mechanisms and Clinical Management. Scientifica 2013:857519. doi:10.1155/2013/857519
208. Cannon A, Thompson C, Hall BR, Jain M, Kumar S, Batra SK (2018) Desmoplasia in pancreatic ductal adenocarcinoma: insight into pathological function and therapeutic potential. Genes & cancer 9 (3-4):78-86. doi:10.18632/genesandcancer.171
209. Mills CD, Lenz LL, Harris RA (2016) A Breakthrough: Macrophage-Directed Cancer Immunotherapy. Cancer Res 76 (3):513-516. doi:10.1158/0008-5472.can-15-1737
210. Riabov V, Kim D, Chhina S, Alexander RB, Klyushnenkova EN (2015) Immunostimulatory early phenotype of tumor-associated macrophages does not predict tumor growth outcome in an HLA-DR mouse model of prostate cancer. Cancer Immunol Immunother 64 (7):873-883. doi:10.1007/s00262-015-1697-1
211. Knight DA, Ngiow SF, Li M, Parmenter T, Mok S, Cass A, Haynes NM, Kinross K, Yagita H, Koya RC, Graeber TG, Ribas A, McArthur GA, Smyth MJ (2013) Host immunity contributes to the anti-melanoma activity of BRAF inhibitors. J Clin Invest 123 (3):1371-1381. doi:10.1172/JCI66236
212. Manzano JL, Layos L, Bugés C, de los Llanos Gil M, Vila L, Martínez-Balibrea E, Martínez-Cardús A (2016) Resistant mechanisms to BRAF inhibitors in melanoma. Ann Transl Med 4 (12):237. doi:10.21037/atm.2016.06.07
213. Ngiow SF, Meeth KM, Stannard K, Barkauskas DS, Bollag G, Bosenberg M, Smyth MJ (2016) Co-inhibition of colony stimulating factor-1 receptor and BRAF oncogene in mouse models of BRAFV600E melanoma. Oncoimmunology 5 (3):e1089381. doi:10.1080/2162402x.2015.1089381

214. Mok S, Tsoi J, Koya RC, Hu-Lieskovan S, West BL, Bollag G, Graeber TG, Ribas A (2015) Inhibition of colony stimulating factor-1 receptor improves antitumor efficacy of BRAF inhibition. BMC Cancer 15 (1):356. doi:10.1186/s12885-015-1377-8
215. Reardon DA, Gokhale PC, Klein SR, Ligon KL, Rodig SJ, Ramkissoon SH, Jones KL, Conway AS, Liao X, Zhou J, Wen PY, Van Den Abbeele AD, Hodi FS, Qin L, Kohl NE, Sharpe AH, Dranoff G, Freeman GJ (2016) Glioblastoma Eradication Following Immune Checkpoint Blockade in an Orthotopic, Immunocompetent Model. Cancer Immunol Res 4 (2):124-135. doi:10.1158/2326-6066.cir-15-0151
216. Kinney SR, Moser MT, Pascual M, Greally JM, Foster BA, Karpf AR (2010) Opposing roles of Dnmt1 in early- and late-stage murine prostate cancer. Mol Cell Biol 30 (17):4159-4174. doi:10.1128/mcb.00235-10
217. Piranlioglu R, Lee E, Ouzounova M, Bollag RJ (2019) Primary tumor-induced immunity eradicates disseminated tumor cells in syngeneic mouse model. 10 (1):1430. doi:10.1038/s41467-019-09015-1
218. Dahmani A, Delisle J-S (2018) TGF-β in T Cell Biology: Implications for Cancer Immunotherapy. Cancers 10 (6):194. doi:10.3390/cancers10060194
219. Nakanishi M, Rosenberg DW (2013) Multifaceted roles of PGE2 in inflammation and cancer. Semin Immunopathol 35 (2):123-137. doi:10.1007/s00281-012-0342-8
220. Munder M (2009) Arginase: an emerging key player in the mammalian immune system. Br J Pharmacol 158 (3):638-651. doi:10.1111/j.1476-5381.2009.00291.x
221. Galluzzi L, Vitale I, Aaronson SA, Abrams JM, Adam D, Agostinis P, Alnemri ES, Altucci L, Amelio I, Andrews DW, Annicchiarico-Petruzzelli M, Antonov AV, Arama E, Baehrecke EH, Barlev NA, Bazan NG, Bernassola F, Bertrand MJM, Bianchi K, Blagosklonny MV, Blomgren K, Borner C, Boya P, Brenner C, Campanella M, Candi E, Carmona-Gutierrez D, Cecconi F, Chan FK, Chandel NS, Cheng EH, Chipuk JE, Cidlowski JA, Ciechanover A, Cohen GM, Conrad M, Cubillos-Ruiz JR, Czabotar PE, D'Angiolella V, Dawson TM, Dawson VL, De Laurenzi V, De Maria R, Debatin KM, DeBerardinis RJ, Deshmukh M, Di Daniele N, Di Virgilio F, Dixit VM, Dixon SJ, Duckett CS, Dynlacht BD, El-Deiry WS, Elrod JW, Fimia GM, Fulda S, Garcia-Saez AJ, Garg AD, Garrido C, Gavathiotis E, Golstein P, Gottlieb E, Green DR, Greene LA, Gronemeyer H, Gross A, Hajnoczky

G, Hardwick JM, Harris IS, Hengartner MO, Hetz C, Ichijo H, Jaattela M, Joseph B, Jost PJ, Juin PP, Kaiser WJ, Karin M, Kaufmann T, Kepp O, Kimchi A, Kitsis RN, Klionsky DJ, Knight RA, Kumar S, Lee SW, Lemasters JJ, Levine B, Linkermann A, Lipton SA, Lockshin RA, Lopez-Otin C, Lowe SW, Luedde T, Lugli E, MacFarlane M, Madeo F, Malewicz M, Malorni W, Manic G, Marine JC, Martin SJ, Martinou JC, Medema JP, Mehlen P, Meier P, Melino S, Miao EA, Molkentin JD, Moll UM, Munoz-Pinedo C, Nagata S, Nunez G, Oberst A, Oren M, Overholtzer M, Pagano M, Panaretakis T, Pasparakis M, Penninger JM, Pereira DM, Pervaiz S, Peter ME, Piacentini M, Pinton P, Prehn JHM, Puthalakath H, Rabinovich GA, Rehm M, Rizzuto R, Rodrigues CMP, Rubinsztein DC, Rudel T, Ryan KM, Sayan E, Scorrano L, Shao F, Shi Y, Silke J, Simon HU, Sistigu A, Stockwell BR, Strasser A, Szabadkai G, Tait SWG, Tang D, Tavernarakis N, Thorburn A, Tsujimoto Y, Turk B, Vanden Berghe T, Vandenabeele P, Vander Heiden MG, Villunger A, Virgin HW, Vousden KH, Vucic D, Wagner EF, Walczak H, Wallach D, Wang Y, Wells JA, Wood W, Yuan J, Zakeri Z, Zhivotovsky B, Zitvogel L, Melino G, Kroemer G (2018) Molecular mechanisms of cell death: recommendations of the Nomenclature Committee on Cell Death 2018. Cell Death Differ 25 (3):486-541. doi:10.1038/s41418-017-0012-4

222. Zhou J, Wang G, Chen Y, Wang H, Hua Y, Cai Z Immunogenic cell death in cancer therapy: Present and emerging inducers. J Cell Mol Med. doi:10.1111/jcmm.14356

223. Calvet CY, Famin D, Andre FM, Mir LM (2014) Electrochemotherapy with bleomycin induces hallmarks of immunogenic cell death in murine colon cancer cells. Oncoimmunology 3:e28131. doi:10.4161/onci.28131

224. Gehl J, Skovsgaard T, Mir LM (1998) Enhancement of cytotoxicity by electropermeabilization: an improved method for screening drugs. Anti-cancer drugs 9 (4):319-325

225. Falk H, Lambaa S, Johannesen HH, Wooler G, Venzo A, Gehl J (2017) Electrochemotherapy and calcium electroporation inducing a systemic immune response with local and distant remission of tumors in a patient with malignant melanoma - a case report. Acta Oncol 56 (8):1126-1131

226. Lens MB, Dawes M (2004) Global perspectives of contemporary epidemiological trends of cutaneous malignant melanoma. Br J Dermatol 150 (2):179-185. doi:10.1111/j.1365-2133.2004.05708.x

227. Apalla Z, Lallas A, Sotiriou E, Lazaridou E, Ioannides D (2017) Epidemiological trends in skin cancer. Dermatol Pract Concept 7 (2):1-6. doi:10.5826/dpc.0702a01
228. Reddy BY, Miller DM, Tsao H (2017) Somatic driver mutations in melanoma. Cancer 123 (S11):2104-2117. doi:10.1002/cncr.30593
229. van Klink F, de Keizer RJ, Jager MJ, Kakebeeke-Kemme HM (1992) Iris nevi and melanomas: a clinical follow-up study. Documenta ophthalmologica Advances in ophthalmology 82 (1-2):49-55. doi:10.1007/bf00156993
230. Roh MR, Eliades P, Gupta S, Tsao H (2015) Genetics of melanocytic nevi. Pigment cell & melanoma research 28 (6):661-672. doi:10.1111/pcmr.12412
231. Wu XC, Eide MJ, King J, Saraiya M, Huang Y, Wiggins C, Barnholtz-Sloan JS, Martin N, Cokkinides V, Miller J, Patel P, Ekwueme DU, Kim J (2011) Racial and ethnic variations in incidence and survival of cutaneous melanoma in the United States, 1999-2006. Journal of the American Academy of Dermatology 65 (5 Suppl 1):S26-37. doi:10.1016/j.jaad.2011.05.034
232. Robert C, Ribas A, Schachter J, Arance A, Grob JJ, Mortier L, Daud A, Carlino MS, McNeil CM, Lotem M, Larkin JMG, Lorigan P, Neyns B, Blank CU, Petrella TM, Hamid O, Su SC, Krepler C, Ibrahim N, Long GV (2019) Pembrolizumab versus ipilimumab in advanced melanoma (KEYNOTE-006): post-hoc 5-year results from an open-label, multicentre, randomised, controlled, phase 3 study. Lancet Oncol 20 (9):1239-1251. doi:10.1016/s1470-2045(19)30388-2
233. Kong BY, Carlino MS, Menzies AM (2016) Biology and treatment of BRAF mutant metastatic melanoma. Melanoma Manag 3 (1):33-45. doi:10.2217/mmt.15.38
234. Ascierto PA, Agarwala SS, Botti G, Budillon A, Davies MA, Dummer R, Ernstoff M, Ferrone S, Formenti S, Gajewski TF, Garbe C, Hamid O, Lo RS, Luke JJ, Michielin O, Palmieri G, Zitvogel L, Marincola FM, Masucci G, Caracò C, Thurin M, Puzanov I (2019) Perspectives in melanoma: meeting report from the Melanoma Bridge (November 29th-1 December 1st, 2018, Naples, Italy). Journal of translational medicine 17 (1):234-234. doi:10.1186/s12967-019-1979-z
235. Ambrosi L, Khan S, Carvajal RD, Yang J (2019) Novel Targets for the Treatment of Melanoma. Current oncology reports 21 (11):97. doi:10.1007/s11912-019-0849-4

236. Yarchoan M, Hopkins A, Jaffee EM (2017) Tumor Mutational Burden and Response Rate to PD-1 Inhibition. The New England journal of medicine 377 (25):2500-2501. doi:10.1056/NEJMc1713444
237. van der Bruggen P, Traversari C, Chomez P, Lurquin C, De Plaen E, Van den Eynde B, Knuth A, Boon T (1991) A gene encoding an antigen recognized by cytolytic T lymphocytes on a human melanoma. Science 254 (5038):1643-1647. doi:10.1126/science.1840703
238. Sharma P, Allison JP (2015) The future of immune checkpoint therapy. Science 348 (6230):56-61. doi:10.1126/science.aaa8172
239. Robert C, Long GV, Brady B, Dutriaux C, Maio M, Mortier L, Hassel JC, Rutkowski P, McNeil C, Kalinka-Warzocha E, Savage KJ, Hernberg MM, Lebbe C, Charles J, Mihalcioiu C, Chiarion-Sileni V, Mauch C, Cognetti F, Arance A, Schmidt H, Schadendorf D, Gogas H, Lundgren-Eriksson L, Horak C, Sharkey B, Waxman IM, Atkinson V, Ascierto PA (2015) Nivolumab in previously untreated melanoma without BRAF mutation. N Engl J Med 372 (4):320-330. doi:10.1056/NEJMoa1412082
240. Andtbacka RH, Kaufman HL, Collichio F, Amatruda T, Senzer N, Chesney J, Delman KA, Spitler LE, Puzanov I, Agarwala SS, Milhem M, Cranmer L, Curti B, Lewis K, Ross M, Guthrie T, Linette GP, Daniels GA, Harrington K, Middleton MR, Miller WH, Jr., Zager JS, Ye Y, Yao B, Li A, Doleman S, VanderWalde A, Gansert J, Coffin RS (2015) Talimogene Laherparepvec Improves Durable Response Rate in Patients With Advanced Melanoma. J Clin Oncol 33 (25):2780-2788. doi:10.1200/jco.2014.58.3377
241. Liu BL, Robinson M, Han ZQ, Branston RH, English C, Reay P, McGrath Y, Thomas SK, Thornton M, Bullock P, Love CA, Coffin RS (2003) ICP34.5 deleted herpes simplex virus with enhanced oncolytic, immune stimulating, and anti-tumour properties. Gene therapy 10 (4):292-303. doi:10.1038/sj.gt.3301885
242. Scapin G, Yang X, Prosise WW, McCoy M, Reichert P, Johnston JM, Kashi RS, Strickland C (2015) Structure of full-length human anti-PD1 therapeutic IgG4 antibody pembrolizumab. Nature structural & molecular biology 22 (12):953-958. doi:10.1038/nsmb.3129
243. Neubert NJ, Schmittnaegel M, Bordry N, Nassiri S, Wald N, Martignier C, Tillé L, Homicsko K, Damsky W, Maby-El Hajjami H, Klaman I, Danenberg E, Ioannidou K, Kandalaft L, Coukos G, Hoves S, Ries CH, Fuertes Marraco SA,

Foukas PG, De Palma M, Speiser DE (2018) T cell-induced CSF1 promotes melanoma resistance to PD1 blockade. Science translational medicine 10 (436):eaan3311. doi:10.1126/scitranslmed.aan3311
244. Erdag G, Schaefer JT, Smolkin ME, Deacon DH, Shea SM, Dengel LT, Patterson JW, Slingluff CL, Jr. (2012) Immunotype and immunohistologic characteristics of tumor-infiltrating immune cells are associated with clinical outcome in metastatic melanoma. Cancer Res 72 (5):1070-1080. doi:10.1158/0008-5472.can-11-3218
245. Gauci CL, Alexander P (1975) The macrophage content of some human tumours. Cancer Lett 1 (1):29-32. doi:10.1016/s0304-3835(75)94826-0
246. Mantovani A, Sica A (2010) Macrophages, innate immunity and cancer: balance, tolerance, and diversity. Current opinion in immunology 22 (2):231-237. doi:10.1016/j.coi.2010.01.009
247. Piras F, Colombari R, Minerba L, Murtas D, Floris C, Maxia C, Corbu A, Perra MT, Sirigu P (2005) The predictive value of CD8, CD4, CD68, and human leukocyte antigen-D-related cells in the prognosis of cutaneous malignant melanoma with vertical growth phase. Cancer 104 (6):1246-1254. doi:10.1002/cncr.21283
248. Jensen TO, Schmidt H, Moller HJ, Hoyer M, Maniecki MB, Sjoegren P, Christensen IJ, Steiniche T (2009) Macrophage markers in serum and tumor have prognostic impact in American Joint Committee on Cancer stage I/II melanoma. J Clin Oncol 27 (20):3330-3337. doi:10.1200/jco.2008.19.9919
249. Massi D, Marconi C, Franchi A, Bianchini F, Paglierani M, Ketabchi S, Miracco C, Santucci M, Calorini L (2007) Arginine metabolism in tumor-associated macrophages in cutaneous malignant melanoma: evidence from human and experimental tumors. Human pathology 38 (10):1516-1525. doi:10.1016/j.humpath.2007.02.018
250. Falleni M, Savi F, Tosi D, Agape E, Cerri A, Moneghini L, Bulfamante GP (2017) M1 and M2 macrophages' clinicopathological significance in cutaneous melanoma. Melanoma Res 27 (3):200-210. doi:10.1097/cmr.0000000000000352
251. Salmi S, Siiskonen H, Sironen R, Tyynela-Korhonen K, Hirschovits-Gerz B, Valkonen M, Auvinen P, Pasonen-Seppanen S (2019) The number and localization of CD68+ and CD163+ macrophages in different stages of cutaneous melanoma. Melanoma Res 29 (3):237-247. doi:10.1097/cmr.0000000000000522

252. Hussein MR (2005) Dendritic cells and melanoma tumorigenesis: an insight. Cancer biology & therapy 4 (5):501-505. doi:10.4161/cbt.4.5.1780
253. Leong SP, Enders-Zohr P, Zhou YM, Stuntebeck S, Habib FA, Allen RE, Jr., Sagebiel RW, Glassberg AB, Lowenberg DW, Hayes FA (1999) Recombinant human granulocyte macrophage-colony stimulating factor (rhGM-CSF) and autologous melanoma vaccine mediate tumor regression in patients with metastatic melanoma. J Immunother 22 (2):166-174. doi:10.1097/00002371-199903000-00008
254. Clark WH, Jr., Elder DE, Guerry Dt, Braitman LE, Trock BJ, Schultz D, Synnestvedt M, Halpern AC (1989) Model predicting survival in stage I melanoma based on tumor progression. J Natl Cancer Inst 81 (24):1893-1904. doi:10.1093/jnci/81.24.1893
255. Clemente CG, Mihm MC, Jr., Bufalino R, Zurrida S, Collini P, Cascinelli N (1996) Prognostic value of tumor infiltrating lymphocytes in the vertical growth phase of primary cutaneous melanoma. Cancer 77 (7):1303-1310. doi:10.1002/(sici)1097-0142(19960401)77:7<1303::aid-cncr12>3.0.co;2-5
256. Taylor RC, Patel A, Panageas KS, Busam KJ, Brady MS (2007) Tumor-infiltrating lymphocytes predict sentinel lymph node positivity in patients with cutaneous melanoma. J Clin Oncol 25 (7):869-875. doi:10.1200/jco.2006.08.9755
257. Krepler C, Sproesser K, Brafford P, Beqiri M, Garman B, Xiao M, Shannan B, Watters A, Perego M, Zhang G, Vultur A, Yin X, Liu Q, Anastopoulos IN, Wubbenhorst B, Wilson MA, Xu W, Karakousis G, Feldman M, Xu X, Amaravadi R, Gangadhar TC, Elder DE, Haydu LE, Wargo JA, Davies MA, Lu Y, Mills GB, Frederick DT, Barzily-Rokni M, Flaherty KT, Hoon DS, Guarino M, Bennett JJ, Ryan RW, Petrelli NJ, Shields CL, Terai M, Sato T, Aplin AE, Roesch A, Darr D, Angus S, Kumar R, Halilovic E, Caponigro G, Jeay S, Wuerthner J, Walter A, Ocker M, Boxer MB, Schuchter L, Nathanson KL, Herlyn M (2017) A Comprehensive Patient-Derived Xenograft Collection Representing the Heterogeneity of Melanoma. Cell reports 21 (7):1953-1967. doi:10.1016/j.celrep.2017.10.021
258. Scali E, Mignogna C, Di Vito A, Presta I, Camastra C, Donato G, Bottoni U (2016) Inflammation and macrophage polarization in cutaneous melanoma: Histopathological and immunohistochemical study. Int J Immunopathol Pharmacol 29 (4):715-719. doi:10.1177/0394632016650895
259. Brown CC, Gudjonson H, Pritykin Y, Deep D, Lavallee VP, Mendoza A, Fromme R, Mazutis L, Ariyan C, Leslie C, Pe'er D, Rudensky AY (2019)

Transcriptional Basis of Mouse and Human Dendritic Cell Heterogeneity. Cell 179 (4):846-863.e824. doi:10.1016/j.cell.2019.09.035
260. Lee JJ, McGarry MP (2007) When is a mouse basophil not a basophil? Blood 109 (3):859-861. doi:10.1182/blood-2006-06-027490
261. Eruslanov EB, Singhal S, Albelda SM (2017) Mouse versus Human Neutrophils in Cancer: A Major Knowledge Gap. Trends Cancer 3 (2):149-160. doi:10.1016/j.trecan.2016.12.006
262. Bassler K, Schulte-Schrepping J, Warnat-Herresthal S, Aschenbrenner AC, Schultze JL (2019) The Myeloid Cell Compartment-Cell by Cell. Annu Rev Immunol 37:269-293. doi:10.1146/annurev-immunol-042718-041728
263. Ingersoll MA, Spanbroek R, Lottaz C, Gautier EL, Frankenberger M, Hoffmann R, Lang R, Haniffa M, Collin M, Tacke F, Habenicht AJR, Ziegler-Heitbrock L, Randolph GJ (2010) Comparison of gene expression profiles between human and mouse monocyte subsets. Blood 115 (3):e10-e19. doi:10.1182/blood-2009-07-235028
264. Joerink M, Savelkoul HF, Wiegertjes GF (2006) Evolutionary conservation of alternative activation of macrophages: structural and functional characterization of arginase 1 and 2 in carp (Cyprinus carpio L.). Molecular immunology 43 (8):1116-1128. doi:10.1016/j.molimm.2005.07.022
265. Edholm E-S, Rhoo KH, Robert J (2017) Evolutionary Aspects of Macrophages Polarization. Results Probl Cell Differ 62:3-22. doi:10.1007/978-3-319-54090-0_1
266. Schneemann M, Schoedon G (2002) Species differences in macrophage NO production are important. Nat Immunol 3 (2):102. doi:10.1038/ni0202-102a
267. DeNardo DG, Ruffell B (2019) Macrophages as regulators of tumour immunity and immunotherapy. Nat Rev Immunol 19 (6):369-382. doi:10.1038/s41577-019-0127-6
268. de Groot AE, Pienta KJ (2018) Epigenetic control of macrophage polarization: implications for targeting tumor-associated macrophages. Oncotarget 9 (29):20908-20927. doi:10.18632/oncotarget.24556
269. Hoeffel G, Ginhoux F (2018) Fetal monocytes and the origins of tissue-resident macrophages. Cellular immunology 330:5-15. doi:10.1016/j.cellimm.2018.01.001
270. Gosselin D, Glass CK (2014) Epigenomics of macrophages. Immunol Rev 262 (1):96-112. doi:10.1111/imr.12213

271. Lavin Y, Winter D, Blecher-Gonen R, David E, Keren-Shaul H, Merad M, Jung S, Amit I (2014) Tissue-resident macrophage enhancer landscapes are shaped by the local microenvironment. Cell 159 (6):1312-1326. doi:10.1016/j.cell.2014.11.018
272. Gosselin D, Skola D (2017) An environment-dependent transcriptional network specifies human microglia identity. 356 (6344). doi:10.1126/science.aal3222
273. Buttgereit A, Lelios I, Yu X, Vrohlings M, Krakoski NR, Gautier EL, Nishinakamura R, Becher B (2016) Sall1 is a transcriptional regulator defining microglia identity and function. 17 (12):1397-1406. doi:10.1038/ni.3585
274. Netea MG, Joosten LAB, Latz E, Mills KHG, Natoli G, Stunnenberg HG, O'Neill LAJ, Xavier RJ (2016) Trained immunity: A program of innate immune memory in health and disease. Science (New York, NY) 352 (6284):aaf1098-aaf1098. doi:10.1126/science.aaf1098
275. Novakovic B, Habibi E, Wang S-Y, Arts RJW, Davar R, Megchelenbrink W, Kim B, Kuznetsova T, Kox M, Zwaag J, Matarese F, van Heeringen SJ, Janssen-Megens EM, Sharifi N, Wang C, Keramati F, Schoonenberg V, Flicek P, Clarke L, Pickkers P, Heath S, Gut I, Netea MG, Martens JHA, Logie C, Stunnenberg HG (2016) β-Glucan Reverses the Epigenetic State of LPS-Induced Immunological Tolerance. Cell 167 (5):1354-1368.e1314. doi:10.1016/j.cell.2016.09.034
276. Quintin J, Saeed S, Martens JHA, Giamarellos-Bourboulis EJ, Ifrim DC, Logie C, Jacobs L, Jansen T, Kullberg B-J, Wijmenga C, Joosten LAB, Xavier RJ, van der Meer JWM, Stunnenberg HG, Netea MG (2012) Candida albicans infection affords protection against reinfection via functional reprogramming of monocytes. Cell Host Microbe 12 (2):223-232. doi:10.1016/j.chom.2012.06.006
277. Kleinnijenhuis J, Quintin J, Preijers F, Benn CS, Joosten LA, Jacobs C, van Loenhout J, Xavier RJ, Aaby P, van der Meer JW, van Crevel R, Netea MG (2014) Long-lasting effects of BCG vaccination on both heterologous Th1/Th17 responses and innate trained immunity. J Innate Immun 6 (2):152-158. doi:10.1159/000355628
278. Welsh RM, Selin LK (2002) No one is naive: the significance of heterologous T-cell immunity. Nat Rev Immunol 2 (6):417-426. doi:10.1038/nri820
279. Taciak B, Białasek M, Braniewska A, Sas Z, Sawicka P, Kiraga Ł, Rygiel T, Król M (2018) Evaluation of phenotypic and functional stability of RAW 264.7 cell line through serial passages. PloS one 13 (6):e0198943-e0198943. doi:10.1371/journal.pone.0198943

280. Weischenfeldt J, Porse B (2008) Bone Marrow-Derived Macrophages (BMM): Isolation and Applications. CSH protocols 2008:pdb.prot5080. doi:10.1101/pdb.prot5080
281. Ray A, Dittel BN (2010) Isolation of mouse peritoneal cavity cells. J Vis Exp (35):1488. doi:10.3791/1488
282. Davies JQ, Gordon S (2005) Isolation and culture of murine macrophages. Methods Mol Biol 290:91-103. doi:10.1385/1-59259-838-2:091
283. Schneider M (2013) Collecting resident or thioglycollate-elicited peritoneal macrophages. Methods Mol Biol 1031:37-40. doi:10.1007/978-1-62703-481-4_4
284. Redente EF, Higgins DM, Dwyer-Nield LD, Orme IM, Gonzalez-Juarrero M, Malkinson AM (2010) Differential polarization of alveolar macrophages and bone marrow-derived monocytes following chemically and pathogen-induced chronic lung inflammation. J Leukoc Biol 88 (1):159-168. doi:10.1189/jlb.0609378
285. Francke A, Herold J, Weinert S, Strasser RH, Braun-Dullaeus RC (2011) Generation of mature murine monocytes from heterogeneous bone marrow and description of their properties. J Histochem Cytochem 59 (9):813-825
286. Giard DJ, Aaronson SA, Todaro GJ, Arnstein P, Kersey JH, Dosik H, Parks WP (1973) In vitro cultivation of human tumors: establishment of cell lines derived from a series of solid tumors. J Natl Cancer Inst 51 (5):1417-1423. doi:10.1093/jnci/51.5.1417
287. Oettgen HF, Aoki T, Old LJ, Boyse EA, de Harven E, Mills GM (1968) Suspension culture of a pigment-producing cell line derived from a human malignant melanoma. J Natl Cancer Inst 41 (4):827-843
288. Meeth K, Wang JX, Micevic G, Damsky W, Bosenberg MW (2016) The YUMM lines: a series of congenic mouse melanoma cell lines with defined genetic alterations. Pigment Cell Melanoma Res 29 (5):590-597. doi:10.1111/pcmr.12498
289. Poste G, Doll J, Hart IR, Fidler IJ (1980) In vitro selection of murine B16 melanoma variants with enhanced tissue-invasive properties. Cancer Res 40 (5):1636-1644
290. Fidler IJ (1973) Selection of successive tumour lines for metastasis. Nature: New biology 242 (118):148-149. doi:10.1038/newbio242148a0
291. Hart IR, Fidler IJ (1980) Role of organ selectivity in the determination of metastatic patterns of B16 melanoma. Cancer Res 40 (7):2281-2287

292. Bellone M, Iezzi G, Manfredi AA, Protti MP, Dellabona P, Casorati G, Rugarli C (1994) In vitro priming of cytotoxic T lymphocytes against poorly immunogenic epitopes by engineered antigen-presenting cells. Eur J Immunol 24 (11):2691-2698. doi:10.1002/eji.1830241118
293. Bellone M, Iezzi G, Martin-Fontecha A, Rivolta L, Manfredi AA, Protti MP, Freschi M, Dellabona P, Casorati G, Rugarli C (1997) Rejection of a nonimmunogenic melanoma by vaccination with natural melanoma peptides on engineered antigen-presenting cells. J Immunol 158 (2):783-789
294. Weigelin B, Bolaños E, Teijeira A, Martinez-Forero I, Labiano S, Azpilikueta A, Morales-Kastresana A, Quetglas JI, Wagena E, Sánchez-Paulete AR, Chen L, Friedl P, Melero I (2015) Focusing and sustaining the antitumor CTL effector killer response by agonist anti-CD137 mAb. Proceedings of the National Academy of Sciences of the United States of America 112 (24):7551-7556. doi:10.1073/pnas.1506357112
295. Bland CL, Byrne-Hoffman CN, Fernandez A, Rellick SL, Deng W, Klinke DJ, 2nd (2018) Exosomes derived from B16F0 melanoma cells alter the transcriptome of cytotoxic T cells that impacts mitochondrial respiration. The FEBS journal 285 (6):1033-1050. doi:10.1111/febs.14396
296. Zhang L, Tao L, Shi T, Zhang F, Sheng X, Cao Y, Zheng S, Wang A, Qian W, Jiang L, Lu Y (2015) Paeonol inhibits B16F10 melanoma metastasis in vitro and in vivo via disrupting proinflammatory cytokines-mediated NF-kappaB and STAT3 pathways. IUBMB life 67 (10):778-788. doi:10.1002/iub.1435
297. Hooijkaas A, Gadiot J, Morrow M, Stewart R, Schumacher T, Blank CU (2012) Selective BRAF inhibition decreases tumor-resident lymphocyte frequencies in a mouse model of human melanoma. Oncoimmunology 1 (5):609-617. doi:10.4161/onci.20226
298. Lee CZW, Kozaki T, Ginhoux F (2018) Studying tissue macrophages in vitro: are iPSC-derived cells the answer? 18 (11):716-725. doi:10.1038/s41577-018-0054-y
299. Qi Z, Wang L, Desai K, Cogswell J, Stern M, Lawson B, Kerkar SP, Vitazka P (2019) Reliable Gene Expression Profiling from Small and Hematoxylin and Eosin-Stained Clinical Formalin-Fixed, Paraffin-Embedded Specimens Using the HTG EdgeSeq Platform. The Journal of molecular diagnostics : JMD 21 (5):796-807. doi:10.1016/j.jmoldx.2019.04.011

300. Overwijk WW, Restifo NP (2001) B16 as a mouse model for human melanoma. Curr Protoc Immunol Chapter 20:Unit-20.21. doi:10.1002/0471142735.im2001s39
301. Trouplin V, Boucherit N, Gorvel L, Conti F, Mottola G, Ghigo E (2013) Bone marrow-derived macrophage production. J Vis Exp (81):e50966-e50966. doi:10.3791/50966
302. Kim CH, Kim WK, Li C, Song JY, Sung JH, Song SY (2015) Antifibrogenic effects of B16 melanoma-conditioned medium. The Journal of surgical research 194 (2):688-695. doi:10.1016/j.jss.2014.10.041
303. Lee CM, Hu J (2013) Cell density during differentiation can alter the phenotype of bone marrow-derived macrophages. Cell Biosci 3:30-30. doi:10.1186/2045-3701-3-30
304. Bradford MM (1976) A rapid and sensitive method for the quantitation of microgram quantities of protein utilizing the principle of protein-dye binding. Analytical biochemistry 72:248-254. doi:10.1006/abio.1976.9999
305. Corraliza IM, Campo ML, Soler G, Modolell M (1994) Determination of arginase activity in macrophages: a micromethod. J Immunol Methods 174 (1-2):231-235. doi:10.1016/0022-1759(94)90027-2
306. Guevara I, Iwanejko J, Dembinska-Kiec A, Pankiewicz J, Wanat A, Anna P, Golabek I, Bartus S, Malczewska-Malec M, Szczudlik A (1998) Determination of nitrite/nitrate in human biological material by the simple Griess reaction. Clinica chimica acta; international journal of clinical chemistry 274 (2):177-188. doi:10.1016/s0009-8981(98)00060-6
307. Kwon M, Choi YJ, Sa M, Park S-H, Shin E-C (2018) Two-Round Mixed Lymphocyte Reaction for Evaluation of the Functional Activities of Anti-PD-1 and Immunomodulators. Immune Netw 18 (6):e45-e45. doi:10.4110/in.2018.18.e45
308. Gehl J, Sersa G, Matthiessen LW, Muir T, Soden D, Occhini A, Quaglino P, Curatolo P, Campana LG, Kunte C (2018) Updated standard operating procedures for electrochemotherapy of cutaneous tumours and skin metastases. 57 (7):874-882. doi:10.1080/0284186x.2018.1454602
309. Franken NA, Rodermond HM, Stap J, Haveman J, van Bree C (2006) Clonogenic assay of cells in vitro. Nature protocols 1 (5):2315-2319. doi:10.1038/nprot.2006.339

310. Tremble LF, Forde PF (2017) Clinical evaluation of macrophages in cancer: role in treatment, modulation and challenges. Cancer Immunol Immunother 66 (12):1509-1527. doi:10.1007/s00262-017-2065-0
311. Jablonski KA, Amici SA, Webb LM, Ruiz-Rosado Jde D, Popovich PG, Partida-Sanchez S, Guerau-de-Arellano M (2015) Novel Markers to Delineate Murine M1 and M2 Macrophages. PloS one 10 (12):e0145342. doi:10.1371/journal.pone.0145342
312. Aras S, Zaidi MR (2017) TAMeless traitors: macrophages in cancer progression and metastasis. Br J Cancer 117 (11):1583-1591. doi:10.1038/bjc.2017.356
313. Benner B, Scarberry L, Suarez-Kelly LP, Duggan MC, Campbell AR, Smith E, Lapurga G, Jiang K, Butchar JP, Tridandapani S, Howard JH, Baiocchi RA, Mace TA, Carson WE, 3rd (2019) Generation of monocyte-derived tumor-associated macrophages using tumor-conditioned media provides a novel method to study tumor-associated macrophages in vitro. J Immunother Cancer 7 (1):140-140. doi:10.1186/s40425-019-0622-0
314. Hamann J, Koning N, Pouwels W, Ulfman LH, van Eijk M, Stacey M, Lin HH, Gordon S, Kwakkenbos MJ (2007) EMR1, the human homolog of F4/80, is an eosinophil-specific receptor. Eur J Immunol 37 (10):2797-2802. doi:10.1002/eji.200737553
315. Holt DJ, Grainger DW (2012) Senescence and quiescence induced compromised function in cultured macrophages. Biomaterials 33 (30):7497-7507. doi:10.1016/j.biomaterials.2012.06.099
316. Rostam HM, Singh S, Salazar F, Magennis P, Hook A, Singh T, Vrana NE, Alexander MR, Ghaemmaghami AM (2016) The impact of surface chemistry modification on macrophage polarisation. Immunobiology 221 (11):1237-1246. doi:https://doi.org/10.1016/j.imbio.2016.06.010
317. Kelley JL, Rozek MM, Suenram CA, Schwartz CJ (1987) Activation of human blood monocytes by adherence to tissue culture plastic surfaces. Exp Mol Pathol 46 (3):266-278
318. Newman SL, Tucci MA (1990) Regulation of human monocyte/macrophage function by extracellular matrix. Adherence of monocytes to collagen matrices enhances phagocytosis of opsonized bacteria by activation of complement receptors and enhancement of Fc receptor function. J Clin Invest 86 (3):703-714. doi:10.1172/jci114766

319. Gaffney EF, Riegman PH, Grizzle WE, Watson PH (2018) Factors that drive the increasing use of FFPE tissue in basic and translational cancer research. Biotech Histochem 93 (5):373-386. doi:10.1080/10520295.2018.1446101
320. Rath M, Müller I, Kropf P, Closs EI, Munder M (2014) Metabolism via Arginase or Nitric Oxide Synthase: Two Competing Arginine Pathways in Macrophages. Front Immunol 5:532-532. doi:10.3389/fimmu.2014.00532
321. Sun S, Pan X, Zhao L, Zhou J, Wang H, Sun Y (2016) The Expression and Relationship of CD68-Tumor-Associated Macrophages and Microvascular Density With the Prognosis of Patients With Laryngeal Squamous Cell Carcinoma. Clin Exp Otorhinolaryngol 9 (3):270-277. doi:10.21053/ceo.2015.01305
322. Gordon S, Plüddemann A, Martinez Estrada F (2014) Macrophage heterogeneity in tissues: phenotypic diversity and functions. Immunol Rev 262 (1):36-55. doi:10.1111/imr.12223
323. Barros MHM, Hauck F, Dreyer JH, Kempkes B, Niedobitek G (2013) Macrophage Polarisation: an Immunohistochemical Approach for Identifying M1 and M2 Macrophages. PloS one 8 (11):e80908. doi:10.1371/journal.pone.0080908
324. Breslow A (1970) Thickness, cross-sectional areas and depth of invasion in the prognosis of cutaneous melanoma. Ann Surg 172 (5):902-908. doi:10.1097/00000658-197011000-00017
325. Torisu H, Ono M, Kiryu H, Furue M, Ohmoto Y, Nakayama J, Nishioka Y, Sone S, Kuwano M (2000) Macrophage infiltration correlates with tumor stage and angiogenesis in human malignant melanoma: possible involvement of TNFalpha and IL-1alpha. Int J Cancer 85 (2):182-188
326. Mantovani A, Locati M (2013) Tumor-associated macrophages as a paradigm of macrophage plasticity, diversity, and polarization: lessons and open questions. Arterioscler Thromb Vasc Biol 33 (7):1478-1483. doi:10.1161/atvbaha.113.300168
327. Bardi GT, Smith MA, Hood JL (2018) Melanoma exosomes promote mixed M1 and M2 macrophage polarization. Cytokine 105:63-72. doi:10.1016/j.cyto.2018.02.002
328. Najafi M, Hashemi Goradel N, Farhood B, Salehi E, Nashtaei MS, Khanlarkhani N, Khezri Z, Majidpoor J, Abouzaripour M, Habibi M, Kashani IR, Mortezaee K (2019) Macrophage polarity in cancer: A review. J Cell Biochem 120 (3):2756-2765. doi:10.1002/jcb.27646

329. Grossman JG, Nywening TM, Belt BA, Panni RZ, Krasnick BA, DeNardo DG, Hawkins WG, Goedegebuure SP, Linehan DC, Fields RC (2018) Recruitment of CCR2(+) tumor associated macrophage to sites of liver metastasis confers a poor prognosis in human colorectal cancer. Oncoimmunology 7 (9):e1470729. doi:10.1080/2162402x.2018.1470729
330. Mantovani A, Sozzani S, Locati M, Allavena P, Sica A (2002) Macrophage polarization: tumor-associated macrophages as a paradigm for polarized M2 mononuclear phagocytes. Trends Immunol 23 (11):549-555
331. Lee WJ, Lee MH, Kim HT, Won CH, Lee MW, Choi JH, Chang SE (2019) Prognostic significance of CD163 expression and its correlation with cyclooxygenase-2 and vascular endothelial growth factor expression in cutaneous melanoma. Melanoma Res 29 (5):501-509. doi:10.1097/cmr.0000000000000549
332. MacMicking J, Xie QW, Nathan C (1997) Nitric oxide and macrophage function. Annu Rev Immunol 15:323-350. doi:10.1146/annurev.immunol.15.1.323
333. Rodriguez PC, Ochoa AC, Al-Khami AA (2017) Arginine Metabolism in Myeloid Cells Shapes Innate and Adaptive Immunity. Front Immunol 8:93. doi:10.3389/fimmu.2017.00093
334. Jeong H, Kim S (2019) Tumor-Associated Macrophages Enhance Tumor Hypoxia and Aerobic Glycolysis. Cancer Res 79 (4):795-806. doi:10.1158/0008-5472.can-18-2545
335. Comunanza V, Corà D, Orso F, Consonni FM, Middonti E, Di Nicolantonio F, Buzdin A, Sica A, Medico E, Sangiolo D, Taverna D, Bussolino F (2017) VEGF blockade enhances the antitumor effect of BRAFV600E inhibition. EMBO Mol Med 9 (2):219-237. doi:10.15252/emmm.201505774
336. Wolchok JD, Chiarion-Sileni V, Gonzalez R, Rutkowski P, Grob JJ, Cowey CL, Lao CD, Wagstaff J, Schadendorf D, Ferrucci PF, Smylie M, Dummer R, Hill A, Hogg D, Haanen J, Carlino MS, Bechter O, Maio M, Marquez-Rodas I, Guidoboni M, McArthur G, Lebbe C, Ascierto PA, Long GV, Cebon J, Sosman J, Postow MA, Callahan MK, Walker D, Rollin L, Bhore R, Hodi FS, Larkin J (2017) Overall Survival with Combined Nivolumab and Ipilimumab in Advanced Melanoma. N Engl J Med 377 (14):1345-1356. doi:10.1056/NEJMoa1709684
337. Engeland K (2018) Cell cycle arrest through indirect transcriptional repression by p53: I have a DREAM. Cell Death Differ 25 (1):114-132. doi:10.1038/cdd.2017.172

338. Schubert C, Schalk-Hihi C, Struble GT, Ma HC, Petrounia IP, Brandt B, Deckman IC, Patch RJ, Player MR, Spurlino JC, Springer BA (2007) Crystal structure of the tyrosine kinase domain of colony-stimulating factor-1 receptor (cFMS) in complex with two inhibitors. J Biol Chem 282 (6):4094-4101. doi:10.1074/jbc.M608183200
339. Lin H, Lee E, Hestir K, Leo C, Huang M, Bosch E, Halenbeck R, Wu G, Zhou A, Behrens D, Hollenbaugh D, Linnemann T, Qin M, Wong J, Chu K, Doberstein SK, Williams LT (2008) Discovery of a cytokine and its receptor by functional screening of the extracellular proteome. Science 320 (5877):807-811. doi:10.1126/science.1154370
340. MacDonald KP, Palmer JS, Cronau S, Seppanen E, Olver S, Raffelt NC, Kuns R, Pettit AR, Clouston A, Wainwright B, Branstetter D, Smith J, Paxton RJ, Cerretti DP, Bonham L, Hill GR, Hume DA (2010) An antibody against the colony-stimulating factor 1 receptor depletes the resident subset of monocytes and tissue- and tumor-associated macrophages but does not inhibit inflammation. Blood 116 (19):3955-3963. doi:10.1182/blood-2010-02-266296
341. Chistiakov DA, Killingsworth MC, Myasoedova VA, Orekhov AN, Bobryshev YV (2017) CD68/macrosialin: not just a histochemical marker. Lab Invest 97 (1):4-13. doi:10.1038/labinvest.2016.116
342. Gottfried E, Kunz-Schughart LA, Weber A, Rehli M, Peuker A, Muller A, Kastenberger M, Brockhoff G, Andreesen R, Kreutz M (2008) Expression of CD68 in non-myeloid cell types. Scand J Immunol 67 (5):453-463. doi:10.1111/j.1365-3083.2008.02091.x
343. Greaves DR, Quinn CM, Seldin MF, Gordon S (1998) Functional comparison of the murine macrosialin and human CD68 promoters in macrophage and nonmacrophage cell lines. Genomics 54 (1):165-168. doi:10.1006/geno.1998.5546
344. Pillai MM, Hayes B, Torok-Storb B (2009) Inducible transgenes under the control of the hCD68 promoter identifies mouse macrophages with a distribution that differs from the F4/80 - and CSF-1R-expressing populations. Exp Hematol 37 (12):1387-1392. doi:10.1016/j.exphem.2009.09.003
345. Mills CD (2012) M1 and M2 Macrophages: Oracles of Health and Disease. Crit Rev Immunol 32 (6):463-488
346. Shima M, Teitelbaum SL, Holers VM, Ruzicka C, Osmack P, Ross FP (1995) Macrophage-colony-stimulating factor regulates expression of the integrins alpha 4

beta 1 and alpha 5 beta 1 by murine bone marrow macrophages. Proc Natl Acad Sci U S A 92 (11):5179-5183
347. Geissmann F, Jung S, Littman DR (2003) Blood monocytes consist of two principal subsets with distinct migratory properties. Immunity 19 (1):71-82
348. Yang J, Zhang L, Yu C, Yang X-F, Wang H (2014) Monocyte and macrophage differentiation: circulation inflammatory monocyte as biomarker for inflammatory diseases. Biomarker Res 2 (1):1-1
349. Zheng J, Yang M, Shao J, Miao Y, Han J, Du J (2013) Chemokine receptor CX3CR1 contributes to macrophage survival in tumor metastasis. Mol Cancer 12 (1):141-141. doi:10.1186/1476-4598-12-141
350. Richards DM, Hettinger J, Feuerer M (2012) Monocytes and macrophages in cancer: development and functions. Cancer Microenviron 6 (2):179-191. doi:10.1007/s12307-012-0123-x
351. Austyn JM, Gordon S (1981) F4/80, a monoclonal antibody directed specifically against the mouse macrophage. Eur J Immunol 11 (10):805-815. doi:10.1002/eji.1830111013
352. Qiu W, Su GH (2013) Development of orthotopic pancreatic tumor mouse models. Methods Mol Biol 980:215-223. doi:10.1007/978-1-62703-287-2_11
353. Zhang Y, Zhang G-L, Sun X, Cao K-X, Ma C, Nan N, Yang G-W, Yu M-W, Wang X-M (2018) Establishment of a murine breast tumor model by subcutaneous or orthotopic implantation. Oncol Lett 15 (5):6233-6240. doi:10.3892/ol.2018.8113
354. McVeigh LE, Wijetunga I, Ingram N (2019) Development of orthotopic tumour models using ultrasound-guided intrahepatic injection. Sci Rep 9 (1):9904. doi:10.1038/s41598-019-46410-6
355. Shultz LD, Goodwin N, Ishikawa F, Hosur V, Lyons BL, Greiner DL (2014) Human cancer growth and therapy in immunodeficient mouse models. Cold Spring Harb Protoc 2014 (7):694-708. doi:10.1101/pdb.top073585
356. Wang W, Green M, Choi JE, Gijon M, Kennedy PD, Johnson JK, Liao P, Lang X, Kryczek I, Sell A, Xia H, Zhou J, Li G, Li J, Li W, Wei S, Vatan L, Zhang H, Szeliga W, Gu W, Liu R, Lawrence TS, Lamb C, Tanno Y, Cieslik M, Stone E, Georgiou G, Chan TA, Chinnaiyan A, Zou W (2019) CD8(+) T cells regulate tumour ferroptosis during cancer immunotherapy. Nature 569 (7755):270-274. doi:10.1038/s41586-019-1170-y

357. Lenos KJ, Miedema DM, Lodestijn SC, Nijman LE, van den Bosch T, Romero Ros X, Lourenco FC, Lecca MC, van der Heijden M, van Neerven SM, van Oort A, Leveille N, Adam RS, de Sousa EMF, Otten J, Veerman P, Hypolite G, Koens L, Lyons SK, Stassi G, Winton DJ, Medema JP, Morrissey E, Bijlsma MF, Vermeulen L (2018) Stem cell functionality is microenvironmentally defined during tumour expansion and therapy response in colon cancer. Nat Cell Biol 20 (10):1193-1202. doi:10.1038/s41556-018-0179-z
358. Ngiow SF, von Scheidt B, Möller A, Smyth MJ, Teng MWL (2013) The interaction between murine melanoma and the immune system reveals that prolonged responses predispose for autoimmunity. Oncoimmunology 2 (2):e23036-e23036. doi:10.4161/onci.23036
359. Chen P, Huang Y, Bong R, Ding Y, Song N, Wang X, Song X, Luo Y (2011) Tumor-associated macrophages promote angiogenesis and melanoma growth via adrenomedullin in a paracrine and autocrine manner. Clin Cancer Res 17 (23):7230-7239. doi:10.1158/1078-0432.ccr-11-1354
360. Yu JW, Bhattacharya S, Yanamandra N, Kilian D, Shi H, Yadavilli S, Katlinskaya Y, Kaczynski H, Conner M, Benson W, Hahn A, Seestaller-Wehr L, Bi M, Vitali NJ, Tsvetkov L, Halsey W, Hughes A, Traini C, Zhou H, Jing J, Lee T, Figueroa DJ, Brett S, Hopson CB, Smothers JF, Hoos A, Srinivasan R (2018) Tumor-immune profiling of murine syngeneic tumor models as a framework to guide mechanistic studies and predict therapy response in distinct tumor microenvironments. PloS one 13 (11):e0206223. doi:10.1371/journal.pone.0206223
361. Haanen JBAG (2013) Immunotherapy of melanoma. EJC Suppl 11 (2):97-105. doi:10.1016/j.ejcsup.2013.07.013
362. Flecknell P (2002) Replacement, reduction and refinement. Altex 19 (2):73-78
363. Flesch IE, Kaufmann SH (1999) Effect of fetal calf serum on cytokine release by bone marrow-derived macrophages during infection with intracellular bacteria. Immunobiology 200 (1):120-127. doi:10.1016/s0171-2985(99)80037-0
364. Bertani FR, Mozetic P, Fioramonti M, Iuliani M, Ribelli G, Pantano F, Santini D, Tonini G, Trombetta M, Businaro L, Selci S, Rainer A (2017) Classification of M1/M2-polarized human macrophages by label-free hyperspectral reflectance confocal microscopy and multivariate analysis. Sci Rep 7 (1):8965. doi:10.1038/s41598-017-08121-8

365. Saha B, Bruneau JC, Kodys K, Szabo G (2015) Alcohol-induced miR-27a regulates differentiation and M2 macrophage polarization of normal human monocytes. J Immunol 194 (7):3079-3087. doi:10.4049/jimmunol.1402190
366. Soncin I, Sheng J, Chen Q, Foo S, Duan K, Lum J, Poidinger M (2018) The tumour microenvironment creates a niche for the self-renewal of tumour-promoting macrophages in colon adenoma. Nat Commun 9 (1):582
367. Schlecker E, Stojanovic A, Eisen C, Quack C, Falk CS, Umansky V, Cerwenka A (2012) Tumor-Infiltrating Monocytic Myeloid-Derived Suppressor Cells Mediate CCR5-Dependent Recruitment of Regulatory T Cells Favoring Tumor Growth. J Immunol 189 (12):5602-5611. doi:10.4049/jimmunol.1201018
368. Sun LX, Li WD, Lin ZB, Duan XS, Xing EH, Jiang MM, Yang N, Qi HH, Sun Y, Li M, Niu YD, Lu J (2015) Cytokine production suppression by culture supernatant of B16F10 cells and amelioration by Ganoderma lucidum polysaccharides in activated lymphocytes. Cell Tissue Res 360 (2):379-389. doi:10.1007/s00441-014-2083-6
369. Zhang F, Wang H, Wang X, Jiang G, Liu H, Zhang G, Wang H, Fang R, Bu X, Cai S, Du J (2016) TGF-β induces M2-like macrophage polarization via SNAIL-mediated suppression of a pro-inflammatory phenotype. Oncotarget 7 (32):52294-52306. doi:10.18632/oncotarget.10561
370. Wan YY, Flavell RA (2008) TGF-beta and regulatory T cell in immunity and autoimmunity. J Clin Immunol 28 (6):647-659. doi:10.1007/s10875-008-9251-y
371. Couper KN, Blount DG, Riley EM (2008) IL-10: The Master Regulator of Immunity to Infection. J Immunol 180 (9):5771-5777. doi:10.4049/jimmunol.180.9.5771
372. Maybruck BT, Pfannenstiel LW, Diaz-Montero M, Gastman BR (2017) Tumor-derived exosomes induce CD8(+) T cell suppressors. J Immunother Cancer 5 (1):65-65. doi:10.1186/s40425-017-0269-7
373. Klarquist J, Tobin K, Farhangi Oskuei P, Henning SW, Fernandez MF, Dellacecca ER, Navarro FC, Eby JM, Chatterjee S, Mehrotra S, Clark JI, Le Poole IC (2016) Ccl22 Diverts T Regulatory Cells and Controls the Growth of Melanoma. Cancer Res 76 (21):6230-6240. doi:10.1158/0008-5472.CAN-16-0618
374. Chen M-L, Pittet MJ, Gorelik L, Flavell RA, Weissleder R, von Boehmer H, Khazaie K (2005) Regulatory T cells suppress tumor-specific CD8 T cell

cytotoxicity through TGF-beta signals in vivo. Proc Natl Acad Sci U S A 102 (2):419-424. doi:10.1073/pnas.0408197102
375. Jiang H, Gebhardt C, Umansky L, Beckhove P, Schulze TJ, Utikal J, Umansky V (2015) Elevated chronic inflammatory factors and myeloid-derived suppressor cells indicate poor prognosis in advanced melanoma patients. Int J Cancer 136 (10):2352-2360. doi:10.1002/ijc.29297
376. Gerber AL, Munst A, Schlapbach C, Shafighi M, Kiermeir D, Husler R, Hunger RE (2014) High expression of FOXP3 in primary melanoma is associated with tumour progression. Br J Dermatol 170 (1):103-109. doi:10.1111/bjd.12641
377. Baumgartner JM, Gonzalez R, Lewis KD, Robinson WA, Richter DA, Palmer BE, Wilson CC, McCarter MD (2009) Increased survival from stage IV melanoma associated with fewer regulatory T Cells. J Surg Res 154 (1):13-20. doi:10.1016/j.jss.2008.04.043
378. Tucci M, Mannavola F, Passarelli A, Stucci LS, Cives M, Silvestris F (2018) Exosomes in melanoma: a role in tumor progression, metastasis and impaired immune system activity. Oncotarget 9 (29):20826-20837. doi:10.18632/oncotarget.24846
379. Kruger-Krasagakes S, Krasagakis K, Garbe C, Diamantstein T (1995) Production of cytokines by human melanoma cells and melanocytes. Recent Results Cancer Res 139:155-168
380. Tremble LF, O'Brien MA, Soden DM, Forde PF (2019) Electrochemotherapy with cisplatin increases survival and induces immunogenic responses in murine models of lung cancer and colorectal cancer. Cancer Lett 442:475-482
381. Tremble LF, O'Brien MA, Forde PF, Soden DM (2018) ICOS activation in combination with electrochemotherapy generates effective anti-cancer immunological responses in murine models of primary, secondary and metastatic disease. Cancer Lett 420:109-115
382. Heppt MV, Eigentler TK, Kahler KC, Herbst RA, Goppner D, Gambichler T, Ulrich J, Dippel E, Loquai C, Schell B, Schilling B, Schad SG, Schultz ES, Matheis F, Tietze JK, Berking C (2016) Immune checkpoint blockade with concurrent electrochemotherapy in advanced melanoma: a retrospective multicenter analysis. Cancer Immunol Immunother 65 (8):951-959

383. Zhou Y, Shi J, Cui J, Deng CX (2008) Effects of extracellular calcium on cell membrane resealing in sonoporation. J Control Release 126 (1):34-43. doi:10.1016/j.jconrel.2007.11.007
384. Barnett A, Weaver JC (1991) Electroporation: a unified, quantitative theory of reversible electrical breakdown and mechanical rupture in artificial planar bilayer membranes. J Electroanal Chem Interfacial Electrochem 320 (2):163-182. doi:https://doi.org/10.1016/0022-0728(91)85625-Y
385. Mir LM, Orlowski S (1999) Mechanisms of electrochemotherapy. Adv Drug Deliv Rev 35 (1):107-118
386. Staresinic B, Jesenko T, Kamensek U, Krog Frandsen S, Sersa G, Gehl J (2018) Effect of calcium electroporation on tumour vasculature. Sci Rep 8 (1):9412
387. Sinha P, Clements VK, Ostrand-Rosenberg S (2005) Reduction of myeloid-derived suppressor cells and induction of M1 macrophages facilitate the rejection of established metastatic disease. J Immunol 174 (2):636-645. doi:10.4049/jimmunol.174.2.636
388. Hao NB, Lu MH, Fan YH, Cao YL, Zhang ZR, Yang SM (2012) Macrophages in tumor microenvironments and the progression of tumors. Clin Dev Immunol 2012:948098. doi:10.1155/2012/948098
389. Chanmee T, Ontong P, Konno K, Itano N (2014) Tumor-associated macrophages as major players in the tumor microenvironment. Cancers 6 (3):1670-1690. doi:10.3390/cancers6031670
390. Sica A, Porta C, Morlacchi S, Banfi S, Strauss L, Rimoldi M, Totaro MG, Riboldi E (2012) Origin and Functions of Tumor-Associated Myeloid Cells (TAMCs). Cancer Microenviron 5 (2):133-149. doi:10.1007/s12307-011-0091-6
391. Song Q, Hawkins GA, Wudel L, Chou P-C, Forbes E, Pullikuth AK, Liu L, Jin G, Craddock L, Topaloglu U, Kucera G, O'Neill S, Levine EA, Sun P, Watabe K, Lu Y, Alexander-Miller MA, Pasche B, Miller LD, Zhang W (2019) Dissecting intratumoral myeloid cell plasticity by single cell RNA-seq. Cancer Med 8 (6):3072-3085. doi:10.1002/cam4.2113
392. Desai BN, Leitinger N (2014) Purinergic and calcium signaling in macrophage function and plasticity. Front Immunol 5:580-580
393. Melcrova A, Pokorna S, Pullanchery S, Kohagen M, Jurkiewicz P, Hof M, Jungwirth P, Cremer PS, Cwiklik L (2016) The complex nature of calcium cation interactions with phospholipid bilayers. Sci Rep 6:38035. doi:10.1038/srep38035

394. Shi X, Bi Y, Yang W, Guo X, Jiang Y, Wan C, Li L, Bai Y, Guo J, Wang Y, Chen X, Wu B, Sun H, Liu W, Wang J, Xu C (2013) Ca2+ regulates T-cell receptor activation by modulating the charge property of lipids. Nature 493 (7430):111-115. doi:10.1038/nature11699
395. Maggio B, Sturtevant JM, Yu RK (1987) Effect of calcium ions on the thermotropic behaviour of neutral and anionic glycosphingolipids. Biochim Biophys Acta 901 (2):173-182. doi:10.1016/0005-2736(87)90113-1
396. Sturtevant JM (1998) The effect of sodium chloride and calcium chloride on the main phase transition of dimyristoylphosphatidylcholine. Chem Phys Lipids 95 (2):163-168. doi:https://doi.org/10.1016/S0009-3084(98)00071-1
397. Provost KA, Smith M, Arold SP, Hava DL, Sethi S (2015) Calcium restores the macrophage response to nontypeable haemophilus influenzae in chronic obstructive pulmonary disease. Am J Respir Cell Mol Biol 52 (6):728-737. doi:10.1165/rcmb.2014-0172OC
398. Link TM, Park U, Vonakis BM, Raben DM, Soloski MJ, Caterina MJ (2010) TRPV2 has a pivotal role in macrophage particle binding and phagocytosis. Nat Immunol 11 (3):232-239. doi:10.1038/ni.1842
399. Diler E, Schwarz M, Nickels R, Menger MD, Beisswenger C, Meier C, Tschernig T (2014) Influence of external calcium and thapsigargin on the uptake of polystyrene beads by the macrophage-like cell lines U937 and MH-S. BMC Pharmacol Toxicol 15:16-16. doi:10.1186/2050-6511-15-16
400. Eguchi Y, Shimizu S, Tsujimoto Y (1997) Intracellular ATP levels determine cell death fate by apoptosis or necrosis. Cancer Res 57 (10):1835-1840
401. Nikoletopoulou V, Markaki M, Palikaras K, Tavernarakis N (2013) Crosstalk between apoptosis, necrosis and autophagy. Biochim Biophys Acta 1833 (12):3448-3459
402. Frandsen SK, Gissel H, Hojman P, Tramm T, Eriksen J, Gehl J (2012) Direct therapeutic applications of calcium electroporation to effectively induce tumor necrosis. Cancer Res 72 (6):1336-1341
403. Frandsen SK, Gissel H, Hojman P, Eriksen J, Gehl J (2014) Calcium electroporation in three cell lines: a comparison of bleomycin and calcium, calcium compounds, and pulsing conditions. Biochim Biophys Acta 1840 (3):1204-1208. doi:10.1016/j.bbagen.2013.12.003

404. Henze A-T, Mazzone M (2016) The impact of hypoxia on tumor-associated macrophages. J Clin Invest 126 (10):3672-3679. doi:10.1172/JCI84427
405. Colegio OR, Chu NQ, Szabo AL, Chu T, Rhebergen AM, Jairam V, Cyrus N, Brokowski CE, Eisenbarth SC, Phillips GM, Cline GW, Phillips AJ, Medzhitov R (2014) Functional polarization of tumour-associated macrophages by tumour-derived lactic acid. Nature 513 (7519):559-563. doi:10.1038/nature13490
406. Chuang Y, Hung ME, Cangelose BK, Leonard JN (2016) Regulation of the IL-10-driven macrophage phenotype under incoherent stimuli. Innate Immun 22 (8):647-657. doi:10.1177/1753425916668243
407. Wang T, Ge Y, Xiao M, Lopez-Coral A, Azuma R, Somasundaram R, Zhang G, Wei Z, Xu X, Rauscher FJ, 3rd, Herlyn M, Kaufman RE (2012) Melanoma-derived conditioned media efficiently induce the differentiation of monocytes to macrophages that display a highly invasive gene signature. Pigment Cell Melanoma Res 25 (4):493-505. doi:10.1111/j.1755-148X.2012.01005.x
408. Hussein MR (2006) Tumour-associated macrophages and melanoma tumourigenesis: integrating the complexity. Int J Exp Pathol 87 (3):163-176. doi:10.1111/j.1365-2613.2006.00478.x
409. Mantovani A, Bottazzi B, Colotta F, Sozzani S, Ruco L (1992) The origin and function of tumor-associated macrophages. Immunol today 13 (7):265-270. doi:10.1016/0167-5699(92)90008-u
410. Elgert KD, Alleva DG, Mullins DW (1998) Tumor-induced immune dysfunction: the macrophage connection. J Leukoc Biol 64 (3):275-290. doi:10.1002/jlb.64.3.275
411. Minami K, Hiwatashi K, Ueno S, Sakoda M, Iino S, Okumura H, Hashiguchi M, Kawasaki Y, Kurahara H, Mataki Y, Maemura K, Shinchi H, Natsugoe S (2018) Prognostic significance of CD68, CD163 and Folate receptor-β positive macrophages in hepatocellular carcinoma. Exp Ther Med 15 (5):4465-4476. doi:10.3892/etm.2018.5959
412. Khazen W, M'Bika J P, Tomkiewicz C, Benelli C, Chany C, Achour A, Forest C (2005) Expression of macrophage-selective markers in human and rodent adipocytes. FEBS Lett 579 (25):5631-5634. doi:10.1016/j.febslet.2005.09.032
413. Wang T, Xiao M, Ge Y, Krepler C, Belser E, Lopez-Coral A, Xu X, Zhang G, Azuma R, Liu Q, Liu R, Li L, Amaravadi RK, Xu W, Karakousis G, Gangadhar TC, Schuchter LM, Lieu M, Khare S, Halloran MB, Herlyn M, Kaufman RE (2015)

BRAF Inhibition Stimulates Melanoma-Associated Macrophages to Drive Tumor Growth. Clin Cancer Res 21 (7):1652-1664. doi:10.1158/1078-0432.CCR-14-1554
414. Knauf JA, Luckett KA, Chen KY, Voza F, Socci ND, Ghossein R, Fagin JA (2018) Hgf/Met activation mediates resistance to BRAF inhibition in murine anaplastic thyroid cancers. J Clin Invest 128 (9):4086-4097. doi:10.1172/jci120966
415. Girotti MR, Pedersen M, Sanchez-Laorden B, Viros A, Turajlic S, Niculescu-Duvaz D, Zambon A, Sinclair J, Hayes A, Gore M, Lorigan P, Springer C, Larkin J, Jorgensen C, Marais R (2013) Inhibiting EGF receptor or SRC family kinase signaling overcomes BRAF inhibitor resistance in melanoma. Cancer Discov 3 (2):158-167. doi:10.1158/2159-8290.cd-12-0386
416. Hutton JE, Wang X, Zimmerman LJ, Slebos RJC, Trenary IA, Young JD, Li M, Liebler DC (2016) Oncogenic KRAS and BRAF Drive Metabolic Reprogramming in Colorectal Cancer. Mol Cell Proteomics 15 (9):2924-2938. doi:10.1074/mcp.M116.058925
417. Hardeman KN, Peng C, Paudel BB, Meyer CT, Luong T, Tyson DR, Young JD, Quaranta V, Fessel JP (2017) Dependence On Glycolysis Sensitizes BRAF-mutated Melanomas For Increased Response To Targeted BRAF Inhibition. Sci rep 7:42604-42604. doi:10.1038/srep42604
418. Edin S, Wikberg ML, Dahlin AM, Rutegard J, Oberg A, Oldenborg PA, Palmqvist R (2012) The distribution of macrophages with a M1 or M2 phenotype in relation to prognosis and the molecular characteristics of colorectal cancer. PloS one 7 (10):e47045. doi:10.1371/journal.pone.0047045
419. Foley JW, Zhu C, Jolivet P, Zhu SX, Lu P, Meaney MJ, West RB (2019) Gene expression profiling of single cells from archival tissue with laser-capture microdissection and Smart-3SEQ. Genome Res 29 (11):1816-1825. doi:10.1101/gr.234807.118
420. Sica A, Larghi P, Mancino A, Rubino L, Porta C, Totaro MG, Rimoldi M, Biswas SK, Allavena P, Mantovani A (2008) Macrophage polarization in tumour progression. Semin Cancer Biol 18 (5):349-355. doi:10.1016/j.semcancer.2008.03.004
421. Dannenmann SR, Thielicke J, Stöckli M, Matter C, von Boehmer L, Cecconi V, Hermanns T, Hefermehl L, Schraml P, Moch H, Knuth A, van den Broek M (2013) Tumor-associated macrophages subvert T-cell function and correlate with reduced

survival in clear cell renal cell carcinoma. Oncoimmunology 2 (3):e23562-e23562. doi:10.4161/onci.23562
422. Kubota K, Moriyama M (2017) CD163(+)CD204(+) tumor-associated macrophages contribute to T cell regulation via interleukin-10 and PD-L1 production in oral squamous cell carcinoma. Sci rep 7 (1):1755. doi:10.1038/s41598-017-01661-z
423. Liu L, Lu Y, Martinez J, Bi Y, Lian G, Wang T, Milasta S, Wang J, Yang M, Liu G, Green DR, Wang R (2016) Proinflammatory signal suppresses proliferation and shifts macrophage metabolism from Myc-dependent to HIF1alpha-dependent. Proc Natl Acad Sci U S A 113 (6):1564-1569. doi:10.1073/pnas.1518000113
424. Kaneda MM, Messer KS, Ralainirina N, Li H, Leem CJ, Gorjestani S, Woo G, Nguyen AV, Figueiredo CC, Foubert P, Schmid MC, Pink M, Winkler DG, Rausch M, Palombella VJ, Kutok J, McGovern K, Frazer KA, Wu X, Karin M, Sasik R, Cohen EEW, Varner JA (2016) PI3Kγ is a molecular switch that controls immune suppression. Nature 539 (7629):437-442. doi:10.1038/nature19834
425. Doedens AL, Stockmann C, Rubinstein MP, Liao D, Zhang N, DeNardo DG, Coussens LM, Karin M, Goldrath AW, Johnson RS (2010) Macrophage expression of hypoxia-inducible factor-1 alpha suppresses T-cell function and promotes tumor progression. Cancer Res 70 (19):7465-7475. doi:10.1158/0008-5472.CAN-10-1439
426. Guo Y, Feng Y, Cui X, Wang Q, Pan X (2019) Autophagy inhibition induces the repolarisation of tumour-associated macrophages and enhances chemosensitivity of laryngeal cancer cells to cisplatin in mice. Cancer Immunol Immunother 68 (12):1909-1920. doi:10.1007/s00262-019-02415-8
427. Rodell CB, Arlauckas SP, Cuccarese MF, Garris CS, Li R, Ahmed MS, Kohler RH, Pittet MJ, Weissleder R (2018) TLR7/8-agonist-loaded nanoparticles promote the polarization of tumour-associated macrophages to enhance cancer immunotherapy. Nat Biomed Eng 2:578-588
428. Ying W, Cheruku PS, Bazer FW, Safe SH, Zhou B (2013) Investigation of macrophage polarization using bone marrow derived macrophages. J Vis Exp (76). doi:10.3791/50323
429. Cassetta L, Pollard JW (2018) Targeting macrophages: therapeutic approaches in cancer. Nat Rev Drug Discov 17 (12):887-904. doi:10.1038/nrd.2018.169

430. van Rooijen N, Hendrikx E (2010) Liposomes for specific depletion of macrophages from organs and tissues. Methods Mol Biol 605:189-203. doi:10.1007/978-1-60327-360-2_13
431. Chen C, Fenk LA, de Bono M (2013) Efficient genome editing in Caenorhabditis elegans by CRISPR-targeted homologous recombination. Nucleic Acids Res 41 (20):e193. doi:10.1093/nar/gkt805
432. Jha AK, Huang SC, Sergushichev A, Lampropoulou V, Ivanova Y, Loginicheva E, Chmielewski K, Stewart KM, Ashall J, Everts B, Pearce EJ, Driggers EM, Artyomov MN (2015) Network integration of parallel metabolic and transcriptional data reveals metabolic modules that regulate macrophage polarization. Immunity 42 (3):419-430. doi:10.1016/j.immuni.2015.02.005
433. Landstrom FJ, Nilsson CO, Crafoord S, Reizenstein JA, Adamsson GB, Lofgren LA (2010) Electroporation therapy of skin cancer in the head and neck area. Dermatol Surg 36 (8):1245-1250. doi:10.1111/j.1524-4725.2010.01617.x
434. Landstrom FJ, Nilsson CO, Reizenstein JA, Nordqvist K, Adamsson GB, Lofgren AL (2011) Electroporation therapy for T1 and T2 oral tongue cancer. Acta Otolaryngol 131 (6):660-664. doi:10.3109/00016489.2010.541937
435. Landstrom FJ, Reizenstein JA, Nilsson CO, Beckerath MV, Lofgren AL, Adamsson GB, Moller C (2015) Electrochemotherapy - possible benefits and limitations to its use in the head and neck region. Acta Otolaryngol 135 (1):90-95. doi:10.3109/00016489.2014.947655
436. Landstrom F, Ivarsson M, Von Sydow AK, Magnuson A, Von Beckerath M, Moller C (2015) Electrochemotherapy - Evidence for Cell-type Selectivity In Vitro. Anticancer Res 35 (11):5813-5820
437. Cemazar M, Parkins CS, Holder AL, Chaplin DJ, Tozer GM, Sersa G (2001) Electroporation of human microvascular endothelial cells: evidence for an anti-vascular mechanism of electrochemotherapy. Br J Cancer 84 (4):565-570. doi:10.1054/bjoc.2000.1625
438. Saczko J, Kaminska I, Kotulska M, Bar J, Choromanska A, Rembialkowska N, Biezunska-Kusiak K, Rossowska J, Nowakowska D, Kulbacka J (2014) Combination of therapy with 5-fluorouracil and cisplatin with electroporation in human ovarian carcinoma model in vitro. Biomed Pharmacother 68 (5):573-580. doi:10.1016/j.biopha.2014.05.005

439. Jarm T, Cemazar M, Miklavcic D, Sersa G (2010) Antivascular effects of electrochemotherapy: implications in treatment of bleeding metastases. Expert Rev Anticancer Ther 10 (5):729-746. doi:10.1586/era.10.43
440. Gehl J, Skovsgaard T, Mir LM (2002) Vascular reactions to in vivo electroporation: characterization and consequences for drug and gene delivery. Biochim Biophys Acta 1569 (1-3):51-58. doi:10.1016/s0304-4165(01)00233-1
441. Green DR, Ferguson T, Zitvogel L, Kroemer G (2009) Immunogenic and tolerogenic cell death. Nat Rev Immunol 9 (5):353-363. doi:10.1038/nri2545
442. Guo ZS, Liu Z, Bartlett DL (2014) Oncolytic Immunotherapy: Dying the Right Way is a Key to Eliciting Potent Antitumor Immunity. Front Oncol 4:74. doi:10.3389/fonc.2014.00074
443. Fernandes P, O'Donovan TR, McKenna SL, Forde PF (2019) Electrochemotherapy Causes Caspase-Independent Necrotic-Like Death in Pancreatic Cancer Cells. Cancers 11 (8):1177. doi:10.3390/cancers11081177
444. Theurich S, Rothschild SI, Hoffmann M, Fabri M, Sommer A, Garcia-Marquez M, Thelen M, Schill C, Merki R, Schmid T, Koeberle D, Zippelius A, Baues C, Mauch C, Tigges C, Kreuter A, Borggrefe J, von Bergwelt-Baildon M, Schlaak M (2016) Local Tumor Treatment in Combination with Systemic Ipilimumab Immunotherapy Prolongs Overall Survival in Patients with Advanced Malignant Melanoma. Cancer Immunol Res 4 (9):744-754. doi:10.1158/2326-6066.cir-15-0156
445. Mozzillo N, Simeone E, Benedetto L, Curvietto M, Giannarelli D, Gentilcore G, Camerlingo R, Capone M, Madonna G, Festino L, Caracò C, Di Monta G, Marone U, Di Marzo M, Grimaldi AM, Mori S, Ciliberto G, Ascierto PA (2015) Assessing a novel immuno-oncology-based combination therapy: Ipilimumab plus electrochemotherapy. Oncoimmunology 4 (6):e1008842. doi:10.1080/2162402X.2015.1008842
446. Perdiguero EG, Geissmann F (2016) The development and maintenance of resident macrophages. Nat Immunol 17 (1):2-8. doi:10.1038/ni.3341
447. Marim FM, Silveira TN, Lima DS, Jr., Zamboni DS (2010) A method for generation of bone marrow-derived macrophages from cryopreserved mouse bone marrow cells. PloS one 5 (12):e15263-e15263. doi:10.1371/journal.pone.0015263
448. Ortiz LA, Moroz K, Liu JY, Hoyle GW, Hammond T, Hamilton RF, Holian A, Banks W, Brody AR, Friedman M (1998) Alveolar macrophage apoptosis and TNF-

alpha, but not p53, expression correlate with murine response to bleomycin. Am J Physiol 275 (6):L1208-1218. doi:10.1152/ajplung.1998.275.6.L1208
449. van den Berg TK, Kraal G (2005) A function for the macrophage F4/80 molecule in tolerance induction. Trends Immunol 26 (10):506-509. doi:10.1016/j.it.2005.07.008
450. Allavena P, Chieppa M, Bianchi G, Solinas G, Fabbri M, Laskarin G, Mantovani A (2010) Engagement of the mannose receptor by tumoral mucins activates an immune suppressive phenotype in human tumor-associated macrophages. Clin Dev Immunol 2010:547179-547179. doi:10.1155/2010/547179
451. Boon T, Coulie PG, Van den Eynde BJ, van der Bruggen P (2006) Human T cell responses against melanoma. Annu Rev Immunol 24:175-208. doi:10.1146/annurev.immunol.24.021605.090733
452. Frandsen SK, Gehl J (2017) Effect of calcium electroporation in combination with metformin in vivo and correlation between viability and intracellular ATP level after calcium electroporation in vitro. PloS one 12 (7):e0181839-e0181839. doi:10.1371/journal.pone.0181839

Appendices

1. Genes regulated by intratumoural $CD68^+$ macrophage density represented in **figure 3.5**

Negatively regulated	**Positively regulated**
RFC4	*TESC*
BRIP1	*MAGEA4*
BIRC5	*MAGEC1*
DEPDC1	*CXCL12*
CDKN3	*VCAM1*
GPAM	*CD40*
SMS	*CP*
MET	
MME	

2. Genes regulated by peritumoural $CD68^+$ macrophage density represented in **figure 3.5**

Negatively regulated	**Positively regulated**
HPN	*CCL21*
BFAR	*SELE*
PTPN11	*LIPA*
	SCUBE2
	CES1
	HOXA9

3. Genes regulated by BRAF status represented in **figure 3.8**

Negatively regulated	**Positively regulated**
OLIG2	IL1RAP
ULK1	ABCB5
WISP1	CKB
FABP4	FLJ10474
CCL14	KIF14
F10	SLC7A5
ADIPOQ	E2F1
PLA2G2A	CDK2
CHAD	SEC22C
JUN	MKI67
RAMP2	UBE2T
DLC1	CDKN3
ANGPT1	ITGA3
MAGEB1	L1CAM
ANGPT2	NPC1

MAGEA1	SLC39A6
TMEM123	
RTN4RL1	
TEK	
MAML2	
BAIAP3	
PDGFC	
VCAM1	
MMP11	
SLIT2	
THBS4	
RARB	
PTN	
HIF3A	